

The Journal of the
**Utah Academy of
Sciences, Arts, & Letters**

Volume 99 • 2022

**Includes selected and refereed articles from the
2022 Annual Conference
held at Brigham Young University
March 19, 2022**

Editor

Kristin L. Kraus

Copyright 2023, Utah Academy of Sciences, Arts, & Letters.
Copyright reverts to authors after publication. Printed in the United States of America by
Brigham Young University Academic Publishing, Provo, Utah. Neither the editors nor the
sponsoring organization assumes responsibility for statements of fact or opinion made by
the contributors.

ISBN-13: 978-0-9988268-6-8
All Rights Reserved

Board of Editors

Arts: **Dmitri Peskov**, Snow College

Biological Science: **Daniel Clark**, Weber State University

Business: **Taowen Le**, Weber State University

Education: **Nichole Gearing**, Utah Valley University

Engineering: **Ali Siapush**, Southern Utah University

Kinesiology and Health Sciences: **L. Nathan Thomas**, Salt Lake
Community College

Humanities, Philosophy, Foreign Language: **Craig Bergeson**,
Weber State University

Language and Literature: **Keith Lawrence**, Brigham Young
University

Physical Sciences: **Chris Monson**, Southern Utah University

Social Sciences: **Emily Putnam**, Salt Lake Community College

Posters: **Jacque Westover**, Utah Valley University

2021-2022 Utah Academy of Sciences, Arts, & Letters Officers

President: **Daniel Poole**, Salt Lake Community College

President-Elect: **Angela Banchemo-Kelleher**, Utah Valley
University

Past President: **Rachel Keller**, Snow College

Secretary: **Colleen Boam**, Weber State University

Treasurer: **Ryan Boam**, Weber State University

Members at Large: **Erin O'Brien**, Dixie State University;

Jonathan Westover, Utah Valley University; **H. Laine
Berghout**, Weber State University

Technology Officer: **Vern Hart**, Utah Valley University

Finance Committee: **Dan Poole**, **Rachel Keller**, **Angie Banchemo-
Kelleher**, **Jonathan Westover**, **Lynn Mckell**

Cover Photo: “Smog and haze hangs over the Salt Lake valley” by Eltiempo10 is licensed under CC BY-SA 4.0. See Jeremy Bryson and Jeff Montague, “Smoke Season: Exploring the Geographies of Transient Wildfire Smoke on the Wasatch Front,” p. 325.

Utah Academy of Sciences, Arts, and Letters

History: Founded 3 April 1908, the Utah Academy of Sciences was organized "to promote investigations and diffuse knowledge in all areas of science." Beginning in 1923, the Academy started publishing the papers presented in its annual meetings in *Proceedings*. In June 1933 at the annual meeting, the Academy was enlarged to include arts and letters, and the name was changed to the Utah Academy of Sciences, Arts, and Letters. Articles of incorporation and non-profit organization status were accepted by the Academy membership at the spring meeting in April 1959. In 1977, the name of the journal of the Academy was changed from *Proceedings* to *Encyclia*. It became a refereed journal at this time. In the mid 1980s, the scope of the Academy was expanded further to include (1) business, (2) education, (3) engineering, (4) library information and instruction, and (5) health, physical education, and recreation. Beginning with the 1998 issue, the journal became *The Journal of the Utah Academy of Sciences, Arts, and Letters*.

Annual Meeting: The Academy's annual meetings are normally held in the spring on one of the Utah campuses of higher education. The plenary session is called the Tanner Lecture, endowed by Mr. O.C. Tanner in 1986.

Best Paper Awards: The best paper presented in every division is given a cash award, which is presented at the Academy's "Awards Evening" held the following fall.

Distinguished Service Awards: The Academy recognizes outstanding contributions to teaching and scholarship by means of annual Distinguished Service Awards, alternating every other year between disciplines.

Membership: When the Academy was founded in 1908, membership was by nomination, ratified by the Council, and elected by a "three-fourths votes of members present." Today, the Academy's membership is available by application.

Institutional Members: All Utah institutions of higher education are members of the Utah Academy. The Academy appreciates their patronage.

Publication Policy

The *Journal of the Utah Academy of Sciences, Arts, and Letters* publishes works in all of the fields of study encompassed in the Academy's mission. Papers published in *The Journal of the Utah Academy of Sciences, Arts, and Letters* are drawn from papers presented by members in good standing at the annual conference of the Utah Academy. To qualify for publication, the papers must be recommended through a refereeing system.

Presenters are encouraged to publish their paper in *The Journal of the Utah Academy*. *The Journal's* criteria are that a submission is (1) fresh, meaningful scholarly insight on its subject; (2) readable and well written; and (3) of general interest for an academic readership beyond the author's field.

If you wish your paper to be considered for publication in *The Journal*, please submit a Microsoft Word document to the section editor of the appropriate section by the indicated deadline. Contact information for the section editors is available on the Utah Academy's website (www.utahacademy.org).

The Journal of the Utah Academy is a refereed journal. Editorial responses will be forthcoming after the resumption of school the following fall when referees have returned their comments to the division chairs.

Papers should be between 10 and 20 double-spaced pages. Detailed instructions to authors are available at http://www.utahacademy.org/Instructions_for_Authors.pdf.

Among the bibliographic services listing at Bowker Serials Bibliographies and The Standard Periodical Direction. Indexing and abstracting services that cite articles in the journal include Arts and Humanities Citation Index, Biosciences Information Services, Current Geographical Publication, Chemical Abstracts, Mathematical Reviews, MLA Biography, Sociological Abstracts, Excerpta Botanica, Social Planning, Policy and Development Abstracts, Language and Language Behavior Abstracts, Index to Scientific Technical Proceedings, and Index to Social Sciences, and Humanities Proceedings.

The Journal of the Utah Academy of Sciences, Arts, & Letters 2022

AWARDS

Distinguished Service Award	11
Academy Fellow 2023	12
John and Olga Gardner Prize	13
O.C. Tanner Lecture	14
Honorary Member 2023	15
2022 Best Paper Awards	16

ARTICLES

BIOLOGY

Conserving Parasites as Keystone Species in the Great Basin Desert	17
Robert L. Bossard, <i>Bossard Consulting</i>	
Electric Hand Dryers Serve as Reservoirs for Antibiotic-Resistant Bacteria	33
Ashlynd Greenwood, Colette Mortensen, Michele Culumber, and Craig Oberg, <i>Weber State University</i>	
One-Sample Survey of <i>Salinivibrio costicola</i> Strain-Specific Phage from the Great Salt Lake	49
Preston D. Capener, Joshua R. Mott, Matthew B. Crook, and Matthew J. Domek, <i>Weber State University</i>	

BUSINESS

- Seasonality of Frequency and Intensity in Consumer Complaints: A Sentiment Analysis Approach** 63

Reagan Siggard and Yong Seog Kim, *Utah State University*

- Bracketed vs. standard difference-in-differences estimation methods with data analysis on medical marijuana laws and violent crimes** 81

Julian Chan,¹ Anthony Frazier², Gavin Roberts,¹

¹Weber State University; ²Colorado State University

EDUCATION

- An Exploratory Tribal-Crit Analysis of Educators Rising's Role in Teacher Recruitment** 105

William J. Davis, *Southern Utah University*

- Story in the Stars: An Autoethnographic Study of Tongan American Situated Storytelling** 105

Belinda 'Ofakihevahanoa Fotu¹ and Latuniua Jesse Fotu

¹Utah State University

ENGINEERING

- Thermodynamics Experiment: Adiabatic Compression of Air** 145

Toby Ian McMurray and Ali Syyed Siahpush, *Southern Utah University*

- Experimental and Theoretical Results of Transient and Steady-State Heat Transfer of a Long Aluminum Fin** 157

Alicyn Astle, Cameron J. Dix, Lee Lorimer, Ali Siahpush
Southern Utah University

- Steady-State and Transient Analysis of a Fin Under Water** 169

Mitchell Halverson, Floyd K. Kimber, Kobe Potter,
Jathen Chaffin, Ali Siahpush, *Southern Utah University*

Scale Analysis of a Solid–Liquid Phase Change Thermal Energy Storage System 187

Jordan Whitlock and Ali Siahpush, *Southern Utah University*

Inward Melting in Cylindrical Coordinate System: Analytical Solution (Derivations) 205

Jordan Whitlock and Ali Siahpush, *Southern Utah University*

Cavitation Demonstration Trials 221

Owen Telford and Ali Siahpush, *Southern Utah University*

KINESIOLOGY AND HEALTH SCIENCES

Exploring Correlates of Domestic Violence and Homelessness: A Review of the Literature 238

Linnette Wong, *Weber State University*

LANGUAGE AND LITERATURE

Rhetorics of Advocacy in Disability Accommodation 249

Rachel Bryson and Peter Call, *Utah State University*

PHYSICAL SCIENCES

Investigation of Manganese Nanoparticles with Various Capping Ligands and Their Effects on *Raphanus sativus* 263

Taytum Stratton,^{1,2} Elizabeth Pierce,¹ Christopher F. Monson¹
¹*Southern Utah University*, ²*SUCCESS Academy*

Creating a Map for Quantum Teleportation Protocols 277

Aidan Gillam and Jean-François Van Huele
Brigham Young University

SOCIAL SCIENCES

Tupac Shakur and Kendrick Lamar: A Legacy of Hip Hop Resistance 293

Theresa A. Martinez, *University of Utah*

Understanding Us: Undergraduate Research to Support a Community Partner Working on Homelessness	309
Kambry Woodbury and Daniel Poole, <i>Salt Lake Community College</i>	
Smoke Season: Exploring the Geographies of Transient Wildfire Smoke on the Wasatch Front	325
Jeremy Bryson and Jeff Montague, <i>Weber State University</i>	
ABSTRACTS	341

DISTINGUISHED SERVICE AWARD 2022

The Distinguished Service Award is given to an academic professional for exceptional service to the higher education community in Utah.

Adrienne Andrews, MA, MS

Weber State University

Andrews earned a Bachelor of Arts degree in Political Science with minors in Ethnic Studies and Spanish in 1993 from the University of Utah. While there, she studied abroad in Cuernavaca, Mexico in addition to completing an internship at the U.S. Supreme Court. She next attended the University of Denver, College of Law as a Chancellor's Scholar, leaving in 1995 and returning to the U of U, where she completed a second Bachelor of Arts in Women's Studies in 1996. Her first master's degree was completed at Minnesota State University, Mankato (MSUM) in Women's Studies in 1997. She completed a master's degree in Political Science at Rutgers, the State University of New Jersey, in 2001.

Andrews completed a postgraduate degree in Conflict Resolution & Mediation, received with honors from the U of U in 2006. Andrews is currently ABD in Education, Culture, and Society at the University of Utah.

During her career, Andrews has worked in a variety of government, higher education, and non-profit capacities including as Director of the Center for Youth Policy and Programs for the State of New Jersey, Staff Associate in the New Jersey Department of State, Political Science Instructor at Rutgers University, Women's Studies Instructor at MSUM, and graduate associate and research associate at the Eagleton Institute of Politics and the Center for American Women and Politics.

A native Utahn, Andrews was raised in Davis County and has a long history of advocacy in social justice and inclusion work with a special capacity for community building. Andrews currently serves as a member of the McKay-Dee and Layton Hospital Boards, the Boys & Girls Club of Weber-Davis Board, and as the Honorary Commander of the Hill Air Force Base 75th Wing. She most recently served on the Utah Governor's Martin Luther King, Jr. Human Rights Commission.

Andrews has received numerous honors, including the 2020 Living Color Gala and Utah Business Educator Award, the 2020 H. Aldous Dixon Award, the 2018 Omega Psi Phi Fraternity Community Service Award, and the 2017 Ogden Weber Chamber Women in Business Athena Award.

ACADEMY FELLOW 2023

Erin O'Brien, PhD

Utah Tech University

Dr. Erin O'Brien is passionate about informal education, having benefited from a long series of mentors and advocates who helped nurture her love for research and the outdoors both in and out of the classroom. As a plant physiological ecologist, she has spent years engaged in research serving the needs of regional public lands and mentoring teams of undergraduate students in restoration and conservation biology. Creating these opportunities for students to engage in research has also resulted in collaborations across a diversity of fields varying from hyperbaric medicine to the use of nature to support mental health.

Providing accessible opportunities for students to engage in research as well as high impact extracurricular experiences has been at the core of her career. As a new professor at Utah Tech University, one of her first responsibilities was to serve on the UASAL Board—initially as the Chair of Biology. She later served as President-Elect, President, Past-President, and a member-at-large for a total of 14 years in UASAL leadership. In addition, she has spent nearly a decade as the Director of the Southern Utah eSMART summer camp, a STEM camp for middle school girls designed to reduce the gender disparity among STEM majors in Southern Utah. Expanding her work in public lands, she worked with the National Park Service to establish the Outdoor Leadership Academy to provide underrepresented young adults the opportunity to meaningfully connect with nature. More recently, this work in nature resulted in the opportunity to create a curriculum to help train others in how to lead inclusive, responsible recreation trips in nature.

Dr. O'Brien currently continues to teach biological research methods and analysis and provide student mentorship while also serving as the Director of Community Engaged Learning at Utah Tech University.

Originally from Virginia, she lives with her partner of 21 years and her daughter in St. George, where she spends her free time hiking and serving the local nonprofit community.

JOHN & OLGA GARDNER PRIZE 2022

The Gardner Prize is awarded annually for exceptional achievement by an academic professional in Utah.

Larry Smith, MS, PhD

Snow College

Larry Smith was raised in Provo, Utah in a family of educators. His interest in math and physics was sparked early, and he devoured the Dewey Decimal 500s and 600s in his junior high library. He also signed up for beginning band and chose to play the clarinet, which he continued through high school. Upon returning to BYU after two years in Chile, he picked up the clarinet again, but spent more time on his double major in physics and math. After graduating from BYU, Larry earned a master's degree in physics and a PhD in science education from The University of Texas at Austin. While in graduate school, Larry married Holly, and they were blessed with two little Texans. He also played in the Austin Community Orchestra.

Larry then accepted a teaching position at Snow College in physics and math. Over time, Larry and Holly added three little Utahns to their family. At Snow College, he has served as chair of the Physics Department twice, as dean of the Division of Natural Sciences and Mathematics, as director of faculty development, and as president of the Faculty Senate. His recent research has centered on the mathematics of music. Larry is involved in the Honors Program and the Great Teachers Movement. His heart remains in the classroom. After the new science building opened, he became the director of the Snow College Planetarium, where he can often be found hosting shows for school groups and the public.

Inspired by the Citizenship in the Community merit badge as a Boy Scout, he served 6 years on the Ephraim Public Library Board and 12 years on the South Sanpete School Board and played his clarinet in the Sanpete Valley Community Orchestra for 25 years. As much as he loves education, his higher priority is his family.

O.C. TANNER LECTURE**“Visualizing the Sciences and Art of Math and Music”****Larry Smith, MS, PhD***Weber State University*

Musicians do not need to be expert mathematicians in order to produce beautiful music, but music is based on mathematical principles that require some choices on the part of musicians, so an understanding of the mathematical underpinnings of music theory is useful. Logarithms are a constructive way to represent frequency or pitch. Ratios of frequencies are used to construct intervals and scales. Mathematical visualizations provide insight into various musical tunings and temperaments. Preferences and choices have changed over time. An understanding of math can enhance the aesthetic enjoyment of music.

HONORARY MEMBER 2023

Dixie Shaheen Rasmussen, DNP, CNM, MSN-Ed

Dr. Dixie Rasmussen is an Advanced Practice Registered Nurse who introduced Nurse Midwifery to Central Utah in 1998. As a Doctoral-prepared Certified Nurse Midwife, Dixie provides culturally competent care for a wide variety of women and newborns with diverse needs. She exemplified this quality as the State of Utah Sexual Assault Examiner of the Year (2010). She is a high-performing, compassionate clinician and manager with 42 years of healthcare experience in hospital and medical office environments. Dixie has delivered over 2200 newborns. She is an advocate for rural healthcare with strong leadership and was awarded the “Nurse of the Year in Leadership” from the Utah Nurse’s Association (1998). Dixie has also been a Nurse-educator in a Licensed Practical Nursing program, Adjunct Professor for the University of Utah, Clinical Instructor for Brigham Young University and currently serves on the Sevier School Board of Education. She continues with her focus in nursing education as she has been a preceptor for scores of Doctoral, Masters’ and undergraduate students. Dixie has a strong academic background. She was awarded the American College of Nursing’s 2017-2018 “Excellence in Advanced Nursing Practice Award.” The award was granted for the nation’s outstanding student in a Doctor of Nursing Practice program for the research and project, “Can a Rural Hospital Reliably Perform an Emergency Cesarean Section in 30 Minutes or Less?” She is also a contributing author in a nursing textbook, *The DNP Professional: Translating Value from Classroom to Practice*. Her contributed chapter is titled “From Mid-Level Midwifery to High-Husbandry – A Rural Certified Nurse Midwife’s Doctoral Journey.

Dixie was born and raised in Salina, Utah. She married her high school sweetheart and has 5 children and 7 grandchildren. She enjoys gardening, reading, and horses.

2022 BEST PAPER AWARDS

Biological Sciences

One-Sample Survey of *Salinivibrio costicola* Strain-Specific Phage from the Great Salt Lake

Preston D. Capener, Joshua R. Mott, Matthew B. Crook, Matthew J. Domek

Weber State University

Business

Seasonality of Frequency and Intensity in Consumer Complaints: A Sentiment Analysis Approach

Reagan Siggard, Yong Seog Kim

Utah State University

Engineering

Thermodynamics Experiment: Adiabatic Compression of Air

Toby I. McMurray, Ali Siapush

Southern Utah University

Social Science

Smoke Season: Exploring The Geographies of Transient Wildfire Smoke on The Wasatch Front

Jeremy Bryson, Jeff Montague

Weber State University

Conserving Parasites as Keystone Species in the Great Basin Desert

Robert L. Bossard

Bossard Consulting

Abstract

Recognition of how pathosystems of parasites and their symbiotes in disease foci are keystone ecological engineers constitutes a revolution in our understanding of ecosystem function. Life zones, biomes, and specialized habitats such as caves are distinct biocenoses of plant and fungal parasites; similarly, animal ectoparasites, such as ticks, mites, mosquitoes, fleas, lice, and internal parasites, such as tapeworms and nematodes, are further associated with their own symbiotic microbiota of protists, bacteria, and the virosphere. Biomes show homeostasis, generally on a small scale but affecting the biosphere and undergoing fairly predictable successions after disturbance resulting in repeated species interactions, notably including those of endemic parasites with their hosts in coevolved subgroup selection that can result counterintuitively in parasites benefitting their hosts. Examples include mistletoe, which parasitizes juniper but feeds birds that aid the seed dispersal of its hosts, and fleas and other parasites, which may regulate seed-eating mice and help regenerate forest after fires. In addition to the charismatic megafauna, flora, and pollinators, parasites and their symbiotes are critical for conservation initiatives such as “30×30” (30% area conserved by 2030) and “Half-Earth” (50% of natural terrestrial and marine areas preserved).

Introduction

Biologists often see parasites as annoyances or perhaps dangers, but a new view during the last several decades is revolutionizing our understanding of terrestrial and aquatic ecosystems: “parasites—usually regarded in terms of their detrimental effects on the individuals they infest—can also have positive impacts... parasites and pathogens act as ecological engineers... [and] challenge the conventional wisdom that parasites have only negative or inconsequential impacts on ecological communities” (Hatcher et al. 2012). Impacts of parasites on ecosystem processes have led to calls to include traditionally ignored parasites in food web and ecosystem studies (McCallum and Dobson 1995, Pojmariska 2002, Hudson et al. 2006, Byers 2009).

Keystone parasites and their pathogens comprise “pathosystems,” an ecosystem’s subsystems of parasites and disease, a term originating from plant–pathogen systems (Robinson 1987) but describing animal–pathogen systems, too. These parasites are likely essential regulatory elements in their communities, but their processes are largely unstudied (Marcogliese and Cone 1997, Hatcher et al. 2008, Watson 2013, Sponchiado et al. 2017), and these unknowns call into question the unintended consequences of global programs designed to eliminate disease, such as malaria (Small 2019, *The Lancet Infectious Diseases* 2020).

In this review, I examine examples from the literature of parasites from a variety of life zones and kingdoms in light of the hypothesis that parasites help regulate populations and establish homeostatic mechanisms in natural ecosystems of the Great Basin Desert (Figure 1).

Parasitic Lifestyles

Terrestrial arthropod parasites are categorized roughly by Di Giovanni et al. (2021): “Short-term micropredators” actively seek out hosts and spend little time in blood or sap sucking, such as most fleas (Siphonaptera), bloodsucking flies (biting midges, blackflies, mosquitoes, sandflies, stable flies, tabanids, tsetse flies), and some true bugs (Triatominae). “Long-term micropredators” actively seek out hosts but stay extensively on or in the host, such as aphids and thrips on plants, bat flies, bed bugs, sheep ked flies, embedding fleas (chigoes in Tungidae), some ticks, and flies whose larvae develop myiasis inside vertebrate tissues, such as blowflies, botflies, and screwflies. Parasites with passive transmission, such as tongue worms (Pentastomidae) and trigonalid hyperparasitoid wasps, depend upon hosts accidentally ingesting them (“trophically transmitted”). Finally, some parasites move between hosts or nests in near contact, such as lice and many types of

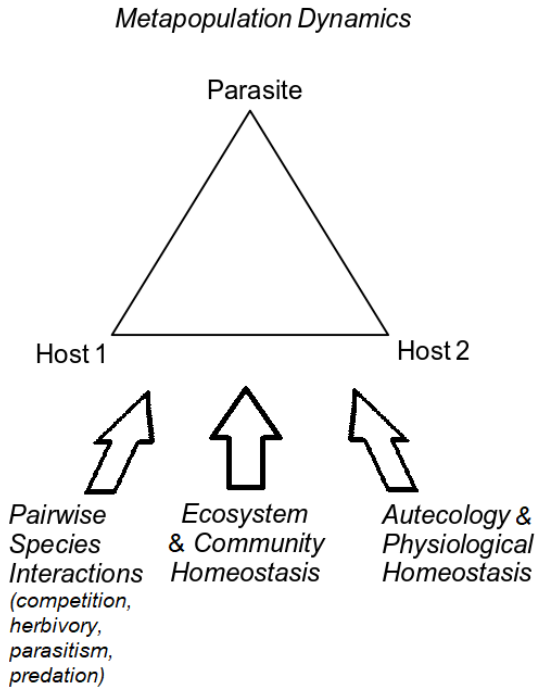


Figure 1. Keystone parasites can affect multiple levels of biological hierarchy, often through indirect, third-party interactions, both trophic and non-trophic, that surprisingly may benefit host populations.

mites (Dermanyssidae, Laelapidae, and Sarcoptidae, the scabies mite). Several examples I discuss are from outside the Great Basin but involve the same species, implying that their interactions may happen within the Great Basin.

Parasites of the Great Basin Desert are often associated with biomes, life zones, or habitat islands (wetlands, nests of mammals and birds, caves) of characteristic complexes of coevolved species (Bossard 2006). Woodrats (*Neotoma*), voles, and others may be infected with helminths and protists (trypanosomes, apicomplexa) and build wonderful nests for complements of fleas, botflies, hard and soft ticks, mites, pseudoscorpions, and spiders (Howell 1955, Howell et al. 1957, Grundmann and Frandsen 1960, Whitaker and Wilson 1974, Smith et al.

2005). The varied life histories of parasites result in pervasive effects on Great Basin Desert ecosystems.

Arthropod Effects

One of these parasite groups, fleas (Siphonaptera), is widespread in Great Basin Desert life zones on a variety of mammals and birds. The “fleas to trees” hypothesis states that fleas and, by implication, other parasites negatively impact abundant and widespread seed-eating rodents, such as deer mice *Peromyscus*, that, if unchecked, would destroy seed banks in the soil of montane and subalpine forests (Zwolak et al. 2013). New seedlings re-establish a successional trajectory to forested landscapes after fire. Thus, the presence of parasites in an area helps determine primary vegetative structure. It is unclear whether other parasites affect biome recovery, such as the gamasid mites in alpine areas in Asia (Medvedev et al. 2014) or mites and endoparasites (hepatozoa, haemosporozoa, nematodes, etc.) that are widely present in the Great Basin Desert (Allred 1956).

Parasites often affect host populations. Fleas, for example, affect nesting behavior, survival rate, the number of young, and in birds, the size of egg clutches and hatching success. Hosts studied include cliff swallow (Brown et al. 1995), tree swallow (Rendell and Verbeek 1996), blue tit (with the hen flea *Ceratophyllus gallinae*, Richner and Tripet 1999, Bouslama et al. 2002, Fitze et al. 2004, Slomczyński et al. 2006), great tit (Richner et al. 1993, Oppliger et al. 1994, Heeb et al. 2000), starling (Mazgajski 1997), kit fox (Kluever 2019), gerbil (with the flea *Synosternus cleopatrae*, Hawlena et al. 2006), Cape ground squirrel (Hillegass et al. 2010), and Columbian ground squirrel (Neuhaus 2003) (infested with *Oropsylla idahoensis* and *Oropsylla tuberculata*). In regard to the Columbian ground squirrel, Roth et al. (2019) declared: “Some subtle short-term effects do manifest but are unlikely to culminate in detrimental long-term fitness consequences unless parasitemia is chronically sustained. As such, fleas, even when experimentally augmented in number to increase their impact, do not strongly affect these hosts. This result suggests that while hosts in poor condition may exhibit high flea loads, flea infestation by itself is unlikely to debilitate hosts.” A model of flea populations corroborated this conclusion (Krasnov et al. 2005), as did Watson’s (2013) meta-analysis of 38 datasets that broadly asserted that diverse parasites did not affect overall breeding success of wild vertebrate hosts, both terrestrial and aquatic, despite the parasites’ significant impacts on other parameters of host populations. This contradiction requires further research: parasite infestation often can have both substantive and negligible effects, which

suggests that parasites may finely tune control elements of ecosystem functioning.

One of the few experiments involving fleas not vectoring disease is with great tit (*Parus major*) nests in Europe. Heeb et al. (2000) manipulated nest humidity and flea infestation levels (again, the flea was *C. gallinae*) and claimed the first experimental results showing: “an ectoparasite acting as a physical ecosystem engineer where nest humidity increased as a result of flea infestations,” “an abiotic factor within nests can affect ectoparasite infracommunity structure,” and “an interspecific association between two ectoparasite species” (the other ectoparasite was *Protocalliphora* flies).

Ticks *Ixodes angustus* and *Ornithodoros parkeri* and endoparasites *Sarcocystis*, *Protospirura* nematodes, and *Wallcomia* pinworms may infest desert rodents in arid areas of Oregon (O’Farrell 1975), as well as other desert biomes (Bajer et al. 2006). Veitch et al. (2020) found interspecific, often positive, co-occurrences among parasites of deer mice. From regeneration at the landscape scale of forests and other biomes to hosts’ nest microclimates, utilization of dens, and physiology, parasitic arthropods affect multiple levels of biological hierarchy.

Effects of Other Parasitic Animals

The helminths (flake, roundworm, tapeworm, etc.) are endoparasites infecting a variety of hosts, including shrews (*Sorex*), marten and other carnivores, and birds, and may require arthropods or mollusks to complete their life cycle. In addition, there are other parasitic animals such as some chordates, leeches, and mollusks.

Helminths and other parasites may help regulate host populations, and are “key indicators for anticipating the consequences of accelerating environmental perturbation... [research] highlights large gaps in our understanding of northern parasites and also documents high rates of new discoveries of parasites and viruses” (Hope et al. 2016).

Parasitic Plant Effects

Parasitic plants affect montane forest. Mistletoe (*Phoradendron californicum*) pilfers light, nutrients, and water from juniper trees (*Juniperus monosperma*). Even so, Van Ommen and Whitham (2002) showed that mistletoe surprisingly *benefits* juniper by interacting with fruit-eating birds (e.g., Townsend’s solitaire (*Myadestes townsendi*) and *Phainopepla nitens*). Mistletoe produces fruit for birds at different times of the year than juniper, fostering retention of the birds for longer times and improving dispersal of juniper and mistletoe seeds. Analogous symbiotes thrive in Great Basin Desert pinyon–juniper woodlands.

Mistletoe proves how parasites may profit their hosts through third-party, indirect interactions. Other parasitic plants such as Indian paintbrush (*Castilleja* spp.) and owl's clover (*Orthocarpus* spp.) are numerous and may affect biotic community diversity and soil nutrients widely in the Great Basin Desert (Ducharme and Ehleringer 1996, Press and Phoenix 2005, Schmidt 2016).

Fungus Effects

Fungi (Laboulbeniales, Ascomycota: Laboulbeniomycetes) flourish as hyperparasites in tritrophic food webs of bat caves (De Groot et al. 2020). In desert caves (Pape 2014, Bossard 2017), fungi are pervasive. In sagebrush biomes, they cause disease in rodents (Bartlow 2017). Fungi appear to shape ecosystems in the Great Basin, including as mutualists, predators, and parasites.

Protist Effects

Microbial eukaryotes occur throughout vertebrate and plant populations and are often transmitted by arthropod vectors. One fascinating example is *Leucocytozoon* (Apicomplexa) afflicting Northern Goshawks in subalpine forests of Northern Great Basin Desert (Jeffries et al. 2015). These hemoparasites cause generally only mild problems for the goshawks and are in the same order (Haemosporida) as malaria, of which there are over 200 species affecting birds, mammals, and reptiles (5 species, vectored by *Anopheles* mosquitoes, affect humans); the goshawk parasites are carried by black flies (Simuliidae), or in some areas, biting midges (Culicoides).

Another eukaryotic apicomplexan endoparasite, gregarines, along with parasitic mites, preferentially infest invasive dragonflies, protecting endemic dragonflies (Mlynarek 2015). In general, parasites may increase their incidence, “sinking” onto invasive hosts and potentially benefitting endemic hosts, or conversely fail to keep up with invasive hosts (“enemy release hypothesis”), leading to population explosions of the invasive species (Dunn 2009, Matthee et al. 2013, Mlynarek 2015, Gozzi et al. 2020).

Prokaryote Effects

Bacteria, too, have the ability to stabilize ecosystems if they are endemic and, if invasive, to transform ecosystems. Tularemia, also known as rabbit fever, circulates through numerous host species, modalities, and mechanisms, including water- and food-borne (Hopla 1955, Foley and Nieto 2010). *Bartonella* show an impressive example of

a positive, indirect effect of fleas on their endemic host (Telfer et al. 2005, Tompkins et al. 2011): “*Bartonella* spp. (a flea-vectored bacterial infection) declined in wood mice *Apodemus sylvaticus* in Ireland as densities of the invading bank vole *Myodes glareolus* increased. The infection was detected in wood mice, but not in bank voles, suggesting that the less competent invader acted as a sink for the parasite.” Again, this invasive host–sink effect has a stabilizing effect on the endemic host and community! Conversely, *Bartonella* can act as an invasive transformer species in ecosystems as climate warms (Foley et al. 2017). Rodents bearing novel viruses are moving north and climbing higher up insular mountains in the Great Basin, exposing endemic birds and mammals, such as American pika *Ochotona princeps*, to disease. In the last 10,000 years since the last Ice Age, biota on Great Basin mountains vanish as alpine environments shrink, with human-induced climate change accelerating the process (Foley et al. 2017, Brinkerhoff et al. 2020).

One of the best-studied experimental systems uses insecticides and plague vaccines on fleas carrying plague bacterium *Yersinia pestis*, an invasive “transformer species” in natural ecosystems (Biggins et al. 2010, Machett et al. 2010, Eads and Biggins 2015, Goldberg et al. 2020). Plague suppression causes direct and indirect trophic effects on hosts, host predators, host food plants, and ancillary species (Figure 2). By causing periodic die-offs of prairie dogs (*Cynomys*), fleas with plague affect the entire ecosystem: nutrient cycling such as carbon storage, nitrogen mineralization, and water infiltration varies. There are increases

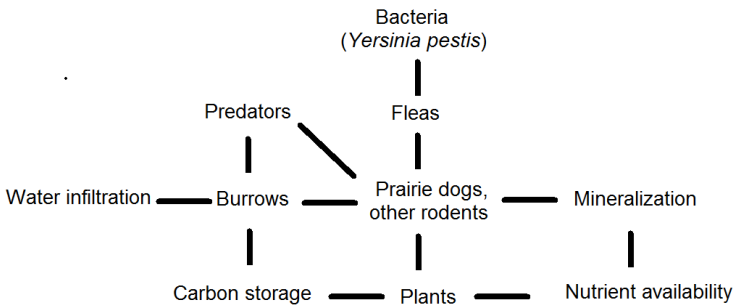


Figure 2. Plague ecosystem interactions; fleas carrying plague bacteria may shift their ecosystem from one stable state to another.

in graminoids, shrubs, and woody plants but loss of nutritious forbs. Burrows used by vertebrates and invertebrates for shelters disappear. Prey decreases for predators such as hawks (*Buteo*) and ferrets (*Mustela*). Prairie dogs remove foundation plants, fleas connect prairie dogs to plague, and plague bacteria extirpate prairie dogs. Ecosystems can shift among stable states (May 1977), thus fleas with plague can change their entire ecosystem.

Virus Effects

Ocean bacteriophages cause large fluctuations in abundance of plankton such as Pelagibacterales, rebalancing food webs (Frada et al. 2014, Dance 2021). By comparison, terrestrial arthropod-borne viruses (arboviruses) circulate through Great Basin Desert ecosystems, the “virosphere,” often vectored by mosquitoes (Crane et al. 1983) or other insects such as plant-sucking Homoptera. Population cycles of mosquito vectors and rabbit hosts in the Great Basin are observed, possibly due to virus dilution (Elbel and Rosenfeld 1990). Arbovirus outbreaks in the Great Basin Desert cause substantial disease in vertebrates and plants.

Implications

In conclusion, species in pathosystems repeatedly interact when their ranges overlap during long periods and result in selection possibly at a variety of levels, including groups of species, or biocenoses (Wilson and Wilson 2007). Genetic feedback contributes to homeostatic regulation, allowing the group to persist despite environmental perturbations; conversely, invasive parasites and pathogens can destabilize and transform landscapes. Homeostatic mechanisms arise at a variety of levels, too, from an individual’s behavioral and physiological homeostasis (autecology), meta-population, paired species interaction (predator–prey, herbivore–plant, parasite–host), and community and ecosystem homeostasis. Local homeostasis helps create biosphere homeostasis, as shown by James Lovelock’s Daisyworld model where life and its environment optimize temperature regulation and maximize biodiversity (Ackland et al. 2003).

Several researchers have referred to the ethical controversy and paradoxes of conserving parasites (Kwak et al. 2019, Carlson et al. 2020). Crozier and Schulte-Hostedde (2014) commented, “One consideration that has not received sufficient attention is that a conservation mandate to protect biodiversity might imply the need to protect pathogens from extinction in part because of their ecological role as consumers. Insofar as wildlife disease eradication programs are aimed at minimizing or extirpating the organism directly responsible for

mortality and morbidity in wildlife, livestock, and human populations, they might undermine biodiversity conservation.” Acosta and Fernandez (2015) wrote, “Parasite conservation may not be a popular topic, but preserving and studying parasite diversity and interactions represent many benefits... for actively modeling community structure and keeping diversity, for being good indicators of ecosystem health..., for their use in biomedicine, and because their DNA may provide a biological record of evolutionary dynamics...”. Some parasites are extinct or endangered because their host went extinct or because the host’s conservation eliminated the host’s ectoparasites (Rozsa and Vas 2015). They observed, “...several reasons why conservationists should care about threatened parasites. They not only constitute a large proportion of global biodiversity but also exert selective pressures to increase host diversity... and therefore harbouring a unique parasitic fauna can increase the conservation value of the host... Furthermore, parasites carry phylogenetic and population genetic information about the evolutionary past of their hosts... Conservationists should consider preserving host specific lice as part of their efforts to save birds or mammals *ex situ*...” (Rozsa and Vas 2015).

In addition to the charismatic megafauna, flora, and pollinators, parasites and their symbiotes are critical for conservation initiatives such as “30×30,” which proposes conservation of 30% of earth’s area by 2030, and “Half-Earth,” with a greater 50% of natural terrestrial and marine areas preserved (Wilson 2016). Biocenoses containing parasites are ubiquitous throughout Great Basin Desert life zones and habitats, and they are important for maintaining community diversity and ecosystem functioning, and for research and conservation.

Literature

Ackland, G.J., M.A. Clark, T.M. Lenton. 2003. Catastrophic desert formation in Daisyworld. *J. Theor. Biol.* 223:39-44.

Acosta, R., J.A. Fernandez. 2015. Flea diversity and prevalence on arid-adapted rodents in the Oriental Basin, Mexico. *Rev. Mex. Biodivers.* 86(4):981-988.

Allred, D.M. 1956. Mites found on mice of the genus *Peromyscus* in Utah. I. General infestation. *Great Basin Nat.* 16(1/4):23-31.

Bajer, A., P.D. Harris, J.M. Behnke, M. Bednarska, C.J. Barnard, N. Sherif, et al. 2006. Local variation of haemoparasites and arthropod vectors, and intestinal protozoans in spiny mice (*Acomys dimidiatus*) from four montane wadis in the St Katherine Protectorate, Sinai, Egypt. *J. Zool.* 270(1):9-24.

Bartlow, A.W. 2017. Ecological factors influencing community structure of parasites and their hosts. PhD diss., University of Utah, Salt Lake City, Utah.

Biggins, D.E., J.L. Godbey, K.L. Gage, L.G. Carter, J.A. Montenieri. 2010. Vector control improves survival of three species of prairie dogs (*Cynomys*) in areas considered enzootic for plague. *Vector-Borne Zoonotic Dis.* 10:17–26.

Bossard, R.L. 2006. Mammal and flea relationships in the Great Basin Desert: from H.J. Egoscue's collections. *J. Parasitol.* 92:260–266.

Bossard, R.L. 2017. Population model for the bat flea *Sternopsylla distincta* (Siphonaptera: Ischnopsyllidae) in temperate caves of the Brazilian free-tailed bat *Tadarida brasiliensis* (Mammalia: Chiroptera). *J. Utah Acad. Sci. Arts Lett.* 94: 71-78.

Bousslama, Z., M.M. Lambrechts, N. Ziane, R. Djenidi, Y. Chabi. 2002. The effect of nest ectoparasites on parental provisioning in a north-African population of the Blue Tit *Parus caeruleus*. *Ibis* 144:E73–E78.

Brinkerhoff, R.J., H.S. Rinsland, S. Sato, S. Maruyama, C. Ray. 2020. Vector-borne pathogens in ectoparasites collected from high-elevation pika. *EcoHealth* 17(3):333-344.

Brown, C.R., M.B. Brown, B. Rannala. 1995. Ectoparasites reduce long-term survival of their avian host. *Proc. Royal Soc. London B* 262(1365):313-319.

Byers, J.E. 2009. Including parasites in food webs. *Trends Parasitol.* 25(2):55-57.

Carlson, C.J., S. Hopkins, K.C. Bell, J. Doña, S.S. Godfrey, M.L. Kwak, et al. 2020. A global parasite conservation plan. *Biol. Cons.* 250:108596.

Crane, G.T., R.E. Elbel, D.B. Francly. 1983. Arboviruses from western Utah, USA, 1967-1976. *J. Med. Entomol.* 20(3):294-300.

Crozier, G.K.D., A.I. Schulte-Hostedde. 2014. The ethical dimensions of wildlife disease management in an evolutionary context. *Evol. Appl.* 7:788-798.

Dance, A. 2021. The incredible diversity of viruses. *Nature* 595:22-25.

De Groot, M.D., I. Dumolein, T. Hiller, A.D. Sándor, T. Szentiványi, M. Schilthuizen, et al. 2020. On the fly: Tritrophic associations of bats, bat flies, and fungi. *J. Fungi* 6(4):361:1-13.

Di Giovanni, F., A.B.B. Wilke, J.C. Beier, M. Pombi, J.A. Mendoza-Roldan, N. Desneux, et al. 2021. Parasitic strategies of arthropods of medical and veterinary importance. *Entomol. Gen.* 41(5):511-522.

Ducharme, L.A., J.R. Ehleringer. 1996. Gas exchange, $\delta^{13}\text{C}$, and heterotrophy for *Castilleja linariifolia* and *Orthocarpus tolmiei*, facultative root hemiparasites on *Artemisia tridentata*. *Great Basin Nat.* 333-340.

Dunn, A.M. 2009. Parasites and biological invasions. *Adv. Parasitol.* 68:161-184.

Eads, D.A., D.E. Biggins. 2015. Plague bacterium as a transformer species in prairie dogs and the grasslands of North America. *Conserv. Biol.* 29:1086-1093.

Elbel, R.E., M.J. Rosenfeld. 1990. Relationship between jackrabbit populations and California serogroup viruses in western Utah. *Proc. Utah Mosq. Abate. Assn.* 43:1-4.

Fitze, P.S., B. Tschirren, H. Richner. 2004. Life history and fitness consequences of ectoparasites. *J. Anim. Ecol.* 73:216–226.

Foley, J.E., N.C. Nieto. 2010. Tularemia. *Vet. Microbiol.* 140(3-4):332-338.

Foley, P., T. Roth, J. Foley, C. Ray. 2017. Rodent-pika parasite spillover in western North America. *J. Med. Entomol.* 54(5):1251-1257.

Frada, M.J., D. Schatz, V. Farstey, J.E. Ossolinski, H. Sabanay, S. Bendor, et al. 2014. Zooplankton may serve as transmission vectors for viruses infecting algal blooms in the ocean. *Curr. Biol.* 24(21):2592-2597.

Goldberg, A.R., C.J. Conway, D.E. Biggins. 2020. Flea sharing among sympatric rodent hosts: Implications for potential plague effects on a threatened sciurid. *Ecosphere* 11(2):e03033.

Gozzi, A.C., M. Lareschi, G. Navone, M.L. Guichon. 2020. The enemy release hypothesis and *Callosciurus erythraeus* in Argentina: Combining community and biogeographical parasitological studies. *Biol. Invasions*. 22(12):3519-3531.

Grundmann, A.W., J.C. Frandsen. 1960. Definitive host relationships of the helminth parasites of the deer mouse, *Peromyscus maniculatus*, in the Bonneville Basin of Utah. *J. Parasitol.* 46(6):673-677.

Hatcher, M.J., J.T. Dick, A.M. Dunn. 2008. A keystone effect for parasites in intraguild predation? *Biol. Lett.* 4(5):534-537.

Hatcher, M.J., J.T. Dick, A.M. Dunn. 2012. Diverse effects of parasites on ecosystems: Linking interdependent processes. *Front. Ecol. Environ.* 10(4):186-194.

Hawlena, H., Z. Abramsky, B.R. Krasnov. 2006. Ectoparasites and age-dependent survival in a desert rodent. *Oecologia* 148:30-39.

Heeb, P., M. Kolliker, H. Richner. 2000. Bird-ectoparasite interactions, nest humidity, and ectoparasite community structure. *Ecology* 81(4):958-968.

Hillegass, M.A., J.A. Waterman, J.D. Roth. 2010. Parasite removal increases reproductive success in a social African Ground Squirrel. *Behav. Ecol.* 21:696-700.

Hope, A.G., S.E. Greiman, V.V. Tkach, E.P. Hoberg, J.A. Cook. 2016. Shrews and their parasites: Small species indicate big changes. *Arctic Report Card* 81-91.

Hopla, C.E. 1955. The multiplication of tularemia organisms in the Lone Star tick. *Am. J. Hyg.* 61:371-380.

Howell, J.F. 1955. A study of the aspectional variations of Siphonaptera associated with the nests of the Thomas wood rat *Neotoma lepida lepida* Thomas. *Great Basin Nat.* 15(1/4):35-49.

Howell, J.F., D.M. Allred, D.E. Beck. 1957. Seasonal population fluctuations of mites in desert wood rat nests in central Utah. *Ecology* 38(1):82-88.

Hudson, P.J., A.P. Dobson, K.D. Lafferty. 2006. Is a healthy ecosystem one that is rich in parasites? *Trends Ecol. Evol.* 21(7):381-5.

Jeffries, M.I., R.A. Miller, M.D. Laskowski, J.D. Carlisle. 2015. High prevalence of *Leucocytozoon* parasites in nestling Northern Goshawks (*Accipiter gentilis*) in the Northern Great Basin, U.S.A. *J. Raptor Res.* 49(3):294-302.

Cluever, B.M., D.T. Iles, E.M. Gese. 2019. Ectoparasite burden influences the denning behavior of a small desert carnivore. *Ecosphere* 10(5):e02749.

Krasnov, B.R., S. Morand, I.S. Khokhlova, G.I. Shenbrot, H. Hawlena. 2005. Abundance and distribution of fleas on desert rodents: linking Taylor's power law to ecological specialization and epidemiology. *Parasitol.* 131:825-837.

Kwak, M. L., A.C.G. Heath, R.L. Palma. 2019. Saving the Manx shearwater flea *Ceratophyllus (Emmareus) fionnus* (Insecta: Siphonaptera): The road to developing a recovery plan for a threatened ectoparasite. *Acta Parasitol.* 64(4):903-910.

Lancet Infections Diseases. Dare we dream of the end of malaria? 2020. *Lancet Infect. Dis.* 20(1):1.

McCallum, H., A. Dobson. 1995. Detecting disease and parasite threats to endangered species and ecosystems. *Trends Ecol. Evol.* 10(5):190-194.

Marcogliese, D.J., D.K. Cone. 1997. Food webs: a plea for parasites. *Trends Ecol. Evol.* 12(8):320-325.

Matchett, M.R., D.E. Biggins, V. Carlson, B. Powell, T. Rocke. 2010. Enzootic plague reduces black-footed ferret (*Mustela nigripes*) survival in Montana. *Vector Borne Zoonotic Dis.* 10:27-35.

Matthee, S., M. Swanepoel, L. Van der Mescht, A.J. Leslie, L.C. Hoffman. 2013. Ectoparasites of a non-indigenous warthog population, *Phacochoerus africanus*, in the Free State Province, South Africa. *Afr. Zool.* 48(2):259-265.

May, R.M. 1977. Thresholds and breakpoints in ecosystems with a multiplicity of stable states. *Nature* 269(5628):471-477.

Mazgajski, T.D., A.H. Kedra, E. Modlinska, J. Samborski. 1997. Fleas (Siphonaptera) influence the condition of starling *Sturnus vulgaris* nestlings. *Acta Ornithol.* 2(32):185-190.

Medvedev, S.G., N.T. Dokuchaev, K.A. Tretyakov, A.V. Yamborko. 2014. Fleas of small mammals from the north of the Russian Far East. *Entomol. Rev.* 94(9):1288-1296.

Mlynarek, J.J. 2015. Testing the enemy release hypothesis in a native insect species with an expanding range. *Peer J.* 3:e1415.

Neuhaus, P. 2003. Parasite removal and its impact on litter size and body condition in Columbian Ground Squirrels (*Spermophilus columbianus*). *Proc. Royal Soc. London B* 270:S213–S215.

O'Farrell, T.P. 1975. Small mammals, their parasites and pathologic lesions on the Arid Lands Ecology Reserve, Benton County, Washington. *Amer. Midl. Nat.* 93(2): 377-387.

Oppliger, A., H. Richner, P. Christe. 1994. Effect of an ectoparasite on lay date, nest-site choice, desertion, and hatching success in the Great Tit (*Parus major*). *Behav. Ecol.* 5:130–134.

Pape, R.B. 2014. Biology and ecology of Bat Cave, Grand Canyon National Park, Arizona. *J. Caves Karst Stud.* 76(1):1–13.

Pojmariska, T. 2002. Parasites as a natural element of any ecosystem. *Wiad. Parazytol.* 48(2):139-154.

Press, M.C., G.K. Phoenix. 2005. Impacts of parasitic plants on natural communities. *New Phytol.* 166:737-751.

Robinson, R.A. 1987. Host management in crop pathosystems. Macmillan, New York.

Rendell, W.B., N.A.M. Verbeek. 1996. Old nest material in nestboxes of Tree Swallows: effects on reproductive success. *Condor* 98:142–152.

Richner, H., A. Oppliger, P. Christe. 1993. Effect of an ectoparasite on reproduction in Great Tits. *J. Anim. Ecol.* 62:703–710.

Richner, H., F. Tripet. 1999. Ectoparasitism and the trade-off between current and future reproduction. *Oikos* 86:535–538.

Roth, J.D., S. Dobson, F. Criscuolo, P. Uhlrich, A. Zahariev, A. Bergouignan, V.A. Viblanc. 2019. Subtle short-term physiological costs of an experimental augmentation of fleas in wild Columbian ground squirrels. *J. Exp. Biol.* 222(12):jeb203588.

Rozsa, L., Z. Vas. 2015. Co-extinct and critically co-endangered species of parasitic lice, and conservation-induced extinction: Should lice be reintroduced to their hosts? *Oryx* 49(1):107-110.

Schmidt, N. 2016. Parasitic plants and community composition: how *Castilleja levisecta* affects, and is affected by, its community. PhD diss., University of Washington, Seattle, Washington.

Slomczyński, R., A. Kaliński, J. Wawrzyniak, M. Bańbura, J. Skwarska, P. Zieliński, J. Bańbura. 2006. Effects of experimental reduction in nest micro-parasite and macro-parasite loads on nesting hemoglobin level in Blue Tits *Parus caeruleus*. *Acta Oecol.* 30:223–227.

Small, E. 2019. In defence of the world's most reviled invertebrate 'bugs.' *Biodiversity* 20(4):168-221.

Smith, A., S. Telfer, S. Burthe, M. Bennett, M. Begon. 2005. Trypanosomes, fleas and field voles: ecological dynamics of a host-vector-parasite interaction. *Parasitology* 131(3):355-365.

Sponchiado, J., G.L. Melo, T.F. Martins, F.S. Krawczak, F.C. Jacinavicius, M.B. Labruna, et al. 2017. Ectoparasites of small-mammals: Determinants of community structure in South American savannah. *Parasitology* 144:475–483.

Telfer, S., K.J. Brown, R. Sekules, I. Begon, T. Hayden, R. Birtel. 2005. Disruption of a host-parasite system following the introduction of an exotic host species. *Parasitology* 130:661–665.

Tompkins, D.M, A.M. Dunn, M. J. Smith, S. Telfer. 2011. Wildlife diseases: from individuals to ecosystems. *J. Anim. Ecol.* 80:19-38.

van Ommeren, R.J., T.G. Whitham. 2002. Changes in interactions between juniper and mistletoe mediated by shared avian frugivores: parasitism to potential mutualism. *Oecologia* 130:281-288.

Veitch, J.S.M., J. Bowman, A.I. Schulte-Hostedde. 2020. Parasite species cooccurrence patterns on *Peromyscus*: Joint species distribution modelling. *IJP: Parasites Wildl.* 12:199–206.

Watson, M.J. 2013. What drives population-level effects of parasites? Meta-analysis meets life history. *IJP: Parasites Wildl.* 2:190–196.

Whitaker, Jr., J.O., N. Wilson. 1974. Host and distribution lists of mites (Acari), parasitic and phoretic, in hair of wild mammals of North America, north of Mexico. *Am. Midland Nat.* 1-67.

Wilson D.S., E.O. Wilson. 2007. Rethinking the theoretical foundation of sociobiology. *Q. Rev. Biol.* 82:327–348.

Wilson, E.O. 2016. *Half-Earth: our planet's fight for life.* Liveright, New York.

Zwolak, R., S. Meagher, J.W. Vaughn, S. Dziemian, E.E. Crone. 2013. Reduced ectoparasite loads of deer mice in burned forest: From fleas to trees? *Ecosphere* 4:1-10.

Electric Hand Dryers Serve as Reservoirs for Antibiotic-Resistant Bacteria

Ashlynd Greenwood, Colette Mortensen, Michele Culumber, and Craig Oberg
Weber State University

Abstract

Electric hand dryers, particularly jet air hand dryers, have been installed in most restrooms on the Weber State University campus to improve convenience and decrease paper waste. Hand dryer manufacturers claim they provide a more hygienic method of hand drying, yet previous research has shown they can act as a reservoir for pathogenic bacteria. The purpose of this experiment was to isolate bacteria from hand dryers, characterize their antibiotic-resistance profiles, and then identify these bacteria. Hand dryers from 32 high-traffic restrooms (16 men's and 16 women's) from four buildings at Weber State University were sampled. A 25-cm² area at the bottom of the drying chamber inside of the hand dryer was sampled using 3M Quikswabs. Swabs were used to inoculate selective and nonselective media, which were incubated at 37°C for 24-48 h. A total of 72 isolates were selected based on unique colony morphology for further characterization. Individual isolates were transferred to tryptic soy broth, grown at 37°C for 24 h, and then screened for resistance to five antibiotics (ampicillin, vancomycin, tetracycline, penicillin, and

chloramphenicol) using the Kirby-Bauer method. Isolates that showed antibiotic resistance were identified using 16S rRNA gene sequence analysis. Forty-five isolates showed resistance to one or more antibiotics (Ant^r), with 42 resistant to at least two of the five antibiotics. The majority of isolates were resistant to penicillin and/or ampicillin, with several isolates resistant to vancomycin. The most numerous penicillin-resistant isolates were common human commensal Staphylococcus sp. including, S. warneri, S. intermedius, S. saprophyticus, and S. aureus. Also identified were representatives of some environmental bacteria including Bacillus pumilus, B. velezensis, and B. subtilis. Less common were gram-negative bacteria such as Enterobacter hormaechei and Mixta calida. All species identified have the potential to cause opportunistic infections. There was no significant difference ($p=0.81$) between the number of antibiotic-resistant strains found in men's and women's bathrooms; however, there was a significant difference ($p<0.001$) in the number of Ant^r isolates found in the different models of dryer. There were more Ant^r colonies in the Mediclinics Dualflow Plus (mean=11.5, SD=2.12, n=2) than in the Dyson Airblade (mean=3.67, SD=1.21, n=6) hand dryers ($t(6)=6.83$, $p<0.0005$). We have shown that antibiotic-resistant bacteria are present in electric hand dryers and may represent a significant source of community-acquired antibiotic-resistant infections. To prevent bacterial contamination and the spread of antibiotic-resistant bacteria during hand drying, the hand dryer's inner chamber should be thoroughly cleaned with a disinfectant on a daily basis.

Introduction

Electric hand dryers, specifically jet air hand dryers, have been installed across Weber State University (WSU)'s campus in an attempt to decrease emissions, reduce paper waste, and create a more environmentally friendly campus. Public restrooms play an underappreciated role in waste generation and greenhouse gas emissions, particularly through the use of paper towels as a drying method. The use of paper towels can also have greater environmental and economic effects for public institutions (Coller et al., 2021), such as WSU. During the Covid-19 pandemic, the general public preferred the use of electric hand dryers over paper because of expressed concerns about contacting SARS-CoV-2 when touching surfaces in public restrooms (Marcenac et al., 2021).

Despite the environmental and economic benefits of electric hand dryers, the inside of the electric hand dryer chamber can act as a reservoir

for pathogenic bacteria (Ma 2021; Nichols et al., 2021). Not only do these hand dryers serve as a reservoir for bacteria, but bacteria can also be emitted when the air dryer is in use, contaminating the air in the restroom (Snelling et al., 2010; Margas et al., 2013; Best et al., 2014, 2018). It has been shown that warm air dryers can deposit pathogenic bacteria onto the hands of users and produce aerosols with the potential to be inhaled (Ansari et al., 1991; Mutters and Warnes, 2019; Reynolds et al., 2020). Alharbi et al. (2016) found the total microbial count on public restroom floors where electric hand dryers were installed was 4.44×10^5 cfu/100 cm² higher than in public restrooms without electric hand dryers. These results show that electric hand dryers produce aerosolized water droplets that can spread greater distances when in contact with the air stream of a hand dryer. Dawson et al. (2016) conducted three experiments to determine the degree to which electric hand dryers spread bacteria and found that electric hand dryers in public restrooms could transfer up to 238 CFU more microorganisms than paper towels per cycle, with 58 CFU transferred on average per use.

Community-acquired infections are infections contracted outside of hospital care and in community settings. Common community-acquired infections include *Staphylococcus aureus* (including methicillin-resistant *S. aureus* (MRSA)), *Streptococcus pneumoniae*, *Streptococcus pyogenes*, *Neisseria meningitidis*, *Salmonella* species, *Campylobacter* species, and *Escherichia coli* (Peyrani et al., 2019). Community-acquired infections can be problematic because these bacteria develop defense strategies and resistance mechanisms against antibiotics (O'Neill, 2016). Antibiotic resistance is a naturally occurring process accelerated by the increased use of antibiotics in modern medicine (Garau et al., 2014). Bacteria can evolve resistance mechanisms to antibiotics and can even become resistant to multiple antibiotics. Community-acquired MRSA and *Clostridioides difficile* are excellent examples of multiple antibiotic-resistant organisms resulting from this phenomenon (Lai et al., 2022).

In public restrooms, antibiotic-resistant bacteria are a concern for community-acquired infections, opportunist microorganisms, and MRSA (Suen et al., 2019). It has also been suggested that public restrooms are sources of these infectious diseases because they have the potential to sustain bacterial resistomes (Mkrtchyan et al., 2013). Their study identified 19 different *Staphylococcal* strains from isolates of 18 toilet sites and found that 37.8% were antibiotic resistant.

The objective with this study was to isolate and identify bacteria in the electric hand dryers on the WSU campus, determine their resistance to five common antibiotics (ampicillin, tetracycline, vancomycin,

penicillin, and chloramphenicol), and evaluate the distribution of these antibiotic-resistant organisms in men's and women's restrooms.

Methods

Sampling Locations

To obtain a representative sample, hand dryers in men's and women's restrooms were swabbed in four buildings at WSU (Ogden, Utah, USA; Figure 1). In one building, Tracy Hall, Mediclinics Dualflow Plus hand dryers (Mediclinics S.A., Barcelona, Spain) are used, whereas Dyson Airblade hand dryers (Dyson Inc., Chicago, Illinois, USA) are used in the other three buildings sampled, Stewart Library, Lindquist Hall, and Shepherd Union. Differences in the number of antibiotic-resistant strains found were compared between men's and women's restrooms and between types of hand dryers using a two-tailed t-test.



Figure 1. Map of Weber State University (WSU) Campus, Ogden, Utah, USA. Sampling locations on WSU Campus are designated in red circles. LH: Lindquist Hall, LI: Stewart Library, SU: Shepherd Union Building, TY: Tracy Hall Science Center.

Swabbing Protocol

Bacterial samples were collected from hand dryers using sterile 3M Quickswabs (3M Microbiology, St. Paul, Minnesota, USA). A 25-cm² surface area in the hand dryer's interior chamber where hands are placed to allow for drying was sampled by rolling the sterile moist swab over a 5 × 5-cm square in the lower one-third of the drying chamber. The swab was returned to the container containing 1 mL of sterile Lethen broth and later vortexed for 30 sec to dislodge the bacteria from the swab into the broth.

Bacterial Isolation Method

For each sample, 0.1 ml of the Lethen broth was spread, with a sterile spreader, on Petri plates containing tryptic soy agar (TSA) (Hardy Diagnostics, Santa Maria, California, USA) as a nonspecific medium, sheep blood agar (SBA) (Hardy Diagnostics) to differentiate *Streptococcus* species based on hemolysis, eosin methylene blue agar (EMB) (Hardy Diagnostics) to select for and detect coliforms, or mannitol salt agar (MSA) (Hardy Diagnostics) for selective isolation of *Staphylococcus* species, especially *S. aureus*.

Plates were incubated at 37°C for 48 h to propagate individual isolates from the hand dryer samples. Colony morphologies were noted, and individual colonies with unique morphologies were transferred to sterile tryptic soy broth (TSB) with a sterile loop and incubated at 37°C for 48 h. Quadrant streak plates were then done on TSA to confirm each isolate was a pure culture, primarily by examination of colony morphology.

Antibiotic Resistance Testing

Once isolates were determined to be pure cultures, isolates were tested for antibiotic resistance using the Kirby-Bauer method (Hudzicki, 2009). This was done by swabbing a 24-h TSB culture on a TSA plate in two directions to create a bacterial lawn. Antibiotic disks were then placed evenly spaced on the plate. Antibiotics tested were ampicillin (AM10, 10 µg), vancomycin (Va30, 30 µg), tetracycline (Te30, 30 µg), penicillin (P10, 10 µg), and chloramphenicol (C30, 30 µg) (Hardy Diagnostics). After the plate was incubated for 24-48 h at 37°C, the diameter of inhibition zones was measured in mm to determine antibiotic resistance. The size of the zones was compared with standard diameters published by the Clinical and Laboratory Standards Institute (Wayne, Pennsylvania, USA) to determine antibiotic resistance or sensitivity according to the manufacturer's protocols (Table 1).

Table 1. Zones of inhibition standards (in mm) for the Kirby-Bauer method to determine isolates' antibiotic resistance			
Antibiotic	Resistant	Intermediate	Susceptible
Ampicillin (<i>Staphylococcus</i>)	≤28	-	≥29
Ampicillin (AM-10*) (other)	≤13	14–16	≥17
Chloramphenicol (C-30*)	≤12	13–17	≥18
Penicillin (P-10*)			
<i>Staphylococcus</i>	≤28	-	≥29
<i>Enterococcus</i>	≤14	-	≤15
β-hemolytic <i>Streptococcus</i>	≤14	15–23	≤24
Tetracycline (Te-30*)			
<i>Streptococcus</i>	≤18	19–22	≥23
<i>Staphylococcus</i>	≤14	15–18	≥19
<i>Enterobacteriaceae</i>	≤11	12–14	≥15
Vancomycin (Va-30*)	≤14	15–16	≥17

*Concentration in micrograms (µg)

16S rRNA Analysis of Isolates

The 16S rRNA gene was sequenced from a random selection of 45 isolates. DNA was extracted from the isolates using the Qiagen DNeasy PowerLyzer Microbial Kit (Hilden, Germany). DNA was quantified using a NanoDrop Lite UV spectrophotometer (Fisher Scientific, Waltham, Massachusetts, USA). The 16S rRNA gene was amplified using bacteria-specific primers (27F 5'-AGAGTTTGATCMTGGCT CAG 3'/1419R 5' ACGGYTACCTTGTTACGACTT 3' (Lane 1991)). PCR cycle conditions were 94°C for 3 min followed by 25 cycles of 94°C for 45 sec, 50°C for 1 min, and 72°C for 2 min. The final extension was at 72°C for 3 min. Each reaction contained 1X GoTaq Green MasterMix (Promega, Madison, Wisconsin, USA), 200 nM of each primer, and 2 µL of DNA template. PCR product was purified using the E.Z.N.A Cycle Pure PCR clean up kit (Omega Bio-Tek, Norcross, Georgia, USA). Sequencing was done at the Molecular Research Core Facility at Idaho State University (Pocatello, Idaho, USA). Assembled full sequences were compared with the NCBI database using the BLAST function.

Results and Discussion

Bacterial Isolation

Two electric hand dryers were sampled from 16 high-traffic restrooms (8 men's and 8 women's) located in four buildings (circled in Figure 1). Tracy Hall, Lindquist Hall, the Student Union Building, and

Stewart Library were chosen based on the high volume of students that use these facilities during an average school day (observational data, not shown). Researchers hoped to obtain a representative sample of microorganisms across the campus by sampling hand dryers in these high-traffic areas. A previous survey of the microbial load in hand driers at WSU found the highest bacterial concentrations were in the Mediclinics Dualflow hand dryers, especially those in the Tracy Hall Science Center and the Student Union (Nichols et al., 2021).

Seventy-two isolates were selected for further characterization. Organisms were selected from each building and each restroom and from most of the selective media. Many isolates were selected based on characteristics suggesting they were either hemolytic organisms (SBA), coliforms (EMB), or *Staphylococcus* (MSA), and a variety of colony morphology isolates were selected from TSA.

Antibiotic Resistance Testing

Only 27 of the 72 selected isolates were sensitive to all five test antibiotics (Figure 2). Four isolates were resistant to one antibiotic, and 41 isolates exhibited antibiotic resistance to two or more antibiotics. More than 90% of the antibiotic-resistant isolates (Ant^r) were resistant to two or more antibiotics, with 23 isolates resistant to two antibiotics, 15 resistant to three antibiotics, and 3 resistant to all five antibiotics (Figure 2). The three isolates resistant to all five antibiotics were collected from Tracy Hall women's restrooms, and all initially were isolated from EMB, indicating they were gram-negative bacteria. Two were identified as *Enterbacter hormanchedi* and one as *Mixta calida*.

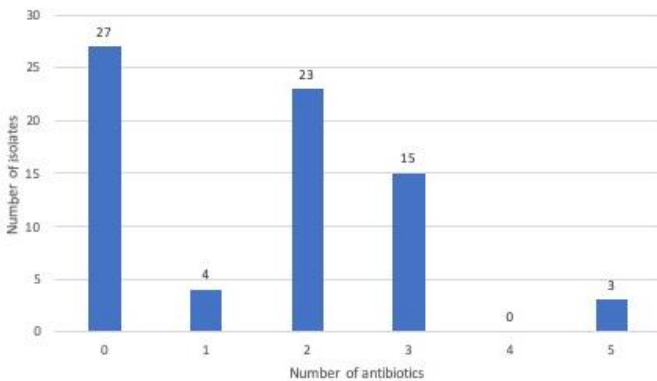


Figure 2. Frequency of resistance to different antibiotics. Of 72 isolates tested with the Kirby-Bauer method (Hudzicki, 2009), 62% were resistant to at least one antibiotic and 4% (3 colonies) were resistant to all of the antibiotics tested.

Of the 45 Ant^r isolates (out of 72 total isolates), the majority of the isolates were resistant to ampicillin (39 isolates) and penicillin (38 isolates). Fewer isolates were resistant to tetracycline (15 isolates), and there were only 8 chloramphenicol-resistant isolates and 6 vancomycin-resistant isolates (Figure 3). Because penicillin and ampicillin have the same cellular targets for growth inhibition, this is to be expected.

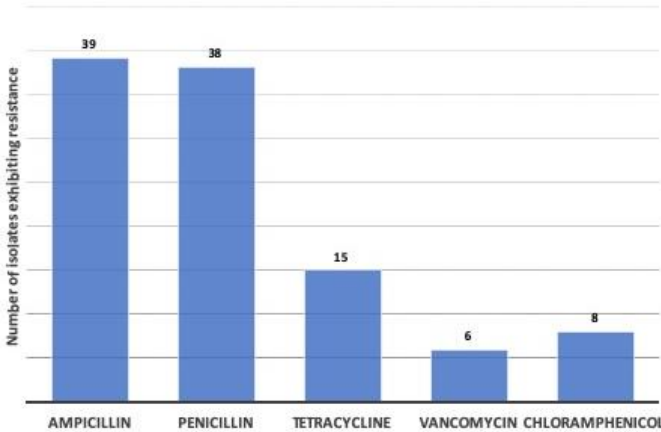


Figure 3. Frequency of isolates for each antibiotic. Forty-five of 72 isolates tested using the Kirby-Bauer method (Hudzicki, 2009) were resistant to at least one antibiotic. Most of the organisms were resistant to ampicillin and penicillin.

Penicillin stops bacterial growth by inhibiting the transpeptidase that catalyzes cell wall biosynthesis, which cross-links polymers during peptidoglycan synthesis. Ampicillin, commonly known as a broad-spectrum penicillin, also interferes with cell wall peptidoglycan synthesis. Organisms resistant to penicillin and ampicillin generally have the capability to secrete β -lactamases or have low-affinity penicillin-binding proteins (Lai et al., 2022). Chloramphenicol, which has a range of activity across gram-negative and gram-positive bacteria, inhibits bacterial protein synthesis by binding to the bacterial ribosomes, inhibiting peptide bond formation and protein synthesis. Tetracycline acts by inhibiting the 30S ribosomal subunit, hindering its ability to bind the aminoacyl-tRNA to the acceptor site on the mRNA complex. Vancomycin, which is most effective against gram-positive bacteria, is a glycopeptide that binds to D-alanyl D-alanine and inhibits peptidoglycan synthesis, preventing the polymerization of the peptidoglycan subunits (Lai et al., 2022).

Overall, the number of Ant^r isolates identified in the women's restrooms (mean=6.0, SD=4.7, n=4) and men's restrooms (mean=5.25, SD=3.40, n=4) were not significantly different ($t(6)=-0.26$, $p=0.81$) (Figure 4). Of the 45 total Ant^r isolates, 21 were obtained from the men's restrooms, while women's restrooms yielded 24 Ant^r isolates. The Tracy Hall Science center had the highest number of Ant^r isolates, 13 in the women's and 10 in the men's. A study by Flores et al. (2011) found that while there was no significant difference in the overall number of bacteria between gendered restrooms, there were variations in taxon. Female restrooms had more vagina-associated *Lactobacillaceae*, which are commonly found in the urine of reproductive-aged women (Flores et al., 2011). In another study by the Cleaning Industry Research Institute (Kennedy et al., 2007), women's restrooms had more bacteria than men's restrooms at a rate of two to one. They also found that female restrooms were three times more likely to be contaminated with *E. coli* than male restrooms.

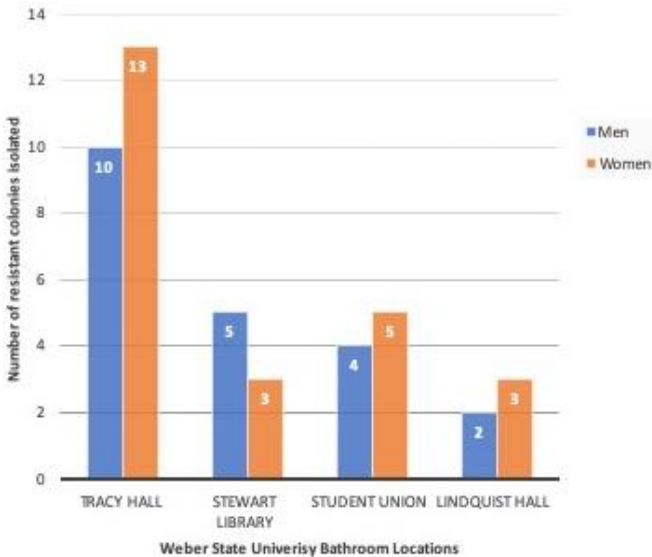


Figure 2. Antibiotic-resistant isolates found in the bathrooms tested at WSU by the Kirby-Bauer method (Hudzicki, 2009). Antibiotic-resistant isolates were found in all of the bathrooms tested. No significant difference ($p=0.81$) was found between men's and women's bathrooms. Tracy Hall had significantly more resistant isolates than the other locations ($p<0.001$), indicating that the type of hand drier may play an important role in harboring bacteria.

There was a significant difference in the number of Ant^r isolates found in the different models of dryer, with more Ant^r colonies in the Mediclinics Dualflow Plus hand dryers (mean=11.5, SD=2.12, n=2) than in the Dyson Airblade hand dryers (mean=3.67, SD=1.21, n=6, t(6)=6.83, $p<0.0005$). Although our sampling size was small, the difference could be due to the ways that excess water drains from the systems. We noticed that more water appears to accumulate in the Dualflow dryers, creating an environment that may favor the growth of bacteria.

16S rRNA identification of Ant^r isolates

Forty-one of the 72 isolates were identified using 16S rRNA gene analysis (Table 2). Forty-five isolates were sequenced, but three had poor-quality sequence data. Interestingly, 80% of the identified isolates were from the genus *Staphylococcus* even though they were not all isolated from the MSA medium. Ten percent were identified as the coliform *Enterobacter hormaechei* in the Enterobacteriaceae family. A single isolate of *M. calida* (formerly *Pantoea calida*), a member of the *Erwiniaceae*, was also found. Seven percent of the identified isolates belonged to the genus *Bacillus*. All of the isolates identified have the potential for opportunistic infections.

The most common Ant^r isolates were gram-positive human commensal *Staphylococcus* species including *S. warneri*, *S. intermedius*, *S. saprophyticus*, *S. epidermidis*, and *S. aureus* (Table 2). *S. epidermidis* is among the most common causes of nosocomial infections in the United States, which can lead to severe complications in compromised individuals. *S. epidermidis* is generally harmless when naturally occurring, but it can be an opportunistic pathogen once it invades the human body through prosthetics or medical devices such as prosthetic valves, cardiac devices, catheters, and intravenous drug equipment (Gomes et al., 2013). *S. aureus* can cause a wide variety of infections and is acquired either as a community-acquired infection or in hospital settings. MRSA is a strain of *S. aureus* that can cause a challenging and life-threatening infection because of its resistance to multiple antibiotics. *S. saprophyticus* is recognized as the most common cause of coagulase-negative urinary tract infection (Lawal et al., 2021).

We also found representatives of environmental gram-positive *Bacillus* sp., including *Bacillus pumilus*, *B. velezensis* and *B. subtilis*. *B. velezensis* is an endospore-forming bacterium that supports plant growth (Rabbee et al., 2019). All of the *Bacillus* species found can be opportunistic pathogens.

Relatively few gram-negative bacteria were identified. The genus *Enterobacter* represents a group of diverse opportunistic pathogens that

Table 2. Species identification and antibiotic resistance of selected hand dryer isolates using 16S rRNA sequencing				
Isolate	Gram reaction	No.*	Isolation medium	Antibiotic resistance
Staphylococcus warneri	Gr+	9	MSA	Tetracycline
Staphylococcus epidermidis	Gr+	8	TSA	Ampicillin, penicillin, vancomycin
Enterobacter hormaechei	Gr-	4	EMB	Ampicillin, penicillin, chloramphenicol, tetracycline, vancomycin
Staphylococcus hominis	Gr+	4	TSA	Ampicillin, penicillin
Staphylococcus aureus	Gr+	3	MSA	Ampicillin, penicillin, vancomycin
Staphylococcus intermedius	Gr+	3	SBA	Ampicillin, penicillin
Staphylococcus saprophyticus	Gr+	2	TSA	None
Staphylococcus pasteurii	Gr+	2	TSA	Ampicillin, penicillin
Staphylococcus capitis	Gr+	2	MSA	Ampicillin, penicillin, tetracycline
Bacillus pumilis	Gr+	1	SBA	None
Bacillus subtilis	Gr+	1	TSA	Ampicillin, penicillin, tetracycline
Bacillus velezensis	Gr+	1	SBA	Ampicillin, penicillin, tetracycline
Mixta calida	Gr-	1	EMB	Ampicillin, penicillin, chloramphenicol, tetracycline, vancomycin

*Number of isolates that were identified for this genus and species.

MSA, mannitol salt agar; TSA, tryptic soy agar; SBA, sheep blood agar; EMB, eosin methylene blue agar

often harbor multiple drug resistance genes and are involved in hospital-acquired infections (Davin-Regli et al., 2019). *E. hormanechei* is fairly widespread in the environment and has been shown to be a causative agent for nosocomial infections (Kamathewatta et al., 2020). *M. calida* is a widespread gram-negative bacterium. It has been isolated from

diverse animal and plant environments (Palmer et al., 2018). In other studies, it has demonstrated significant antibiotic resistance, especially when cultured aerobically (Kovale et al., 2021).

Conclusions

These results show that electric hand dryers can serve as a microbial reservoir for antibiotic-resistant bacteria. Most of the organisms found in this study were of human origin and have potential to be human pathogens. Cleaning and maintaining the hand dryers on a regular basis could decrease the risk of exposure and infection. By frequent and regular decontamination, we could see a lower rate of spread to the community by these opportunists and community pathogens. Although paper towels generate a significant amount of waste, they may be better at preventing the spread of pathogens in public restrooms. Amid the SARS-CoV-2 pandemic, these efforts could also be incredibly beneficial to decrease the spread not only of everyday microorganisms, but the epidemics and pandemics our community and the students at WSU will face today and in the future.

Acknowledgments

Thank you to Microbiology Lab Manager, Karen Mann, and Weber State's Microbiology Department.

References

- Alharbi, S.A., S.H. Salmen, A. Chinnathambi, N.S. Alharbi, M. Zayed, B.O. Al-Johny, M. Wainwright. 2016. Assessment of the bacterial contamination of hand air dryer in washrooms. *Saudi J Biol Sci* 23:268-271. doi: 10.1016/j.sjbs.2015.06.020
- Ansari, S.A., V.S. Springthorpe, S.A. Sattar, W. Tostowaryk, G.A. Wells. 1991. Comparison of cloth, paper, and warm air drying in eliminating viruses and bacteria from washed hands. *Am J Infect Control* 19:243-249. doi: 10.1016/s0196-6553(05)80256-1
- Best, E., P. Parnell, M. Wilcox. 2014. Microbiological comparison of hand-drying methods: the potential for contamination of the environment, user, and bystander. *J Hosp Infect* 88:199-206. doi: 10.1016/j.jhin.2014.08.002

Best, E., P. Parnell, J. Couturier, F. Barbut, A. Le Bozec, L. Arnoldo, et al. 2018. Environmental contamination by bacteria in hospital washrooms according to hand-drying method: a multi-centre study. *J Hosp Infect* 100:469-475. doi: 10.1016/j.jhin.2018.07.002

Coller, G., M Schiavon, M. Ragazzi. 2021. Environmental and economic sustainability in public contexts: the impact of hand-drying options on waste management, carbon emissions, and operating costs. *Environ Dev Sustain* 23:11279-11296. doi: 10.1007/s10668-020-01109-x

Davin-Regli, A., J.-P. Lavigne, J.-M. Pagès. 2019. *Enterobacter* spp.: update on taxonomy, clinical aspects, and emerging antimicrobial resistance. *Clin Microbiol Rev* 32(4):e00002. doi: 10.1128/CMR.00002-19

Dawson, P., J. Northcutt, M. Parisi, I. Han. 2016. Bioaerosol formation and bacterial transfer from commercial automatic hand dryers. *J Food Microbiol Saf Hyg* 1:108. doi: 10.4172/jfmsh.1000108

Flores, G.E., S.T. Bates, D. Knights, C.L. Lauber, J. Strombaugh, R. Knight, N. Fierer. 2011. Microbial biogeography of public restroom surfaces. *PLoS ONE* 6(11): e28132. doi: 10.1371/journal.pone.0028132

Garau, J., D.P. Nicolau, B. Wullt, M. Bassetti. 2014. Antibiotic stewardship challenges in the management of community-acquired infections for prevention of escalating antibiotic resistance. *J Glob Antibiot Resist* 2:245-253. doi: 10.1016.jgar.2014.08.002

Gomes, F., P. Teixeira, R. Oliveira. 2013. Mini-review: *Staphylococcus epidermidis* as the most frequent cause of nosocomial infections: old and new fighting strategies. *J Bioadhes Biofilm Res* 30:131-141. doi: 10.1080/08927014.2013.848858

Hudzicki, J. 2009. Kirby-Bauer disk diffusion susceptibility test protocol. *American Society for Microbiology*. Retrieved August 22, 2022, from <https://asm.org/Protocols/Kirby-Bauer-Disk-Diffusion-Susceptibility-Test-Pro>

Kamathewatta, K., R. Bushell, F. Rafa, G. Browning, H. Billman-Jacobe, M. Marena. 2020. Colonization of a hand washing sink in a veterinary hospital by an *Enterobacter hormaechei* strain carrying multiple resistances to high importance antimicrobials. *Antimicrob Resist Infect Control* 9:163. doi: 10.1186/s13756-020-00828-0

Kennedy, D.I., C.E. Enriquez, C.P. Gerba. 2007. Enteric bacterial contamination of public restrooms. CIRI Cleaning Industry Research Institute. Retrieved July 5, 2022 from <https://ciriscience.org/ieq-measurement/enteric-bacterial-contamination-of-public-restrooms/>

Kovale, L., Y.S., Nimonkar, S.J. Green, Y.S. Shouche, O. Prakash. 2021. Antibiotic susceptibility of human gut-derived facultative anaerobic bacteria is different under aerobic versus anaerobic test conditions. *Microbes Infect* 23: 9-10:104847. doi: 10.1016/j.micinf.2021.104847

Lane D.J. 1991. 16S/23S rRNA sequencing. In Stackebrandt E., Goodfellow, M. (eds.), *Nucleic Acid Techniques in Bacterial Systematics*, pp. 115-175. John Wiley & Sons, New York.

Lai, C.K.C., R.W.Y. Ng, S.S.Y. Leung, M. Hui, M. Ip. 2022. Overcoming the rising incidence and evolving mechanisms of antibiotic resistance by novel drug delivery approaches – An overview. *Adv Drug Deliv Rev* 181:114078. doi: 10.1016/j.addr.2021.114078

Lawal, O.U., M.J. Fraqueza, O. Bouchami, P. Worning, M.D. Bartels, M.L. Gonçalves, et al. 2021. Foodborne origin and local and global spread of *Staphylococcus saprophyticus* causing human urinary tract infections. *Emerg Infect Dis* 27:880-893. doi: 10.3201/eid2703.200852.

Ma, J.J. 2021. Blowing in the wind: Bacteria and fungi are spreading from public restroom hand dryers. *Arch Environ Occup Health* 76:52-60. doi: 10.1080/19338244.2020.1799183

Marcenac, P., S. Kim, N.A. Molinari et al. 2021. Knowledge, attitudes and practices around hand drying in public bathrooms during the COVID-19 pandemic in the United States. *Am J Infect Control* 49:1186-1188. doi: 10.1016/j.ajic.2021.03.021

Margas, E., E. Maguire, C.R. Berland, F. Welander, J.T. Holah. 2013. Assessment of the environmental microbiological cross contamination following hand drying with paper hand towels or an air blade dryer. *J Appl Microbiol* 115:572-582. doi: 10.1111/jam.12248

Mkrtchyan, H. V., C. A. Russell, N. Wang, and R. R. Cutler. 2013. Could public restrooms be an environment for bacterial resistomes? *PLoS ONE* 8(1): e54223. doi: 10.1371/journal.pone.0054223

Mutters, R. and S. L. Warnes. 2019. The method used to dry washed hands affects the number and type of transient and residential bacteria remaining on the skin. *J Hosp Infect* 101:408-413. doi: 10.1016/j.jhin.2018.12.005

Nichols, R., H. Packard, M. Culumber, C. Oberg. 2021. Electric hand dryers serve as a microbial reservoir for contamination. *Journal of the Utah Acad Sci Arts Letts* 97:65-77

O'Neill, J. 2016. Tackling drug-resistant infections globally: Final report and recommendations. *The Review on Antimicrobial Resistance*. Retrieved August 22, 2022, from <https://amr-review.org/Publications.html>

Palmer, M., E.T. Steenkamp, M.P.A. Coetzee, J.R. Avontuur, W. Chan, E. van Zyl, et al. 2018. *Mixta* gen. nov., a new genus in the *Erwiniaceae*. *Int J Syst Evol Microbiol* 68:1396-1407. doi: 10.1099/ijsem.0.002540

Peyrani, P., L. Mandell, A. Torres, G. S. Tillotson. 2019. The burden of community-acquired bacterial pneumonia in the era of antibiotic resistance. *Expert Rev Respir Med* 13:139-152. doi: 10.1080/17476348.2019.1562339

Rabbee, M.F., M.S. Ali, J. Choi, B.S. Hwang, S.C. Jeong, K.H. Baek. 2019. *Bacillus velezensis*: A valuable member of bioactive molecules within plant microbiomes. *Molecules* 24:1046. doi: 10.3390/molecules24061046

Reynolds, K., J. Sexton, A. Norman, D. McClelland. 2020. Comparison of electric hand dryers and paper towels for hand hygiene: A critical review of the literature. *J Appl Microbiol* 120:1-15. doi: 10.1111/jam.14796

Snelling, A., T. Saville, D. Stevens, C. Beggs. 2010. Comparative evaluation of the hygienic efficacy of an ultra-rapid hand dryer vs conventional warm air hand dryers. *J Appl Microbiol* 110:19-26. doi: 10.1111/j.1365-2672.2010.04838.x

Suen, L.K.P., G.K.H. Siu, Y.P. Gou, S.K.W. Yeung, K.Y.K. Lo, M. O'Donoghue. 2019. The public washroom—friend or foe? An observational study of washroom cleanliness combined with microbiological investigation of hand hygiene facilities. *Antimicrob Resist Infect Control* 8:47. doi: 10.1186/s13756-019-0500-z

One-Sample Survey of *Salinivibrio costicola* Strain-Specific Phage from the Great Salt Lake

Preston D. Capener, Joshua R. Mott, Matthew B. Crook, and Matthew J. Domek
Weber State University

Abstract

Bacteria growing in the Great Salt Lake (GSL) are halophilic in nature because of the high salt concentration and are represented by a large number of diverse species. Previous studies from this laboratory have led to the isolation of various phages that infect GSL halophiles, including Halomonas, Idiomarina, Salinivibrio, and Marinobacter. In this study, we collected a single sample from Bridger Bay in the GSL and plated it on three different halophilic media formulations. A unique bacterial isolate was recovered from each media formulation, which were named HB3, CB6, and TH4. Sequencing of the 16S rRNA gene of the three isolates revealed that they are all unique strains of the same species: Salinivibrio costicola. Concurrently, a portion of the water sample was centrifuged and filtered through a 0.2-micron filter for bacteriophage isolation. We challenged each bacterial isolate with the filtered water sample and measured growth on a plate reader at 25°C for 30 hours. An increase of absorbance, followed by a rapid decrease, was taken as evidence of the presence of a lytic phage. Three samples showed evidence of phage infection—one for each host. We recovered

phage lysates for each of these three samples and confirmed that they were lytic against the original host by performing spot tests. Remarkably, there was no cross-reactivity of phage infections among the three samples, revealing each phage as not only species-specific but strain-specific.

Introduction

The genus *Salinivibrio* is characterized as gram-negative, motile, catalase-positive, facultative anaerobic bacteria. These bacteria are typically isolated from saline environments, such as salty foods or extreme aquatic habitats. *Salinivibrio costicola* was first identified on bacon rib meat (Smith, 1938), and further related species and strains have been identified around the world (de la Haba et al., 2019). The Great Salt Lake (GSL) supports the growth of a diverse group of halophilic bacteria including *Salinivibrio* (Weimer et al., 2009). The salinity of the GSL varies from 8% to >25%, because of a variety of environmental factors (Gwynn, 1996). Previous studies have identified bacteriophage that infect *Salinivibrio* species in the GSL (Savage et al., 2013; Shen et al., 2012). Bacteriophage play an important role in the ecology of the GSL, as they participate in nutrient cycles by releasing key compounds taken up by the bacteria (Sime-Ngando, 2014). Since the GSL has undergone significant changes in the depth of the lake and increased salinity, we sought to determine whether similar pairs of host bacteria and phage could be isolated using similar sampling techniques that were used in previous studies. In this study, we give a preliminary description of the bacterial host and associated phage that were found in this single sample.

Methods

Isolation of Halophilic Bacteria

A one-gallon water sample was obtained from the surface of Bridger Bay in the GSL, about 20 feet from the shoreline (41.049169 N, 112.259736 W), in November 2021. Spread plates were made from dilutions of water samples onto three separate agar formulations (HB, CB, TH; see **Table 1**), all supplemented with 8% NaCl. Isolates were selected based on unique colony morphology and restreaked to obtain pure cultures.

Table 1: Media formulations of three modifications of <i>Halobacterium</i> medium (Atlas, 1993) used to isolate bacteria from the GSL			
Ingredient	HB	CB	TH
NaCl	80.0	80.0	80.0
MgSO ₄ ·7H ₂ O	10.0	8.0	12.5
Casamino acids	5.0	5.0	2.5
KCl	5.0	2.0	—
Disodium citrate	3.0	3.0	1.5
KNO ₃	1.0	—	—
Yeast extract	1.0	5.0	2.5
CaCl ₂ ·6H ₂ O	0.2	—	—
Proteose peptone	—	—	1.25
Pancreatic digest of casein	—	2.5	—
Sodium acetate	—	—	0.1
Agar	15.0	15.0	15.0

All amounts are in g/L, pH adjusted to 7.5 for each medium. The names of the formulations were chosen arbitrarily.

Identification of Phage and Bacteria Pairs

A portion of the water sample was centrifuged at 10,000×g for 5 minutes and filtered through a 0.2-micron filter. This filtrate served as a phage source. Another portion of the water sample was autoclaved. Using a 48-well plate, 200 μL of media was placed in a well, followed by 200 μL of the autoclaved GSL water. One μL of the bacteria culture was placed in the well. In the adjacent well, 200 μL of media and 200 μL of phage filtrate were placed, with 1 μL of the same bacterial isolate. This method was repeated for an additional 12 isolates. The autoclaved GSL water served as a control. The well plate was placed in a Tecan 200M Multimode plate reader at 30°C for 24 hours, and absorbance readings at 600 nm were obtained every 20 minutes. The two wells were then compared. Phage infection was identified by a steady growth followed by a rapid decline in absorbance. The wells indicating a phage infection were removed by syringe and filtered through a 0.2-micron filter. Phage spot plates were performed to confirm the phage infection of the bacterial isolates. Briefly, bacteria were added to molten top agar (10 g/L of agar), which was overlaid on the appropriate agar for that strain and allowed to solidify. An amount of 5 μl of phage was added to the surface of the top agar and incubated at 30°C overnight. The appearance of a plaque at the point of inoculation was taken as confirmation of infection.

Identification of Bacteria

DNA extractions of the bacterial isolates were performed using the Qiagen DNeasy UltraClean Microbial Kit and protocol. PCR was then performed on the DNA extracts for the 16S rRNA gene using primers oJG1035 (5' -ACTCCTACGGGAGGCAGCAGT-3') and oJG1036 (5' -TACGGTTACCTTGTTACGACTT-3'). The 16S rRNA amplifications were sent to Idaho State University's Molecular Research Core Facility (<https://www.isu.edu/mrcf/>) for sequencing. The resulting sequences were then submitted to BLASTn (<https://blast.ncbi.nlm.nih.gov/Blast.cgi>) and the RDP SeqMatch tool (http://rdp.cme.msu.edu/seqmatch/seqmatch_intro.jsp) for identification, with both analyses limited to comparisons with extant type material.

Propagation and Precipitation of Phage

Propagation and precipitation of phage is based on the protocol of Summer (2009). Briefly, five mL of overnight bacterial culture was added to a flask of 150 mL of media and incubated on a shaker at 30°C for 3 hours. Once slight turbidity was noted ($OD_{600} = \sim 0.2$), 50 μ L of phage was added to the flask and allowed to incubate for 21 hours on the shaker. Following the incubation period, if the flask was still turbid, chloroform solution was added to a final concentration of 2% and incubated 10 minutes. The contents were then centrifuged at 5000 $\times g$ for 10 minutes, and supernatants were filtered through a 0.2-micron filter. PEG-8000 was added to the filtrate at a ratio of 1:2 and gently mixed. The solution was then incubated at 4°C overnight.

Purification of Phage

The PEG-8000 and phage filtrate were centrifuged at 11,000 $\times g$ for 20 minutes. Supernatant was removed by pouring without disturbing the translucent pellet. A micropipette was used to remove the remaining liquid. The pellet was then resuspended in 500 μ L of STE buffer. One μ L was removed to measure titer levels. We then added 1 M $MgCl_2$ (12.5 μ L/mL) and mixed. Then, 1 μ L/mL of DNase (2000 U/mL) and RNase (100 mg/mL) were added to each suspension. The tubes were then incubated at 37°C for 30 minutes. Following the incubation, 0.5 M EDTA (40 μ L/mL), Proteinase K (10 mg/mL), and 10% SDS (50 μ L/mL) were all added. The solutions were then incubated at 55°C for 60 minutes, with mixing occurring every 20 minutes.

Phage DNA Extraction and Precipitation

In a chemical fume hood, we added phenol-chloroform-isoamyl alcohol in a 1:1 ratio to the phage solution. The solution was inverted to mix. The sample was then centrifuged at 13,000×g for 5 minutes. The aqueous layer was then removed and placed into a new tube, and 1 mL of 95% ethanol and 50 µL of sodium acetate were added. The sample was then placed on ice for 30 minutes. Following the ice incubation, the solution was mixed by gently swirling. The tubes were then centrifuged at 13,000 rpm for 10 minutes and decanted. Following the decanting, 500 µL of 70% ethanol was used to wash the pellet. The sample was then centrifuged again at 13,000 rpm for 10 minutes and decanted. The cap was then left off the tube and the contents allowed to air dry for 20 minutes. The DNA pellet was then dissolved in 50 µL of TE buffer. The concentration and purity of each sample was measured by Nanodrop, and agarose gel electrophoresis (1% agarose, TAE running buffer) was used to confirm that the DNA was unfragmented. The remaining sample was stored in the -20°C freezer for further analysis.

Sequencing, Assembly, and Annotation

DNA samples of each phage were sent to Idaho State University's Molecular Research Core Facility for sequencing. Libraries were prepared using an NEBNext Ultra II DNA Library Prep Kit and then cleaned using a Zymo Select-a-Size DNA Clean & Concentrator Kit to remove small fragments. The libraries were sequenced using an Illumina MiSeq Reagent Kit NANO v2 500-Cycle sequencing kit. Sequence files in FastQ format were uploaded to the Galaxy Server (<https://usegalaxy.org/>). Sequence reads were filtered using fastp v.0.23.2 (Chen et al., 2018) and PrinSeq v.0.20.4 (Schmieder & Edwards, 2011), assembled using Shovill v.1.1.0 (<https://github.com/tseemann/shovill>), and annotated using Prokka v.1.14.6 (Seemann, 2014). Genome maps were created using ApE v3.1.2 (<https://jorgensen.biology.utah.edu/wayned/ap/>) and touched up using InkScape v.1.0 (<https://inkscape.org/>). Submission of the nucleotide sequences to GenBank is in progress.

Results

A water sample taken from the GSL was plated on three different media (**Table 1**). The water sample was measured to be 11% salt by refractometry at sampling time, which falls within the range of past GSL samplings (Benson et al., 2012; Savage et al., 2013). Thirteen strains were recovered and named according to the medium they were isolated on. These strains were then challenged with filtered GSL water to look

for lytic phages. We found lytic phages against three of the strains (CB6, HB3, and TH4), based on a decrease in absorbance compared with growth of the same strain when treated with autoclaved (*i.e.*, phage-free) GSL water (**Figure 1**). This decline in absorbance began at about 8 hours for the CB6 strain (**Figure 1B**) and the TH4 strain (**Figure 1C**). The HB3 strain grew much more slowly, and a drop in absorbance was not noted until around 15 hours (**Figure 1A**). Each of the host–phage pairs showed a similar pattern of growth and lysis; however, the phage-treated CB6 sample showed some growth recovery after 14 hours (**Figure 1B**). Phage were isolated from these three samples, which we provisionally named ϕ CB6, ϕ HB3, and ϕ TH4, for the bacterial strains they were capable of infecting. Lysis was confirmed by spot tests. Spot tests also revealed that all three phages were host-specific—they were only able to infect their original host. We then repeated the spot tests on the three different media. All three bacterial strains grew best on the CB medium, while the highest titers of phage infection occurred on the HB medium (data not shown).

We sequenced the 16S rRNA of the three bacterial strains and submitted the sequences to BLASTn and RDP for analysis. BLASTn identified all three as isolates of *S. costicola* (percent identities between 98.68% and 99.71%), as did RDP (scores between 0.988 and 1.000).

We purified DNA from all three phage isolates and submitted them for high-throughput genome sequencing. To our surprise, the assemblies for ϕ HB3 and ϕ TH4 both yielded two separate genomes, which we named ϕ HB3a, ϕ HB3b, ϕ TH4a, and ϕ TH4b. The genome of ϕ CB6 was the smallest genome, at 33,866 bp (**Table 2**). It has 61 coding sequences which are arranged into a set of genes related to capsid assembly and lysis and a second set of genes related to genome replication (**Figure 2**). The genome of ϕ HB3a had considerable overlap with the genome of ϕ HB3b, which created difficulties in assembling the genome of ϕ HB3b. Consequently, assembled data for ϕ HB3b are unavailable at present. The genome of ϕ HB3a is 131,431 bp (**Table 2**). It has 226 coding genes, 3 noncoding RNAs, and 3 tRNAs. It has multiple gene clusters related to capsid assembly and multiple gene clusters related to replication (**Figure 3**). The genomes of ϕ TH4a and ϕ TH4b only overlapped by ~1400 bp, in a gene that was annotated as “major tropism determinant” in both genomes. The genome of ϕ TH4a is 127,643 bp (**Table 2**). It has 220 coding genes, 2 noncoding RNAs, and 1 tRNA. It has multiple gene clusters related to capsid assembly and multiple gene clusters related to replication (**Figure 4**). The genome of ϕ TH4b is 40,983 bp (**Table 2**). It has 73 coding sequences, which are arranged into multiple gene clusters related to capsid assembly and multiple gene clusters related to replication (**Figure 5**).

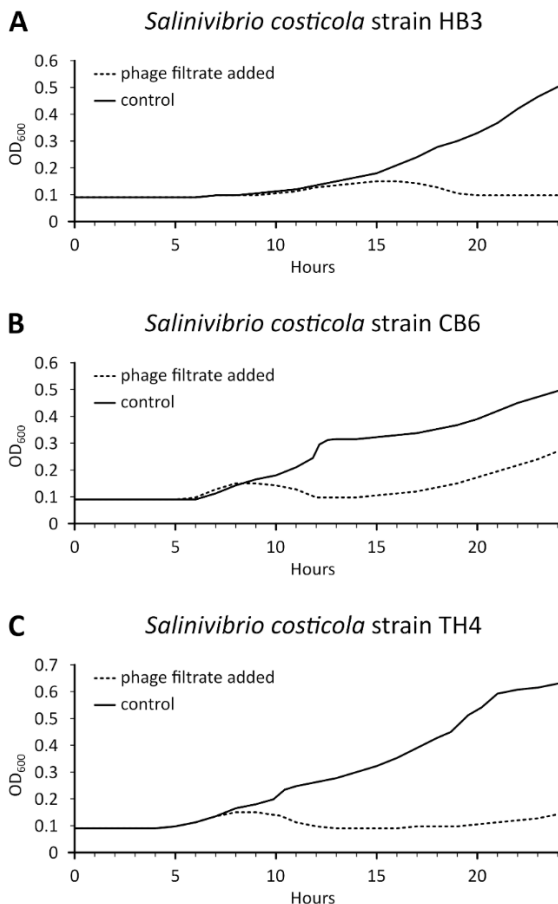


Figure 1. Growth of *S. costicola* strains HB3 (A), CB6 (B), and TH4 (C) over time in the presence (dotted line) or absence (solid line) of filtered GSL water, as measured by absorbance at 600 nm. The decline in absorbance in the test condition suggests the presence of a lytic bacteriophage.

Table 2: Phage genome size, and number of coding genes (CDSs), non-coding RNAs (ncRNAs), and tRNAs				
Phage	Size (bp)	CDSs	ncRNAs	tRNAs
φCB6	33,866	61	0	0
φHB3a	131,431	226	3	3
φTH4a	127,643	220	2	1
φTH4b	40,983	73	0	0

The genome of φHB3b is not included due to incomplete assembly.

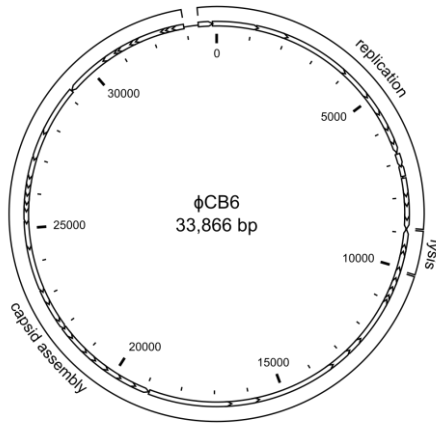


Figure 2: A graphical map of the ϕ CB6 genome. Brackets indicate groups of genes with shared functions (capsid assembly, lysis, or replication).

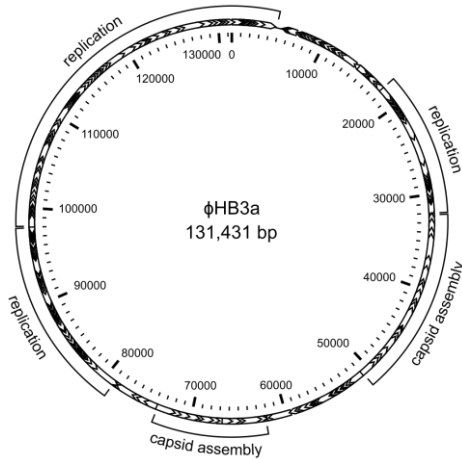


Figure 3: A graphical map of the ϕ HB3a genome. Brackets indicate groups of genes with shared functions (capsid assembly or replication). Genes without brackets did not have an obvious shared function.

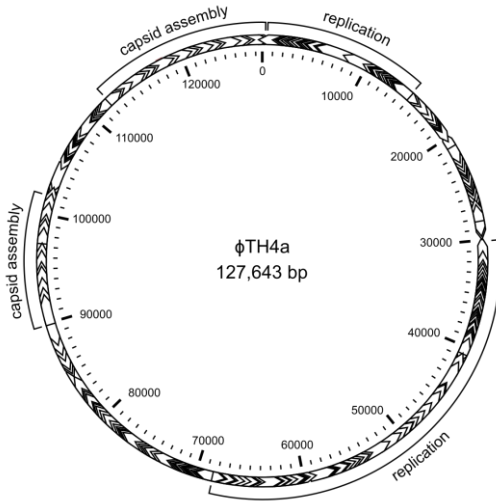


Figure 4: A graphical map of the ϕ TH4a genome. Brackets indicate groups of genes with shared functions (capsid assembly or replication). Genes without brackets did not have an obvious shared function.

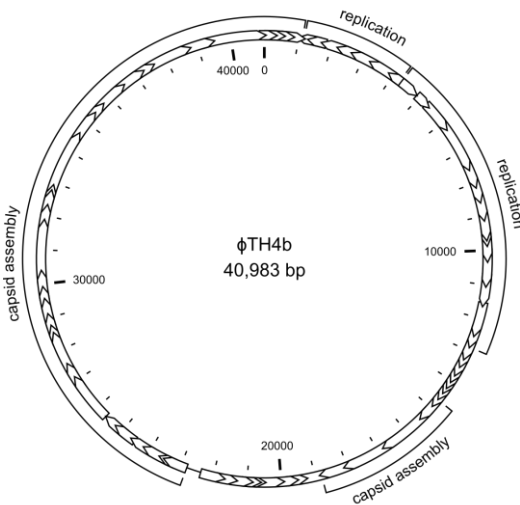


Figure 5: A graphical map of the ϕ TH4b genome. Brackets indicate groups of genes with shared functions (capsid assembly or replication). Genes without brackets did not have an obvious shared function.

Discussion

Preliminary evidence shows that we have isolated three strains of similar, but unique bacteria, as observed in previous studies (Benson et al., 2012; Shen et al., 2012; Simon et al., 2012; Savage et al., 2013). A metagenomic study would be important to determine what other host bacteria are present in the GSL, but it is clear that *Salinivibrio* plays an important role in the ecology of the GSL. There are some differences among the media formulations that we used. Some of the most obvious differences between the two media that may have contributed to these differences (HB and CB) include the increase of yeast extract in the CB medium that promotes better bacterial growth, while the added magnesium and calcium in the HB medium may assist in better phage infection.

The genome sequencing and annotation of the phage are preliminary, but they point to some major differences and interesting questions. The differences in the size of the genomes and the juxtaposition of the gene grouping (capsid assembly, replication, etc.) suggest the phages are not closely related. Deeper analysis is required to determine whether any of the genes for replication or capsid structure are of a similar lineage. Similar functional gene groups, such as three regions of replication genes in phage CB6 and two regions of capsid assembly genes in phages ϕ HB3a, ϕ TH4a, and ϕ TH4b, might reveal evidence of gene duplication upon additional analysis. A full genomic analysis of these phages awaits the final assembly of the ϕ HB3b genome.

It is surprising that two of our samples yielded pairs of phages: ϕ HB3a and ϕ HB3b were found coinfecting *Salinivibrio costicola* strain HB3 and ϕ TH4a and ϕ TH4b were found coinfecting *Salinivibrio costicola* strain TH4. It is possible that both phages infected their shared host strain simultaneously and do not depend on each other to complete their infection cycles. The other possibility is that one phage is a satellite and cannot complete its infection cycle without the other, such as the dependence of satellite phage P4 on helper phage P2 (Kahn et al. 1991). Experiments to distinguish these two possibilities are currently in progress.

Conclusions

The fact that we were able to isolate three separate strains of *Salinivibrio*, on three different medium formulations, each with a unique phage infection pattern, is an indication that the GSL is a rich growth environment and that the ever-changing salinity and other environmental factors favor microbial diversity. The phages we isolated are also considerably diverse, which suggests that there is still much to be

discovered about the microbial interactions taking place within this unique body of water.

References

Atlas, R.M. (1993). *Handbook of Microbiological Media*. Japan: CRC-Press, 415.

Benson, C.M., Domek, M.J., Zwolinski, M.D., Oberg, C.J. (2012). Isolation of a novel phage from the Great Salt Lake that infects *Idiomarina*. *Journal of the Utah Academy Science, Arts and Letters* 89: 31–44.

Chen, S., Zhou, Y., Chen, Y., Gu, J. (2018). Fastp: An ultra-fast all-in-one FASTQ preprocessor. *Bioinformatics* 34 (17): i884–90.

de la Haba R.R., López-Hermoso C., Sánchez-Porro C., Konstantinidis K.T., Ventosa A. (2019). Comparative Genomics and Phylogenomic Analysis of the Genus *Salinivibrio*. *Frontiers in Microbiology*. 10: 2104.

Gwynn, J. (1996). *Commonly asked questions about Utah's Great Salt Lake and Lake Bonneville*. Utah Geological Survey. Retrieved on September 12, 2022, from <https://geology.utah.gov/popular/great-salt-lake/commonly-asked-questions/>

Kahn, M.L., Ziermann, R., Dehó, G., Ow, D.W., Sunshine, M.G., Calendar, R. (1991). Bacteriophage P2 and P4. *Methods in Enzymology* 204: 264–280.

Savage, N.E., Sexton, Z., Waters, C., Domek, M.J., Oberg, C.J. (2013). Bacterial predation by bacteriophage isolated from the Great Salt Lake. *ERGO* 7: 46–53.

Schmieder, R., Edwards, R. (2011). Quality control and preprocessing of metagenomic datasets. *Bioinformatics* 27 (6): 863–4.

Seemann, T. (2014). Prokka: rapid prokaryotic genome annotation. *Bioinformatics* 30 (14): 2068–9.

Shen, P.S., Domek, M.J., Sanz-García, E., Makaju, A., Taylor, R.M., Hoggan, R., et al. (2012). Sequence and structural characterization of Great Salt Lake bacteriophage CW02, a member of the T7-like supergroup. *Journal of Virology* 86 (15): 7907–7917.

Sime-Ngando, T. (2014). Environmental bacteriophages: Viruses of microbes in aquatic ecosystems. *Frontiers in Microbiology* 5: fmicb.2014.00355.

Simon, T.B., Oberg, C.J., Culumber, M.D., Domek, M.J. (2012). Characterization of *Marinobacter* bacteriophage TS22 isolated from the Great Salt Lake, UT. *Journal of the Utah Academy Science, Arts and Letters* 89: 55–68.

Smith F.B. (1938) An investigation of a taint in rib bones of bacon. The determination of halophilic vibrios. *Proceedings of the Royal Society Queensland* 1938; 49: 29–52.

Summer, E.J. (2009). Preparation of a phage DNA fragment library for whole genome shotgun sequencing. *Methods in Molecular Biology* 502: 27–46.

Weimer, B.C., Rompato, G., Parnell, J., Gann, R., Ganesan, B., Navas, C., et al. (2009). Microbial biodiversity of Great Salt Lake, Utah. *Natural Resources and Environmental Issues* 15: 15–22.

Seasonality of Frequency and Intensity in Consumer Complaints: A Sentiment Analysis Approach

Reagan Siggard and Yong Seog Kim

Utah State University

Abstract

Is there a time of year when consumers are more intense in their complaints regarding financial products and services? Consumer complaints and reviews are pervasive in current competitive digital marketplaces, where they provide consumers with valuable information about services and products. Consumers may refrain from purchasing items when they find strong negative reviews more frequently than positive reviews. At the same time, consumer behavior is known to be affected by seasonal changes and events. This phenomenon forces many business entities to develop their marketing and operational strategies around shifts in consumers' seasonal needs. This paper focuses on detecting the seasonality of frequency and intensity in consumer complaints of financial products and services over multiple years using data obtained from the Consumer Financial Protection Bureau (CFPB). Our research focuses on temporal patterns and their potential relationship with seasonal dynamics by measuring the change in the number of positive and negative complaints and the emotional intensity

of the complaint narratives. Our analysis identifies various outcomes, including seasonal frequency patterns of consumer complaints that differ from the intensity of the narratives. We identify root causes across all quarterly dimensions that affect the frequency and intensity of complaint narratives.

Introduction

Consumer complaints and reviews are crucial in modern online markets because they provide consumers and competitors with important information about companies, services, and products. Consumers may opt not to purchase services or products when they find strong negative reviews more frequently than positive reviews. Reviews also benefit service and product suppliers with valuable information about instances of service failure (Crié, 2003), which can be helpful in the development of service recovery strategies oriented to customer retention. Thus, companies must be aware of and address consumer complaints to stay in competition.

At the same time, consumer behavior is known to be affected by changes in the seasons and by seasonal events. These changes can be expressed in the number of purchases, the amount spent on purchases, the number of reviews, or the number of consumer complaints (Lee et al., 2018). This phenomenon forces many business entities to develop their marketing and operational strategies around shifts in consumers' seasonal needs. A thorough understanding of seasonal dynamics is critical for businesses to maximize productivity and profitability.

This research investigates the seasonality of consumer complaint behaviors in the financial sector. The analysis strives to detect seasonality of frequency (the number of complaints) and intensity (the emotional strength—positive or negative—of the complaint) in consumer complaints over multiple years by examining temporal patterns that show seasonal dynamics measured by changes in 1) the number of positive and negative complaints and 2) the intensity of those complaints. The analysis also identifies, by using the consumer complaint database made publicly available by the Consumer Financial Protection Bureau (CFPB), whether there are financial services or products that need improvement to limit the number of consumer complaints and accrue more positive sentiments. In a broader view, this study bridges the gap between two fields of research, namely 1) technical natural language processing, where, similar to humans, algorithms learn the ability to understand text; and 2) seasonality in digital consumer

marketplaces, by harnessing the power of both to provide insight into how they can be used to track consumer experiences.

This research will benefit the CFPB (which tracks and manages the consumer complaint database) as it enforces the proper laws to protect the consumer, writes better rules and regulations, and supervises financial companies. According to a report released early in 2019, "...more than 223,000 grievances resulted in relief for consumers. More than 75,000 people got money back from companies they complained about" since the establishment of the CFPB complaint database (Singletary, 2019, para. 4). The semiannual reports from the CFPB are limited because they only consider the frequency of consumer complaints (Bureau of Consumer Financial Protection, 2019). The research offers a framework for identifying seasonal dynamics by consolidating temporal patterns of frequency and intensity in consumer complaints to aid CFPB in accomplishing its purpose.

Literature Review on Sentiment and Seasonality Analysis

This study addresses two research streams: sentiment and seasonality analysis of consumers' opinions. Sentiment analysis (or opinion mining) aims to detect and extract someone's opinion and attitudes from textual data. Sentiment analysis assesses whether someone has positive, neutral, or negative views toward a product or a service (Pang & Lee, 2008; Liu, 2009). Detecting and identifying others' attitudes has always interested many people, from political leaders aiming to stabilize their political regimes to ordinary individuals strengthening social relationships. Administering votes and questionnaires has been regarded as one of the most traditional methods to quantify and measure public opinions on political policy (Droba, 1931). Modern sentiment analysis based on natural language processing, which started to appear in the mid-2000s, focuses on analyzing online conversations and feedback of consumers to identify their sentiment toward products, brands, or services, which are eventually used to tailor products and services (Nassirtoussi et al., 2014; Ji et al., 2018). Over the years, sentiment analysis has been applied to numerous other areas such as financial markets (Nassirtoussi et al., 2014), national security (Burnap et al., 2014), social Web (Thelwall et al., 2012), and fraud detection (Saumya & Singh, 2018).

Identifying people's emotions can be critical for maintaining successful consumer retention rates because businesses can tailor their products and services based on consumers' sentiments. Sentiment analysis becomes particularly valuable when customers can express their

feelings more openly through survey responses, social media conversations, or websites. Sentiment analysis often focuses on detecting emotions (e.g., happiness, frustration, anger, sadness) based on lexicons (i.e., lists of words and the emotions they convey) (Taboada et al., 2011; He et al., 2018; Srikanth et al., 2022). It also focuses on identifying aspects that customers are mentioning in a positive, neutral, or negative way at different levels of granularity, whether a clause, a sentence, a paragraph, or a whole document (Najmi et al., 2015). Comprehensive reviews of the historical evolution and techniques of sentiment analysis can be found in Feldman (2013), Mäntylä et al. (2018), and Birjali et al. (2021).

Because of the rapid evolution of mobile and social media platforms, consumers easily share their experiences through third-party agencies (e.g., complaints.com or CFPB) and significantly impact other consumers' purchase decisions (Frey & Meier, 2004). When consumers' complaints or feedback have been accumulated over the years, it is natural to investigate seasonal variations. According to many studies in marketing, seasonal weather (e.g., temperature, snowfall, light levels) and seasonal events directly impact consumers' moods (Murray et al., 2010; Ehrenthal et al., 2014). For example, the lower mood of consumers during the winter season influences the frequency of filing complaints (Murray, 2006). In addition, some consumers may feel stress and happiness in making holiday purchasing (Chowdury et al., 2009), while others may feel joyful in holiday gift-giving or decorating.

Although this study also investigates complaint seasonality, it differs significantly from prior studies in several perspectives. First, many studies focus on identifying the characteristics and effects of seasonality on consumers' purchasing behavior, but we focus on detecting seasonal patterns in consumers' complaining behavior. Second, our study is also different from studies (Lee et al., 2018) that investigate seasonal patterns in consumers' complaining behavior because it considers the frequency and intensity of the complaint to detect notable seasonal characteristics of filing complaint behaviors over multiple years. Finally, our study adopts a sentiment analysis approach to analyze the polarities of the full text of complaints to reflect the intensity of the complaints.

Methods

The primary data source for analysis is the consumer complaint database, obtained from CFPB at Data.Gov in January 2020. The file contained 1,143,264 rows of consumer complaint records collected between 12/5/2004 and 1/12/2020. This data set consists of 17 variables,

as summarized in Table 1. Most of the variables in these data come directly from consumers who filed their complaints to the CFPB.

Table 1: List of Variables	
Variable	Description
Company	Which company the complaint is about
Company public response	The company's optional, public-facing response to a consumer's complaint
Complaint ID	The unique identification number for a complaint
Consumer complaint narrative	Description by the consumer about the complaint
Consumer consent provided	Describes whether the consumer opted in to publish their consumer complaint
Consumer disputed	Describes whether the consumer disputed the company's response
Date received	Date CFPB received the complaint from the consumer
Date sent to company	Identifies the date the CFPB sent the complaint to the company
Issue	Issue the consumer identified in the complaint
Product	Product type the consumer identified in the complaint
State	Consumer's mailing address state
Sub issue	Sub-issue the consumer identified in the complaint
Sub product	Sub-product types the consumer identified in the complaint
Submitted via	How the complaint was submitted to the CFPB
Tags	Data that supports easier searching and sorting of complaints
Timely	Indicates whether the company gave a timely response or not
Zip code	The mailing zip code provided by the consumer

When filing their complaints, consumers identify the product and sub-product about which they are complaining and the main issue and sub-issue of the complaint. Overall, consumer complaints were filed against 13 products (and 50 sub-products) on 16 main issues (and 84 sub-issues). The consumers' state and zip codes are extracted from their reported mailing addresses. The 'Consumer complaint narrative' column is an optional field where consumers can explain the details of their complaints. The CFPB then edits the field to desensitize any potentially identifiable information. Consumers can opt to share their narratives and

their consent is indicated in the ‘Consumer consent provided’ column. Finally, the complaint submission type (e.g., phone, website) is recorded, and the unique number is assigned to each complaint.

Once consumers’ complaints are recorded into the CFPB database, each complaint is sent back to the associated company. The company can respond to the consumer as indicated in the ‘Company response to consumer’ field. The ‘Company public response’ field is an optional field where the company can express its publicly accessible response to the complaint. The ‘Timely response’ and ‘Consumer disputed’ fields indicate whether the company gives a timely response to the consumer and whether the consumer disputes the company’s response, respectively.

To perform the data analysis, the data were loaded into Microsoft SQL Server, and SQL queries were used for tasks of primitive data cleansing. The most significant data preprocessing task was to remove records that did not have a consumer complaint narrative (e.g., records with NULL values or spaces in the narrative column) because the analysis required the field to calculate the polarity values of each complaint narrative. These polarity values were then used to compute frequencies and intensities of complaint narratives among time windows. This approach distinguishes this research from other regular reports from the CFPB, which do not apply any text mining analysis on complaint narratives (Bureau of Consumer Financial Protection, 2019).

After removing records without consumer complaint narratives, there are 160,490 records left in the data set. A SQL statement created a calendar dataset to indicate the day type (i.e., holiday, business, or weekend) for each date when consumers submitted their complaints. The CFPB and calendar datasets were joined on each dataset’s date field to enable future analysis.

Results and Discussion

After completing the above methods and data engineering practices, text mining practices were utilized to understand the sentiment of consumer complaints.

Sentiment Analysis on Consumer Complaint Narratives

Sentiment analysis can detect polarity (e.g., a positive or negative opinion) using textual data. Although there are several different ways of performing sentiment analysis on reviews depending on the levels of granularity (e.g., a word, clause, sentence, paragraph, or whole document), this research reviewed the polarity of each complaint narrative in a lump sum instead of sentence by sentence. The lump-sum

approach is appropriate for this analysis because all complaint narratives are typically negative. Thus, there is no need to divide the complaint narrative into good and bad sections (Najmi et al., 2015). The analysis utilized the text sentiment analysis library (TextBlob) using Python version 3.7, a data analytics programming language, to rate the polarity (intensity) of the consumer complaint narratives. Polarity scores range from [-1.0] to [1.0], where [1.0] means a positive statement and [-1.0] means a negative statement. The computed polarity values over 160,490 consumer complaint narratives ranged between -1.0 and 1.0, with an average of .002921.

To investigate seasonal trends of polarity in consumer complaint narratives, two aggregate measures (average polarity of narratives, number of negative or positive narratives) were calculated from the sentiment analysis output. First, average values of polarity scores were plotted across temporal dimensions (e.g., month, quarter, year) to reflect and compare the intensity of consumer complaints. Through this assessment, the research aims to find transitions of emotional polarity scores from strongly negative to strongly positive (or vice versa) within temporal windows. The second measure is the frequency dimension, which reflects the number of records of consumer complaint narratives with positive or negative polarity scores. Technically, it is possible to regard all records with less (or greater) than 0 polarity scores as negative (or positive) complaint narratives. However, to decipher strongly positive versus strongly negative scores and to avoid potential misclassification of narratives, narratives were counted as strongly positive if the polarity score is greater than .6 or strongly negative if the polarity score is less than -.6. To defend this approach, many consumer complaint narratives contain many 'XX's entered by the CFPB to desensitize sensitive information for public viewing, which can impact the polarity score of the text sentiment analysis. In the following sections, we use the terms strongly positive and strongly negative narratives as positive and negative narratives without adjectives for simplicity.

Frequency and Intensity of Positive and Negative Polarity by Day Type

The analysis begins by presenting frequencies of consumer complaint narratives investigating temporal trends across a small dimension, day types (Figure 1). The number of positive and negative complaint narratives are plotted for day types (business day, holiday, and weekend) for positive and negative complaint narratives. As expected, there are many more positive narratives reported on business days (940

records) than on weekends (200 records) and holidays (6 records) simply because there are more business days than weekends and holidays. Similarly, there are many more negative narratives on business days (336 records) than on weekends (82 records) and holidays (5 records).

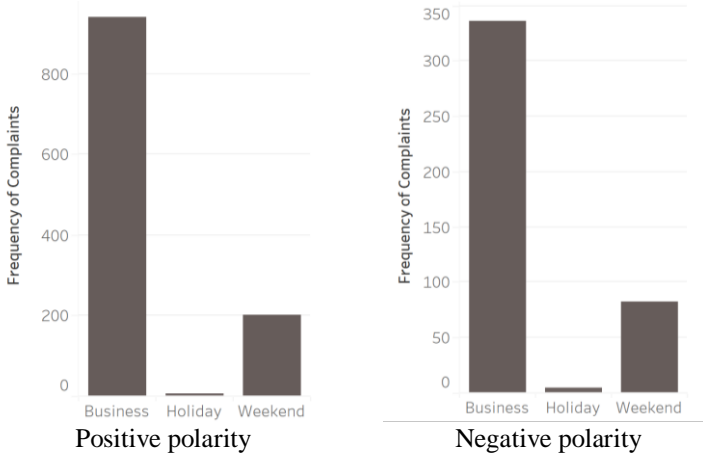


Figure 1. Frequency of positive and negative polarity by day type.

Additionally, there is a significantly greater number of positive narratives than negative narratives across all day types. This finding is somewhat unexpected because, people tend to remember and express their negative emotions more strongly and frequently (Baumeister et al., 2001). This well-known psychological phenomenon reflects the fact that negative emotion receives more information processing and leaves stronger impressions than positive emotion through the positive-negative asymmetry effect (Skowronski & Carlson, 1989; Baumeister et al., 2001).

In Figure 2, the polarity intensities of complaint narratives are computed by calculating the average scores of narrative polarity for data types. Figure 2 shows narratives on holidays are most positive followed by weekends and regular business days. This finding was against the researchers' initial expectations that consumer complaint narratives will be more sentimentally negative on holidays as consumers would be even more unhappy to file complaints on holidays. However, this finding in Figure 2 is understandable under the assumption that consumers may be more likely to be happier on holidays and may try to convey politeness through their complaints.

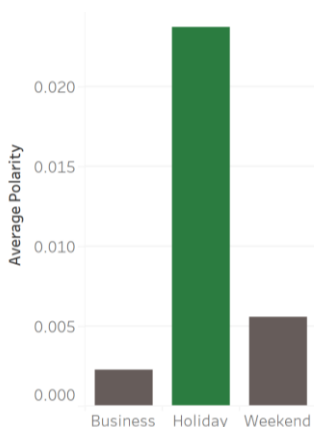


Figure 2. Intensity of polarity by day type.

Temporal Trends of Polarity Intensity of Complaint Narratives

The analysis focuses on temporal trends of polarity intensity over the past five years to create a more longitudinal, seasonality approach. Figure 3 displays the quarterly trends of polarity intensity over five years by calculating average scores of narrative polarities for each quarter in each year. (Note, although the data range is longer than five years, the data cleansing process removed all null complaint narratives, resulting in an analysis of five years.)

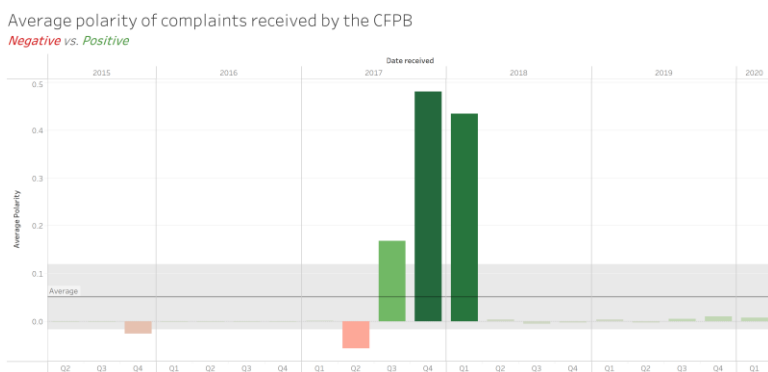


Figure 3: Temporal trends of polarity intensity

Figure 3 presents several notable exceptions of complaint narrative intensity in the past five years, with a 95% confidence interval in gray color. First, abnormal negative polarity patterns were observed in the 4th Quarter of 2015 and the 2nd Quarter of 2017. In contrast, irregular positive polarity patterns were observed in the 3rd and 4th Quarters of 2017 and the 1st Quarter of 2018. Although claims cannot be made that this pattern will repeat, some organizational, financial, economic, or societal triggers are assumed to cause such exceptional temporal patterns. Identification of the dramatic changes in polarity intensities between the 2nd Quarter of 2017 and the 1st Quarter of 2018 warranted additional investigation. During this time, Equifax's data breach exposed the sensitive, private information of 147 million people and ended in a settlement of \$425 million (Federal Trade Commission, 2020). The data breach instance of Equifax itself might have contributed to the increase in the number of filing complaints, while the way Equifax publicly acknowledged their mistakes in the 4th Quarter of 2017 and agreed to pay \$425 million as a settlement in the 1st Quarter of 2018 may have resulted in substantially higher polarity intensity of Equifax during these periods (0.50 and 0.47 during the 4th Quarter of 2017 and 1st Quarter of 2018, respectively).

Figure 4 displays the computed polarity intensity of complaint narratives for each month over five years. Note that, for each month, Figure 4 shows average polarity values in each month and hence does not convey sequential trends over months and quarters of years as shown in Figure 3.

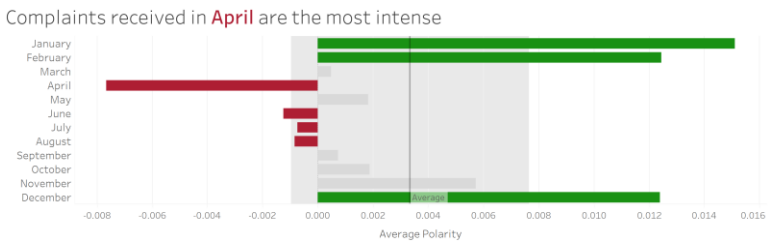


Figure 4: Monthly comparison of polarity intensity

According to Figure 4, the month of April shows the most negative polarity, while January, February, and December show the most positive polarity. In addition, these polarity intensity scores are statistically significantly different from those of other months, as indicated by the 95% confidence interval band in the gray background. Furthermore,

polarity intensity scores in June, July, and August are also negative, although not to the same level as April.

Why do consumer complaints to the CFPB increase in intensity during April? One explanation could be that more people are likely to inquire about their credit scores in April and the following months when they apply for preapproval with mortgage lenders. Our speculation is partially endorsed by another study (Whiteman, 2021), which indicated that houses tend to sell the fastest in June, leaving the credit reporting and credit inquiries happening in the months leading up to June. Around this time of year, consumers strongly desire to receive an accurate credit report to qualify for a mortgage and consider it of utmost importance. Thus, if they find an error on the report and do not receive help from their financial companies during this crucial time, they are more likely to express their intense negative emotions to the CFPB.

To further investigate this hypothesis, Figure 5 presents the polarity intensity of complaint narratives for each issue type that consumers identified when they filed their complaints to the CFPB. A 95% confidence interval band visually demonstrates the statistical significance of differences between negative and positive polarity intensity for each issue category. According to Figure 4, financial services and products dealing with credit reporting tend to have the most intense negative polarity, followed by different loans, including vehicle loans or leases, credit cards or prepaid cards, mortgages, and title loans.

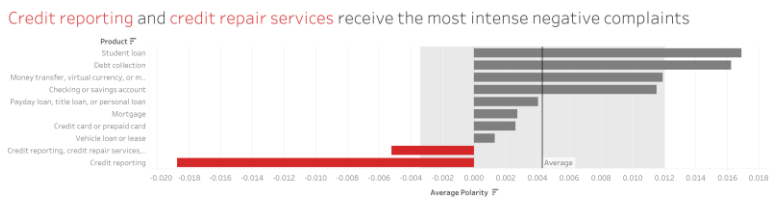


Figure 5: Comparison of polarity intensity by financial product

In addition, Figure 6 (top) shows that credit reporting services tend to have the most intensive negative polarity in April, followed by June and July. Another closely related service, mortgage services, tends to have the most intensive negative polarity in March, as shown in Figure 6 (bottom). We also note that credit reporting services and mortgages have the most intensive negative polarity around similar times (March through August, as shown in Figures 5 and 6). In contrast, intensities of negative polarity of credit reporting and mortgage services become weaker during the winter months, providing additional speculation support. These findings from Figures 4–6 support our hypothesis that

consumers tend to complain more negatively during this time of the year (mainly in April followed by June and July) because they are likely to use financial services that deal with the process of buying a home (credit reporting in Figure 6 (top) and mortgage services in Figure 6 (bottom)).

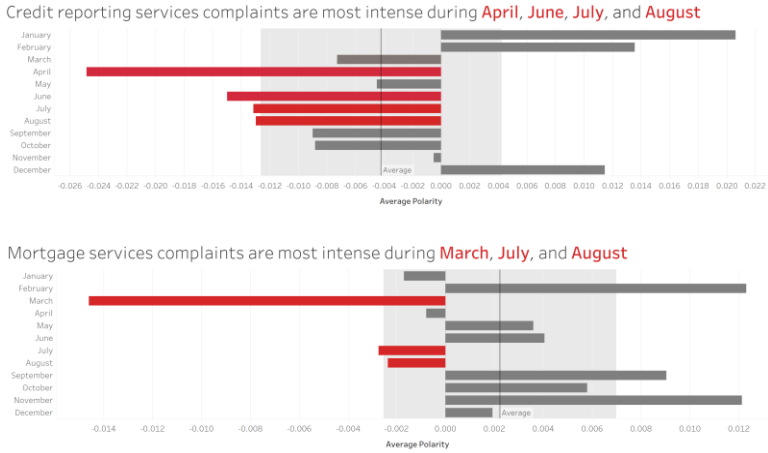


Figure 6: Monthly comparison of polarity intensity for business services. (Top) Credit reporting services; (bottom) mortgage services.

Temporal Trends of Polarity Frequency of Complaint Narratives

Frequencies of positive and negative complaint narratives over the last two years are shown in Figure 7. Initially, the analysis did not identify consistently meaningful temporal patterns in the frequency dimension. For example, months in the 3rd and 4th Quarters in 2018 present much higher frequencies of negative narratives than other months in 2018, while months in the 1st and 2nd Quarters in 2019 present much higher incidents than months in other quarter periods. Similarly, months in the 3rd and 4th Quarters in 2018 show much higher frequencies of strongly positive narratives than other months in 2018. These patterns did not repeat themselves in 2019. For example, months in the 1st and 2nd Quarters in 2019 show much higher incidents than months in other quarter periods in 2019, contradicting the findings in 2018. These findings suggest no strong temporal pattern associated with an increase or decrease in the number of strongly positive or negative narratives.

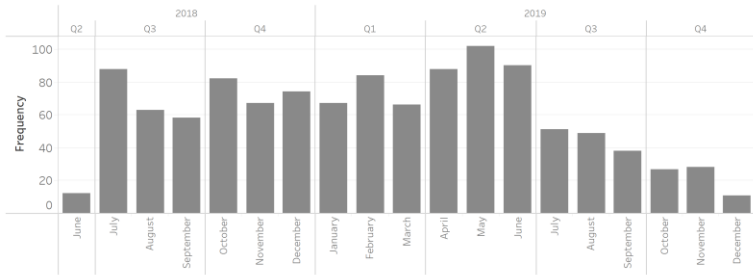
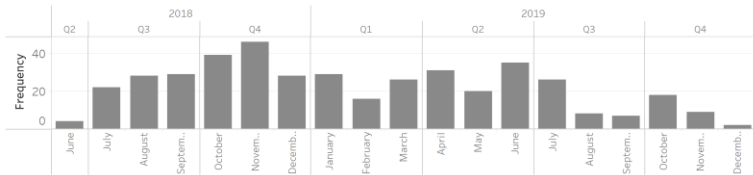
Seasonality of frequency of **positive complaints**Seasonality of frequency of **negative complaints**

Figure 7: Temporal patterns of positive (A) and negative (B) polarity frequency

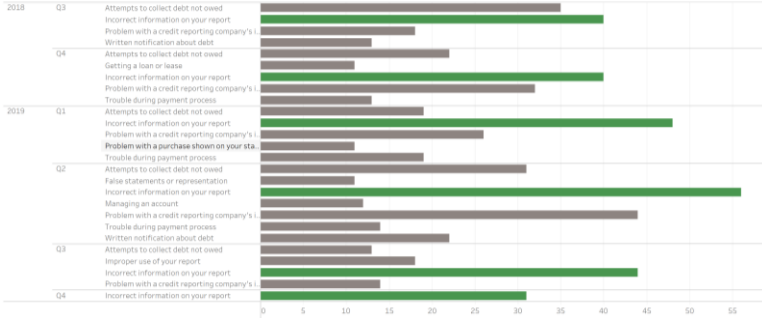
One interesting observation from Figure 7 is that there is a much higher frequency of positive narratives than negative narratives across all months from June 2018 to December 2019. Note that this figure only considered the frequency of positive or negative polarity, not the intensity of complaint narratives. Because the polarity intensity is the most negative in April from Figure 4, polarity values of negative complaints must be extremely negative to compensate for negative narratives not being as frequent as positive ones. These extremely negative complaints should be of particular concern for the companies receiving them, as the consumer may pursue additional action and/or there may be an underlying issue.

Temporal Polarity Frequency of Complaint Narratives by Issue

To find the most prominent financial services and product issues in the complaint narratives (see Figure 8), the total number of positive and negative frequencies were divided by each issue. One of the most interesting observations from the temporal frequency of positive polarity in Figure 8 is that in almost all quarters, ‘Incorrect information on your report’ is the most prominent issue that makes consumers’ sentiments positive. Two prominent other issues that make consumers feel negatively are when (1) there is a problem with their credit reporting and

(2) when the company tries to collect debt not owed. The incorrect information on the report issue links back to our speculation that severely negative complaints in April through June are related to financial products and services of buying a home. Companies should operationally focus on additional resources and strategies to minimize the number of credit report issues, particularly around the months identified (i.e., April, June).

Incorrect Information on Your Report has the most positive complaints



Incorrect Information on Your Report has the most negative complaints

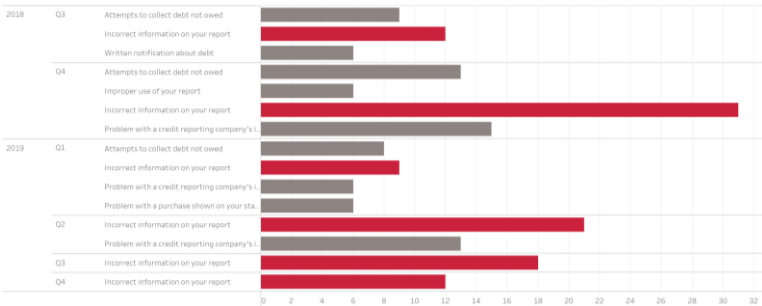


Figure 7: Temporal frequency of polarity by issue. (Top) Positive polarity frequency; (bottom) negative polarity frequency.

Conclusion and Future Work

This paper used consumer sentiments from their complaint narratives on financial products and services to detect seasonal patterns in both frequency and intensity dimensions. Our analysis shows an observed difference in seasonal patterns of the frequency dimension and intensity dimension of consumer complaints. For example, there were nearly double the number of positive narratives than negative ones in the frequency dimension. However, overall sentiments of complaint

narratives on temporal checkpoints (e.g., monthly and quarterly) were positive even though there were many strongly negative narratives, resulting in changes in seasonal patterns. Finally, potential root causes across all quarterly dimensions were discussed that affect the frequency and intensity of complaint narratives.

One possible extension of the current research is to model the probability of receiving company responses from consumers' perspectives. It will be interesting to see whether consumers from a specific geographical area, demographic, or who show strong negative (or positive) emotions tend to receive a company's response first. More interestingly, an analysis of whether company responses demonstrate seasonality in terms of frequency and intensity in their responses could prove helpful to companies as they navigate their duties to consumers and their need to adhere to the CFPB. Furthermore, future research should assess whether certain companies are receiving more or fewer complaints per year and whether that correlates with them responding to prior consumer complaints. The current and future research together will benefit the CFPB and financial companies as they try to remedy or relieve consumer's complaints and maximize productivity and profitability through merchandising, marketing, and operational strategies.

The original consumer complaint dataset is a powerful tool for analysis. It can tell many stories outside the realm of natural language processing. To continue analyzing the dataset using sentiment analysis, the subjectivity score (a measure of factual information or personal opinion) is a significant data point that has much potential to identify the validity of the consumer complaints. The subjectivity score could help determine which complaints should be addressed in terms of their validity by the company and the CFPB.

The intensity of the complaints is a crucial measurement. The intensity of the complaints could play a key role in how far the consumer will pursue the issue. The more upset a consumer is, the more he or she will demand of the company. This could lead the CFPB to critique the company responsible for the more intense negative consumer complaint more demandingly. This research pinpoints specific times of the year when consumers tend to be more negative (spring and summer) and then identifies issues and products that companies should address in terms of their accuracy, ability, and usefulness to consumers. Lowering the number of intense negative complaints could help companies maintain a good consumer base and retain a better profile, according to the CFPB.

References

- Baumeister, R.F., Bratslavsky, E., Finkenauer, C. & Vohs, K. D., 2001. Bad is stronger than good. *Review of General Psychology*, 5(4), 323-370.
- Birjali, M., Kasri, M. & Beni-Hssane, A., 2021. A comprehensive survey on sentiment analysis: Approaches, challenges, and trends. *Knowledge-Based Systems*, 226, 107134.
- Bureau of Consumer Financial Protection, 2019. *Semi-Annual Report of the Bureau of Consumer Financial Protection*, Washington, DC: Bureau of Consumer Financial Protection.
- Burnap, P. et al., 2014. Tweeting the terror: modelling the social media. *Social Network Analysis and Mining*, 4(1), 1-14.
- Chowdury, T.G., Ratneshwar, S. & Mohanty, P., 2009. The time-harried shopper: exploring the differences between maximizers and satisficers. *Marketing Letters*, 20, 155-167.
- Críe, D., 2003. Consumers' complaint behavior. Taxonomy, typology, and determinants: towards a unified ontology. *Journal of Database Marketing and Customer Strategy Management*, 11(1), 60-79.
- Droba, D.D., 1931. Methods used for measuring public opinion. *American Journal of Sociology*, 37(3), 410-423.
- Ehrental, J.C.F., Honhon, D. & Van Woensel, T., 2014. Demand seasonality in retail inventory management. *European Journal of Operational Research*, 238, 527-539.
- Federal Trade Commission, 2020. *Equifax Data Breach Settlement*, Washington, DC: Federal Trade Commission.
- Feldman, R., 2013. Techniques and applications for sentiment analysis. *Communications of the ACM*, 56(4), 82-89.
- Frey, B.S. & Meier, S., 2004. Social comparisons and prosocial behavior: testing "conditional cooperation" in a field experiment. *American Economic Review*, 94, 1717-1722.

He, W., Zhang, Z. & Akula, V., 2018. Comparing consumer-produced product reviews across multiple websites with sentiment classification. *Journal of Organizational Computing and Electronic Commerce*, 28(2), 142-156.

Ji, P., Zhang, H.-Y. & Wang, J.-Q., 2018. A fuzzy decision support model with sentiment analysis for items comparison in e-commerce: the case study of <http://PConline.com>. *IEEE Transactions on Systems, Man, and Cybernetics: Systems*, 49, 1993-2004.

Lee, S., Park, J., Hyun, H., Back, S., Lee, S.B., Gunn, F., Ahn, J., 2018. Seasonality of consumers' third-party online complaining behaviour. *Social Behavior and Personality*, 46(3), 459-470.

Liu, B., 2009. Sentiment analysis and subjectivity. In *Handbook of Natural Language Processing* (eds. N. Indurkha & F.J. Damerau). New York: Marcel Dekker.

Mäntylä, M.V., Graziotin, D. & Kuuttila, M., 2018. The evolution of sentiment analysis—a review of research topics, venues, and top cited papers. *Computer Science Review*, 27, 16-32.

Murray, G.W., 2006. *Seasonality, Personality and the Circadian Regulation of Mood*. 1st ed. Hauppauge: Nova Science Publishers.

Murray, K.B., Di Muro, F., Finn, A. & Leszczyc, P.P., 2010. The effect of weather on consumer spending. *Journal of Retailing and Consumer Services*, 17, 512-520.

Najmi, E., Hashmi, K., Malik, Z., Rezgui, A., Khan, H.U., 2015. CAPRA: a comprehensive approach to product ranking using customer reviews. *Computing*, 97(8), 843-867.

Nassirtoussi, A.K., Aghabozorgi, S., Wah, T.Y. & Ngo, D.C.L., 2014. Text mining for market prediction: a systematic review. *Expert Systems with Applications*, 41(16), 7653-7670.

Pang, B. & Lee, L., 2008. Opinion mining and sentiment analysis. *Foundations and Trends in Information Retrieval*, 2(1-2), 1-135.

Saumya, S. & Singh, J.P., 2018. Detection of spam reviews: a sentiment analysis approach. *CSIT*, 6, 137-148.

Singletary, M., 2019, September 22. The fight over shutting down the CFPB consumer complaint database is over. It's staying. *Boston Globe*. Retrieved March 15, 2019, from <https://www.bostonglobe.com/business/2019/09/22/the-fight-over-shutting-down-cfpb-consumer-complaint-database-over-staying/m1y0fE1Xod10eEthCjteSN/story.html>.

Skowronski, J.J. & Carlson, D.E., 1989. Negativity and extremity biases in impression formation: A review of explanations. *Psychological Bulletin*, 105(1), 131-142.

Srikanth, J., Damodaram, A., Yeekaraman, Y., Kuppusamy, R., Thelkar, A.R., 2022. Sentiment analysis on COVID-19 Twitter data streams using deep belief neural networks. *Computational Intelligence and Neuroscience*, 2022, 8898100.

Taboada, M., Brooke, J., Tofiloski, M., Voll, K., Stede, M., 2011. Lexicon-based methods for sentiment analysis. *Computational Linguistics*, 37(2), 267-307.

Thelwall, M., Buckley, K. & Paltoglou, G., 2012. Sentiment strength detection for the social web. *Journal of the American Society for Information Science and Technology*, 63(1), 163-173.

Whiteman, D., 2021. When is the best time of year to buy a house? *MoneyWise.com*. Retrieved May 10, 2021, from <https://moneywise.com/mortgages/mortgages/best-and-worst-times-to-buy-a-house>.

Bracketed vs. standard difference-in-differences estimation methods with data analysis on medical marijuana laws and violent crimes

Julian Chan,¹ Anthony Frazier², Gavin Roberts,¹

¹Weber State University; ²Colorado State University

Abstract

The difference-in-differences (DiD) estimator is a widely used tool for research in economics, political science, and public policy to evaluate the effects of public policy on a response variable. In this paper, we use simulations to compare the standard DiD estimator with the bracketed difference-in-differences (bDiD) approach of Hasegawa et al. (2019) that is robust to the existence of unobserved confounding variables in certain conditions. We highlight trade-offs between these approaches in a variety of cases that vary assumptions about the influence of confounding variables. We then apply both approaches in an analysis of the effect of medical marijuana legalization on violent crime. We do not find a negative effect of medical marijuana legalization on violent crime

as some recent analyses have. We show that the context provided by our simulations is helpful in interpreting the results in this data application.

Introduction

The difference-in-differences (DiD) model is a popular statistical model in a variety of disciplines. The model compares the change in an outcome variable of interest in a treatment group that receives an intervention with a control group that does not receive the intervention. It is often difficult for researchers to assess the validity of the assumptions of the DiD model when using observational data. One violation that might commonly occur is the influence of unobservable confounding variables on the outcome variable of interest. Hasegawa et al. (2019) introduce a bracketed DiD (bDiD) approach that provides an unbiased interval estimate of the treatment effect in some such cases when the influence of the confounder meets certain assumptions. However, we use simulations to show that adoption of the bDiD approach can lead to a loss of statistical power relative to the standard DiD approach. Therefore, analysts face a trade-off when deciding which approach to adopt. The use of simulations allows us to compare these approaches across many cases with varying assumptions about the influence of unobserved confounders.

We also implement both DiD approaches to estimate the effect of medical marijuana legislation (MML) on violent crime rates using a sample of 15 states. Here we show how to implement the bracketing approach of Hasegawa et al. (2019) to the two-way fixed effects DiD estimator. Recent estimates of the effect of MML on violent crime rates vary significantly: several studies found a negative effect of MML on violent crime while others have found a positive effect. These differences may result from unobservable confounders and control group selection. Visual inspection of our data reveals the possibility of influential confounders of the type discussed by Hasegawa et al. (2019) and analyzed in our simulations. We estimate a large and statistically significant negative effect of MML on violent crime using the standard two-way fixed-effects DiD approach but cannot reject the null hypothesis of no effect using the bracketed approach. These results are consistent with our simulations that implement a data generating process similar to what is observed based on visual inspection of the violent crime data across states that have and have not implemented MML.

Background

The DiD method has become an increasingly popular tool to measure the effects of policy interventions in a variety of disciplines (Meyer, 1995; Cook et al., 2002; Dimick and Ryan, 2014; Bernal et al., 2017). However, assessing whether the assumptions on which causal inference are based in DiD can be difficult. The assumptions of the standard DiD model are:

1. Treatment status is independent of the outcome variable of interest, e.g., violent crime does not affect the probability that a state will implement MML.
2. The treatment and control groups exhibit parallel trends in the outcome variable in the absence of treatment, e.g., if the treatment state had not passed MML, it would exhibit the same crime trends as control states on average. Figure 1 illustrates the parallel trends assumption. Note that the parallel trends assumption is in fact not testable because the outcome variable in the treatment group in the post-treatment period in the absence of treatment is not observable, so analysts rely on parallel trends in the pre-treatment period for evidence that the assumption holds.

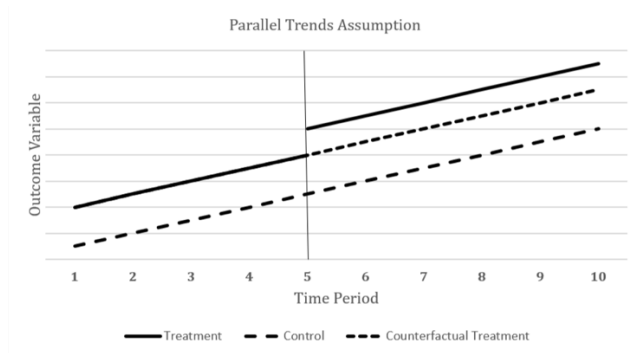


Figure 1. The parallel trends assumption requires that the treatment group would have experienced similar trends in the outcome variable to the control group in the absence of treatment. The “counterfactual treatment” line illustrates this assumption. Note that the counterfactual treatment is unobserved in the data, and analysts generally rely on parallel trends before the treatment period as evidence that this assumption holds.

3. There are no spillover effects from the treatment group to the control group and/or vice versa, e.g., MML enactment in the

treatment states does not lead to changes in the violent crime rates in control states.

In most cases, the primary focus of DiD analyses is validating the parallel trends assumption. Several methods for directly assessing the validity of the parallel trends assumption are used in practice. For example, one can assess the validity of the parallel trends assumption by visual inspection of the pretreatment data and extrapolate that pretreatment parallel trends evidence post-treatment counterfactual parallel trends (Dimick and Ryan, 2014). Several analysts have proposed estimators that adjust for violations to the parallel trends assumption (Lee et al., 2016; Roth, 2018; Andrews and Kasy, 2019). In particular, Hasegawa et al. (2019) propose a bDiD estimator that attempts to control for the effects of an unobserved confounding variable that may lead to a biased estimate of the treatment effect through violation of the parallel trends assumption. In the case analyzed by Hasegawa et al. (2019), visual inspection of the pretreatment trends is not valid because they focus on confounding variables that do not impact the outcome variable until after treatment occurs. An example of a confounding variable in an analysis of the effect of MML on violent crime might be poverty in the group population if the extent of poverty interacts with the implementation of MML in a manner that impacts violent crime rates.

The Hasegawa et al. (2019) estimator requires the identification of two control groups; a lower control group for which the unobserved confounder leads to smaller observations of the outcome variable relative to the treatment group and an upper control group for which the confounder leads to larger observations of the outcome variable relative to the treatment group. Similar to the standard DiD, the assumptions made about the distribution of the unobserved confounder and its effect on the dependent variable might be difficult to assess. The analyst will always have the option of combining the lower control group and the upper control group into a single control group and applying the standard DiD estimator. The upper and lower control groups are identified by inspection of the outcome variable across groups before treatment occurs. Hasegawa et al. (2019) suggest using data from before the statistical sample period, e.g., before time period 1 in Figure 1, for identification of control groups.

The Hasegawa et al. (2019) bracketing model makes some specific assumptions about the nature of the unobserved confounding variable, which are:

1. The outcome variable is monotonic in the unobserved confounder, e.g., higher levels of poverty in the group lead to more violent crime after MML implementation.

2. The level of the confounding variable in the groups does not change over the sample period, e.g., the poverty rate does not change significantly within a group over the sample period.
3. Control and treatment groups can be ordered in terms of the unobserved confounder, e.g., a control group exists that has a lower poverty rate than the treatment group, and a control group exists that has a higher poverty rate than the treatment group. Note that this assumption, like the parallel trend assumption, is not explicitly testable because the confounder is unobservable by definition.

In essence, the assumptions of the Hasegawa et al. (2019) bracketing model replace the parallel trends assumption of the standard DiD model. The existence of an unobserved confounder that impacts the control and treatment outcomes differentially in the post-treatment period violates the parallel trends assumption.

We perform a variety of simulations that mirror situations that might arise in typical analysis. Each simulation explores how violating assumptions to varying degrees affects the results for both the standard and bracketed models. The results of these simulations offer guidance to analysts considering the trade-offs between using a standard DiD estimator or bDiD estimator. We employ simulations to allow for the comparison of a large number of cases in a manner similar to Bertrand et al. (2004). Further, interval estimates associated with the bracketing approach of Hasegawa et al. (2019) provide a *minimum* confidence level so simulations allow us to compute the empirical confidence level for purposes of comparison. The next section provides a description of the methodology of our simulations. The fourth and fifth sections present the results of our simulations and the results of an application to the effect of MML on violent crime, respectively. For additional reading and foundational texts on standard DiD estimation, we refer the reader to Card & Krueger (1995), and Angrist & Pischke (2009). For reading on bracketing the DiD estimator, we refer the reader the authors who invented the method: Hasegawa et al. (2019).

Methods

Our simulations are based on a DiD model with an unobserved confounder for each group i , U_i , which varies across three groups—a lower-control group, treatment group, and upper-control group. We assume the outcome variable in each group follows the data-generating processes

$$y_{i,c,p} = x + b_{i,c} + m_{i,c}p + \gamma \mathbb{1}_{p \geq p^*} U_{i,c} p + \delta \mathbb{1}_{p \geq p^*} U_{i,c} - \gamma \mathbb{1}_{p \geq p^*} U_{i,c} p^* + \epsilon_{i,c,p}, \quad (1)$$

$$y_{t,p} = x + b_t + m_t p + \gamma \mathbb{1}_{p \geq p^*} U_t p + \delta \mathbb{1}_{p \geq p^*} U_t - \gamma \mathbb{1}_{p \geq p^*} U_t p^* + \mathbb{1}_{p \geq p^*} TE + \epsilon_{t,p}, \quad (2)$$

and

$$y_{uc,p} = x + b_{uc} + m_{uc} p + \gamma \mathbb{1}_{p \geq p^*} U_{uc} p + \delta \mathbb{1}_{p \geq p^*} U_{uc} - \gamma \mathbb{1}_{p \geq p^*} U_{uc} p^* + \epsilon_{uc,p}, \quad (3)$$

respectively. The data-generating process in each group is a piece-wise linear function plus white noise, $\epsilon_{i,p}$. For each equation, $y_{i,p}$, represents the outcome variable of interest in group i in time period p . The variable x , which represents the time variable for DiD, controls for the average rate of change of $y_{i,p}$. The next terms on the righthand sides of equations (1), (2), and (3), which are b_{ic} , b_t , and b_{uc} , are the expected values of the outcome in the first period of the sample, $p = 0$, or the constants of the trend equations. For clarity, we assume $b_{ic} < b_t < b_{uc}$. The next terms on the righthand sides are the baseline trends in the three series—a time slope m multiplied by the period value, p . Note that m is common to each of the three data-generating processes, so the trends are parallel in expectation in the pretreatment period. However, this does not ensure that the parallel trends assumption holds because it requires trends to be parallel in the counterfactual post-treatment period, i.e., it requires that trends would have been parallel between the treatment and control groups in the absence of treatment.

For simplicity, we assume that the confounder only affects the outcome variable starting from the treatment period, p^* . The assumptions in Hasegawa et al. (2019) require that the confounders, U_i , are time-invariant within each group and can be stochastically ordered such that

$$E[f(U_{ic})] \leq E[f(U_t)] \leq E[f(U_{uc})] \quad (4)$$

for all bounded and increasing functions f . This is an equivalent definition of the third assumption listed earlier for the Hasegawa et al. (2019) bracketing model.

The fourth and fifth terms on the righthand sides of equations (1), (2), and (3) represent our assumptions about the impact of the unobserved confounder, U_i , on the outcome across groups. The fourth terms allow the confounder to shift the post-period outcomes by magnitude δU_i , while the fifth terms allow the confounder to change the trajectory of the outcome variable relative to the pretreatment trend by magnitude γU_i . The γ and δ parameters allow the confounder to affect the intercept and slope differently in different simulation specifications. For example, if $\gamma = 0$ and $\delta > 0$, then the confounder only affects the trend of the outcome variable, but does not shift it at $p = p^*$.

The sixth terms in each equation are constants that adjust the overall height of each group in the post-period. This term ensures that, without the presence of any treatment effect or other post-treatment

jumps, the post-treatment values would connect to the pretreatment values in a linear manner.

The seventh term in equation (2) represents the implementation of treatment. Treatment occurs at $p = p^*$ and shifts the outcome variable by magnitude TE for the remainder of the post-treatment period. This is the effect that DiD aims to identify. The last terms in equations (1), (2), and (3) are mean zero error terms.

The standard DiD estimate is unbiased if the assumptions of the ordinary least squares model hold in addition to the assumption of parallel trends (Bertrand et al., 2004; Abadie, 2005). The parallel trends assumption requires that treatment group observations of the outcome variable after implementation of treatment *would* have exhibited the same trend as control observations in the post-treatment period in the absence of treatment. The parallel trend assumption could be violated if an unobserved confounding variable is present (Hasegawa et al., 2019). For example, the parallel trend assumption will be violated in our simulations between the lower control group and the treatment group if $\gamma = 0$, $\delta > 0$, and $E(U_{lc}) < E(U_t)$, because the trends between these groups will diverge in the post-treatment period in that case. We focus our simulation results on the effectiveness of the methods when these assumptions are violated in these specific ways.

The expected value of the DiD estimator based on our assumed data-generating processes with the lower control group is

$$\begin{aligned} E(DiD)_{lc} &= [E(y_t|p \geq p^*) - E(y_{lc}|p \geq p^*)] - [E(y_t|p < p^*) - E(y_{lc}|p < p^*)] \\ &= TE + \gamma[E(U_t) - E(U_{lc})]p + (\delta - \gamma p^*)[E(U_t) - E(U_{lc})]. \end{aligned} \quad (5)$$

Therefore, the DiD will be biased upwards if $E(U_t) > E(U_{lc})$ and the lower control group is used. This is the upper bound for the Hasegawa et al. (2019) bDiD interval estimate. Similarly, the expected value of the DiD estimator with the upper control group is

$$E(DiD)_{uc} = TE + \gamma[E(U_t) - E(U_{uc})]p + (\delta - \gamma p^*)[E(U_t) - E(U_{uc})], \quad (6)$$

which will be biased downwards if $E(U_t) < E(U_{uc})$ and the upper control group is used. This is the lower bound for the Hasegawa et al. (2019) bDiD interval estimate. So, the expected value of the bDiD estimate, $E(bDiD)$, based on our assumed data-generating processes in equations (1) to (3) is

$$E(bDiD) = \{\max(E(DiD)_{lc}, E(DiD)_{uc}), \min(E(DiD)_{lc}, E(DiD)_{uc})\}$$

The logic underlying the Hasegawa et al. (2019) approach is that the two DiD estimates are biased in opposite directions, so the true treatment effect should lie within the bracketed interval. However, the

size of the interval is increasing in $E(U_t) - E(U_{lc})$ and $E(U_t) - E(U_{lc})$, so large confounding effects will lead to substantial losses in statistical power when the bracketing approach is applied because this directly affects the size of the bracket by equations (5) and (6).

One alternative to bracketing is to treat the upper and lower control groups as one control group unit and perform regular DiD estimation. We refer to this method as the standard DiD (sDiD) approach, which leads to a single point estimate. The analyst can still build confidence intervals (CIs) using standard techniques. The CIs from the sDiD method have specific margins of error rather than the minimum ones provided by the Hasegawa et al. (2019) approach. Furthermore, the standard error of the standard approach will be smaller because of the larger pooled control sample. The sDiD estimator will be unbiased in cases where the biases associated with the lower and upper control group are symmetric around the treatment group. Therefore, the sDiD approach is optimal when biases associated with the upper and lower control group are symmetric because it will lead to more precise interval estimates, but the sDiD approach will lead to erroneous (statistically biased) results in cases where the biases are not symmetric.

Finally, we will also explore the option of generating a new control group, done by taking the arithmetic mean of output values of each control group at each time period and performing sDiD estimation using the new control group and the treatment group. This approach amounts to tempering the variation caused by the unobserved confounder in the underlying data. We refer to the resulting estimate as the Gavin estimator (gDiD). All three of these estimators will be available in any analysis where an upper and lower control group can be identified in the data.

Simulations

In this section, we run simulations for different scenarios related to the unobserved confounding variable. In each scenario, we compare the sDiD, the bDiD, and the gDiD. We start with a scenario in which the unobserved confounder does not lead to violations of the parallel trends assumption. We then move on to simulations that violate the assumptions of the standard DiD model, exploring how variations in violations to the parallel trends assumption lead to different results for each method. We run 1000 simulations for every scenario using sample sizes of 100 for each group. We compare the accuracy and precision of the sDiD, bDiD, and gDiD estimators by calculating the mean of each of the three-point estimates over the 1000 simulations, the standard error of the three-point estimates, the mean lower and upper 95% confidence bounds, the proportion of the simulations for which the point estimates fall within

their respective theoretical 95% CIs on average, and the proportion of the simulations for which the true TE falls within the bDiD interval.

Simulation 1: No Violation of Parallel Trends Assumption

We first simulate the results when each line has the same expected slope ($m = 1$) in both the pre-treatment ($p < p^*$) and post-treatment ($p > p^*$) periods, so the parallel trends assumption holds. This is implemented by applying values of $\gamma = \delta = 0$ in equations (1)–(3). We use intercepts of $b_{lc} = 0$, $b_t = 1$, and $b_{uc} = 2$ on the interval $p \in (0, 1)$, and apply unit variance to the mean-zero error terms for each group. Table 1 shows the results of this scenario for different sizes of the underlying true TE used in equation (2) in the generation of the treatment data.

Table 1a: Comparison of regular and Gavin estimators when confounding variable does not lead to violations of the standard DiD assumptions

TE	TE_d	$sd(TE_d)$	CI	$CI\%$	\overline{TE}_g	$sd(\overline{TE}_g)$	CI_g	$CI_g\%$
0	0	0.02	(-.05, .05)	0.95	0	0.02	(-.05, .05)	0.95
.5	0.5	0.02	(.45, .55)	0.94	0.49	0.02	(.45, .55)	0.95
1	1	0.02	(.95, 1.05)	0.94	1	0.02	(.95, 1.05)	0.93
5	5	0.02	(4.95, 5.05)	0.95	5	0.02	(4.95, 5.05)	0.96

Table 1b: Performance of bracketed and extended bDiD approaches when confounding variable does not lead to violations of the standard DiD assumptions

TE	\overline{TE}_L	\overline{TE}_U	$sd(\overline{TE}_L)$	$sd(\overline{TE}_U)$	$BR\%$	$Ext\ CI$	$Ext\ CI\%$
0	-0.01	0.01	0.03	0.03	0.28	(-.07, .07)	0.99
.5	0.49	0.51	0.03	0.03	0.33	(.43, .57)	0.99
1	0.99	1.01	0.03	0.03	0.34	(.93, 1.07)	0.99
5	4.99	5.01	0.03	0.03	0.32	(4.93, 5.07)	0.99

The first column of Table 1 shows the different treatment effect parameter applied in each row of results. The second to fifth columns of Table 1a show results of our simulations associated with the different DiD estimators. The second column, labeled TE_d , shows the simulation-mean estimate of the TE using the sDiD method, the third column shows

the simulation-standard error of TE_d , the fourth column shows the mean confidence-interval bounds, and the fifth column shows the proportion of the time that the true TE is inside the 95% CI. The sixth to tenth columns display corresponding results for the gDiD estimator.

In table 1b, \widehat{TE}_L and \widehat{TE}_U are the estimated treatment effects between the treatment group and upper and lower controls respectively using sDiD estimates. Similarly, $sd(\widehat{TE}_L)$ and $sd(\widehat{TE}_U)$ are the standard errors of these estimates. The reported CI represents the average CI for the bDiD 95% CI. BR CI% is the simulated level of confidence for the bDiD 95% CI and BR% is the proportion of time the interval that is the maximum and minimum value of the point estimate contain the treatment effect. In what follows we will report all of the above information, but the first column will indicate which parameter(s) change in the given scenario.

The second to fifth columns of Table 1a indicate that the sDiD performs well, as expected, when the parallel trends assumption is not violated. All simulation-mean sDiD estimates are within 0.01 of the true TE . Further, the 95% CIs perform as expected with approximately 95% of the 1000 sDiD estimates landing within a 95% CI. Because the parallel trends assumptions hold in this scenario, gDiD performs about as well as sDiD.

Table 1b shows the performance of the bDiD estimates in our scenario without violations to the parallel trends assumption. The \widehat{TE}_L and \widehat{TE}_U estimates are biased on average because of the ex post ordering that occurs in choosing the lower and upper bounds of the bracketed interval.¹ Hence, although the bounds associated with the *bDiD* approach are individually unbiased in the absence of a problematic confounder, the analyst might introduce bias through ex post selection of the upper and lower bounds for the *bDiD* interval. On the other hand, the midpoint between the lower and upper control groups is an unbiased estimate of TE in this case as the variance of the error terms in the data generation was the same in the lower and upper control groups (Nadarajah and Kotz, 2008). This is less likely to occur in observational data.

Simulation 1 also indicates that use of the bracketed approach leads to a significant loss of statistical power. When $TE = 0.5$, the *sDiD* leads to a 95% CI that does not contain zero, while the average CI associated with the *bDiD* contains zero. This loss of power can also be seen by the fact that the 95% CI associated with the *bDiD* hovers around 99%.

¹ See Nadarajah and Kotz (2008) for the theoretical distributions of the maximum and minimum of two Gaussian random variables like these.

The main conclusion to be drawn from the results of Simulation 1 are that the *bDiD* approach leads to a large loss of statistical power and this is not associated with any gain in the case that the parallel trends assumption is not violated.

Simulation 2: Violation of Parallel Trends in One Control Group

In this simulation, we violate the parallel trends assumption in a manner that violates the assumptions of the *sDiD* model but does not necessarily violate the looser assumptions of the *bDiD* model. Assumption (2) in Hasegawa et al. (2019) requires that the outcome variable of interest is monotonic in the confounding variable. In this set of simulations, we increase the expected slope of the upper control group in the post-treatment period by applying $\delta = 1$, $U_{uc} \geq 0$, $U_t = 0$, and $U_{lc} = 0$ when generating the data using equations (1)–(3). This leads to a violation to the parallel trends assumption when $U_{uc} > 0$ as the slope of the upper control group will not be the same as the counterfactual treatment slope. The *sDiD* estimate associated with the upper control group will be biased because of the confounder as shown in equation (6). However, the outcome variable is monotonic in the unobserved confounder and the expected value of the unobserved confounder is higher in the upper control group than in the lower control or treatment groups so the *bDiD* assumptions are not violated.

We run five simulations associated with this type of violation for different post-treatment upper control slopes (Table 2). The pretreatment control ranges from 0 to 2, with values shown in the first columns of Table 2. The $TE = 1$ in each of the rows is displayed in Table 2. The first row of Table 2 shows the baseline case without violations to the parallel trends assumption, i.e., the post-treatment upper-control slope is one and the results dovetail with those of Simulation 1.

Several important observations can be drawn from the remaining rows with $U_{uc} > 0$. The *sDiD* and *gDiD* estimates labeled TE_d and \widehat{TE}_g become increasingly downward biased as the impact of the confounder grows and leads to larger and larger violations of the parallel trends assumption—the slope of the pooled control data is becoming increasingly large relative to the counterfactual slope of the treatment data. The same increasing downward biases \widehat{TE}_L because the effect of the confounder is not dampened through pooling as it is in the *sDiD* approach. Interestingly, the \widehat{TE}_L estimate becomes less biased as the impact of the confounder grows. This occurs because the lower control group becomes increasingly likely to produce the larger of the two

bounds associated with the *bDiD* approach whereas each control group was equally likely to produce the larger DiD estimate in Simulation 1.

Table 2a: Comparison of regular and Gavin estimators with violations to the parallel trends assumption

U_{uc}	TE_d	$sd(TE_d)$	CI	CI%	\overline{TE}_g	$sd(\overline{TE}_g)$	CI_g	$CI_g\%$
0	0.99	0.02	(.95, 1.05)	.95	1	0.02	(.95, 1.0)	0.95
.5	0.94	0.03	(.89, .99)	.34	0.94	0.02	(.89, .99)	0.30
1	0.87	0.03	(.81, .93)	.01	0.87	0.03	(.82, .93)	0
1.5	0.81	0.04	(.74, .88)	0	0.81	0.03	(.76, .87)	0
2	0.74	0.04	(.66, .83)	0	0.75	0.03	(.69, .81)	0

Table 2b: Performance of bracketed and extended bDiD approaches with violations to the parallel trends assumption

U_{uc}	\overline{TE}_L	\overline{TE}_U	$sd(\overline{TE}_L)$	$sd(\overline{TE}_U)$	BR %	Ext CI	Ext CI%
0	0.99	1.01	0.03	0.03	0.35	(.93, 1.07)	1
.5	0.88	1	0.03	0.03	0.53	(.82, 1.06)	.97
1	0.75	1	0.03	0.03	0.51	(.68, 1.06)	.97
1.5	0.62	1	0.04	0.03	0.50	(.54, 1.06)	.97
2	0.49	1	0.05	0.03	0.48	(.40, 1.05)	.97

Comparison of the CIs across the *sDiD*, *gDiD*, and *bDiD* approaches in Table 2 indicates that while the *sDiD* and *dDiD* approach is not useful, the *bDiD* approach only improves the situation in the case of a relatively small impact of the confounder. In cases with a large impact of the confounder, the *bDiD* approach leads to such wide interval estimates that they may not be useful for statistical inference. The optimal choice to an analyst confronted with data of the type confronted in Simulation 2 would be to identify the control units for which the parallel trends are holding and apply the *sDiD* approach using only those control units. However, this information will not be directly available to the analyst. An analyst could however compare pooled DiD estimates with estimates using different control units and look for the types of patterns that are apparent in Table 2.

Simulation 3: Violation of Parallel Trends in One Control Group (Sim3 B)

We now simulate a scenario in which all groups have slopes of zero in the pretreatment period or $m = 0$. The intercept of the upper, treatment, and lower control groups are 2, 1, and 0. In this simulation, the slope of the lower control group increases in the post-treatment period by $U_{lc} > 0$. This leads to a violation of the parallel trends assumption because we impose $U_{uc} = 0 < U_{lc}$. This simulation was motivated by visual inspection of violent crime data in 15 states collected for the data analysis in the next section. Figure 2 (below) displays data from lower control, treatment, and upper control states. The violent crime rate from the lower control group appears to increase relative to the treatment and upper control groups in the post-treatment period (approximately after the year 2000).

We run Simulation 3 with different magnitudes of U_{lc} and different treatment effects. The results of Simulation 3 are displayed in Table 3, with the first column showing the treatment effect and U_{lc} applied in that row of results. The first set of five rows all apply $TE = 0$, the second set of five rows all apply $TE = 1$, and the third set all apply $TE = -1$.

Within each treatment effect, specification results with $U_{lc} = 0$ are displayed first. Consistent with the results of Simulation 1, the sDiD approach is preferred in these cases because it is unbiased and more powerful than the bDiD approach in these cases.

On the other hand, the sDiD and gDiD estimate becomes increasingly downward biased as U_{lc} gets larger. In fact, the sDiD approach leads to a Type I error in the case with $TE = 0$ and $U_{lc} = 2$. The lower bound from the bDiD becomes increasingly downward biased at an even faster rate as U_{lc} grows because the bias is not dampened through pooling with the upper control group, which does not produce biased results. In this case, the bDiD estimate is preferred to the sDiD because the former does not result in any Type I errors. However, if the analyst knew they were in this case, the optimal option would be to choose the estimate associated with the upper control group that is the least biased in this case.

Note that visual inspection of the observational violent crime data led us to run Simulation 3b, and Simulation 3b shows that selection of the control group that is unaffected by the unobserved confounder leads to the best results. This shows how simulations can be used in conjunction with analysis on observational data to make better decisions associated with inference.

Table 3a: Comparison of regular and Gavin estimators with violations to both sDiD and bDiD

(TE, U_{ic})	TE_d	$sd(TE_d)$	CI	CI%	\widehat{TE}_g	$sd(\widehat{TE}_g)$	CI_g	$CI_g\%$
(0,0)	0.00	0.02	(-.05, .05)	.95	0.00	0.02	(-.05, .05)	.95
(0,.5)	-0.06	0.03	(-.11, -.01)	.34	-0.06	0.02	(-.11, -.01)	.30
(0,1)	-0.13	0.03	(-.19, -.11)	0	-0.13	0.03	(-.18, -.07)	0
(0,2)	-0.25	0.04	(-.34, -.17)	0	-0.25	0.03	(-.31, -.19)	0
(1,0)	1	0.02	(.95, 1.05)	.95	1	0.02	(.95, 1.05)	.95
(1,.5)	0.94	0.03	(.89, .99)	.29	0.94	0.02	(.89, .99)	.27
(1,1)	0.87	0.03	(.81, .93)	.01	0.87	0.03	(.82, .93)	0
(1,2)	0.75	0.04	(.66, .83)	0	0.75	0.03	(.69, .81)	0
(-1,0)	-1	0.02	(-1.05, -.95)	0.95	-1	0.02	(-1.05, -.95)	0.95
(-1,.5)	-1.06	0.03	(-1.12, -1.01)	0.31	-1.06	0.02	(-1.11, -1.01)	0.27
(-1,1)	-1.13	0.03	(-1.19, -1.07)	0.01	-1.13	0.03	(-1.18, -1.07)	0
(-1,2)	-1.25	0.04	(-1.34, -1.17)	0	-1.25	0.03	(-1.31, -1.19)	0

Table 3b: Performance of bracketed and extended bDiD approaches with violations to both sDiD and bDiD

(TE, U_{ic})	\widehat{TE}_L	\widehat{TE}_U	$sd(\widehat{TE}_L)$	$sd(\widehat{TE}_U)$	BR%	EX CI	EX BR%
(0,0)	-.01	.01	.03	.03	0.34	(-.07, .07)	.99
(0,.5)	-.13	0	.03	.03	0.54	(-.18, .06)	.97
(0,1)	-.25	0	.03	.03	0.5	(-.32, .06)	.98
(0,2)	-.51	0	.05	.03	0.51	(-.60, .06)	.97
(1,0)	.99	1.01	.03	.03	0.33	(.93, 1.07)	.99
(1,.5)	.87	1	.03	.03	0.49	(.82, 1.06)	.98
(1,1)	.75	1.00	.03	.03	0.51	(.68, 1.06)	.98
(1,2)	.50	1	.05	.03	0.48	(.40, 1.06)	.97
(-1,0)	-1.01	-0.99	0.03	.03	0.38	(-1.06, -.93)	0.99
(-1,.5)	-1.13	-1	0.03	.03	0.50	(-1.19, -.94)	0.98
(-1,1)	-1.25	-1	0.03	.03	0.53	(-1.32, -.94)	0.97
(-1,2)	-1.51	-1	0.05	.03	0.48	(-1.60, -.95)	0.97

Simulation 4: Violation of Parallel Trends in Both Control Groups

In this section, we violate the parallel trends assumption in both control groups, but in a manner that is consistent with the bDiD assumptions. In this setting, we apply different levels of the confounders U_{lc} and U_{uc} such that $U_{lc} < 0$, $U_{uc} > 0$, and $|U_{lc}| = U_{uc}$. We impose $\delta = 1$ and $\gamma = 0$ as in the previous simulation so the expected slope in the lower control group is $m + U_{lc} < m$ in the post-treatment period and the slope of the upper control group is $m + U_{uc} > m$ in the post-treatment period, while the counterfactual treatment slope is m throughout. This scenario will lead the sDiD estimate associated with the lower control group to be biased upwards and the sDiD estimate associated with the upper control group to be biased downwards. However, although these DiD estimates are individually biased, if $|U_{lc}| = U_{uc}$, then these individual biases will cancel each other out in the pooled data, leading to an unbiased DiD. This is confirmed in the results of Simulation 4 presented in Table 4.

Table 4a: Comparison of regular and Gavin estimators with violations to the parallel trends assumption								
$ U_{uc} = U_{lc} $	TE_a	$sd(TE_a)$	CI	CI%	\overline{TE}_g	$sd(\overline{TE}_g)$	CI_g	$CI_g\%$
0	1	0.02	(.95, 1.05)	.94	1	0.02	(.95, 1.05)	0.94
.5	1	0.03	(.94, 1.06)	.98	1	0.02	(.95, 1.05)	0.95
1	1	0.04	(.92, 1.08)	1	1	0.02	(.95, 1.05)	0.95
1.5	1	0.06	(.89, 1.11)	1	1	0.02	(.95, 1.05)	0.95
2	1	0.07	(.86, 1.14)	1	1	0.02	(.95, 1.05)	0.95

Table 4b: Performance of bracketed and extended bDiD approaches with violations to the parallel trends assumption								
$ U_{uc} = U_{lc} $	\overline{TE}_L	\overline{TE}_U	$sd(\overline{TE}_L)$	$sd(\overline{TE}_U)$	BR %	Ext CI	Ext CI%	
0	0.99	1.01	0.03	0.03	0.31	(.93, 1.07)	0.99	
.5	0.87	1.13	0.03	0.03	1	(.81, 1.13)	1	
1	0.75	1.25	0.03	0.03	1	(.68, 1.25)	1	
1.5	0.62	1.38	0.04	0.04	1	(.54, 1.38)	1	
2	0.49	1.50	0.05	0.05	1	(.40, 1.50)	1	

We run five simulations in this setting. All groups have slope $m = 0$ in the pretreatment period with intercepts are 2, 1, and 0 for the upper control, treatment, and lower control groups, respectively. The treatment group receives a treatment of 1 in all five simulation results displayed in

Table 4. For purposes of comparison, the first row is the baseline case in which there is no violation of parallel trends.

The results show that combining the control groups and using the gDiD estimate performs better because this method leads to unbiased results and the simulated level of confidence remains approximately at the true 95% level of confidence throughout all five levels of $|U_{ic}| = U_{uc}$. On the other hand, while the sDiD and bDiD interval estimates contain the true treatment effect of q in each simulation, the CIs are much wider than those associated with the gDiD approach. In fact, the CI using the bDiD approach becomes so wide when $|U_{ic}| = U_{uc} = 1$, the use of the bDiD approach would result in a Type II error in that case.

The assumption that $|U_{ic}| = U_{uc}$ used in Simulation 4 is quite strong but leads to an important observation through comparison to Simulation 2: when the unobserved confounder leads to offsetting individual biases in the lower and upper DiD estimates, pooling can lead to unbiased results and a more powerful statistical analysis. Further, the midpoint of the bDiD interval is unbiased in this case. An analyst can gather evidence associated with which situation they are in by comparing the sDiD or gDiD estimate to the midpoint of the bDiD interval. If they find themselves in a situation like Simulation 4, it is likely efficacious to pool the control groups.

Data analysis

In this section, we apply both the standard and bDiD approaches to estimate the effect of MML on violent crime rates. There are economic reasons why MML might increase or decrease violent crime. If legalization decreases black market activity, it might decrease crime, whereas it might increase violent crime if it leads to more marijuana use and marijuana use increases the propensity of citizens to commit violent crimes.

Historical unobserved confounders might also impact violent crime rates in U.S. states after the implementation of MML. For example, states with strict marijuana laws might have more established black markets, which is difficult to measure. Recent analyses find that MML reduces crime (Shepard and Blackley, 2016; Gavrilova et al., 2019). However, other recent studies do not find a statistically significant change in crime rates as a result of MML (Green et al., 2010; Morris et al., 2014; Chu and Townsend, 2019).

We collected annual violent crime data from the FBI's Uniform Crime Reporting System from 1983 to 2014. The total violent crime rate, which is the sum of the murder, rape, robbery, and aggravated assault rates, is our outcome variable of interest. Dates of implementation of

legalized medical marijuana were collected from the National Conference of State Legislators. We divided states that had not implemented MML during our sample period into an upper and lower control group based on visual inspection of crime rate trends in these control states relative to treatment states. Five states are included in each group, and crime rate trends for these states are plotted in Figure 2.²

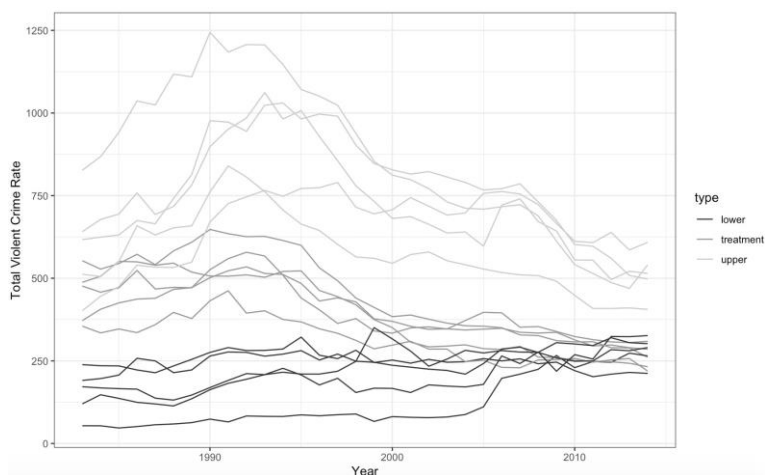


Figure 2: Crime rate trends in the upper control group, MML treatment group, and lower control group. Crime rates are measured per 100,000 residents.

Note from Figure 1 that the slope of the lower control group appears to increase relative to the slopes of the treatment group and upper control group after 2000. This change provides evidence of an unobserved confounder that affects each group differently. These violent crime data dovetail with our simulations in which the lower control group experiences a slope change that is inconsistent with the assumptions of the bDiD model after treatment resulting from an unobserved confounder.

The treatment states in our data enacted MML in different years.³ This requires the use of a more generalized DiD regression known as the

² The treatment states are Colorado, New Jersey, Oregon, Rhode Island, and Washington. The lower control states are Idaho, North Dakota, South Dakota, West Virginia, and Wisconsin. The upper control states are Florida, Louisiana, South Carolina, Tennessee, and Texas.

³ Oregon and Washington enacted in 1998, Colorado in 2000, Rhode Island in 2007, and New Jersey in 2009.

two-way fixed-effects DiD model in which state dummy variables replace the treatment group dummy variable and year dummy variables replace the post-treatment period dummy variable that we use in our simulations (Angrist and Pischke, 2009; Goodman-Bacon, 2018).

We estimate

$$y_{st} = \alpha + \gamma_s + \lambda_t + \beta D_{st} + \epsilon_{st} \tag{8}$$

using ordinary least squares in R, where α is a constant term, γ_s is a state fixed effect, λ_t is a year fixed effect, and D_{st} is equal to one if a violent crime observation occurs in a treated state after enactment of MML. β is the treatment effect.⁴ Individual state fixed effects replace the treatment group dummy variable to increase precision by controlling for heterogeneity within states. We estimate the sDiD by pooling the upper and lower control groups when estimating Eq. (8). We estimate the bDiD by estimating Eq. (8) with the lower control group and the upper control group separately.

Table 5 provides our different treatment effect estimates associated with the estimation of Eq. (8). The sDiD estimate is negative and very statistically significant. However, the bDiD estimate contains zero and has an upper bound indicating a large increase in the violent crime rate. The CI for the bDiD is much larger and indicates the possibility of a large negative effect, no effect, or a large positive effect.

Table 5: Comparison of standard and bracketed DiD estimates of impact of medical marijuana legalization on violent crime.			
	Standard	Lower	Upper
TE estimate	-77.699***	-161.853***	26.780
<i>t</i> statistics	(-4.257)	(-12.609)	(1.521)
95% CI	[-113.57, -41.82]	[-187.12, -136.59]	[-7.87, 61.43]
bDiD		[-161.853, 26.780]	
95% CI bDiD		[-187.12, 61.43]	

* $p < 0.05$, ** $p < 0.01$, *** $p < 0.001$

The estimates provided in Table 5 make the tradeoff between the two approaches clear: the standard approach provides much more power but may lead to erroneous conclusions in the presence of unobserved

⁴ See Goodman-Bacon (2018) for a detailed discussion of the two-way fixed-effects DiD regression. Abraham and Sun (2018), Borusyak and Jaravel (2017), and de Chaisemartin and D’Haultfœuille (2018) show that the two-way fixed-effects DiD regression generates an estimated treatment effect that is a weighted average of all possible two-by-two comparisons between treatment and control units including comparison between groups that are treated at different times (Goodman-Bacon, 2018).

confounders whereas the bracketed approach provides very wide interval estimates making it difficult to identify small effects. However, we saw from Simulation 4 that the estimate associated with the upper control group displayed the smallest bias when $U_{lc} > 0$ and $U_{uc} = 0$. If we have properly characterized the violent crime data as being in this category, the best estimate of the impact of MML on violent crime is the upper one that indicates MML increased violent crime by 26.78 per 100,000 per year. This estimate is not statistically significant, however. This result provides less evidence that MML decreased violent crime as compared with several previous analyses that find a statistically significant negative effect. Based on Figure 2 and the simulations, it is likely that the gDiD does not provide an improvement over sDiD or bDiD, hence we focus our analysis on these two estimators for the purposes of data analysis.

Conclusion

We ran several simulations to compare the bDiD approach of Hasegawa et al. (2019) with the sDiD estimator. The primary result is that application of the bDiD approach can make DiD analysis possible in situations where an unobserved confounding variable leads to violations of the parallel trends assumption, but this comes at a significant expense in terms of statistical power.

Our first simulation showed that application of the bDiD approach in the absence of confounding variables leads only to a loss of statistical power, and if an analyst is confident that the parallel trends assumption holds, the bDiD approach will only increase the probability of Type II errors. That simulation also showed that the bounds associated with the bDiD approach will be individually biased in such cases as a result of the ex post choice of the upper and lower bounds for the bDiD interval. Our second and third simulations showed a situation in which the bDiD could be more successful as a result of violations to the parallel trends assumption in one of the control groups. In the fourth simulation, we found that when the parallel trends assumption is broken in a mirrored way across the upper and lower control, the Gavin estimator provided accurate yet sufficiently powerful results, unlike sDiD or bDiD. Specifically, pooling and applying the sDiD might be optimal if unobserved confounders lead to bias in opposite directions in DiD estimates. The overall simulation results indicate that a best choice strategy would involve removing control units that are affected by the unobserved confounder to the extent this is possible.

We also showed how to estimate the bDiD interval using a two-way fixed effects DiD model and applied this method to an analysis of

the impact of MML on violent crime rates. Visual inspection of violent crime rate data in the control and treatment states motivated Simulation 3, and we argue that running such simulations based on visual inspection of data can help analysts confront potential biases in the different estimators. Our data analysis leads to a less clear picture of the impact of MML on violent crime relative to other analyses that find a large negative impact: we cannot reject the possibility of no impact and our best estimate is that there is a positive impact, although this estimate is statistically insignificant.

Our simulations and data analysis that compare the sDiD, bDiD, and gDiD can point analysts in the right direction when confronted with the possibility that unobserved confounding variables might lead to biased DiD estimates. Analysts can use the tables to guide their methods and weigh the costs and benefits of each method. Neither method is clearly superior, and choosing one depends on weighing the relative risks of an error and the size of the treatment effect in each scenario.

Future work

This paper assesses the performance of several DiD estimators in a broad range of scenarios so that a data analyst can determine which estimator is best used in each scenario. Although performance of a statistical method is important, it is also important to assess the assumptions of a statistical test. We would like to assign a p-value to the specific assumptions of bDiD estimation in a similar way that one can test the assumption of normality with, say, the p-value of a Shapiro test. In the paper by Ye et al. (2020), the authors have identified a negative correlation strategy for a falsification test using bootstrapping for partial identification of bDiD estimation; however, the test developed requires assumptions about the data. We are also interested in applying this statistical methodology to the shelter-in-place policies implemented during COVID-19 to determine the effectiveness of the policy. This study would be of interest to many economists, politicians, epidemiologists, and public health officials. Because almost every state at some point during the COVID-19 pandemic executed a stay-at-home order and these orders were issued at different times, we would typically use the methodology discussed by Goodman-Bacon for DiD estimation with multiple timing groups. Because of the nature of the data set, death rates are likely to be affected by a variety of unobserved confounding factors, and this suggests the use of bracketing to estimate the effect of shelter-in-place policies. In this instance, the data analysis of COVID-19 shelter-in-place policies and methodology would both be novel.

References

Abadie, A. (2005). Semiparametric difference-in-differences estimators. *The Review of Economic Studies* 72(1), 1–19.

Abraham, S. & L. Sun (2021). Estimating dynamic treatment effects in event studies with heterogeneous treatment effects. *Journal of Econometrics* 225(2), 175–199

Andrews, I. & M. Kasy (2019). Identification of and correction for publication bias. *American Economic Review* 109(8), 2766–2794.

Angrist, J.D. & J.-S. Pischke (2009). *Mostly Harmless Econometrics: An Empiricist's Companion*. Princeton, NJ: Princeton University Press.

Bernal, J., S. Cummins, A. Gasparrini (2017). Interrupted time series regression for the evaluation of public health interventions: a tutorial. *International Journal of Epidemiology* 46, 348–355.

Bertrand, M., E. Duflo, S. Mullainathan (2004). How much should we trust differences-in-differences estimates? *Quarterly Journal of Economics* 119(1), 249–275.

Borusyak, K. & X. Jaravel. (2017). Revisiting event study designs. *Harvard University Working Paper*. Retrieved April 20, 2022 from <https://arxiv.org/abs/2108.12419>.

Card, D. & Krueger, A.B. (1995). Time-series minimum-wage studies: a meta-analysis. *American Economic Review*, 85(2), 238–243.

Chu, Y.-W.L. & W. Townsend (2019). Joint culpability: The effects of medical marijuana laws on crime. *Journal of Economic Behavior & Organization* 159, 502–525.

Cook, T., D. Campbell, & W. Sadish (2002). *Experimental and Quasi-Experimental Design for Generalized Causal Inference*. Boston, MA: Houghton Mifflin.

de Chaisemartin, C. & X. D'Haultfœuille (2018). Fuzzy difference-in-differences. *Review of Economic Studies* 85(2), 999–1028.

Dimick, J.B. & A.M. Ryan (2014). Methods for evaluating changes in health care policy: The difference-in-differences approach. *JAMA* 312(22), 2401–2402.

Gavrilova, E., T. Kamada, F. Zoutman (2019). Is legal pot crippling Mexican drug trafficking organisations? The effect of medical marijuana laws on US crime. *Economic Journal* 129(617), 375–407.

Goodman-Bacon, A. (2021). Difference-in-differences with variation in treatment timing. *Journal of Econometrics* 225(2), 254–277.

Green, K.M., E.E. Doherty, E.A. Stuart, M.E. Ensminger (2010). Does heavy adolescent marijuana use lead to criminal involvement in adulthood? evidence from a multiwave longitudinal study of urban African Americans. *Drug and Alcohol Dependence* 112(1-2), 117–125.

Hasegawa, R.B., D.W. Webster, D.S. Smalls (2019). Evaluating Missouri’s handgun purchaser law: A bracketing method for addressing concerns about history interacting with group. *Epidemiology* 30(3), 371–379.

Lee, J.D., D.L. Sun, Y. Sun, J.E. Taylor (2016). Exact post-selection inference, with application to the lasso. *Annals of Statistics* 44(3), 907–927.

Meyer, B. (1995). Natural and quasi-experiments in economics. *Journal of Business & Economic Statistics* 13, 151–161.

Morris, R.G., M. TenEyck, J.C. Barnes, T.V. Kovandzic (2014). The effect of medical marijuana laws on crime: evidence from state panel data. *PLoS One* 9(3), 7–31.

Nadarajah, S. & S. Kotz (2008). Exact distribution of the max/min of two gaussian random variables. *IEEE Transactions on Very Large Scale Integration (VLSI) Systems* 16(2), 210–212.

Roth, J. (2018). Should we adjust for the test for pre-trends in difference-in-difference designs? *arXiv*, 1804.01208

Shepard, E.M. & P.R. Blackley (2016). Medical marijuana and crime: further evidence from the Western states. *Journal of Drug Issues* 46(2), 122–134.

Ye, T., L.J. Keele, R. Hasegawa, D.S. Small (2020). A negative correlation strategy for bracketing in difference-in-differences with application to the effect of voter identification laws on voter turnout. *arXiv*, 2006.02423.

An Exploratory TribalCrit Analysis of Educators Rising's Role in Teacher Recruitment

William J. Davis

Southern Utah University

Abstract

This intrinsic case study analyzed the community-based framing of the work of Educators Rising, a nationwide organization that aims to develop a pipeline between secondary students and the teaching profession. Using TribalCrit to examine publicly available documents, videos, and websites, the study found Educators Rising primarily framed community as a place: communities are physical locations that need teachers, the original impetus for Educators Rising's existence and work. Through its partnerships with schools and districts, Educators Rising seeks to cultivate market-oriented views of knowledge and teaching in these communities. The organization's standards and activities privilege certain academic knowledge over cultural knowledge. Building from this view of certain academic knowledge, Educators Rising packages conceptions of teaching forged by external entities like the National Board for Professional Teaching Standards, which participants are expected to assimilate through their involvement in the organization. Additionally, Educators Rising attempts to enforce

assimilation of external conceptions of teaching through competitions and micro-credentials. Communities, from Educators Rising's perspective, are sites to assimilate certain knowledge and narrow conceptions of teaching and teacher learning, primarily through student participation in competitive activities. Recommendations for effective partnerships are discussed.

Community is a central focus in several Utah teacher recruitment initiatives. One source of this community focus is Utah's Grow Your Own Teacher and School Counselor Program (2021) legislation, which provided funding to recruit community members like paraprofessionals as professional teachers (Reed, 2021). In a separate initiative, Utah's Career and Technical Education (CTE) office has attempted to seize on the promise of potential teachers in local communities by developing secondary-level teacher career exploration courses for students interested in teaching careers (Career Pathway: K-12: Teaching as a Profession, 2021). Through career cluster pathways and teacher endorsement requirements, Utah's CTE office promotes co-curricular participation in Educators Rising, a nationwide career and technical student organization with its own community-based recruitment focus: Educators Rising (2020) claims that nearly 60% of teachers end up teaching within 20 miles of their own K-12 schools, leading the organization to promote the development of school-based chapters that seek to generate interest in the teaching profession among secondary students. Educators Rising's goal is to create a pathway between local communities and the teaching profession.

Although Educators Rising's community-based recruitment emphasis seems sensible, it reflects a singular view of community—specifically schools—as a physical place for which Educators Rising seeks to provide teachers. This singular view of community demonstrates the narrow, Western-dominant interpretations of community traditionally adopted in education research and work (Kulago, 2012; Nieto et al., 2008). As Educators Rising expands in states like Utah, the organization is likely to come into contact with Indigenous peoples, who may possess fundamentally divergent views concerning community (Kulago, 2012) and how participation in an organization like Educators Rising may impact their communities. The purpose of this paper is to examine Educators Rising through an analysis of publicly accessible documents using a divergent Indigenous lens, specifically using Brayboy's (2005) Tribal Critical Race Theory.

Theoretical Framework

Teacher Shortages and Recruitment: Trends and Initiatives

K-12 teacher recruitment and retention challenges in Utah have mirrored challenges across the United States. Teacher shortages have been identified as the product of supply and demand imbalances, which have periodically occurred since at least the 1990s (Barry & Shields, 2017). However, key events during the preceding 15 years have greatly exacerbated staffing challenges in the US and Utah. First, college/university teacher preparation programs were struck by a 35% reduction in enrollments between 2009 and 2014 (Sutcher et al., 2016). Second, the COVID-19 pandemic is thought by some to have impacted teacher preparation program enrollments and K-12 school staffing. Although researchers have debated the impact of the pandemic on teacher attrition and mobility (e.g., Goldhaber & Theobald, 2021), 20% of teacher preparation programs reported double-digit declines in enrollment (Will, 2022), and school systems continue to report staffing challenges (Carver-Thomas et al., 2021; Gecker, 2021). These trends have been observed across Utah during this same period (Jackson, 2022; Lindberg, 2016), particularly in school districts with higher percentages of Indigenous students. Both San Juan District (49% Native American) and Uintah School District (7% Native American) reported teacher vacancies on the first day of the 2021-2022 school year; both districts also reported teacher turnover rates greater than 14%, the fifth and sixth highest rates among Utah's 41 school districts (State of Utah Legislative Auditor General, 2021).

In response to teacher shortages, Utah and other US states and school districts have employed an array of initiatives, including “grow-your-own” programs. Some initiatives have focused on incentives for teachers, including increased salaries, tax credits, fellowships, grants, and even loan forgiveness (Barry & Shields, 2017). In Utah, low salaries are thought to be linked to staffing challenges (Jackson, 2022), which may explain the emphasis in Utah on salary increases (Smith & Ho, 2019). With the passage of the Grow Your Own Teacher and School Counselor Program (2021) legislation, the State of Utah joined the states and school systems that have sought to develop pipeline programs to recruit existing community members like paraprofessionals to the teaching profession (Gist et al., 2019; Simmons, 2018; Valenzuela, 2017). Grow-your-own programs have expanded in recent years to include initiatives aimed at secondary students such as high school courses, dual credit enrollment offerings, mentorship programs, and career and technical organizations like Educators Rising (Audrain &

Googins, 2020; Davis, 2021; Gist et al., 2019; Googins, 2019). In some cases, including Educators Rising as well as the university-based program described by Gist et al. (2019), grow-your-own programs have placed special emphasis on the recruitment of teachers of color.

Market-Based Reform and Community in Teacher Education

Amid these teacher recruitment initiatives, there has been a precipitous increase in market-based reforms in teacher education. Market-based reforms draw from neoliberal views of free-market capitalism that emphasize top-down government directives, demand strict accountability measures, deregulate public entities like schools, normalize competition, and/or emphasize uniformity (Jess et al., 2021; Philip et al., 2019; Werler, 2016; Zeichner, 2010). Rather than a strictly American phenomenon, neo-liberal, market-based reformers have impacted teaching and teacher education across the world (Zeichner, 2010). In some instances, market-based reforms take the form of “travelling policy ideas” like the Teach for All movement, leading to the proliferation of boot-camp-style pathways to teacher certification (Ellis et al., 2016, p. 64; see also Friedrich, 2014). As these ideas move, so too do particular, narrow approaches to or framings of teaching, such as the emphasis on core instructional practices to learn in teacher preparation programs (e.g., Philip et al., 2019) and the privileging of the psychological sciences in teaching and learning (e.g., Friedrich, 2014). By centering these and other narrow approaches to or framings of teaching, teacher learning is recast as a commodity to be transmitted—through courses, boot-camp-style preparation, and even the purchasing of micro-credentials (Werler, 2016; Zeichner, 2010).

The proliferation of market-based reforms in teacher education, including the commodification of teacher learning, directly challenges teacher preparation programs’ emphases on democratic education and community resources or assets. Democratic teacher education, in which teacher preparation is “a public enterprise for the common good” that centers equity and justice in democratic societies, differs from top-down, managerial or entrepreneurial, hyper-pragmatic forms of teacher education promoted in some teacher preparation programs (Cochran-Smith et al., 2018, p. 581). Cochran-Smith et al. (2018) argued that democratic teacher educator reformers view market-based reforms as antithetical to “community knowledge traditions” and other democratic education goals like equity and justice (p. 582). Indeed, as Paine and Zeichner (2012) pointed out, while it may be impossible in the modern world to ignore change efforts elsewhere in the world while reforming

teacher education in a given context, community knowledge traditions like “historical and cultural practices, traditions, and institutions” are important mediators of policies and practices originating in external contexts (p. 579). Local conditions and challenges cannot be ignored when drawing ideas from external contexts, whether such ideas are state/provincial, national, or even global in origin.

Examining Community through a TribalCrit Lens

To orient this inquiry towards the local, specifically towards the Indigenous communities of Utah, this study utilizes Tribal Critical Race Theory (hereafter referred to as TribalCrit). TribalCrit was developed by Brayboy (2005) from Critical Race Theory, through which racism has been positioned as endemic in society. However, as multiple scholars have noted, Critical Race Theory’s focus on racism—at times presented as a Black-White binary (Solórzano & Yosso, 2002, p. 39)—does not adequately address the particular needs and challenges of Indigenous peoples (Brayboy, 2005; Carter Andrews et al., 2019; Martinez-Cola, 2020). Brayboy (2005) outlined nine tenets of his variant of Critical Race Theory:

1. Colonization is endemic to society.
2. U.S. policies toward Indigenous peoples are rooted in imperialism, White supremacy, and a desire for material gain.
3. Indigenous peoples occupy a liminal space that accounts for both the political and racialized natures of our identities.
4. Indigenous peoples have a desire to obtain and forge tribal sovereignty, tribal autonomy, self-determination, and self-identification.
5. The concepts of culture, knowledge, and power take on new meaning when examined through an Indigenous lens.
6. Governmental policies and educational policies toward Indigenous peoples are intimately linked around the problematic goal of assimilation.
7. Tribal philosophies, beliefs, customs, traditions, and visions for the future are central to understanding the lived realities of Indigenous peoples, but they also illustrate the differences and adaptability among individuals and groups.
8. Stories are not separate from theory; they make up theory and are, therefore, real and legitimate sources of data and ways of being.
9. Theory and practice are connected in deep and explicit ways such that scholars must work towards social change. (pp. 429-430)

Although TribalCrit scholars view colonization as endemic in society, Brayboy's (2005) theory also engages with the role of racism in the interactions between Indigenous and Western peoples.

TribalCrit has been used by scholars to study Indigenous peoples and perspectives in education, including teacher education and learning. Such scholarship has included TribalCrit analyses of court rulings and school segregation for Indigenous peoples (e.g., Martinez-Cola, 2020), examinations of how Indigenous peoples and issues are portrayed in social studies curricula (e.g., Krueger, 2021), and Indigenous teacher mentorship aimed at supporting responsive educators (e.g., Anthony-Stevens et al., 2022), among others. Teacher educators also have recognized the power of TribalCrit to unmask, expose, and confront "continued colonization within educational contexts and societal structures," leading to examinations of multicultural teacher education (e.g., Writer, 2008, p. 1), teacher preparation for Aboriginal teachers (e.g., Kitchen et al., 2010), and teacher educators' experiences in community-based Aboriginal teacher education programs (e.g., Kitchen & Hodson, 2013). Writer and Oesterreich's (2011) study is particularly noteworthy; using TribalCrit to study a teacher recruitment and retention initiative for Pueblo people, they noted that teacher education, including retention and recruitment, must be "a collective effort" consisting of "partnership[s] for and with native communities" (p. 519). Such calls for an emphasis on community and partnership building in teacher education and recruitment for Indigenous communities have inspired the present study, which is undergirded by the following research question: what does a TribalCrit analysis of Educators Rising's publicly accessible documents reveal about its "community-oriented" emphasis?

Method

The present study is an intrinsic case study of Educators Rising, one that focuses on Educators Rising to understand the organization itself rather than understand other organizations or entities (see Stake, 1995). Qualitative document analysis, an approach that involves a "systematic procedure for reviewing or evaluating documents" (Bowen, 2009, p. 27), was used to study Educators Rising. Documents in this study are viewed as "social products" that reflect "wider norms and values" as opposed to objective facts (Wood et al., 2020, p. 458). As social products, documents may suggest a reality that researchers describe through their inquiry. In addition, documents can serve as "actors in their own right," which are not strictly passive and may be used in certain ways within a social sphere; research can help explain how the document "functions in patterns and structures of social

activity” (p. 459; see also Prior, 2008). This study examines both the wider norms and values suggested by its documents as well as the use of those documents.

Study Context

Educators Rising is the focal case for this study. Educators Rising is a nationwide organization that is administered by PDK International and Curriculum Management Solutions, Inc. The organization’s stated goal is to employ a community-based model to promote teacher recruitment across the country so that a pathway exists between every school in the country and the teaching profession. Thirty-five states have started their own Educators Rising affiliates, typically administered by state-level CTE offices; the remaining 15 states have at least some Educators Rising presence in them. Whereas the national organization develops standards for secondary-level teacher career exploration classes and hosts an annual conference with competitions in various areas, state-level Educators Rising affiliates primarily work with schools and districts to develop local chapters. These chapters may be coupled with high school classes, or they may exist as standalone clubs in schools and colleges/universities. Participants qualify for the national-level competitions by participating in state-level competitions. Educators Rising also has partnered with companies like Digital Promise to produce a system of five micro-credentials that secondary students can complete. This analysis examines documents describing and/or related to Educators Rising, rather than offering an empirical examination of the program’s implementation and variability at the school/chapter level, or an investigation of multiple elements of the professional learning continuum for teachers (e.g., preservice teacher education; in-service professional development; see Feiman-Nemser, 2001).

Data Sources

Data sources for this study included Educators Rising’s publicly accessible documents, videos, and websites. These sources included Educators Rising’s teaching standards, promotional or recruitment fliers, and video anecdotes or stories available on online platforms like YouTube. All documents and videos were downloaded or otherwise captured using NVivo 12, a qualitative data analysis program. In addition to Educators Rising’s publicly accessible documents, the study included documents, rubrics, and websites from Educators Rising partners like Digital Promise, as well as college/university sites that documented their involvement with Educators Rising. All data were stored in an NVivo 12 project for data analysis.

Data Analysis

Initial coding of all data used a form of structural coding (see Saldaña, 2016). A node was created for each tenet of Brayboy's (2005) TribalCrit, and all data sources were coded using these nine nodes. Once all data sources were reviewed using structural coding, a subsequent round of coding was conducted using axial coding to identify the characteristics, attributes, or dimensions of each original node's contents (Saldaña, 2016). Axial coding was conducted simultaneously with analytic memoing (Birks et al., 2008), which was used to examine similarities in axial coding across the TribalCrit nodes. As similarities became more pronounced in axial coding, the data was themed (Saldaña, 2016) through the drafting of phrases that helped to explain the connection and meaning of the common data points. Preliminary findings were critiqued at regional conferences through peer-review and in-person discussion, then revised and expanded based on these reviews (see McGloin, 2008). These connections were further explored in coding and in memos, ultimately yielding the categories presented below in the findings.

Positionality

TribalCrit's use as an analytical lens demands an examination of my own positionality as a researcher. I began my teaching career in northwest New Mexico in a school that was 80%+ Navajo. Socialized into a white, Anglo-American, middle-class culture situated thousands of miles from where I was teaching, I was an outsider in this New Mexico community, one who only began to develop a beginning awareness of Indigenous cultures and perspectives. Although an outsider perspective may have some merit in research (Merriam et al., 2001), it may have limitations and even present problems (Banks, 1998), perhaps most notably the "partial understanding of and little appreciation for the values, perspectives, and knowledge of the community" (p. 8). This study does not examine a particular community group, but I am cognizant of the limitations of my understanding of Indigenous peoples and cultures. My intent in using TribalCrit is not to appropriate an Indigenous perspective, but rather to position myself on the periphery of both teacher recruitment and Indigenous communities to develop a "more robust, more accountable, [and] more usable" perspective on Educators Rising (see Meyer, 2010, p. 123), and thus transform our understanding of the organization and its recruitment work.

Findings

The Privileging of Academic over Community or Cultural Knowledge

Educators Rising privileges the accumulation of acontextual academic knowledge over locally developed or community or cultural knowledge. In Educators Rising’s standards, rising educators—a reference to secondary-aged participants in the program—are said to “know that teachers utilize content knowledge and pedagogical expertise within their planning and practice.” Rising educators build content and pedagogical knowledge and expertise by “taking classes, reading and discussing ideas, observing the instruction of effective teachers, or researching topics that fascinate them.” In addition to content and pedagogical knowledge, learning to teach requires understanding of “educational theories and cognitive science,” including theories of child development. Teaching requires explicit planning that combines content standards and knowledge, curricular goals, and student needs and interests.

Although the standards ask that rising educators learn about K-12 students, students are expected to do this using academic knowledge from the psychological sciences. To understand students is in large part to apply theories of “social, emotional, physical, and cognitive development.” Students’ capacities to build knowledge and skill are said to vary by stage of development “from infancy to adulthood,” requiring rising educators to use these perspectives to “[form] relationships with [students] as people and [distinguish] them as learners.” Thus, Educators Rising frames the K-12 student as a primarily psychological being, making the psychological sciences the central lens of teaching and learning to teach.

When community or cultural knowledge is invoked by Educators Rising’s documents, it is secondary to forms of academic knowledge like the psychological sciences. From their social, emotional, physical, and cognitive understanding of students, rising educators are expected to “learn about students and develop cultural competence” in order to “[respond] positively to students’ individual needs to help them succeed and to elevate their voices.” However, the connection between cultural competence and students using their voices is unclear. Cultural competence is identified in the standards as a cross-cutting theme that reflects rising educators’ abilities “to successfully teach students who come from a culture or cultures other than one’s own.” Another cross-cutting theme of the standards is social justice and advocacy, including the ability to “promote the interests of students and communities”;

advocacy is framed in terms of the teachers'—rather than the students'—abilities to promote these interests. Interestingly, words like culture, social justice, and advocacy do not appear to be included in the rubrics for Educators Rising competitions like the “impromptu lesson” or “public speaking.” One reference to culture can be found in the rubrics: students are permitted to wear head covers “required for religious purposes or to honor cultural tradition[s].”

The view of knowledge espoused by Educators Rising is one that emphasizes acontextual, externally constructed academic knowledge, which reflects Friedrich's (2014) critique of certain neo-liberal teacher education reforms as privileging certain knowledge. The accumulation of such knowledge, whether it is as a K-12 student or as a teacher, is framed as orderly and predictable, with the when and how of student learning developed according to knowledge of human development and a static view of content knowledge. These views of teaching and learning as certain and static are codified by various professional teaching organizations, including those that partner with Educators Rising.

Assimilating Conceptions of Teaching and Professionalism Developed Outside the Community

Participating in Educators Rising requires rising educators to consider the privileging of certain, academic knowledge while assimilating particular views of teaching promoted by a number of professional teaching organizations that almost always exist far away from school communities. Educators Rising's curriculum was developed in conjunction with the National Board for Professional Teaching Standards (NBPTS), along with support from the National Education Association and American Federation of Teachers. The standards also drew from Pearson's edTPA portfolio assessment. Educators Rising, the NBPTS, and edTPA all promote a normative, universal “cycle” of teaching consisting of planning, instruction, assessment, and reflection. This cycle also is commonly found in state teaching evaluations for professional teachers, which local schools are often required to utilize for teacher evaluation.

The psychological sciences, along with a certain and predictable view of learning, sit at the center of the “cycle” of teaching. Learning objectives perhaps best illustrate psychology's presence within the cycle. Popularized in education circles by Tyler (1949/2013) as part of a psychology of learning, objectives were put forth as a way to isolate “results to be achieved from learning” (p. 37). When combined with assessments, the authoring of objectives helped to create curricular goals, which enabled the measurement of learning. Educators Rising's

standards emphasize the importance of measuring learning; teachers are said to measure learning using an array of assessments along with “curricular goals and objectives as well as the diverse needs of students.” The close relationship between objectives and assessment is perhaps most obvious in the Digital Promise formative assessment micro-credential, which requires student learning objectives in a lesson plan, as well as a written rationale for both learning objectives and assessments.

Through its standards, competitions, and micro-credentials, Educators Rising can bypass communities and college/university teacher preparation programs and introduce its psychology-centric view of teaching directly to program participants in local chapters. A major thrust of Educators Rising’s marketing is the establishment of a pipeline between communities and the teaching profession. Yet communities to Educators Rising are little more than a place for teachers to work, with special characteristics that are alluded to in the standards and micro-credentials without meaningful consideration. Similarly, the role of college/university teacher preparation programs is underplayed; even though more than three-quarters of teachers are prepared in traditional, college/university-based teacher preparation programs (National Center for Education Statistics, 2022), the nature of teacher learning within these programs is barely addressed by Educators Rising. Instead, the standards include 19 statements of what rising educators will do “[a]fter high school,” including “refine their planning skills” and “collaborate with stakeholders throughout the learning environment,” without addressing the site(s) where such skills are developed. The expectations of professional teaching organizations, based on a singular psychology-centric view of teaching derived outside of schools and communities, are thus mapped back into activities by Educators Rising, without concern for local views of teaching, either in communities themselves or college/university teacher preparation programs.

External Validation and Verification of (Teacher) Learning

Educators Rising’s competitive activities and micro-credentials do more than introduce the “cycle” of teaching and professional teaching standards produced beyond individual communities. They portray professional learning as something that should be validated and verified by those outside the community. Knowledge and skills related to teaching and learning are created beyond communities where rising educators will teach, and mastery of such knowledge and skills must be approved by outsiders as well.

State and national competitions hosted by Educators Rising are one example of validation and verification of certain forms of (teacher)

learning. Competitions may include a variety of different activities, such as delivering a creative lecture or mock presentation, discussing an ethical dilemma, delivering impromptu lessons or speeches, and sharing a planned lesson. Educators Rising has established rules and rubrics for these competitions, which are evaluated by a panel of judges. Judges may come from a variety of roles and positions, although judging is pitched as a particular pathway for “collegiate” Educators Rising advisors to participate in the program. Rising educators may participate in state-level competitions, which can help them qualify for the annual national-level conference and competitions. Competitions represent something of a paradox in terms of community: the more successful rising educators are, the larger the competition they participate in, and the more decontextualized the judging becomes since participants are evaluated by judges from beyond their own home states and communities.

External validation and verification of learning is also conducted through the earning of Digital Promise’s micro-credentials. Educators Rising offers micro-credentials in five areas: anti-bias instruction, classroom culture, collaboration, formative assessments, and learning engagement. Each micro-credential costs \$75 and requires documentation of learning in the chosen area. For example, the learning engagement micro-credential requires submission of a particular form, which captures information about a written plan and a 4–6-minute video-recorded lesson that must be submitted. Rising educators must demonstrate through their plan, video, and submission form that they have completed a teaching cycle where they have planned, taught, assessed, and analyzed their own teaching. Micro-credentials frame learning as something marketed, designed, and assessed by external forces, while educators are presented as “market-oriented customer[s] of learning opportunities” (Werler, 2016, p. 69). Learning to teach, then, necessarily involves someone other than educators themselves, typically an individual who is not part of the educator’s own community and culture.

Competitive activities focusing on both teaching and soft skills, as well as micro-credentials, enculturate rising educators into a profession where external review and competition are considered normal elements of being a teacher. Educators Rising describes both competitive activities and micro-credentials as opportunities to “demonstrate...knowledge, skills, and leadership in education” or “showcase...growing skills” in teaching. Micro-credentials in particular represent an effort to equip rising educators with paper qualifications, although it is unclear whether schools/colleges of education and school districts recognize micro-credentials. Tooley and Hood (2021) traced the origins of micro-credentials to Digital Promise, which began to develop and market these

credentials in 2014. Despite nearly a decade in existence, micro-credentials are not universally used in education, and even Educators Rising has noted that it is “working with” different institutions and employers “to recognize and value micro-credential achievement.” The effort to find institutions and employers who will recognize micro-credentials continues despite questions surrounding the implementation of micro-credential systems and the link between micro-credentials and teacher performance and/or student learning (e.g., Aydarova, 2021; Reider, 2022).

Discussion and Conclusion

This intrinsic case study analyzed the community-based framing of the work of Educators Rising, a nationwide organization that aims to develop a pipeline between secondary students and the teaching profession. Using Brayboy’s (2005) TribalCrit to examine publicly accessible documents, videos, and websites, the study found Educators Rising primarily framed community as a place: communities are physical locations that need teachers, the original impetus for Educators Rising’s existence and work. Through its partnerships with schools and districts, Educators Rising seeks to cultivate market-oriented views of knowledge and teaching in these communities. The organization’s standards and activities privilege certain academic knowledge (see Friedrich, 2014) over community or cultural knowledge. Building from this view of certain academic knowledge, Educators Rising packages conceptions of teaching forged by external entities like the NBPTS, which participants are expected to assimilate through their involvement in the organization. Additionally, Educators Rising attempts to enforce assimilation of external conceptions of teaching through competitions and micro-credentials. Communities, from Educators Rising’s perspective, are sites to assimilate certain knowledge and narrow conceptions of teaching and teacher learning, pursued primarily through student participation in competitive activities.

Analyzing Educators Rising’s goals and work may depend, in part, on how the organization is situated in the teacher recruitment and preparation landscape. If Educators Rising is viewed as the former, and its goal is simply to establish guidelines for state affiliates and local chapters as they promote teacher recruitment, then labeling the organization’s work as assimilative could be seen as unfair, as its very goal would be to scale its program up in the name of recruitment. However, the stronger case can be made for the latter: by integrating professional teaching standards and frameworks like those of the NBPTS and edTPA into its programming, Educators Rising, in effect, extends

the professional learning continuum for teachers into secondary schools. Instead of formal studies as a teacher beginning in college or university teacher preparation programs, the continuum Feiman-Nemser (2001) outlined is being reconceptualized to begin, at least in some states and schools, with secondary-level programming. From this view, Educators Rising—along with teacher academies, internships, and teacher career exploration courses—represent a new curricular frontier for teacher learning. Taken as a curriculum, as Educators Rising sometimes markets its program as, Educators Rising’s programming can—and, I think, should—be critiqued as a form of teacher preparation.

Regardless of whether it is viewed as a recruitment initiative or as part of a secondary-level curriculum of teacher education, Educators Rising exemplifies reform through “the neoliberal playbook” described by Philip and colleagues. Market-based, neoliberal “solutions” like competition and uniformity are presented in response to “problem[s]” presented by public schooling as well as teacher education (Philip et al., 2019, p. 251). In Educators Rising’s case, the problem, rather than the kinds of “manufactured calamit[ies]” Philip et al. (2019) critiqued (p. 252), is real: public schools across the country are struggling to find adequate numbers of certified and qualified teachers to staff their openings (Carver-Thomas et al., 2021; Gecker, 2021; Jackson, 2022). The solution presented is the cultivation of a more uniform, if not standardized, view of knowledge and teaching (see Friedrich, 2014; Philip et al., 2019), one introduced and drilled into secondary students before they enter college/university teacher preparation programs. In other words, Educators Rising doubles down on what it regards as the essence of teaching, claiming greater and earlier understanding of this essence will spur recruitment. This belief persists despite precipitous declines in teacher preparation program enrollments during a period in which the plan-teach-assess-reflect cycle, measurable objectives, and other aspects of Educators Rising’s psychology-centric view of teaching have remained central elements of public school teaching (Sutcher et al., 2016; Will, 2022). Rather than consider the working conditions of teachers or other aspects of their work and lives (see Aydarova, 2021), Educators Rising frames the problem entirely as an issue of teacher supply.

The arrival of Educators Rising into Indigenous communities risks alienation, if not outright rejection. Although Educators Rising presents itself as a community-based initiative, little evidence of an authentic, two-way partnership was uncovered in this study. Moreover, all the knowledge of teaching and learning that Educators Rising appears to value originates in professional organizations or Educators Rising itself, reflecting white, middle-class cultural expectations for schools (Kulago,

2012). To partner with Educators Rising is to submit to the organization's view of teaching, along with the competitive activities the organization promotes at state and national levels. Indigenous, or even just *different*, ways of knowing, which Brayboy (2005) identified as crucial elements in meeting the needs of Indigenous communities, are not considered or prioritized in Educators Rising's documents, videos, and websites. Furthermore, Educators Rising's emphasis on competition is antithetical to the way many Indigenous children are raised, where cooperation is preferred to competition (Brayboy, 2005). Instead of the kind of "collective effort" that results in a "partnership for and with native communities" (Writer & Oesterreich, 2011, p. 519), Educators Rising appears to partner with schools and districts to oversee secondary students' assimilation of certain forms of knowledge and teaching.

Establishing a teacher recruitment pipeline is a laudable goal, but creating such a pipeline through authentic community partnerships requires a more inclusive, contextualized effort. At the most fundamental level, secondary students must be viewed as learners who have an array of experiences in schools to draw upon; this group's assets for teacher learning are seldom recognized, and in some cases are even pathologized by teacher educators and policymakers. To cultivate authentic partnerships with Indigenous communities is to privilege tribal sovereignty and self-determination by developing a shared academic capital rather than risking further colonization from external institutions (Brayboy, 2005; Writer & Oesterreich, 2011). Such partnerships necessarily involve the integration of community and tribal knowledge in the standards and curriculum of teacher preparation. If the curriculum of teacher preparation spans high schools and college/university teacher preparation programs, which now seems to be the case in a number of states, the integration of community and tribal knowledge should be an essential element of this curriculum in all settings. Teacher recruitment is not something done *to* or *for* communities; it requires a multilateral collaboration focused on the community's specific needs beyond simply staffing teaching positions.

Educators Rising's structure, with its local chapters, state affiliates, and national organization—including events that take place at the state and national levels—offers tremendous potential for such multilateral collaborations in teacher learning. Bringing together rising and professional educators across a state provides opportunities to surface different ways of knowing, learning, and teaching, which groups of educators could analyze using approaches that parallel the collaborative ways professional learning communities work in schools. Instead of tapping teachers, teacher educators, and others to serve as judges, secondary students could partner with these educators to evaluate

teaching and planning demonstrations to identify which best reflect dynamic local innovation and/or a successful demonstration of professional teaching expectations. Within the existing structure, Educators Rising could promote teacher learning demonstrations and discourse where community practice and knowledge are valued and shared with the widest possible audience. Sharing and valuing community practice and knowledge could spur interest in the teaching profession and learning as teachers as much, if not more, than mock presentations and other competitive activities, assuming community knowledge and teaching practices were viewed as equal to, if not greater than, decontextualized knowledge and conceptions of teaching practice.

Although this study, like all others, has limitations, its findings warrant additional research. This particular study focused on Educators Rising's publicly accessible documents, videos, and websites. Consequently, the perspectives of Educators Rising staff members, along with youth and adult participants of the organization, are absent from this inquiry. This omission also excludes accounts of local (and Indigenous) implementation of Educators Rising's standards and various activities. These perspectives, along with longitudinal studies that follow rising educators into teacher preparation and the teaching profession to assess the effectiveness of Educators Rising as a recruitment vehicle, represent important next steps for researchers in understanding teacher recruitment and the preparation of teachers.

References

Anthony-Stevens, V., Moss, I., Jacobson, A., Boysen-Taylor, R., & Campbell-Daniels, S. (2022). Grounded in relationships of support: Indigenous teacher mentorship in the rural west. *The Rural Educator*, 43(1), 88-104. <https://doi.org/10.35608/ruraled.v43i1.1209>

Audrain, R.L., & Googins, J. (2022). Beyond teaching teddy bears: Generating and sustaining high school students' interest in the teaching profession through clinical practice. In D. Polly & E. Garin (Eds.), *Preparing Quality Teachers: Advances in Clinical Practice*. Information Age Publishing, Charlotte, NC

Aydarova, E. (2021). *NEPC Review: Harnessing Micro-credentials for Teacher Growth*. National Educational Policy Center, Boulder, CO. Retrieved on November 14, 2022, from <https://nepc.colorado.edu/thinktank/microcredentials>

Banks, J.A. (1998). The lives and values of researchers: Implications for educating citizens in a multicultural society. *Educational Researcher*, 27(7), 4-17. <https://doi.org/10.3102/0013189X027007004>

Barry, B., & Shields, P.M. (2017). Solving the teacher shortage: Revisiting the lessons we've learned. *Phi Delta Kappan*, 98(8), 8-18. <https://doi.org/10.1177/0031721717708289>

Birks, M., Chapman, Y., & Francis, K. (2008). Memoing in qualitative research: Probing data and processes. *Journal of Research in Nursing*, 13, 68-75. <https://doi.org/10.1177/1744987107081254>

Bowen, G.A. (2009). Document analysis as a qualitative research method. *Qualitative Research Journal*, 9(2), 27-40. <https://doi.org/10.3316/QRJ0902027>

Brayboy, B.M.J. (2005). Toward a Tribal Critical Race Theory in education. *The Urban Review*, 37(5), 425-446. <https://doi.org/10.1007/s11256-005-0018-y>

Carter Andrews, D.J., Brown, T., Castillo, B.M., Jackson, D., & Vellanki, V. (2019). Beyond damage-centered teacher education: Humanizing pedagogy for teacher educators and preservice teachers. *Teachers College Record*, 121(6), 1-28. <https://doi.org/10.1177%2F016146811912100605>

Carver-Thomas, D., Leung, M., & Burns, D. (2021). *California teachers and COVID-19: How the pandemic is impacting the teacher workforce*. Learning Policy Institute. Retrieved on November 17, 2022, from <https://doi.org/10.54300/987.779>

Cochran-Smith, M., Stringer Keefe, E., & Carney, M.C. (2018). Teacher educators as reformers: Competing agendas. *European Journal of Teacher Education*, 41(5), 572-590. <https://doi.org/10.1080/02619768.2018.1523391>

Davis, W.J. (2021). Recruitment of teachers of color: On “gifts and talents.” *Kappa Delta Pi Record*, 57(2), 52-54. <https://doi.org/10.1080/00228958.2021.1890436>

Educators Rising. (2020). Retrieved on November 17, 2022 from <https://educatorsrising.org>

Ellis, V., Maguire, M., Trippstad, T.A., Liu, Y., Yang, X., & Zeichner, Z. (2016). Teaching other people's children, elsewhere, for a while: The rhetoric of a travelling educational reform. *Journal of Educational Policy*, 31(1), 60-80. <https://doi.org/10.1080/02680939.2015.1066871>

Feiman-Nemser, S. (2001). From preparation to practice: Designing a continuum to strengthen and sustain teaching. *Teachers College Record*, 103(6), 1013-1055. <https://doi.org/10.1111/0161-4681.00141>

Friedrich, D. (2014). "We brought it upon ourselves": University-based teacher education and the emergence of boot-camp-style routes to teacher certification. *Educational Policy Analysis Archives*, 22(2). <https://doi.org/10.14507/epaa.v22n2.2014>

Gecker, J. (2021, September 22). COVID-19 creates dire US shortage of teachers, school staff. US News & World Report. <https://www.usnews.com/news/business/articles/2021-09-22/covid-19-creates-dire-us-shortage-of-teachers-school-staff>

Gist, C.D., Bianco, M., & Lynn, M. (2019). Examining grow your own programs across the teacher development continuum: Mining research on teachers of color and nontraditional educator pipelines. *Journal of Teacher Education*, 70(1), 13-25. <https://doi.org/10.1177/0022487118787504>

Goldhaber, D., & Theobald, R. (2021). Teacher attrition and mobility over time. *Educational Researcher*. 51(3), 235-237. <https://doi.org/10.3102/0013189X211060840>

Googins, J.C. (2019). *A life in teaching is a stitched together affair: Teacher academy instructors' narratives and ideologies*. Doctoral dissertation. Miami University, Oxford, OH.

Grow Your Own Teacher and School Counselor Pipeline Program, 53F-5-218, Utah Code Annotated 1953. (2021).

Jackson, C. (2022, April 22). Utah schools most impacted by teacher shortages. *abc4.com*. Retrieved on November 17, 2022, from <https://www.abc4.com/news/teacher-shortages-in-utah/>

Jess, M., McMillan, P., Carse, N., & Munro, K. (2021). The personal visions of physical education student teachers: Putting the education at the heart of physical education. *The Curriculum Journal*, 32(1), 28-47. <https://doi.org/10.1002/curj.86>

Kitchen, J., & Hodson, J. (2013). Living alongside: Teacher educator experiences working in a community-based Aboriginal teacher education program. *Canadian Journal of Education*, 36(2), 144-174. <https://www.jstor.org/stable/10.2307/canajeducrevucan.36.2.144>

Kitchen, J., Cherubini, L., Trudeau, L., & Hodson, J. (2010). Weeding out or developing capacity? Challenges for Aboriginal teacher education. *The Alberta Journal of Educational Research*, 56(2), 107-123. <https://doi.org/10.11575/ajer.v56i2.55393>

Krueger, J. (2021). TribalCrit, curriculum mining, and the teaching of contemporary Indigenous issues. *Multicultural Perspectives*, 23(2), 78-86. <https://doi.org/10.1080/15210960.2021.1914048>

Kulago, H.A. (2012). Theorizing community and school partnerships with Diné youth. *Journal of Curriculum Theorizing*, 28(2), 60-75.

Lindberg, K.J.P. (2016). Facing the teacher shortage: Why Utah struggles to keep educators, and what the U is doing to help. *University of Utah Magazine*. Retrieved on November 17, 2022, <https://continuum.utah.edu/web-exclusives/facing-the-teacher-shortage/>

Martinez-Cola, M. (2020). Visibly invisible: TribalCrit and Native American segregated schooling. *Sociology of Race and Ethnicity*, 6(4), 468-482. <https://doi.org/10.1177%2F2332649219884087>

McGloin, S. (2008). The trustworthiness of case study methodology. *Nurse Researcher*, 16(1), 45-55. <https://doi.org/10.7748/nr2008.10.16.1.45.c6752>

Merriam, S.B., Johnson-Bailey, J., Lee, M., Kee, Y., Ntseane, G., & Muhamad, M. (2001). Power and positionality: Negotiating insider/outsider status within and across cultures. *International Journal of Lifelong Education*, 20(5), 405-416.

Meyer, M. (2010). The rise of the knowledge broker. *Science Communication*, 32, 118-127. <https://doi.org/10.1177/1075547009359797>

National Center for Education Statistics. (2022). Characteristics of public school teachers who completed alternative route to certification programs. *Condition of Education*. U.S. Department of Education, Institute of Education Sciences. Retrieved on November 17, 2022, <https://nces.ed.gov/programs/coe/indicator/tlc>

Nieto, S., Bode, P., Kang, E., & Raible, J. (2008). Identity, community, and diversity: Rethorizing multicultural curriculum for the postmodern era. In F.M. Connelly, M.F. He, and J. Phillion (Eds.), *The Sage Handbook of Curriculum and Instruction* (pp. 176-197). Sage Publications, Thousand Oaks, CA.

Paine, L., & Zeichner, K. (2012). The local and the global in reforming teaching and teacher education. *Comparative Education Review*, 56(4), 569-583. <https://www.jstor.org/stable/10.1086/667769>

Philip, T.M., Souto-Manning, M., Anderson, L., Horn, I., Carter Andrews, D.J., Stillman, J., & Varghese, M. (2019). Making justice peripheral by constructing practice as “core”: How the increasing prominence of core practices challenges teacher education. *Journal of Teacher Education*, 70(3), 251-264. <https://doi.org/10.1177/0022487118798324>

Prior, L. (2008). Repositioning document in social research. *Sociology*, 42(5), 821-836. <https://doi.org/10.1177/0038038508094564>

Reed, J. (2021, April 27). *Utah launches ‘grow your own’ teacher programs statewide*. KUER90.1. Retrieved on November 17, 2022, from <https://www.kuer.org/education/2021-04-27/utah-launches-grow-your-own-teacher-program-statewide>

Reider, A.T. (2022). Using micro-credentials and digital badges in education and training: A literature review. In E. Langran (Ed.), *Proceedings of the Society for Information Technology & Teacher Education International Conference, April 11, 2022* (pp. 246-251). Association for the Advancement of Computing in Education, San Diego, CA. Retrieved on November 17, 2022, from <https://www.learntechlib.org/p/220734/>

Saldaña, J. (2016). *The Coding Manual for Qualitative Researchers* (3rd ed.). SAGE Publications, Thousand Oaks, CA

Simmons, A. (2018, February 12). Teacher recruitment starting in high school. *edutopia*. Retrieved on November 17, 2022, from <https://www.edutopia.org/article/teacher-recruitment-starting-high-school>

Smith, M., & Ho, S. (2019, August 23). Teacher shortage, protests complicate educator pay dynamics. *US News & World Report*. Retrieved on November 17, 2022, from <https://www.usnews.com/news/politics/articles/2019-08-23/teacher-shortage-protests-complicate-educator-pay-dynamics>

Solórzano, D.G., & Yosso, T.J. (2002). Critical race methodology: Counter-storytelling as an analytical framework for educational research. *Qualitative Inquiry*, 8(1), 23-44. <http://qix.sagepub.com/cgi/content/abstract/8/1/23>

Stake, R.E. (1995). *The Art of Case Study Research*. SAGE Publications, Thousand Oaks, CA.

State of Utah Legislative Auditor General. (2021). *A Performance Audit of Teacher Retention within Utah's Public Education System*. Retrieved on November 17, 2022, from https://olag.utah.gov/olag-doc/2021-13_RPT.pdf

Sutcher, L., Darling-Hammond, L., Carver-Thomas, D. (2016, September 15). A coming crisis in teaching? Teacher supply, demand, and shortages in the U.S. Retrieved on November 17, 2022, from <https://learningpolicyinstitute.org/product/coming-crisis-teaching>

Tooley, M., & Hood, J. (2021). *Harnessing micro-credentials for teacher growth: A national review of early best practices*. New America, Washington, DC. Retrieved on November 17, 2022, from <https://files.eric.ed.gov/fulltext/ED612409.pdf>

Tyler, R.W. (2013). *Basic Principles of Curriculum and Instruction*. The University of Chicago Press, Chicago, IL. (Original work published 1949)

Utah Board of Education. Career pathway: K-12: Teaching as a Profession. (2021). Retrieved on November 17, 2022, from <https://www.schools.utah.gov/file/53c71fc0-47f8-4574-88fd-fb7f8d44fda8>

Valenzuela, A. (2017). Grow your own educator programs: A review of the literature with an emphasis on equity-based approaches. *Intercultural Development Research Center*, San Antonio, TX. Retrieved on November 17, 2022, from <https://files.eric.ed.gov/fulltext/ED582731.pdf>

Werler, T. (2016). Commodification of teacher professionalism. *Policy Futures in Education*, 14(1), 60-76. <https://doi.org/10.1177/1478210315612646>

Will, M. (2022, March 4). ‘How bad could it get?’ State and district leaders work to combat teacher shortages. *EducationWeek*. Retrieved on November 17, 2022, from <https://www.edweek.org/leadership/how-bad-could-it-get-state-and-district-leaders-work-to-combat-teacher-shortages/2022/03>

Wood, L.M., Sebar, B., & Vecchio, N. (2020). Application of rigour and credibility in qualitative document analysis: Lessons learnt from a case study. *The Qualitative Report*, 25(2), 456-470. <https://doi.org/10.46743/2160-3715/2020.4240>

Writer, J.H. (2008). Unmasking, exposing, and confronting: Critical Race Theory, Tribal Critical Race Theory and Multicultural Education. *International Journal of Multicultural Education*, 10(2), 1-15. <https://doi.org/10.18251/ijme.v10i2.137>

Writer, J.H., & Oesterreich, H.A. (2011). Native women teacher candidates “with strength”: Rejecting deficits and restructuring institutions. *Action in Teacher Education*, 33(5-6), 509-523. <https://doi.org/10.1080/01626620.2011.627040>

Zeichner, K. (2010). Competition, economic rationalization, increased surveillance, and attacks on diversity: Neo-liberalism and the transformation of teacher education in the U.S. *Teaching and Teacher Education*, 26, 1544-1552. <https://doi.org/10.1016/j.tate.2010.06.004>

Story in the Stars: An Autoethnographic Study of Tongan American Situated Storytelling

Belinda 'Ofakihevahanoa Fotu¹ and Latuniua Jesse Fotu

¹*Utah State University*

Abstract

Past, present, and future stories are important devices for transferring culture and knowledge while connecting communities. Narratives of self are apparent in the types of stories we tell each other as well as the venues in which we tell them. In this autoethnography, I investigate specifically through a Tongan American lens the community built through stories: ancestors ancient and living as well as those outside of the Tongan American culture. This is especially relevant for members of the Tongan diasporic community born into or living within land-locked states. Situated spaces and storytelling play an important role in the success of Tongan American storytelling: the diasporic execution and reception of generational stories, parental advice (akonaki), or reciprocal conversations (talanoa). Contexts of audience and venues disrupt those spaces. This disruption is the truest space for Tongan American learning, as we navigate generational promises and

expectations that cross continents, mingling with the immediate demands of westernized systems of knowledge reproduction. Implications of this study include the need for educators to adjust learning spaces to better integrate epistemologies and learning strategies that feature strengths of community and genres of literacy-building centered in Pasifika epistemologies of respect, sacrifice, and humility.

When I was a teenager, I would compete in storytelling competitions using stories that my mother had written down from my dad's recollection of Tongan mythology. They were ancient Tongan tales, usually of male heroes who were kind, wise, and very clever. I would say they were similar to Odysseus, but with a large side of humor. While Dad was the original storyteller, he was not really a father who changed the telling according to the cognitive developmental level of the child and so many of the stories were lost on us. Instead, my palangi (white) mother wrote them down, translated them through a western palate/narrative construct, and painstakingly coached my sister and me to recite and later perform them. This is how I learned the ancient folklore of my father's origin. More recently, I have read the stories on different websites or in different books recording the folklore and have noticed that authors and translators added elements or left out important embellishments. In my father's more recent retelling of the stories, his versions of the stories have also changed, adding in the elements I know my mother had long ago adjusted to keep the stories, as she said, "PG-13 and not R."

Stories continue to play a central role in how I navigate and analyze the world and specifically my Tongan American culture. Autoethnography is a methodology that has the capacity to hold important stories within critical analysis to reveal essential aspects of the culture that created those stories. Analysis interplays heavily with interpretation in this research methodology, where the analysis extracts bits and pieces of the data to observe under a microscope while the interpretation pulls the researcher into a macro view of how the research data fits into a larger schema of culture as a whole. Through various data collecting, such as interviews, artifacts, and field notes, as well as storytelling, autoethnography is a methodology that has the capability to hold and explore facets of culture less accessible within more traditionally validated forms of research. Autoethnography has the flexibility, yet rigor, as a tool to better understand important aspects of culture. I use it here to interrogate the liminal space of Tongan American culture as it is nurtured by situated storytelling.

As a Tongan American, I am within the culture I intend to study, looking specifically at an aspect of Tongan American culture that seems often to float in the background of conversations: belonging and liminality of ownership within Tongan American spaces. The stories of my childhood continue to direct how I understand and navigate my experiences in my present and how I extend my imagination of self and culture into the future. Although the traditional Tongan tales and myths I grew up learning and telling are not common knowledge among all Tongan Americans, they represent well the epistemologies that carry old traditions and present expectations that have continued relevance in the Tongan American consciousness. They were created anciently in Tonga and, through the oral tradition of storytelling from parent to child, were passed on to me. I have already passed on several of these same stories to my son, who listens to them and corrects them according to how he imagines the past and his present.

There was one story that made me emotional in every retelling: *The Humu and the Toloa*. Integrated in the retelling of this ancient tale are all the elements previously mentioned: the translation between two different generations, two different languages, and two different cultures. I tell the story now as a tool to hold these ideas and also as a way to present autoethnography as an essential method necessary in unknitting and reweaving important stories in Tongan American culture. To understand the interplaying influences as well as the organic ever-arriving culture of Tonga America, the analysis and storytelling must be intertwined in this study. Therefore, autoethnography, with its emphasis on both analysis and evocative description, becomes an important tool in this study of a culture that is pulled by space and time, but essentially grounded in values. In the retelling of *The Humu and the Toloa*, I am distinctly aware of how old gods and new ones populate my storytelling: Tangaloa and Aho'eitu sit uneasily with Christ and Joseph Smith; my ancestors on both sides of my family tree gather quietly waiting for me to start. I imagine all of them in the audience listening to my retelling, leaning in to see if I include them as they raised me to. I start with the trepidation of one who knows she is in the act of disappointing.

Section I: The Alienated Storyteller; Fictional Account

“There once was a king,” I shift my ta'ovala, distractedly pulling at the woven fabric as I catch my grandfather, Kafokuota's, eyes. The ancient chief is focused on me, the result of his and his descendants' many sacrifices: a woman whose lips curve around the language of the Christian missionaries he resisted for so long.

I let go of my vala and promptly bend my elbows and hold my hands. “A chief. There once was a chief, and one day he went to the ocean to bathe.”

“Ikai—na'e ne 'alu pe ki he vaikaukau,” Grandma Mafile'o interjects waving at me with her tiny knotted hand, smiling at already recognizing the story.

“Huh?”

“She says that he went to the pond,” Great-grandma Hannah, daughter of Mormon pioneers, says gently, as Mafile'o puts her arm through Hannah's, linking arms like old friends. They are near mirror images of encouragement, watching me. I breathe out and try again. This time with my eyes closed. I'm trying to re-remember.

“Once a great chief went to the wade pools to wash his body. He used a sponge from the rocks to scrub his skin smooth. He did not know that watching him was an immortal being, a goddess...” I open my eyes remembering the cadence, “...of incredible strength, wit, and power. Pleased with the chief's strong form, the goddess transformed into a sponge, and when the chief reached for the sponge to soak against his skin, he reached instead for the goddess. The moments of relief they shared in that pool resulted in her pregnancy of twins: Ma'afutoka and Ma'afulele. The goddess raised the twins in... the heavens,” I pause, unsure of this word choice. “As the twins grew, they began to wonder about their father and his people. They would ask their mother about him often, and she would tell them about a blessed land and a noble chief. One day, when they were old enough, she sent them to the mortal world to live with their father.” My hands, now raised above my head to the side, turn around each other and sweep to my hip. In this story, dance plays a role in the retelling. That was how I was taught to tell it.

“At first, their chief-father was so proud to have these demi-gods as his children, and he showed them to his people with joy. There were great celebrations, and the villagers welcomed the boys into their homes, but the time for excitement waned, and the resources required to appease the appetites of two growing demi-gods began to dwindle. The village's joy turned to bitterness as resources ran low and their own children's bellies grew swollen with hunger. While the twins were off joy-riding megalodons on the horizon at dawn, the villagers called a meeting.

‘Our wells run dry; our livestock are running out!’

‘The children cry for food!’

‘The twins break everything they touch!’

‘They cannot stay!’

‘Then they must go.’ This last voice came from the chief, the boys' father. ‘They cannot live among us.’ The village stood still in the weight of the chief's decision.

Finally, one woman broke the silence ‘Then what do we do?’

The chief lifted his eyes to the east horizon, and a breeze sifted through the crowd.

‘The Humu,’ an elder whispered, and the village buzzed in anxiety of words only heard in nightmares echoing the voice from the choking lungs of the sole survivor of the fishing crew who voyaged many years ago to that eastern island. In search of new fishing grounds, he and the crew landed on a strangely silent island. In his final gasps, he spoke of an ancient well and a monster of the deep that emerged from within, soon devouring the other shipmates. The sailor escaped death only long enough to relay the message to his people: avoid the silent island of the east.

‘I will lead a hunting crew to the island of the Humu, where we will sail with my sons.’ The chief stopped to swallow the catch in his throat, ‘We will sail with my sons and leave them on the island for the Humu.’”

I look up at the audience of ancestors. The fabric of the puletaha I wear pinches under my arms. It was made with a smaller frame in mind.

Autoethnography vs Autobiography: Keeping it Critical

Storytelling in autoethnography is as much process as it is product. One of the reasons autoethnography as a methodology is helpful in studying culture is that it is a genre of study that gives the necessary space, the essential authorial license, for writing that communicates something more true in evocative form than it could possibly portray in plain description. I never stood in front of a room of myths and ancestors from both my Tongan and white heritage lines, but in setting up the retelling this way, I can communicate that my position as a Tongan American woman is to acknowledge all of their conflicting presences in my choices and in my simple being. That I characterize myself as standing on a stage where the audience is benevolent and accepting, and yet that that portrayal of me is self-conscious and stammering, is a device autoethnography allows to hold two thick ideas: performance and disenfranchisement.

Storytelling Spaces

There are many venues in which to tell stories, fananga, in Tongan tradition. Some are from pulpits, in front of congregations, some are among women in the fale-hanga weaving, pounding, and painting mats, ngatu, and tapas, tapestries that stretch sometimes over 50 meters made out of bark pounded thin like paper and soft like cloth. The work these artists create is called koloa, the translation of which is “treasure.” Imagery from fananga, such as the geometric representation of the Humu

often are included in the kupesi (Latu, 2020), the painting on the tapa or the ngatu, of these community art pieces. Storied spaces, specifically for the ancient tales, include the nofo'aki-putu, night-long vigils at funerals kept by the women in the deceased family and community. Other spaces for storytelling are within circles of men drinking kava and singing songs with stories incorporated throughout. While gendered, these are Indigenous spaces and the social expectations of gender are very different from that of their colonizers (Fa'avae, 2021). Although there are many different venues for fananga, or storytelling, to take place, “the most common is a form of domestic entertainment: the stories are recounted by a senior family member at night as the family settles down to sleep” (Moyle, 1995, p. 3). My father’s recountings of family folklore were merely reenactments of the tradition he had also inherited from his grandparents.

In Tongan fananga, telling and listening share a mutual onus to the success of the story, and both skills are necessary cultivated crafts within the Tongan tradition. For example, when I was little, I remember the rigorous lessons on listening my siblings and I learned while waiting patiently for speakers in church functions or at celebrations to finish their speeches so we could eat. The food sat inches from our salivating mouths, but we were not allowed to speak nor to touch the food until the speeches and prayers had been made. Breaking this expectation would be our acquiescing to a dreaded flick to our ear or smart spank, lovingly dealt out by either my father or nearest auntie. Within this context, we were being taught respect, and our stamina to listen to stories grew. Later, we would feel accountability to participate not just as listeners but as speakers at functions where our contribution was an implied responsibility. Although imperfect in our language and style, we all understood the feeling of that responsibility as it was taught to us and, awkwardly or not, we fulfilled it in congruence with the culture that had raised us to understand the importance of that participation. Listening and speaking were a way to tauhi-vā, “an ancient Moanan system of conceptualizing and acting...an indigenous artistic device that uses symmetry to reconcile sociospatial conflicts and create harmonious and beautiful sociospatial relations” (Ka’ili, 2017, p. 5). Litts et al. (2021) recognizes that “[r]esearch on Indigenous storytelling argues that how we listen and tell stories are culturally based activities” (p. 844), and so the way my siblings and I learned how to tauhi-vā through listening and telling stories had strong direct ties to our Tongan culture as it was nestled in our Western culture/environment. Litts et al. (2021) further clarifies that often in Indigenous storytelling, “it is incumbent upon the listener to understand the story rather than on the narrator to make the story clear” (p. 844). In the intimacy of our home, we learned and were

taught these dispositions, and so when Dad tells me a story, I know how to listen in a way that one cannot be sure strangers, even those from the Tongan diaspora, across the internet may have learned. Tecun et al. (2018) notes that “the protocols and cultural knowledge aid and support the process of striving for balance in engagement between people, places, and energies” (p. 14). Stories and storied spaces aid in teaching those protocols and cultural knowledge not just through the content of the story but through the context of the storytelling.

When I gift stories to my son, it is as he lays on my shoulder, moments away from sleep. This is called *kaliloa*, and my father once told me stories this way as well. The Tongan phrase for someone who adheres to the *akonaki*, wisdom of previous generations, is *fielau na’e moheofi*. *Moheofi*, which directly translates to “sleep near,” is a reference to a person who has been attentive in *kaliloa* and has learned the generational lessons well.

In the earlier evocative narration, I stand in front of, separate from, an audience of ancestors and belief figures. That separation shows how there is an element of distance from them in both relation and responsibility. In the Western context, standing in front of a crowd is often an act to lead the congregation in an activity or as an act of shaming. The only times I have stood in front of a Tongan congregation were to enact a responsibility I had to the community; otherwise, I would only be sitting amongst others. The stage with its blinding spotlight and dark, non-participatory audience is a disingenuous construction for telling Tongan tales. It is a scenario better left for violin quartets and acting performances where the fourth wall remains intact. There are no walls in the Tongan tales I whisper to my son as he lies cradled in my arms. He is as much a part of the story, as the listener, as I am, as the teller. In our living room, we listen and sometimes interrupt each other in the telling, always laughing—occasionally yelling. It is the nurturing of the relationships through the stories that is the focus of the storytelling, not the actual stories. The stories are merely the vehicle that carries our expectations of ourselves and each other. They carry our celebrations and our love.

In the portrayal of my retelling of *The Humu and the Toloa* to an audience of ancestors and deities, I start in the setting of how I once told stories to audiences of white families in state and national storytelling festivals. I am distant from my audience at this point in the story. The retelling is a performance rather than a contribution to an ongoing conversation, as it would be within a more intimate setting within a close community. Even so, I chose the audience in this portrayal to be those of ancestors who at once feel distant and yet are familiar through their love of parents to children, relationships easily recognizable and relatable to

me in contemporary contexts. Once again, the idea of proximity is in play. I am at once distanced by the time and space of when and where they once lived, displaced by decades and oceans. At the same time, I am close to them as the relationships are held at a higher esteem than that of colonialist notions of blood quantum or language gatekeepers (Ofahengaue Vakalahi & Hafoka, 2017). The distance and space is specifically significant in Moanian (Oceanic) theories. *Tā-vā* is an extensive tempospatial theory that encompasses the epistemologies that drive Moanian ontology (Māhina and Ka’ili, 2017). In this *tā-vā* theory, “one’s ancestral lands, ancestors, and roots are highly significant” (Ka’ili, 2017, p. 4). My presence on the stage embodies the distance from my ancestors I feel even as the act of storytelling, though imperfect and halting, draws them nearer. They encourage this and even call out to me from the audience, breaking that contrived social separation and drawing us closer. My ancestor audience reminds me that the separations of time and space—those decades, those oceans and land masses—are all categories made outside Indigenous epistemologies (Ka’ili, 2017; Hau’ofa, 1994). My ancestors cross over those imagined Western narratives to draw me into a shared, reciprocated space (Tecun et al., 2018). This is not to say that my actions as a character in the story or as a writer and researcher are without the external context of whiteness and racial hierarchies inherent in being Tongan American in predominantly white spaces. I am not just knee deep in the context of whiteness, but it, like my Tongan heritage, courses simultaneously through my veins and animates my every action. Hau’ofa (1997) refers to this mixture of culture as Tongans “doing what their ancestors did in earlier times: enlarging their world as they go, on a scale not possible before... expanding kinship networks through which they circulate themselves, their relatives, their material goods, and their stories all across their ocean” (p. 155). Māhina noted that for Tongans, especially the diaspora, the Indigenous and colonizer are “inseparable—what is left is mediation by way of liberation by both parties.” Māhina is adamant that he does not condone colonization, “because colonization is one of imposition and domination. ... We want to decolonize ourselves by moving to mediation and liberation. There is no end to it. We will always be working on it—our progeny will continue to work for it.” (Māhina et al. 2021). As a Tongan American researcher who is also centering my studies on my diasporic culture, I use autoethnography to carry all these complementing contradictions both ontological and epistemological.

Section II: Stories Among Family; Fictional Account

“They rode in their boats and canoes...”

“Canoes like Indians?”

“Yes, and other ones much bigger, but a lot of them looked like canoes from Indians.”

“How do you know?” My little sister, Mafile’o, questions as she leans against the counter, one hand on her hip, the other on her baby bump.

“We bought a replica the first time we went to Tonga. It’s just downstairs. It’s basically a canoe with a tapa sail.”

“Hhh! Laupisi—’io, koe vaka tatau pe. Tuku ho fa’a fakatonotonu kae tuku ho tokoua ke ne fai ‘a e talanoa,” Grandma Tipaleli gently chides.

“Sai pe ia—’oku fakalata pe ia,” her grandmother, Tuipe, counters, defending my little sister, whom she has pulled in to help her with cutting up the sapaui noodles with scissors at the stovetop. Here in this story/space where time and context are suspended and we can sit in ease with the ancestors past and present who love us most, Grandma Tuipe is a young woman, pregnant with her firstborn, my great-grandpa, Hokafonu, a benevolent leader of his community and the man who raised my father. My little sister is pregnant with the niece I cannot wait to meet. My sister has told us she plans to name her baby “Tuipe.”

“They rode in their canoes with the twins to the eastern island.”

“The quiet island.”

“Fakalongolongo.”

“Ue! Sorry!”

“Ikai—na’a nau folau ange pe ki he motu ko fakalongolongo ‘i he hahake.”

“Right,” I say, taking the cleaver my cousin, Pepe, had just finished sharpening for me and carefully cubing the frozen chicken thighs. Pepe is not an ancestor, but he likes the stories as much as I do, even when I am the one telling them. Mom is air frying fries behind me with Great-grandma Hannah cutting the tips off the green beans across our kitchen island. Tipaleli, the grandma I never got to meet, still 28, is shucking the corn with my older sister, who took her name. Grandma Louise sits opposite Great-grandma Mafile’o, who still excitedly corrects the story as it unfolds.

She is reminding us of what is important.

“When they got to the island, the twins jumped out and pulled the canoes full of sailors onto the beach, but none of the other men got out of the boats.”

“*Right there. They should have known right then and there,*” Grandma Louise points for emphasis.

“But they didn’t. They still trusted their father and the villagers.”

“*Chumps.*”

“Probably. In any case, their dad, Ma’afu, gets out of the boat and tells them something like that the sailors are thirsty and tired from the journey and if they would please go fetch water from the well on the other side of the island.”

“Uh oh.”

“So, the twins start walking across the island. As soon as they were no longer in sight of the ships, the boats set sail back to the village, certain that the twins were sure as dead.

They walked through the eerie landscape with only the sound of their footsteps and a breeze, ominous for its lack of seagull cries.”

“Ooh, I love it when she does that.”

“Io, koe polofesinolo 'ia!” My grandmas laugh, and I continue.

“As they reach the height of the island, they see the ruins of an enormous well, the size of a rugby field. Thirsty, the twins reach into the water to retrieve a drink but instead pull out wet bones of various sizes floating on the surface of the water.

‘This water is weird,’ Ma’afutoka grimaces.

‘Let’s go to the other side where the water gets darker and pull from there. There’s nothing floating on that side.’

The twins strode alongside the well wall, and the water got darker and darker until on the far side it was nearly black in its deepness.

‘I’m not sure about this place,’ Ma’afulele said, looking off into the undergrowth around them...

“Finally they pick up. Good grief.”

‘Mo’oni. 'Okapau koe ongo ta’ahine kinaua, ne na 'osi 'ilo koe feitu'u fakatu'utamaki ia.’

‘Mahalo. Hoko'atu, 'Ofa.’

“‘I’m going to keep watch while you pull from the well...’ he said.”

“Welp. Can’t win for losing, I guess.”

“Ma’afutoka leaned deep into the well, reaching ever farther for the cooler water. He did not see the glint of a scale nor the flick of a fin in the deep of the water. Ma’afulele, though, raised his hele in front of him, all his senses screaming to him of impending danger. He looked toward the bushes, then back at his twin nearly chest deep into the liquid darkness. Ma’afulele reacted before he saw it—a flash of light as the Humu burst through the surface. Ma’afutoka was safe, if sputtering, on the ground by the well, pushed to safety by his twin who in one fluid movement, blocked the Humu from his brother and embedded his hele deep into the monstrous fish as it thrust itself from the water into the sky. Ma’afulele held onto the hele as it sliced the animal from gill to fin. The Humu landed on the wall of the well, its flight cut short by the blade of the watchful twin. Its jaws jolted to snatch the legs of the boys, but Ma’afutoku, recovered, sidestepped the jaws of dagger-like teeth and

clenched the Humu's side fin and back fin with his fists, lifting the monster off the ground as the centrifugal force turned the pair into a tornado. The twin released the animal, flying all the way across the island, across the waters until it landed, WOMP!" I smash the cleaver I am holding into the chicken leg I have been working on for effect. "Right on the returning boat of the sailing party that left them, killing everyone but their traitorous father!" I look around the room, expecting surprise, but my Tongan grandmas instead look concerned.

Critical Analysis of Section II

There is a flexibility in the storying process that allows for representation of storytelling innate to the research and the researcher. The flexibility allows for the melding of writing genres in order to better investigate elements of culture accessible through the intersecting of stories and analysis. Holdman Jones et al. (2016) wrote, "We turned our energy to joining social science and humanities to make scholarship more human, useful, emotional, and evocative...I do autoethnography less as a way to live and relate the story of research and more as a way *into* researching and storying living" (p. 9). This approach gives the researcher the creative space to best represent the intimacies of translating literacies of a lived embodiment into a written format. This can take the form of different writing genres in order to create the necessary communication of emotion and context. It is not uncommon in autoethnography to use fiction and evocative writing to communicate and then analyze an element of culture (Chang, 2008). While the writing genres can be diverse, there are some strong pillars that bear into autoethnography: "the autoethnographer is expected to satisfy the following conditions: (a) be a member of the social world under study, (b) engage in reflexivity and analyse data on one's self, (c) be visible and actively present in the text, (d) include other informants in similar situations in data collection, and (e) be committed to theoretical and critical analysis" (Fa'avae, 2018, p. 129).

In this second storytelling, the scene is of the storytelling happening in a more authentic way among the women of my immediate community of ancestors and living family members. We work on a common project and we tell stories, often taking turns to add missing details or throw jokes. We build from each other's presence, the communication of our proximity, our actions, and our tone, as well as from the words we speak, the already established power structures inherent in our interactions. Women occupy this space together. We talanoa, our intergenerational conversation building from our shared space of ancestors and progeny (Tecum et al., 2018). In the previous part of the story, where I stood on

a stage, that was an example of Talaloto (Naufahu, 2018) where I hold the space to tell my story or speak my truth uninterrupted. Talanoa is a more collaborative space, and while I use this space to continue the story arc, talanoa often is not linear (Vaiotele, 2006). This is acknowledged by beginning this section in a topic apart from the center of the story. This is a space of sharing and gathering, where stories can be exchanged by participants or picked up by those just listening.

Within the talanoa, patterns of respect are enacted and upheld. As in the descriptive fiction of the kitchen scene with female ancestors, the highest matriarch or oldest matriarch, in this case Tuipe, can tell her daughters to be quiet and give space for her granddaughter to speak. The younger cannot interrupt the elders. Grandma Louise, not part of the Tongan tradition, happily interrupts the story whenever she likes. Outside the sociospatial expectations of interaction, she does not need to follow any unwritten rules. As one of the youngest in the room, I am allowed to tell my story, because I'm being actively nurtured and encouraged by the older women.

Section III: Stories on the *Shoulder-Pillow*, Kaliloa; Non-fictional Account

“The villagers decided to call another meeting. So, while the boys were off enjoying a sauna break in some distant volcanoes...”

“*No. They were riding megalodons again,*” my seven-year-old reminds me. We lie in bed, his head on my shoulder, my arm around him. This is *kaliloa*, the most intimate form of storytelling, between a parent to their child. Kaliloa are *akonaki* (advice) and bedtime stories told to children just before sleep so as to populate the child's dreams and remind them in so many ways of the things that are most important. My son, transfixed on the earlier imagery of the twins riding megalodons, insists that they do it again while the second meeting of the villagers takes place. Why not? This is as much his story as it has been mine.

“Ok. They went again to ride megalodons.”

“*In the sunset.*”

“In the sunset. And the village met.

‘All our food is gone.’

‘Our wells run dry!’

‘Our children hunger!’

‘The twins must be stopped!’

‘They can't stay here!’

‘Then they must go.’ The chief says again, this time knowing to save his people the twins have to leave. ‘But how?’

The village was quiet in thought, then another elder from the center of the crowd pointed to the chief and called, ‘The Toloa!’ The name whispered throughout the crowd, until the chief quieted the people with his arms raised above them.

‘That demon is only legend,’ he said, glaring into the crowd.

‘It is real!’ the old man insisted.

‘Tangata ‘eiki, tell us what you know.’ The chief took the old man’s hand and helped him stand and speak. We always need to listen to our elders, yes, Bubbah?”

“Yes. What did the old guy say?”

“Elder. You mean what did the elder say.”

“Yes. What did the elder say?”

“Many generations ago, my grandfather’s grandfathers once told of an island to the west, beautiful with high cliffs and abundant fruit. They once went there to hunt when a hurricane and sudden darkness came upon the island. The sky filled with thunder and the earth shook. It was not a hurricane, but the beating of mighty wings on a body so large it hid the sun and engulfed the earth in night—not thunder but a monstrous QUACK!”

I wait. This is an important part of the retelling: timing.

“Did you say ‘quack’?”

“Yes. A MONSTROUS quack.”

“...it’s a duck?”

“Yup.”

“Seriously?”

“Seriously. A seriously huge duck that picks people off the earth like they were breadcrumbs. The chief along with new sailors equipped their boats for the voyage that would take them past the sunset, far to the west, to the island of the Toloa.”

“Toloa.” My son tries out the word. I’m surprised at his diction. His pronunciation is spot on, where the “t” in Tongan nearly sounds like a “d” and the accent is on the second to last vowel. I never pointed these patterns of language out to him. He picks up implicitly.

The twins understood by now that they could not live with the villagers; they could not stay with their father. And so they took the skeleton remains of the Humu and the Toloa with them up into the heavens where they placed the two animals into the sky.”

My son looks up at me, wondering why my voice has cracked and I’ve paused in the story. He watches me, confused at my tears.

“The Humu and the Toloa are constellations, the Coalsack and the Southern Cross, that Ma’afutoka and Ma’afulele gifted to the Tongan sailors so that no matter where they were, they could look up into the sky and find their way back home.”

We lie silently in the stillness of our dark bedroom and I ask, “Did you like my story?”

“Yes.” His voice is quiet and his speech is slower.

“Do you want to hear another one?”

“...mmm.”

We lie in the darkness and after a couple minutes I can hear my son’s breath become heavy and rhythmic.

Implications

The kind of storytelling I have described in the previous sections speaks to a type of cultural inheritance of learning. Inheritors of Tongan storytelling (talanoa and akonaki along with more formal stories) are taught values and worthy attributes on how to contribute to their communities in appropriate ways and how to maintain strong sociospatial relationships (vā) with each other and others. These are all attributes that could contribute to stronger communities in general, not just in Tongan diasporic spaces. These are all attributes that would strengthen learning spaces.

Learning spaces like classrooms from preschool to higher education could better integrate spaces for Indigenous stories, not in the alienated formats of “cultural experiences” but in transforming the climate of the classroom to embrace and not censor plurality. Specifically, this would look like relationships in classrooms that created productive storytelling/story-living spaces that are not limited or censored by a western lens. Perhaps this could be in how teachers construct expectations and accountability around large and small group discussions to better give space for reciprocation and community building rather than only content building. How that kind of community speaking and listening skills are validated in grades could be better imagined to validate Indigenous strengths in literacy. Pasifika diasporic students come with the cultural capital wealth (Yosso, 2005) of the thick literacies passed onto them through their home and cultural communities. Paired with growing up in America with the insidiously pervasive western gaze, they actively learn that majority cultural lens for literacy as well. These children are vessels of literacies unvalidated by majority cultures, literacies that would benefit their school community. Educators could do better to create classroom environments that created space for these kinds of literacies to be shared and validated in the curriculum/grades as equally as the western literacies are validated. An educator need not be an expert at every type of literacy to build a space for that kind of validation; they need only be active learners themselves, creatively creating contexts for students to show and build

strengths/skills. If educators are majority culture with no experience of Indigenous epistemologies or teaching styles, they can actively seek out how to remedy their inexperience (and to stimulate their imagination of their craft) by reading how Indigenous teachers constantly bridge that cultural gap and manage to teach western standards in Indigenous contexts (Delpit, 2006; Cajete, 2019).

Students and instructors could better learn the craft of listening, of sitting in a story rather than refuting or tolerating. Both “refuting” and “tolerating” are acts of reifying the center of the classroom in western lore, to the inherent exclusion and othering of multiplicity. If instead, the classroom curriculum included story-listening and discouraged lens-arrogance, the classroom would be more ethical and equitable to learning for all students. There will be dissonance in initial understanding when stories are shared outside of different cultural norms, specifically for majority culture students who understand curriculum with their own consciousness and learning at the center. The lessons in that dissonance are as important as those in the plot, characters, and ending of the actual stories.

Maybe majority-culture students will be confused by the nobility of a chief willing to sacrifice his sons for his village. Maybe dominant-culture students will initially refuse to see the recorded concrete lines of Tongan lineage to creatures of the sea, the very stars in the sky, or even to oceans. As a teacher, I have heard the responses of dominant-culture students collapsing time to include old and new knowledge that refutes ancient tales as myths. I have sat in classrooms as a student, hearing instructors condescendingly call Indigenous stories the quaint, metaphoric products of third-world nations. Using that same technique, I could just as easily collapse time and judge majority-culture stories using past and present Indigenous knowledge coupled with the majority-culture arrogance: how Johnny Appleseed was an irresponsible spreader of invasive species or how *The Three Pigs* and *Goldilocks and the Three Bears* were both stories of the western world’s obsession with property and revenge. This strategy of minimizing stories to the mere scope of rationality severely limits understanding the cultures that made and continue to tell those stories. Stories exist outside of the hyper-rational, one-sided colonizer lens of “fact” and “worth.” Beauty, emotion, context, and especially community connection validate stories far past plot lines and narrative arcs.

Learning spaces could be better transformed to better hold ancient stories in the simultaneous space of truth and myth—and cultivate the craft of listening as importantly as the skill of speaking or producing. If teachers and Education could shift away from centering the western lens in both content and processes of production/skills, there would be more

room to validate incredibly rich indigenous literacies. Indigenous literacies and paradigms would strengthen all school communities.

Conclusion

“One characteristic that binds all autoethnographies is the use of personal experience to examine and/or critique cultural experience” (Holman Jones et al, 2016, p. 22). Because the theory and methodology drive this analysis, it is distinct from mere autobiographies or writing within the memoir genre. It is a type of personal writing that has specific purposes: “While all personal writing could be considered examinations of culture, not all personal writing is autoethnographic; there are additional characteristics that distinguish autoethnography from other kinds of personal work. These include (1) *purposefully commenting on/critiquing of culture and cultural practices*, (2) *making contributions to existing research*, (3) *embracing vulnerability with purpose*, and (4) *creating a reciprocal relationship with audiences in order to compel a response*” (Holman Jones et al, 2016, p. 22).

This critical autoethnography uses storytelling as its center of analysis, specifically the Tongan storytelling in my Tongan American family. Through an analysis of language, metaphor, and transfer, the roadmap for Tongan American diaspora to find connection in the Moana is more apparent.

References

- Cajete, G. (2019). Culturally responsive science education at the Institute of American Indian Arts, Santa Fe, New Mexico: A retrospective 1974-1989. In P.P. Trifonas & S. Jagger (Eds.), *Handbook of Cultural Studies and Education* (pp. 175–189). Taylor & Francis, New York.
- Chang, H.V. (2008). *Autoethnography as Method*. Routledge, Milton Park, Abingdon.
- Delpit, L. D. (2006). *Other People's Children: Cultural Conflict in the Classroom*. New Press, New York.
- Fa'avae, D. (2018). Giving voice to the unheard in higher education: Critical autoethnography, Tongan males, and educational research. *Mai Journal*, 7(2), 126-138.

Fa'avae, D. (2021). Critical autoethnographic encounters in the moana: Wayfinding the intersections of to'utangata Tonga and indigenous masculinities. In A. Harris, S. Holman Jones, & F. Iosefo (Eds.), *Wayfinding and Critical Autoethnography* (pp. 69–79). Routledge, Milton Park, Abingdon.

Hau'ofa, E. (1994). Our sea of islands. *The Contemporary Pacific*, 6(1), 147–161.

Holman Jones, S., Adams, T.E., & Ellis, C. (Eds.). (2016). Introduction, In A. Harris, S. Holman Jones, & F. Iosefo (Eds.), *Handbook of Autoethnography* (p. 9–47). Routledge, Milton Park, Abingdon.

Ka'ili, T.O. (2017). *Marking Indigeneity: The Tongan Art of Sociospatial Relations*. The University of Arizona Press, Tucson.

Māhina, 'O., Ka'ili, T.O., & Vaeatangitau, M. (2021, June 24). *10 Webber Images: Critical analysis from Dr. 'Okusitino Mahina, Dr. Tevita Ka'ili, and Manuha'apai Vaeatangitau. Lagi-Maama Academy & Consultancy*. [Paper presentation.] Lagi-Maama Academy & Consultancy's Third Lagi-Maama Talanoa Thursdays, Auckland, New Zealand.

Latu, V. (2020). *Unraveling Lalava: Uncovering the Cultural Knowledge Embodied in Lalava*. Master's thesis. Auckland University of Technology, Auckland.

Litts, B.K., Searle, K.A., Brayboy, B.M., & Kafai, Y.B. (2020). Computing for all?: Examining critical biases in computational tools for learning. *British Journal of Educational Technology*, 52(2), 842–857. <https://doi.org/10.1111/bjet.13059>

Māhina, 'O., & Ka'ili, T. O. (2017). Talamu'aki: Forward. In *Marking Indigeneity: The Tongan Art of Sociospatial Relations* (pp. 3–11). The University of Arizona Press, Tucson.

Moyle, R. M. (1995). *Fananga: Fables from Tonga in Tongan and English* (Vol. 2). Friendly Islands Bookshop, Nuku'alofa.

Naufahu, M. (2018). A Pasifika RESEARCH Methodology: Talaloto. *Waikato Journal of Education*, 23(1), 15–24. <https://doi.org/10.15663/wje.v23i1.635>

Ofahengaue Vakalahi, H.F., & Hafoka, O.K.L. (2017). Beyond words. *Amerasia Journal*, 43(1), 1–12. <https://doi.org/10.17953/aj.43.1.1-11>

Tecun (Daniel Hernandez), A., Hafoka, 'I., 'Ulu'ave, L., & 'Ulu'ave-Hafoka, M. (2018). Talanoa: Tongan epistemology and indigenous research method. *AlterNative: An International Journal of Indigenous Peoples*, 14(2), 156–163. <https://doi.org/10.1177/1177180118767436>

Vaioleti, T.M. (2006). Talanoa research methodology: A developing position on Pacific research. *Waikato Journal of Education*, 12(1), 21–34. <https://doi.org/10.15663/wje.v12i1.296>

Yosso, T.J. (2005). Whose culture has capital? A critical race theory discussion of community cultural wealth. *Race Ethnicity and Education*, 8(1), 69–91. <https://doi.org/10.1080/1361332052000341006>

Thermodynamics Experiment: Adiabatic Compression of Air

Toby Ian McMurray and Ali Syyed Siahpush
Southern Utah University

ABSTRACT

Thermodynamics concepts are complicated and hard to understand. In the undergraduate mechanical engineering lab, we studied and built a cost-effective thermodynamic cycle of ideal gases. In this study, air (ideal gas) was considered as the working fluid. The experiment was conducted by compressing and expanding air in a sealed container (two-liter pop bottle). This process may be considered confusing and complicated, but breaking down the ideal gas processes as adiabatic and isometric will simplify it to demonstrate the concept. This simplified model was applied to predict the ratio of specific heats of air (c_p/c_v). The results for the specific heat ratio of air was very close to the published value.

NOMENCLATURE	
Symbol	Description
P	Absolute pressure (kPa)
V	Volume (m ³)
γ	Specific heat ratio
C_p	Specific heat at constant pressure (kJ/kg.K)
C_v	Specific heat at constant volume (kJ/kg.K)
T	Absolute temperature (K)

INTRODUCTION

Adiabatic cycles are used to model complex and commonly used machines such as engines, refrigerators, and heating/cooling devices [1-4]. Thus, it's important that thermal engineers fully understand these adiabatic processes. Technical literature is saturated with applications of the ideal gas law. An example is determining the gas volumes in various chemical reactions. The ideal gas law can be used to calculate the volume of gases consumed or produced in these reactions. The ideal-gas equation is also frequently used to convert between volumes and molar amounts in chemical equations [2].

Hands-on and experimental demonstrations are a crucial part of the engineering curriculum. To understand the thermodynamics of the ideal gas law, a simple and cost-effective engineering demonstration (undergraduate mechanical engineering thermodynamics lab) is extremely helpful [5-9].

The primary purpose of this paper is to design and develop an apparatus to demonstrate an adiabatic compression and expansion cycle by compressing a 2-liter bottle to determine the specific heat ratio of air. From the literature review, it was found that an experiment of this nature has already been developed [5]. However, it was not presented as a full technical paper. Without a lab instructor and due to the lack of knowledge of materials, processes, and equipment used in this experiment, it was not a complete demonstration of the ideal gas law. Using reference 5 as a baseline to explore and understand the concept, the first iteration of the apparatus was built as shown in Fig. 1.

The first iteration of the apparatus, approximately 4 ft long, was simple to build and designed to validate and demonstrate the approach presented in reference 5. Using this apparatus, it was exciting to experimentally validate and provide accurate results for determining the specific heat ratio of air. However, it was too bulky and difficult to use. The bottle was also not initially pressurized so it couldn't fully re-expand after the compression process.

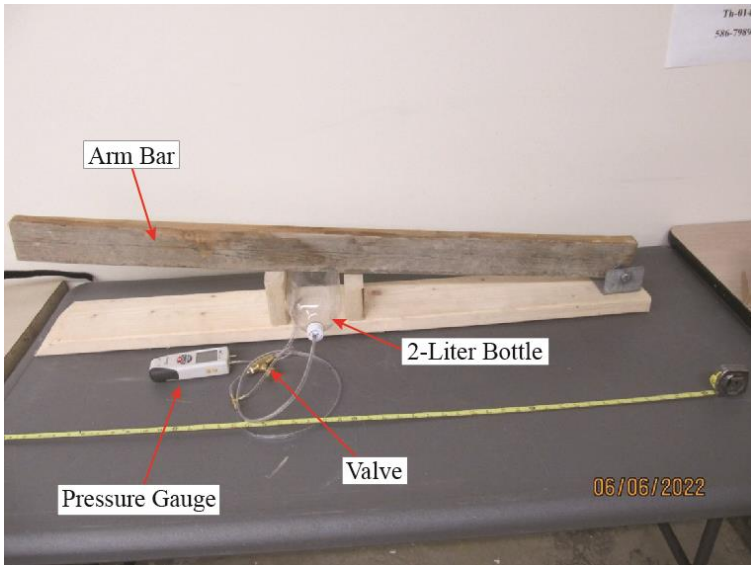


Figure 1. First iteration of the testing apparatus.

The purpose of this paper is to build and test the second iteration of the apparatus. The second iteration was designed to be much smaller and easier to use. The 2-liter bottle was also going to be initially pressurized when tests were conducted to allow for quick repetition of testing due to the re-expansion of the bottle.

THEORY

The thermodynamic cycle described in this experiment consists of four processes which are displayed in Fig. 2, the PV diagram.

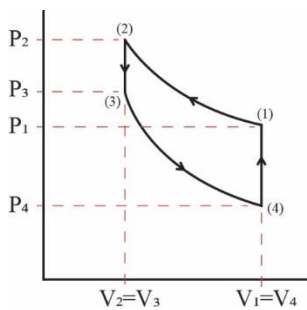


Figure 2. PV diagram of the thermodynamic cycle.

As seen in Fig. 2, process 1 (P_1 is slightly higher than the atmospheric pressure) to 2 describes the rapid compression of the bottle by the arm bar. This process is modeled as adiabatic (no heat added or removed from the system) compression since there is no time for the compressed air to exchange heat with the environment. In process 2 to 3, the bottle is held compressed in place until it reaches equilibrium with the environment (room temperature). This process is modeled as an isometric (constant volume) process and takes approximately 2-3 minutes. In process 3 to 4, the arm bar is released from the bottle and the rapid expansion of the bottle is observed. This process is modeled as adiabatic expansion since, similar to the compression process, there is no time for heat exchange with the environment. Finally, in process 4 to 1, the uncompressed bottle is left to reach equilibrium with the environment (room temperature). As with process 2 to 3, process 4 to 1 is also modeled as isometric and takes approximately 2-3 minutes to reach equilibrium with the environment (room temperature).

The curves from (1-2) and (3-4) in Fig. 2 are described as adiabats. From Boyle's Law, the relationship between absolute pressures may be modeled as [1]

$$P_1 V_1^\gamma = P_2 V_2^\gamma \quad (1)$$

$$P_3 V_3^\gamma = P_4 V_4^\gamma \quad (2)$$

where P is the absolute pressure inside the bottle (kPa), V is the volume of the bottle (m^3), and γ is the ratio of specific heats. The ratio of specific heats is defined as

$$\gamma = \frac{C_p}{C_v} \quad (3)$$

where C_p is the specific heat at constant pressure (J/kg·K) and C_v is the specific heat at constant volume (J/kg·K). Using Eqs. (1) and (2), γ can be determined for each adiabat as

$$\gamma = \frac{\log\left(\frac{P_1}{P_2}\right)}{\log\left(\frac{P_1}{P_3}\right)} \quad (4)$$

$$\gamma = \frac{\log\left(\frac{P_3}{P_4}\right)}{\log\left(\frac{P_3}{P_1}\right)} \quad (5)$$

where Eq. (4) represents the adiabatic compression process 1 to 2 and Eq. (5) represents the adiabatic expansion process 3 to 4. See the Appendix for the derivation of Eqs. (4) and (5).

From Eq. (4), it can be seen that the specific heats ratio can be determined when P_1 , P_2 , and P_3 are known. Thus, taking a pressure measurement before compression (P_1), right after compression (P_2), and after holding the bottle compressed for 2-3 minutes (P_3), allows for the specific heat ratio of air to be determined.

MATERIALS AND PROCEDURE

Shown in Fig. 3 is the second iteration of the testing apparatus. This apparatus has a final length of approximately 2 ft which is half the length of the first iteration at 4 ft. This size difference allows for much easier handling and reproduction. It also features a metal arm bar wrapped in foam alongside a Velcro strap which can hold the armbar in place.

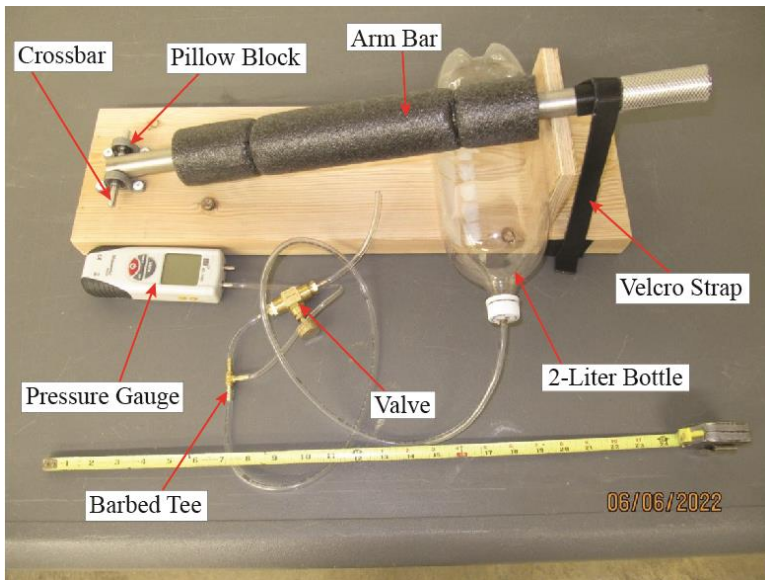


Figure 3. The second iteration of the testing apparatus.

Table 1 presents the parts required for the construction of the second iteration apparatus shown in Fig. 2.

Table 1. The parts used to construct the second iteration apparatus	
Part Name	Part Details
Barbed tee fitting	3/16" × 3/16" × 3/16"
Needle valve	1/4" NPT female × 1/4" NPT female
Barbed to male fitting adapter	1/8" barbed × 1/4" NPT male
Steel tubing	Stainless steel 304 grade, 16 gauge, 1" OD, 24" long
Foam noodle	1" ID, 50" long
Plastic tubing	1/8" ID, 1/4" OD
2-liter pop bottle	N/A
Digital monometer	RISEPRO
Pillow Block with Bearing	8-mm Bearing ID
Crossbar	8-mm OD
Wood stop	4" tall, same width as base

The following steps explain how the experiment was conducted.

1. Connect the hose on the open end of the needle valve to a pressurized air source. With the needle valve open, pressurize the 2-liter pop bottle to around 35 kPag and close the needle valve. Then slowly release air by slightly opening the valve until 25 kPag is achieved.
2. Allow the pressurized bottle to rest for 2-3 minutes to reach room temperature. Room temperature is achieved when the pressure reading on the monometer stabilizes.
3. Record the stable pressure measurement from the monometer as the initial pressure (P_1).
4. Rapidly press the arm bar down onto the wood stop, compress the bottle, and hold it in place. Quickly record the pressure measurement as the pressure right after compression (P_2).
5. Use the Velcro strap to secure the arm bar to the wood stop and let the compressed bottle rest for 2-3 minutes to reach room temperature again.
6. Record the new stable pressure measurement as the pressure after holding compressed (P_3).
7. Use Eq. (4) to calculate the specific heat ratio.
8. Repeat this process three times taking the average of the calculated specific heat ratios and comparing it to published values.

RESULTS AND DISCUSSION

The experiment was conducted using the first iteration of the apparatus, and the gauge pressure measurements are presented in Table 2.

Trial	$P_{1,gauge}$ (kPa)	$P_{2,gauge}$ (kPa)	$P_{3,gauge}$ (kPa)
1	-0.06	6.94	5.00
2	0.00	7.21	5.15
3	0.00	6.89	5.25
4	0.01	6.76	5.28
5	0.10	7.20	5.40
Average	0.01	7.00	5.21

To calculate the specific heat ratio, absolute pressure must be used. The atmospheric pressure during the experiment using the first iteration apparatus was 81.49 kPa. Thus, using the average gauge pressure from Table 2 with the atmospheric pressure yields the absolute pressure shown in Table 3.

	P_1	P_2	P_3
Abs. Pressure	81.5 kPa	88.49 kPa	86.7 kPa

Using Eq. (3) and the absolute pressure measurements from Table 3, the specific heat ratio of air using the first iteration apparatus was calculated to be 1.3304. The specific heat ratio of air is reported to be 1.4 [1]. Therefore, the experiment using the first iteration apparatus yielded a percent error of 4.97%. Although this percent error is low, it can be improved upon.

The experiment was also conducted using the second iteration of the apparatus and the pressure measurements were recorded in Table 4.

	P_1	P_2	P_3
Gauge Pressure	27.35 kPa	33.15 kPa	31.5 kPa

The atmospheric pressure during the experiment using the second iteration apparatus was 82.5 kPa. Combining the atmospheric pressure

with the gauge pressure measurements in Table 4 gives the absolute pressure measurements, shown in Table 5.

Table 5. Absolute pressure using the second iteration apparatus			
	P₁	P₂	P₃
Abs. Pressure	129.79 kPa	135.59 kPa	13.94 kPa

Using Eq. (3) and the absolute pressure measurements from Table 5, the specific heat ratio of air using the second iteration apparatus was calculated to be 1.389. This value is very close to the reported value of 1.4 [1]. The experiment using the second iteration apparatus yielded a percent error of 0.79%. The results from using the second iteration apparatus were very accurate.

Overall, the second iteration apparatus provided more accurate results while being smaller, cheaper, and easier to use. It was also observed that initially pressurizing the bottle before testing did not adversely affect the results.

SOURCES OF ERROR

While the results of the tests were accurate, there was still some error. Possible sources of this error may include inaccurate measurements from the pressure gauge, inconsistent compression on the bottle, and air leaks at connection points. It is also possible that the bottle was not fully allowed to reach room temperature after being compressed.

To minimize these sources of error, the pressure gauge can be calibrated before testing occurs, the Velcro strap can be used to lock the armbar in place after compression, and PTFE tape can be used at all connection points. It may also be beneficial to implement a temperature measurement system that can monitor the internal temperature of the bottle. This would help ensure the bottle reaches room temperature before being released

CONCLUSION AND RECOMMENDATIONS

The purpose of this paper is to develop the second iteration of an apparatus that could accurately determine the specific heat ratio of air. As a result, the second iteration apparatus was built and proved to be more effective and accurate than the first iteration. Specifically, the first iteration apparatus showed a percent error of 4.97% while the second iteration apparatus showed only 0.79% discrepancy. The second iteration apparatus is also much lighter and half the size of the first iteration

making it much easier to operate. It is also worth mentioning that initially pressurizing the bottle didn't affect the results.

To improve upon the second iteration of the apparatus, a temperature system that displays the internal temperature of the bottle should be implemented.

ACKNOWLEDGMENTS

This project would not have been possible without the help and support of the Department of Engineering and Technology at Southern Utah University. Their contributions included providing the equipment and assistance from faculty. Also, the undergraduate research funding was partially provided by the NASA Utah Space Grant Consortia.

REFERENCES

- [1] Cenge Y. A., Boles, M. A. *Thermodynamics: An Engineering Approach*, Eighth Edition, McGraw-Hill, New York, NY, 2015.
- [2] LibreTexts Chemistry. "6.4: Applications of the Ideal Gas Equation." Retrieved June, 3, 2022, from [https://chem.libretexts.org/Bookshelves/General_Chemistry/Map%3A_General_Chemistry_\(Petrucci_et_al.\)/06%3A_Gases/6.4%3A_Applications_of_the_Ideal_Gas_Equation](https://chem.libretexts.org/Bookshelves/General_Chemistry/Map%3A_General_Chemistry_(Petrucci_et_al.)/06%3A_Gases/6.4%3A_Applications_of_the_Ideal_Gas_Equation)
- [3] Byjus.com. "What is a real life example of ideal gas law?" Retrieved June 3, 2022, from <https://byjus.com/jee-questions/what-is-a-real-life-example-of-ideal-gas-law/>
- [4] Saylor Academy. The Ideal Gas Law and Some Applications. Retrieved June, 3, 2022, from https://saylordotorg.github.io/text_introductory-chemistry/s10-05-the-ideal-gas-law-and-some-app.html
- [5] Foothill College. Phys 4c. "Lab 3 Experiment 2 Adiabatic Compression–Gamma Ratio." Retrieved June, 3, 2022, from <https://www.coursehero.com/file/14043213/Lab-3-Exp-2-Adiabatic-Gas/>
- [6] "Physics 23 Fall 1993 Lab 2 - Adiabatic Processes." Retrieved June, 3, 2022, from <https://fliphtml5.com/kdgg/nyxz/basic>

[7] Memorial University of Newfoundland, Department of Physics and Physical Oceanography. “Physics 2053 Laboratory, Isothermal and Adiabatic Processes.” Retrieved June, 3, 2022, from <https://www.physics.mun.ca/~cdeacon/labs/2053/adiabatic.pdf>

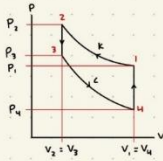
[8] University of Texas – San Antonio. “Ideal gas law.” Retrieved June, 3, 2022, from <https://www.utsa.edu/physics/resources/lab-1611/IdealGasLaw.pdf>

[9] Clemson University. “223 Physics Lab: Ideal Gas Laws.” Retrieved June, 3, 2022, from <http://science.clemson.edu/physics/labs/labs/223/gaslaws/index.html>

APPENDIX

In this Appendix, the derivations of Eqs. (4) and (5) are provided. The equations are derived from Boyle’s Law, the Ideal gas law, and information from the PV diagram of the thermodynamic cycle in Fig. 2.

DERIVATION



KNOWN

$$P_1 V_1 = K$$

K IS SOME CONSTANT

$$P_2 V_2 = K$$

L IS SOME CONSTANT

$$P_3 V_3 = C$$

$$P_4 V_4 = C$$

$$T_3 = T_4 \text{ (ROOM TEMP)}$$

BOYLES LAW

$$P_1 V_1^\gamma = P_2 V_2^\gamma \quad \text{AND} \quad P_3 V_3^\gamma = P_4 V_4^\gamma$$

$$\frac{P_1}{P_2} = \left(\frac{V_2}{V_1} \right)^\gamma \quad \rightarrow \quad \text{LOG} \left(\frac{P_1}{P_2} \right) = \gamma \text{LOG} \left(\frac{V_2}{V_1} \right) \quad \rightarrow \quad \gamma = \frac{\text{LOG} \left(\frac{P_1}{P_2} \right)}{\text{LOG} \left(\frac{V_2}{V_1} \right)} \quad (1)$$

IDEAL GAS LAW

$$P_1 V_1 = nRT_1 \quad \text{AND} \quad P_3 V_3 = nRT_3$$

SINCE n AND R ARE CONSTANT WITH AIR
AND $T_1 = T_3$

$$P_1 V_1 = P_3 V_3 \quad \rightarrow \quad \frac{P_1}{P_3} = \frac{V_3}{V_1} \quad \rightarrow \quad \text{SINCE } V_3 = V_2 \quad \rightarrow \quad \frac{P_1}{P_3} = \frac{V_2}{V_1} \quad (2)$$

SUBSTITUTING (2) INTO (1) GIVES

$$\gamma = \frac{\text{LOG} \left(\frac{P_1}{P_2} \right)}{\text{LOG} \left(\frac{P_1}{P_3} \right)}$$

THE SAME PROCESS CAN BE USED WITH $P_3 V_3^\gamma = P_4 V_4^\gamma$ TO GET $\gamma = \frac{\text{LOG} \left(\frac{P_3}{P_4} \right)}{\text{LOG} \left(\frac{V_3}{V_4} \right)}$ SINCE $V_4 = V_1$

Experimental and Theoretical Results of Transient and Steady-State Heat Transfer of a Long Aluminum Fin

Alicyn Astle, Cameron J. Dix, Lee Lorimer, Ali Siahpush

Southern Utah University

ABSTRACT

There are several important concepts in heat transfer, including conduction, convection, and radiation. Most heat transfer analysis is assumed to be one-dimensional, steady-state, and uniform, if possible. These simplifications make solving complicated problems easier. Convection heat transfer is enhanced by enlarging the surface area and exposing it to the surrounding fluid, air. This can be done by adding fins. Fins are used over a broad range of industries to cool down or heat devices. Fins are highly conductive and made from various materials like aluminum. The purpose of this experiment is to analyze the heat transfer throughout a fin, an aluminum rod suspended in air, assumed to be infinitely long (the end of the rod is at room temperature). This is done by using experimental data and known transient and steady-state heat transfer equations for a fin to predict the temperature profiles. Then to

get an accurate heat transfer coefficient, the value can be found by changing the value until the temperature curves match. The value found for the natural convection heat transfer coefficient was $10 \left(\frac{W}{m.K}\right)$. The temperature profiles between the theoretical and measured steady-state were compared and the average difference between them was 1.34. The transient state was also compared and the average difference between all the nodes was 0.2912. The difference values between both the steady and transient states are extremely small and show that the data gathered was correct.

NOMENCLATURE		
Symbol	Description	Value / Unit
A_c	Cross-sectional area	$3.17 \times 10^{-5} \text{ (m}^2\text{)}$
A_f	Surface area of fin	$0.020 \text{ (m}^2\text{)}$
D	Diameter	(m)
h	Convection heat transfer coefficient	$10 \left(\frac{W}{m^2.K}\right)$
k	Thermal conductivity of 6061 Aluminum	$177 \left(\frac{W}{m.K}\right)$
L	Length of fin	1 (m)
N	Nodal point	-
P	Perimeter of fin	0.01995 (m)
f	Heat loss rate	(W)
T	Temperature	(°C)
T_0	Base temperature	(°C)
T_∞	Ambient temperature	21.7 (°C)
τ	Time constant	-
X	Axial location	(m)
$\theta(x)$	Excess temperature ($T(x) - T_\infty$)	(°C)

INTRODUCTION

Heat transfer is used in a variety of devices such as electronic components, heat exchangers, and heating and air conditioning systems. In many such devices, extended surfaces (fins) are used to enhance the heat transfer rate between a solid surface and the surrounding air [1]. Fins combine conduction and convection heat transfer effects to either cool or heat devices over a broad range of industries. One of the many parameters to consider in fin design is the convection heat transfer coefficient. The heat transfer coefficient, however, is generally found with values based on uniform heat flux source or uniform temperature at

the base of the fin [1]. For fin analysis, this is inaccurate because fins exhibit a decaying exponential temperature distribution across the fin. The correct convection heat transfer coefficient is important because it is used extensively in the analysis of heat transfer for both transient and steady-state conditions [2]. The experimental value can be found by estimating a value and comparing the experimental data and the theoretical value.

The purpose of this research is to construct an apparatus that can accurately model the transient and steady-state heat transfer across a fin. The set-up involves an aluminum rod, assumed to be infinitely long (the end of the rod is at the same temperature as the environment), attached to a base with a heating pad and insulation to surroundings to prevent heat loss. The heat transfer is assumed to be one-dimensional. Then, by developing transient and steady-state heat transfer equations for a fin, a prediction and analysis of the temperature profile across the fin can be found, as well as the convection heat transfer coefficient that matches the temperature decay across the fin.

THEORY

In this analysis, these assumptions are considered:

1. No heat generation.
2. Thermal conductivity k remains constant.
3. Convection heat transfer coefficient h is constant and uniform over the entire surface of the fin
4. The heat transfer through the rod is one-dimensional and uniform cross-section ($A_c = \text{Constant}$).
5. Neglect heat loss at tip ($T_{\text{fin tip}} = T_{\infty}$).

Steady-State

Under the assumptions listed above, the equation for the temperature profile in a fin is [2]:

$$T(x) - T_{\infty} = (T_0 - T_{\infty})e^{-\sqrt{\frac{hp}{kA_c}}x} \quad (1)$$

where $T(x)$ is the temperature ($^{\circ}\text{C}$) at a given distance (x) from the base, T_{∞} is the ambient temperature (21.7°C), T_0 is the temperature of the base ($^{\circ}\text{C}$), h is the convection heat transfer coefficient ($\frac{\text{W}}{\text{m}^2\cdot\text{K}}$), ρ is the density of aluminum ($\frac{\text{kg}}{\text{m}^3}$), k is the thermal conductivity of aluminum ($\frac{\text{W}}{\text{m}\cdot\text{K}}$), and A_c is the cross-sectional area (m^2) of the aluminum rod. The equation for the energy leaving the plate is defined for long fin as [2]:

$$\dot{Q}_f = \sqrt{hPkA_c} (T_0 - T_\infty) \quad (2).$$

The expected temperature profile is shown in Figure 1.

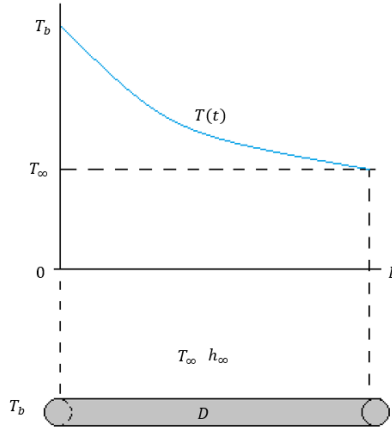


Figure 1. The expected curve of the temperature throughout the length of the fin.

Transient

If time-dependent (transient) behavior of the fin is required, the energy balance equation for a control volume of material is [1]:

$$\dot{Q}_{in} - \dot{Q}_{out} = \Delta \dot{E}_{syst} \quad (4)$$

where \dot{Q}_{in} is the rate of heat transfer into the system (W), \dot{Q}_{out} is the rate of heat transfer leaving the system (W), and $\Delta \dot{E}_{syst}$ is the change of energy of the material (W). The change in energy of the material can be described as [2]:

$$\Delta \dot{E}_{syst} = \rho c_p A_c \Delta x \frac{dT}{dt} \quad (5)$$

where Δx is the length of an element of the cross-section (m). One-dimensional conductive heat transfer (Fig. 2) through two internal nodes of a cross-section of material is described as [2]:

$$\dot{Q}_{cond} = kA_c \frac{(T_m - T_{m+1})}{\Delta x} \quad (6)$$

where T_m is the temperature at the first node (K) and T_{m+1} is the temperature at the next node (K). Convective heat transfer from a surface of an element is [1]:

$$\dot{Q}_{\text{conv}} = hA_s(T_m - T_\infty) \quad (7).$$

Figure 2 shows how conduction and convection heat transfer are acting on several sections of a cylindrical fin. By doing finite difference numerical analysis, the energy balance the system can be represented as follows:

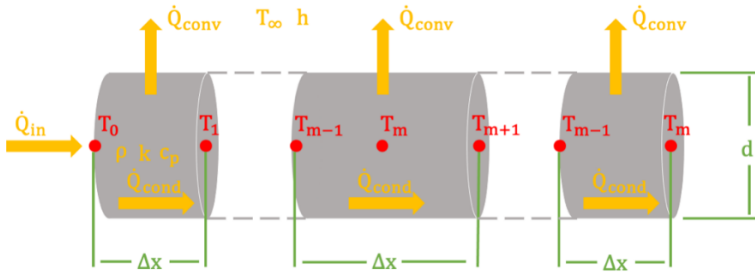


Figure 2. Heat transfer throughout sections of the aluminum rod.

The energy balance at the heated end of the fin (node 0) is described as

$$\dot{Q}_{\text{in}} - kA_c \frac{T_0 - T_1}{\Delta x} - h \frac{A_s}{2} (T_0 - T_\infty) = \rho c_p A_c \frac{\Delta x}{2} \frac{dT}{dt} \quad (8).$$

Similarly, the energy balance at any internal node of the fin (m) is described as

$$kA_c \frac{T_{m-1} - T_m}{\Delta x} - kA_c \frac{T_m - T_{m+1}}{\Delta x} - hA_s(T_m - T_\infty) = \rho c_p A_c \Delta x \frac{dT}{dt} \quad (9).$$

Assuming the final node of the fin (m) to be at the ambient temperature (long fin assumption), the energy balance yields

$$kA_c \frac{T_{m-1} - T_m}{\Delta x} - hA_s(T_m - T_\infty) = \rho c_p A_c \frac{\Delta x}{2} \frac{dT}{dt} \quad (10).$$

Equations (8-10) share two common terms that may be denoted as

$$\tau = \frac{kdt}{\rho c_p \Delta x^2}; \quad D = \frac{4h_\infty \Delta x^2}{kd} \quad (11).$$

It is possible to predict the temperature with respect to time and position using a finite difference numerical analysis. The implicit Euler

method was used in this analysis [2]. The implicit Euler method uses a forward difference approach to predict the next temperature stepping through time

$$\Sigma \dot{Q}^{i+1} = \Delta \dot{E}_{\text{sys}}^i \quad (12)$$

where $i+1$ denotes the next time step, and i is the current time step. The temperature derivative with respect to time from Eq. (5) becomes

$$\frac{dT}{dt} = \frac{T_m^{i+1} - T_m^i}{\Delta t} \quad (13).$$

Substituting Eqs. (11) and (13) into Eqs. (4)-(7) and using the implicit method described in Eq. (12), Eq. (8-10) become

$$-(2\tau + D\tau + 1)T_0^{i+1} + (2\tau)T_1^{i+1} + T_0^i + \frac{8\tau \dot{Q}_{\text{in}} \Delta x}{k\pi d^2} + D\tau T_\infty = 0 \quad (14)$$

$$(\tau)T_{m-1}^{i+1} - (2\tau + D\tau + 1)T_m^{i+1} + (\tau)T_{m+1}^{i+1} + T_m^i + \tau D T_\infty = 0 \quad (15)$$

$$(2\tau)T_{m-1}^{i+1} - (2\tau + D\tau + 1)T_m^{i+1} + T_m^i + D\tau T_\infty = 0 \quad (16).$$

Equations (14-16) are a system of equations with m unknowns that can be solved simultaneously at each time step to find the numerical solution for the temperature at each node (m) through time.

EQUIPMENT AND MATERIALS

1. 6061 Aluminum rod (0.635-cm diameter, 1-m length) with 1.27-cm-long threaded end
2. 6061 Aluminum plate (7.62×7.62-cm, 1.27-cm thickness) with threaded hole in center
3. 1-in.-thick foam board insulation
4. 11 thermocouples (in-house thermocouple system provided by instructor)
5. Power source (https://hybridatelier.uta.edu/uploads/equipment/manual_pdf/27/B1OyuYQCw9S.pdf)
6. Clamps
7. Thermal paste (https://www.amazon.com/dp/B00M5G6AHY/ref=cm_sw_r_sms_api_glt_fabc_N922TFPYVJC15SNJRVW2?_encoding=UTF8&th=1)
8. Sealant
9. Rubber cooking mold
10. Metal baking mold
11. Heating pads (https://www.amazon.com/24V-Flexible-Polyimide-Heater-Plate/dp/B074SXKPZL/ref=rvi_sccl_14/ 132-

2730684-5203027?pd_rd_w=DVRtc&content-id=amzn1.
 sym.f5690a4d-f2bb-45d9-9d1b-736fee412437&pf_rd_p=
 f5690a4d-f2bb-45d9-9d1b-736fee412437&pf_rd_r=
 RAVH1G9TNZNQ8GVM8FET&pd_rd_wg=snhzG&pd_rd_r=
 =f5292700-b3a3-4bca-90f1-8ef7f285d5f7&pd_rd_i=
 B074SXXPZL&th=1)

PROCEDURE

Setup and Preparation

The basic experimental setup consisted of an insulation shell surrounding a $7.62 \times 7.62 \times 1.27$ -cm aluminum plate with a circular aluminum rod, 0.636 cm in diameter and 1 m long, attached perpendicularly to the plate. Holes, which are represented by nodes in a theoretical analysis, were drilled into the center of the rod at varying intervals. A baking mold was used as a barrier between the heating pad and the insulation to protect against melting or burning the insulation. Insulation encapsulated the entire plate, heating pad, and baking mold, with a hole cut for the rod to ensure that all of the heat energy was transferred through the fin. Clamps were used to keep the insulation together and to balance the fin on the table. A metal baking mold was also used to keep the shape of the apparatus; it was located outside of the insulation so that it did not affect the heat transfer rate of the insulation. The experimental setup is shown in Figure 3.

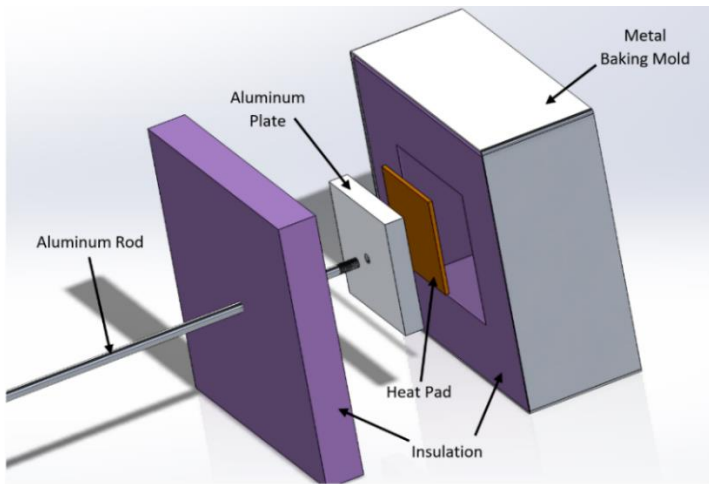


Figure 3. 3D SolidWorks model expansion of the fin and insulation assembly.

For node placement in the fin, the first hole is located 1.9 cm from the base of the rod; this hole represents the first node outside of the plate. The next hole is located 6.35 cm from the base; this hole represents the first node outside of the insulation. The next 5 holes are located 10.16 cm apart from the first hole outside the insulation. The last 3 holes are 15.25 cm apart. This setup is shown in Figure 4. There is a larger amount of heat transfer closer to the heat pad than at the end of the rod, which is the reason for more nodes located in the first half of the the rod.

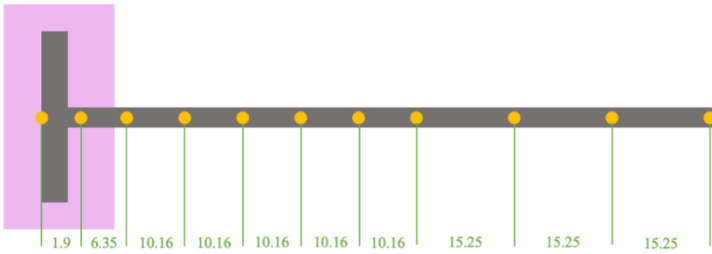


Figure 4. Thermocouple/node placement of the rod in centimeters.

Thermocouples were coated in thermal paste and placed in each hole. A sealant was then applied over the thermocouples to act as an adhesive and prevent them from slipping out of position (Fig. 5). After test runs, it was determined that a constant voltage of 5 volts and 0.37 amps would give the heating pad a temperature of approximately 45°C at the fin base.

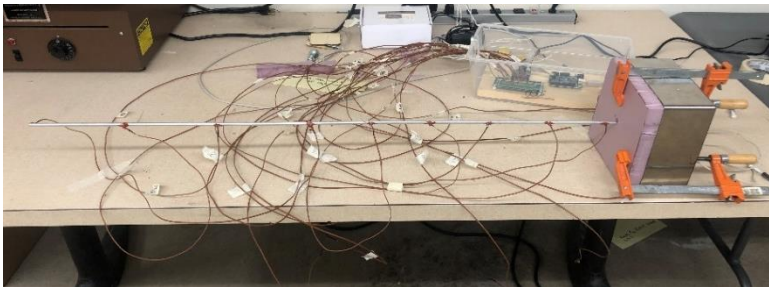


Figure 5. Entire experimental setup ready for testing.

Experiment

After the proper setup and preparation, the experiment was run as follows:

1. Ensure that all thermocouples are properly sealed in the fin.
2. Begin monitoring the temperature readings from the thermocouples, looking for irregularities and malfunctioning thermocouples.
3. Begin recording the temperatures.
4. Begin heat transfer by applying a current to the heat pad. Be sure the voltage and current inputs are 5 V and 0.37 A, respectively.
5. Take temperature data at about 1-minute intervals for approximately 3 hours or until steady-state is reached.

RESULTS AND DISCUSSION

The temperature at each node was recorded until the temperatures reached steady-state. The steady-state temperature data were plotted and compared with the prediction found using Eq. (1) as shown in Figure 6. The temperature data at each node over time were plotted and compared with the predictions found using Eqs. (13-15) as shown in Figure 6. The convective heat transfer coefficient was adjusted in the calculations until the plot of the theoretical temperatures matched the experimental data for both the transient and steady-state scenarios. A heat transfer coefficient of $10 \left(\frac{\text{W}}{\text{m.K}} \right)$ provided the best fit for both plots. This heat transfer coefficient is natural convection coefficients and is expected to be low [2].

Figure 6 shows strong correlation between the predicted values and the measured values once the system reached steady-state. We are interested in the maximum temperature difference. The average difference between the measured and theoretical values of T was 1.34°C , which indicates that the experiment is valid and that it represents an infinite fin quite well. The measured temperatures were lower than the predicted temperatures as expected because of various losses (heat loss to ambient) that were not included in the theoretical analysis.

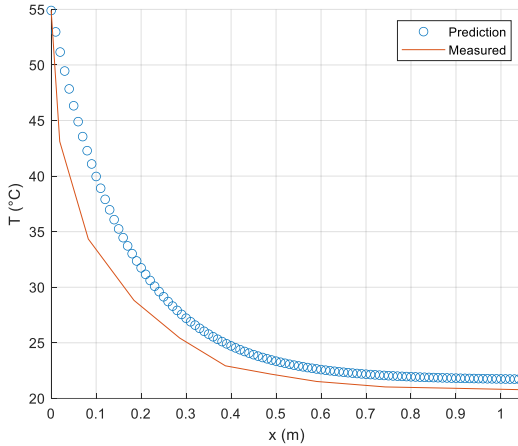


Figure 6. The predicted and measured temperatures for each node at steady-state.

In addition to the temperatures at steady-state, the predictions and the measured values for the transient state are shown in Figure 7.

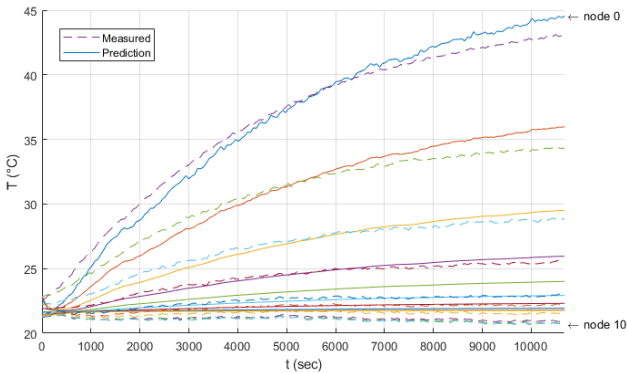


Figure 7. Temperature versus time over a 3-hour interval.

Figure 7 displays the recorded temperatures and the predicted temperatures as functions of time for the entire duration of the experiment. The temperatures at the beginning of the experiment vary widely from the predicted values. As time goes on, the experimental data follows the theoretical data more closely. Although the temperatures at the beginning vary largely, the maximum difference between the

predicted and measured values was 0.2912°C . The maximum difference between the predicted and measured values are extremely close to each other, and all the nodes follow similar trend lines with the measured temperature lower than predicted. This indicates that there are losses other than the fin to which the difference can be attributed.

SOURCES OF ERROR

One notable source of error was within the insulation shell. Although the insulation shell covered the majority of the plate, holes had to go through the backside of the insulation so thermocouples and wires for the power source could reach inside of the experiment. The hole in the insulation to fit the rod was not completely touching the rod. It should also be noted that the insulation may not have been perfect; the insulation may have let a small amount of heat transfer pass through it. This experiment assumed that all heat transfer was happening through the fin, but if any heat transfer was lost through the holes or the insulation, the data would be affected.

Another source of error could have resulted if the thermocouples were not properly sealed into the hole, in which case the temperature of the air leaking in could have affected the readings. The air conditioning vent above the experiment could have affected the experiment as well. If the air conditioning was blowing directly onto the experiment, it could have changed the temperature of the rod. The initial temperatures of the thermocouples also may have been incorrect as residual body heat from installing the thermocouples in the fin could have affected the initial temperature readings.

All equipment has some limitations to the accuracy of the results. For example, every thermocouple had a different reading when first tested at room temperature. Although all of the readings were fairly close to each other, none were the same. This could lead to minor errors in temperature readings. The power source would occasionally fluctuate the amps applied to the heating pad as well. Although the fluctuations were only 0.01 amperes, this could in turn fluctuate the heat coming from the heating pad.

CONCLUSION AND RECOMMENDATIONS

Fins can be an effective way to exchange heat between the surface and the fluid passing by it. In this experiment, the fluid in contact with the surface was air. By using a fin, the surface area is increased, thereby increasing the rate of heat exchanged. Depending on the surface being cooled or heated by a fin, it is important to be able to predict the temperature to achieve a desired result. When analyzing the fin under

steady-state conditions, the theoretical calculations were very close to the measured data. Exponential decay was also expected for the temperature profile of the fin and was confirmed during the experiment.

After the steady-state conditions were analyzed, the heat transfer coefficient of 10 (W/mK) had the best fit for the data, and a transient test was done over time. The rod and the plate started at room temperature, and as the temperature was recorded at each node over time it was plotted against the predicted values. There was only a slight difference in the values. This experiment shows temperatures at a certain location on a fin can be calculated and are very close to the actual measured temperature of the node over time.

A recommendation for future adaptations could be to use a larger-diameter rod. The 0.635-cm-diameter rod proved hard to machine nodes into, with the risk of bending or snapping the rod. There are more considerations for a wider-diameter rod, but accurate results could still be obtained.

REFERENCES

- [1] Abu-Mulaweh, H.I. “*Integration of a Fin Experiment into the Undergraduate Heat Transfer Laboratory.*” International Journal of Mechanical Engineering Education, vol. 33, no. 1, pp. 83-92, 2005.
- [2] Cengel, Y.A., and A.J. Ghajar. *Heat and Mass Transfer: Fundamentals and Applications*, 5th ed., McGraw-Hill Professional, 2014.

Steady-State and Transient Analysis of a Fin Under Water

**Mitchell Halverson, Floyd K. Kimber, Kobe Potter,
Jathen Chaffin, Ali Siahpush**
Southern Utah University

ABSTRACT

This paper describes an analysis that was performed on a fin underwater to better understand the convective coefficient of heat transfer, h , while giving experience into real-life engineering projects. The experiment was set up by making an aluminum fin using an aluminum plate and rod, where the rod is submerged in a plastic tub filled with water and the plate is heated via a heating pad outside of the tub of water. The plate and heat pad are insulated, so that heat from the heat pad is not lost to the environment. Thermocouples attached at specified distances from the heat source measured the temperature throughout the rod. To analyze the heat transfer through the rod, steady-state and transient conditions were considered, with models created on MATLAB to predict how the rod would lose heat and compare it with the data collected through experimentation. To collect the data, two 8-channel thermocouple data loggers were used. The general solution for finding the temperature and heat flux throughout the fin proves useful under conditions where the fin is assumed to be very long.

INTRODUCTION

A fin is an extended heat surface attached to a body to increase the rate of convection heat transfer. The rate of convective heat transfer can be enhanced by the application of fins as heat exchanging devices. Examples of fins include computer CPU heatsinks, radiators, and heat exchangers in power plants [1]. The main purpose of fins is to increase the surface area and thus directly increase the rate of convective heat transfer between a fluid and the heated surface to which the fin is attached. Increasing the surface area of an object, without greatly increasing the volume and mass of that object, is one of the most effective ways to improve convective heat transfer. Studies were done to alter the geometry of a fin to increase heat transfer. In these studies, notches were made into the fin as well as hollowing the fin, and both increased heat transfer [1]. To design effective fins, it is important to predict temperature distributions along the fin.

In the process of this experiment, a cylindrical aluminum fin was placed within a tank full of water at room temperature. The base of the fin was attached to an aluminum plate located on the exterior of the tank. This base was adjacent to an electrical heating pad, and both were well insulated from the surrounding air. Thus, the electrical energy supplied to the heat pad was conducted through the base to the fin and then dissipated via convection heat transfer through water. There were 16 thermocouples used to measure the change in temperature over time at various places along the rod and on either side of the plate.

Fins have practical applications to control the heat experienced within and external to a boundary. Some applications use fins to cool down storage spaces that use little electricity but want to find powerless ways to provide cooling [2]. Further analysis determined the effect that fin geometry has on heat transfer through a boundary [2], which is useful because it allows us to enter fields of innovation that have to do with temperature control within a space.

Understanding the effects of the coefficient of convective heat transfer and how it is affected by fin design is important to better allow for the proper design of a system that will allow for the maximum heat transfer out of the system.

THEORY

This experiment utilized two different methodologies to analyze convective heat transfer through a fin. In this section, we will derive the theory's relationship needed for the analysis of a general longfin, as shown in Figure 1.

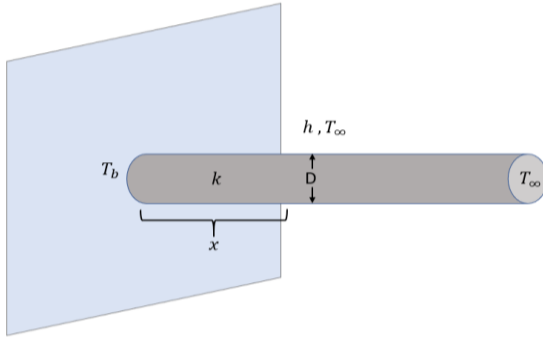


Figure 1. A model of a general fin.

These theories will then be applied to the specific fin used in this experiment. The first methodology will be used to determine the temperature distribution in the fin for a steady-state heat transfer condition. The second methodology will be used to determine the temperature distribution in the fin for a transient heat transfer condition, via a finite-difference approach.

STEADY-STATE ANALYSIS

To analyze the steady-state fin condition, we first assume that the fin is long enough that all the heat transfer into the fin via the base is transferred to the environment via convection. This means that at the full length of the fin, the temperature of the fin is the same as the temperature of the surrounding fluid.

To begin the steady-state analysis of the fin, the first law of thermodynamics is expressed as [3]

$$\Delta \dot{E} = \dot{Q}_{in} - \dot{Q}_{out} \quad (1)$$

where $\Delta \dot{E}$ is the change in energy in a given section of the fin (W), \dot{Q}_{in} is the rate of heat transfer going into a given section of the fin (W), and \dot{Q}_{out} is the rate of heat transfer going out of a given section of the fin (W).

At the steady-state condition, the total energy of a given section of the fin is constant (no change in the energy of the system), therefore, $\dot{Q}_{in} = \dot{Q}_{out}$. Analyzing any section of the fin, \dot{Q}_{in} is through conduction heat transfer, either from the heat pad or the previous section of the fin, and \dot{Q}_{out} is conduction to the further section of the fin and convection to the surrounding fluid. Applying the steady-state conditions to Eq. (1) yields [3]

$$\dot{Q}_{cond, x} = \dot{Q}_{cond, x+\Delta x} + \dot{Q}_{conv} \quad (2)$$

where $\dot{Q}_{cond, x}$ is the rate of conductive heat transfer into a given section of the fin starting at position x (W), $\dot{Q}_{cond, x+\Delta x}$ is the rate of conductive heat transfer going out of a given section of fin starting at position x and ending at position $x + \Delta x$ (W), and \dot{Q}_{conv} is the rate of convective heat transfer going out of a given section of the fin, starting at position x and ending at position $x + \Delta x$, into the surrounding fluid.

The rate of conductive heat transfer can be defined as [3]

$$\dot{Q}_{cond} = -kA \frac{dT}{dx} \quad (3)$$

where k is the thermal conductivity ($\frac{W}{m.K}$), A is the cross-sectional area of the given section of the fin (m^2), $\frac{dT}{dx}$ is the change in temperature over the change in position along the length of the fin ($^{\circ}C/s$)

The rate of convective heat transfer can be defined as [3]

$$\dot{Q}_{conv} = h(p \Delta x)(T - T_{\infty}) \quad (4)$$

where h is the coefficient of convective heat transfer of the fluid that surrounds the fin ($\frac{W}{m^2.K}$), p is the perimeter of the fin at the given section (m), T is the temperature of the given section of the fin ($^{\circ}C$), and T_{∞} is the uniform temperature of the fluid that surrounds the fin ($^{\circ}C$).

Combining Eqs. (2-4), assuming steady-state conditions, results in the second-order ordinary differential equation

$$\frac{d^2T}{dx^2} - \frac{hp}{kA}(T(x) - T_{\infty}) = 0 \quad (5)$$

where $T(x)$ is the temperature of the given section fin at position x ($^{\circ}C$). Solving Eq. (5), we arrive at the general solution as

$$T(x) - T_{\infty} = c_1 e^{\sqrt{\frac{hp}{kA}}x} + c_2 e^{-\sqrt{\frac{hp}{kA}}x} \quad (6)$$

Assuming the end of the fin remains at the same temperature as the surrounding fluid, $c_1 = 0$. Solving for the initial condition at $x = 0$ (m), $c_2 = T_b - T_{\infty}$, where T_b is the temperature of the base of the fin ($^{\circ}C$). We can then solve for $T(x)$, which will yield the temperature of any section of the rod.

$$T(x) = (T_b - T_{\infty})e^{-\sqrt{\frac{hp}{kA}}x} + T_{\infty} \quad (7)$$

Equation (7) is the theoretical prediction (steady-state exact solution) needed to analyze steady-state heat transfer through the fin.

Transient Analysis

To analyze the fin in a transient heat transfer condition, the second portion of the experiment will utilize the explicit finite-difference approach [3]. To perform the numerical analysis, the fin was divided into several nodes. Then, with the initial temperature of the system (T at $t=0$), we predict the temperature of each fin section one-time step later [3]. As before, the first law of thermodynamics, Eq. (1), was utilized. In the steady-state analysis, the left-hand side of Eq. (1) was equal to zero. In a transient analysis, the change in energy in the section of fin being analyzed, $\Delta \dot{E}$, changes in time and can be presented as

$$\Delta \dot{E} = \frac{m c_p \Delta T}{\Delta t} \quad (8)$$

where m is the mass of the fin (kg), c_p is the specific heat of the fin ($\frac{J}{kg^\circ C}$), ΔT is the change in temperature of that given section of the fin ($^\circ C$), and Δt is time step (s) [3]. Applying the transient heat transfer, Eq. (2) can be rewritten as

$$\dot{Q}_{cond\ in} - \dot{Q}_{cond\ out} - \dot{Q}_{conv\ out} = \frac{m c_p \Delta T}{\Delta t} \quad (9)$$

In a finite-difference approximation of the heat transfer, the fin is approximated by dividing the entire length of the fin into a finite number of smaller sections. In each of these sections, we assume that the temperature is uniform in that given section of the rod, convection is uniform across the section, and the section length is Δx . The points (nodes) between these given sections are then analyzed. By knowing the properties of the fin, and at a certain time, we can predict the temperature of the fin after a short time-step.

In our analysis, there are three general forms that the nodes will take: the initial node (Fig. 2), the internal nodes (Fig. 3), and the final node (Fig. 4).

The initial node is different from the internal nodes, because it has the fin only on one side of it, not surrounding it. This means there is half as much surface area exposed to the fluid for convection between the initial node and the first internal node as there is between two internal nodes. Another difference is that the heat transfer entering the node is directly from the heat pad, rather than conducted from the previous node. The heat transfer coming into the fin from the heat pad, \dot{Q}_{pad} , was measured through an analysis of the one-dimensional heat transfer through the fin inside of the insulation before it comes in contact with the fluid, so there was no convection as seen in Figure 3.

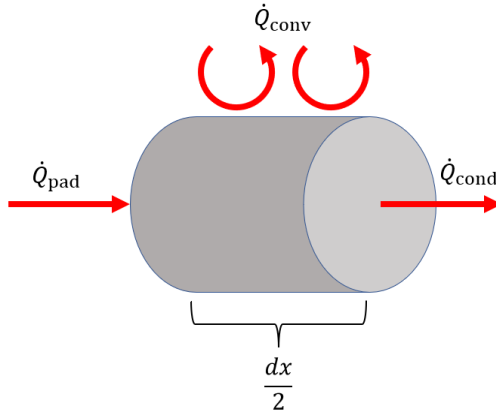


Figure 2. The heat transfer about the initial (base) node of the fin.

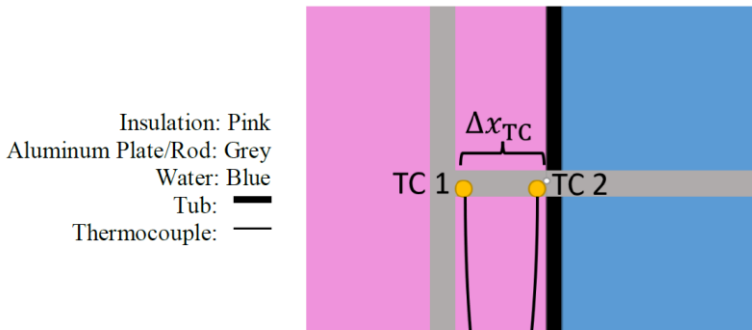


Figure 3. The thermocouple arrangement needed to measure the heat coming into the fin from the heat pad, \dot{Q}_{pad} .

By taking the temperature of the fin at two points inside of the insulation, and knowing the distance between the points, we can use Eq. (3) to determine the heat conduction coming from the heating pad. Adapting Eq. (3) to the temperatures measured by the thermocouples in the insulation, we get

$$\dot{Q}_{pad} = -kA \frac{T_{TC2} - T_{TC1}}{\Delta x_{TC}} \quad (10)$$

Recording the temperature at the thermocouples in intervals of Δt , we can approximate the heat transfer into the fin \dot{Q}_{pad} over each time interval.

The one-dimensional assumption can be made based on the knowledge that most of the heat between the two points on the rod inside of the insulation will only move along the fin, not out into the insulation. The insulation should keep most of the heat flowing along the rod rather than being lost to the surroundings.

The heat transfer equation for the initial node can be defined as

$$\Delta \dot{E}_{node\ 1} = \dot{Q}_{pad} - \dot{Q}_{cond\ out} - \dot{Q}_{conv\ out} \tag{11}$$

where $\Delta E_{node\ 1}$ is the change in energy (W) in the initial node, or node 1, and all other variables are as previously defined in Figure 2.

To simplify this and the following equations, further variables need to be defined based on the coefficients and constants of the experiment. The first variable is the thermal diffusivity, α , $\left(\frac{m^2}{s}\right)$, which is expressed as [3]

$$\alpha = \frac{k}{\rho c_p} \tag{12}$$

where ρ is the density of the fin. The second variable to be defined is τ (time constant), which is expressed as ref

$$\tau = \frac{\alpha \Delta t}{\Delta x^2} \tag{13}$$

where Δt is the time-step. Substituting Eqs. (3), (4), and (8) into Eq. (11), solving for the temperature at $i+1$, and simplifying using the variables expressed in Eqs. (12) and (13), the result can be written as

$$T_0^{i+1} = 2 \dot{Q}_{pad} \frac{\Delta t}{\rho A \Delta x c_p} - 2 \tau (T_1^i - T_0^i) + \frac{h p \Delta t}{\rho A c_p} (T_\infty - T_0^i) + T_0^i \tag{14}$$

where T_0^i is the temperature at the initial node at time-step i . The T_1^i is the temperature at node 1, the internal node adjacent to the initial node, and T_0^{i+1} is the temperature of the initial node one time-step in the future.

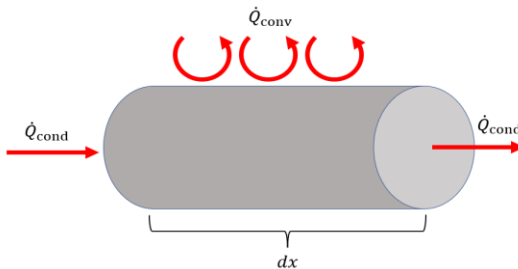


Figure 4. The heat transfer about the intermediate nodes of the fin.

The internal nodes all have the same interactions with the environment and the nodes adjacent, and so they will have the same symbolic equations. Analyzing the fin at any node m , using the first law of thermodynamics, we get

$$\Delta \dot{E}_{node\ m} = \dot{Q}_{cond\ in} - \dot{Q}_{cond\ out} - \dot{Q}_{conv\ out} \quad (15)$$

Again, substituting Eqs. (3), (4), and (8) into Eq. (10), solving for the temperature one time-step ahead at node m , and simplifying using the variables expressed in Eqs. (11) and (12), the result can be written as

$$T_m^{i+1} = \tau(T_{m-1}^i - 2T_m^i + T_{m+1}^i) + \frac{h\ p\ \Delta t}{\rho\ A\ c_p}(T_\infty - T_m^i) + T_m^i \quad (16)$$

The final node of the fin has a unique equation as well because there is no conduction out of the tip of the fin (Fig. 5). Applying the first law of thermodynamics to the final node of the fin, we get

$$\Delta \dot{E}_{node\ f} = \dot{Q}_{cond\ in} - \dot{Q}_{conv\ out} \quad (17)$$

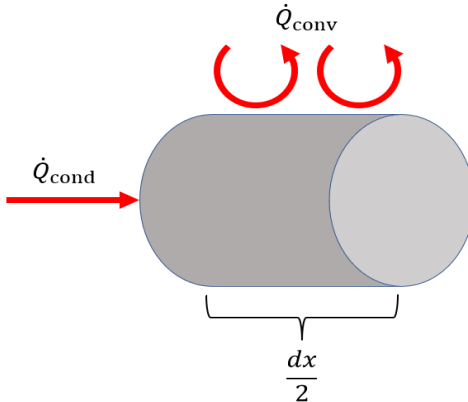


Figure 5. The heat transfer about the final node of the fin.

As the initial node, the final node has only half as much surface area exposed to the fluid for convection between the final internal node and the final node as there is between two internal nodes.

Substituting in Eqs. (3), (4), and (8) into Eq. (10), solving for the temperature one time-step ahead, and simplifying using the variables expressed in Eqs. (11) and (12), the result can be written as

$$T_f^{i+1} = 2\tau(T_{f-1}^i - T_f^i) + \frac{h p \Delta t}{\rho A c_p}(T_\infty - T_f^i) + T_f^i \quad (18)$$

where T_{f-1}^i is the temperature of the internal node just before the final node at time-step i , T_f^i is the temperature of the final node at time-step i , and T_f^{i+1} is the temperature of the final node one time-step in the future.

EQUIPMENT/MATERIALS

- An aluminum rod of $\frac{3}{8}$ -in. diameter and 27-in. length
- An aluminum plate of dimensions 6×8 in.
- Plastic tote to act as a water container
- Waterproof thermocouple (<https://www.amazon.com/-/es/HUATO-S220-T8-Registrador-alimentaci%C3%B3n-certificado/dp/B07SJRG6Y8>)
- Thermal paste to increase thermal conduction between the threaded plate and rod (<https://www.amazon.in/Protronix-Extreme-Performance-Thermal-Compound/dp/B07PQTT3WZ>)
- Uniseal to create a waterproof seal around the rod and the hole in the tote
- Moldable epoxy to create a waterproof seal around the thermocouples in the rod

PROCEDURE

Preparing the Materials

1. Thread the rod, and drill and tap the plate, so they will screw together.
2. Drill 13 holes $1/16$ in. deep into the aluminum rod, at the following positions.
 - a. Just after the thread on the rod, as close to the base plate as possible.
 - b. 0.5 in. from the base plate
 - c. 1.0 in. from the base plate
 - d. 1.5 in. from the base plate
 - e. 2.0 in. from the base plate
 - f. 3.0 in. from the base plate
 - g. 4.0 in. from the base plate
 - h. 6.0 in. from the base plate
 - i. 9.0 in. from the base plate
 - j. 13.0 in. from the base plate

- k. 16.0 in. from the base plate
- l. 20.0 in. from the base plate

Preparing the Experiment

- 3. Drill a single hole where the fin will be inserted into the tub.
- 4. Fill all of the holes on the fin with thermal paste and epoxy regardless of whether the hole will be in the water or not.
- 5. Label each thermocouple from base to tip, 1, 2, 3, etc. after the base thermocouple. From here, the fin is screwed into the base plate.
- 6. Enclose the base plate and the heat pad inside the pink insulation. All the sides of the plate are enclosed by the insulation and taped down to ensure that the holes on the insulation are closed.
- 7. Apply thermal paste and epoxy to the thermocouple inside the tub to ensure that they are stationary during testing.
- 8. Label each thermocouple wire and determine a location to be set up and the corresponding place on the meter to be measured.
- 9. When the testing begins, measure the temperature at each spot on the fin, in 10-second increments.
- 10. The voltage, current, power of the testing is 5 V, 2.5 A, respectively.
- 11. See Figures 6 and 7 for the assembled system.



Figure 6. The complete set-up of the entire apparatus.

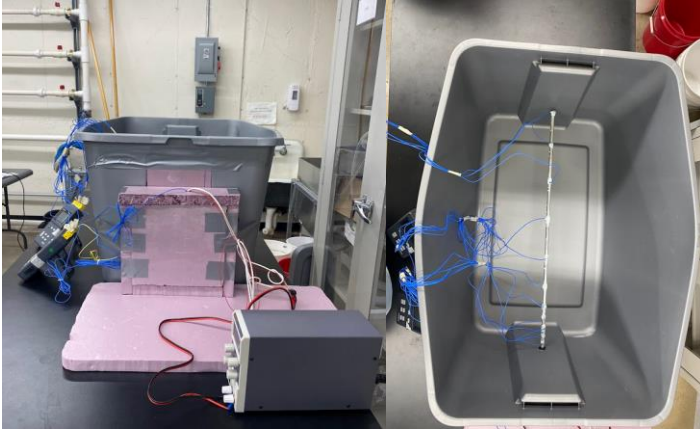


Figure 7. (Left) Representation of how the plate and heat pad is insulated. (Right) Configuration of the thermal couples in the bin.

Results and Discussion

In our experiment, we first calculated the heat transfer into the fin from the pad, \dot{Q}_{pad} , using Eq. (3). The amount of energy entering the fin increased quickly at the beginning and then began to taper off as time progressed, until gradually approaching 4.713 W after about 3 hours and 40 minutes, as can be seen in Figure 9.

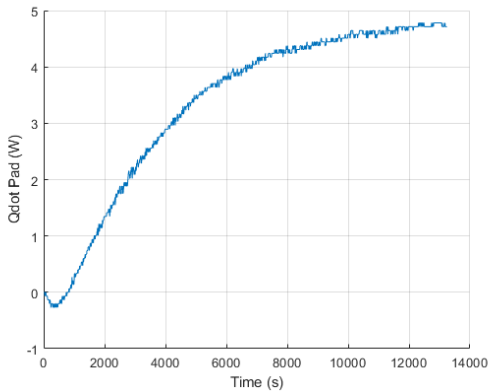


Figure 9. The power supplied to the fin through conduction.

In the mathematical models described in the theory section, the only unknown variable needed to determine the temperatures is the convective heat transfer coefficient, h . The temperatures at the end of the experiment were determined to be nearly steady-state, so they were used to approximate the h value for the models. An h value of $550 \left(\frac{w}{m^2 \cdot k} \right)$ best aligned the temperatures of the mathematical models with the temperatures collected out of the many h values tested. The final temperatures measured in the experiment along are presented in Figure 10, along with the temperatures predicted using the model described in the theory section at an h of $550 \left(\frac{w}{m^2 \cdot k} \right)$.

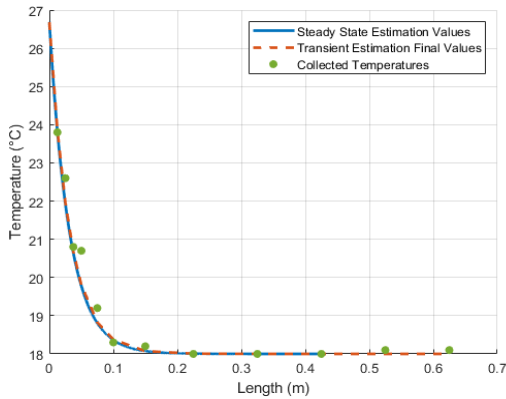


Figure 10. Temperature distribution along the fin.

The data seem to align well on the plot, and using a percent difference comparison (Appendix) it is easy to see that the models align well with <5% difference on both models. Transient analysis of the fin as it is being heated can be seen in Figure 11.

Observing the graph, the transient analysis follows the temperatures observed in the experiment well. The transient model does not appear to consistently overestimate or underestimate the temperatures observed.

The temperatures collected by the thermocouples farther from the base of the fin barely rose in temperature over the course of the experiment. The theory predicted that past 15 cm out from the base of the fin the temperature should be constant. This can be seen in Figure 10 clearly; looking at the temperatures of the thermocouples plotted on

Figure 11, it is easy to see that the temperature at the thermocouples past 15 cm experience minimal rises in temperature.

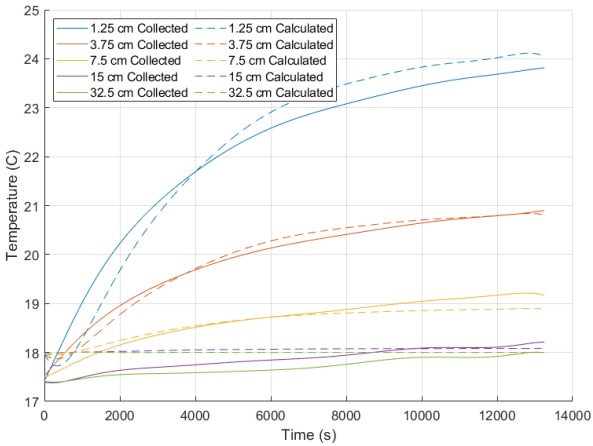


Figure 11. The calculated temperature of the fin at a variety of distances from the base.

The temperature of the base of the fin is off much further than the rest of the temperatures as can be seen in Figure 12.

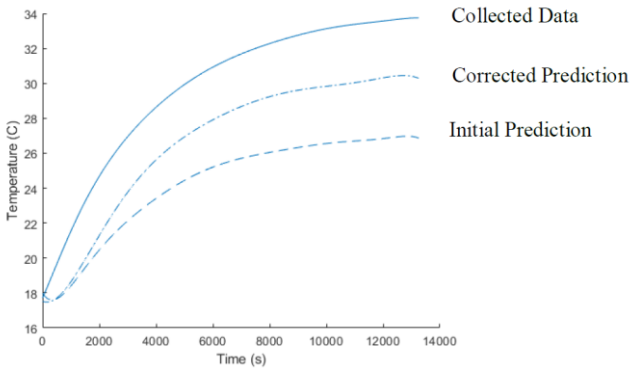


Figure 12. The recorded temperature of the base, the predicted temperature of the base, and a corrected prediction of the temperature of the base.

The temperature measured by the thermocouple at the base of the fin is much greater than the temperature predicted by the base transient model, or the corrected model discussed in the theory.

The fact that the base node is the only one that is not following the analysis is a cause for concern. This may be due to the placement of the thermocouple measuring the temperature at the base of the fin. The thermocouple was placed on the outside of the tank on the opposite side of the uniseal. As a result, the true temperature of the base of the fin was not collected. An attempt to correct the data was made using an assumption of one-dimensional heat transfer along the fin between the point where data was collected and that where the true base of the fin is. This can be done with a modified version of Eq. (10). If we assume the heat transfer through the fin in the section of fin inside the uniseal is \dot{Q}_{pad} , we can rearrange Eq. (10) to solve for the temperature of the fin on the outside of the uniseal.

$$T_{corrected} = T_{measured} - \frac{\dot{Q}_{pad}}{kA} \Delta x_{uniseal} \quad (19)$$

where $T_{corrected}$ is the corrected temperature of the base of the fin, $T_{measured}$ is the temperature measured opposite the uniseal from the base of the fin, and $\Delta x_{uniseal}$ is the width of the uniseal. The corrected base temperature found from this equation is shown in Figure 12. The correction does not account for all the differences, and so the assumption of heat transfer in that section of the fin may not be correct. This area of the fin is not insulated and is in contact with the tub holding the water, so the temperature may drop more than the one-dimensional analysis accounts for.

The collected data appear to follow the models developed in the theory section well at an h value of 550 $\left(\frac{W}{m^2k}\right)$. The temperatures collected along the fin match the temperatures estimated using the steady-state analysis except for the initial node. Although the temperatures collected do not exactly match the predicted temperatures, the fact that the predicted value is sometimes higher and sometimes lower than the actual value leads us to believe that the predictions are off because of random error rather than a systemic error in our prediction methods.

The h value of 550 $\left(\frac{W}{m^2k}\right)$ is within the range of known values for the convective heat transfer coefficient of water [4]. Likely, the convective heat transfer coefficient is not constant along the length of the fin because natural convection is heavily reliant on the buoyant forces, so the sections of the fin that heat the water more quickly will have higher buoyant forces, and thus more convection.

The steady-state model of heat transfer out of a fin, Eq. (7), and the transient model used as described in the theory section are supported by the fact that after about 15 cm the temperature is nearly constant. Both models predict the change in temperature to be nearly zero as fin extends past 15 cm. As the temperature of the fin does not rise past this point, any part of the fin past 15 cm is unnecessary to dissipate the heat. As such, we can approximate any fin past 15 cm in our experiment to be an “infinite” fin.

SOURCES OF ERROR

Throughout this experiment, there were various possible sources of error. The measurements done to determine the distance from the base plate may have been slightly incorrect when they were machined. The calibration on the thermocouples may have been off slightly. In one of our tests, there were various data points where the temperature was recorded as 0°C and that was assumed to be due to poor connection in the thermocouple cables. Another source of error may be the assumption that there was one-dimensional heat transfer from the insulation to the rod and along the length of the rod were not true. The uniseal may have allowed for greater heat loss in a different dimension than the insulation. It is also important to remember that aluminum has varying degrees of k values at different temperatures. It was also assumed that the water would remain the same throughout the tests. Our pool may not have been large enough because the temperature rose by about 1 degree over each test. Although our fin was not infinitely long, it was assumed that steady-state was reached, although it never truly will. If these assumptions are not true, then that may affect the accuracy of our experiments.

CONCLUSION AND RECOMMENDATIONS

In conclusion, we found that given the temperatures along the length of a fin and the heat entering the fin we can determine a value for the convective heat transfer coefficient that will allow us to predict the temperature of the fin throughout the transient portion of heating the fin.

The data collected and the models verified in this paper will aid those who define fins to increase convective heat transfer to both find a way to measure the convective heat transfer coefficient of the fluid in which their fin will operate and design the fin that will be needed to dissipate the energy being supplied to it.

For those that are interested in building on our research, we would advise using caution in the placement of the thermocouples. The correction made in the discussion section to correct the temperature of

the base of the fin could have been avoided had we placed the thermocouple in a better location.

The next step we would take in analyzing convective heat transfer with our experimental setup would be to explore forced convection by forcing the fluid around the fin to move. This could be done in the air via a fan or by inducing a flow in the water.

REFERENCES

- [1] Mohankumar D, Shashank, Pazhaniappan Y, Nithesh Kumar RA, Ragul R, Manoj Kumar P, Nikhil Babu P (2021) *Computational study of heat-transfer in extended surfaces with various geometries*. IOP Conf Ser Mater Sci Eng 1059:012055.
- [2] Gharebaghi M, Sezai I (2007). *Enhancement In Heat Transfer In Latent Heat Storage Modules With Internal Fins*. Num Heat Transf A Applic 53(7):749-765.
- [3] Çengel YA, Ghajar AJ (2015). *Heat and Mass Transfer: Fundamentals & Application* (5th ed.). New York: McGraw Hill.
- [4] Engineering ToolBox (2003). *Convective Heat Transfer*. [online] Retrieved December 17, 2021, from https://www.engineeringtoolbox.com/convective-heat-transfer-d_430.html.

APPENDIX

This table shows percent difference calculations for both steady-state analysis and transient analysis.

Distance (cm)	Experimental temp. (°C)	Steady-state analysis		Transient analysis	
		Temp. (°C)	% difference	Temp. (°C)	% difference
0 (Initial)	33.8	26.88	22.8	26.87	22.8
1.25	23.8	24.03	0.8	24.05	0.8
2.5	22.6	22.09	1.7	22.12	1.6
3.75	20.8	20.77	0.0	20.81	0.0
5	20.7	19.88	2.7	19.91	2.6
7.5	19.2	18.87	1.1	18.89	1.0
10	18.3	18.39	0.3	18.41	0.4
15	18.2	18.08	0.4	18.08	0.4
22.5	18.0	18.00	0.0	18.00	0.0
32.5	18.0	18.00	0.0	18.00	0.0
42.5	18.0	18.00	0.0	18.00	0.0
52.5	18.1	18.00	0.3	18.00	0.3
62.5 (Final)	18.1	18.00	0.3	18.00	0.3

Scale Analysis of a Solid–Liquid Phase Change Thermal Energy Storage System

Jordan Whitlock and Ali Siahpush
Southern Utah University

Abstract

A detailed scale analysis study has been carried out to evaluate the heat transfer performance of a solid–liquid phase change thermal energy storage system. The phase-change material, 99% pure eicosane with a melting temperature of 36.5°C, was contained in a vertically oriented test cylinder that was heated at its outside boundary, resulting in radially inward melting. Detailed quantitative time-dependent temperature distributions and melt-front motion and shape data were obtained in previous research. A heat transfer scale analysis was used to help interpret the data and development of heat transfer correlations. In this scale analysis, conduction and natural convection heat transfer were considered. Comparison of experimental data with scale analysis predictions of the solid–liquid interface position and temperature distribution was performed. The analytical scale heat transfer results demonstrated good agreement with the experimental results and confirmed the existence of four melting regions.

INTRODUCTION

Passive thermal energy storage is a possible solution for many of the problems that arise in the modern world. Passive thermal energy storage has many uses in the temperature control systems of building designs, satellites, and in applications where access to an external power source is limited. In passive thermal energy storage, the energy is stored in the form of either sensible heat or latent heat. In using sensible heat, the temperature of the storage material increases as the energy stored increases. This may become an issue in many applications. By storing the energy in the form of latent heat, the energy is stored in the form of a phase change rather than increased temperature. Because the temperature is stable throughout the heat storage process, latent heat storage is often preferred when cryocoolers and active cooling systems are not available or not desired because of vibration [1].

To better understand the passive thermal energy storage via latent heat, we are building on previous research that has been conducted at Southern Utah University (SUU) over three years. The previous students designed and constructed a test system that consists of a vertical copper test cylinder that was heated and cooled inwardly by using copper tubing wrapped in a counter-flow arrangement around the outside of the test cylinder. The copper tubing was connected to a constant temperature bath that provides fluid to heat and cool the test cylinder at a range of -20°C to 100°C . The temperature of the phase-change material (PCM) inside of the test cylinder is monitored by an array of more than 100 thermocouples. The experimental setup with the insulation removed is shown in Figure 1 [2].

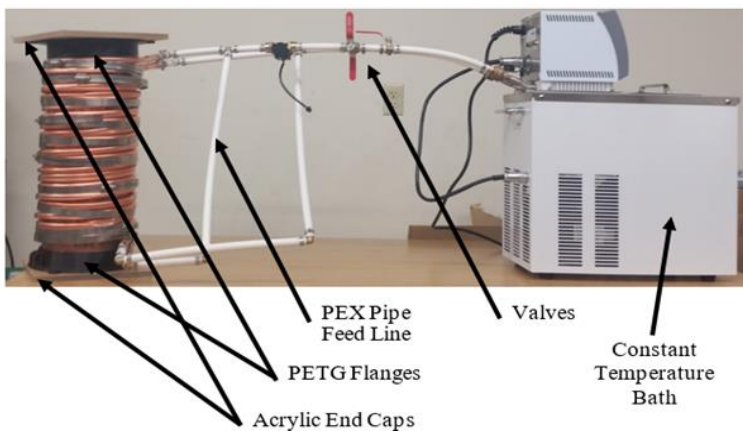


Figure 1. The testing apparatus and its pieces labeled.

In our analysis, the copper test cylinder was filled with solid eicosane cooled to a temperature of 10°C by the fluid from the constant temperature bath (CTB). The eicosane was then heated via the CTB system and counterflow heat exchanger to a temperature of 50°C. As the test cylinder heated, the eicosane changed phase from solid to liquid. Data was gathered on the location of the melt front and the amount of heat transferred to the eicosane via the thermocouple array.

In this paper, we conducted a scale analysis of the melting behavior of PCM in a cylindrical system and compared the behavior predicted by the scale analysis to the behavior observed in eicosane in the test cylinder as it went through its melting process using the Nusselt number as the comparative metric.

EXPERIMENTAL RESULTS

The heat transferred into the PCM was provided via a CTB. To determine the heat transfer to the PCM from the CTB, we must consider the fluid in the CTB. In our case, the heat transfer has three components [3], the heat removed from the CTB, Eq. (1), the sum of heat transfer absorbed by all of the components of the testing apparatus, Eq. (2), and the heat transfer from the CTB to the PCM, Eq. (3).

$$Q_1 = \dot{m}_{CTB} c_{p, CTB} (T_{out} - T_{in}) \Delta t \quad (1)$$

$$Q_2 = \sum m_{comp} c_{p, comp} (T_{2, comp} - T_{1, comp}) \quad (2)$$

$$Q_3 = Q_1 - Q_2 \quad (3)$$

where Q_1 is the heat removed from the CTB (kJ), \dot{m}_{CTB} is the mass flow rate in and out of the CTB (kg/s), $c_{p, CTB}$ is the specific heat of the CTB fluid (J/kg.K), T_{out} is the temperature of the fluid leaving the CTB (°C), and T_{in} is the temperature of the fluid returning to the CTB (°C), Δt is the time that the fluid is outside of the CTB before returning (s), Q_2 is the sum of heat transfer absorbed by all of the components in the testing apparatus (kJ), m_{comp} is the mass of the component (kg), $c_{p, comp}$ is the specific heat of the component (kJ/kg.K), $T_{2, comp}$ is the temperature of the component after some time (°C), $T_{1, comp}$ is the temperature of the component before that time (°C), and Q_3 is the heat transfer added to the PCM (kJ).

The cumulative heat transfer to the PCM (Q_3) has three components [3]. The first component, Eq.(4), is the sensible heat added

to the solid PCM ($Q_{s \rightarrow f}$) (kJ), at T_i to heat the eicosane to fusion temperature (T_{fus}). The second term is the heat of fusion (Q_{fus}) absorbed by the PCM at the fusion temperature to change phase (kJ), Eq.(5), and the third component ($Q_{f \rightarrow l}$) is the sensible heat that was absorbed by the liquid PCM to heat it from fusion temperature to the wall/set-point temperature (kJ), Eq. (6).

$$Q_{s \rightarrow f} = m_{PCM\ s} c_{p\ s} (T_f - T_i) \quad (4)$$

$$Q_f = m_l \Delta h_f = \rho_l \pi (r_w^2 - r_f^2) H \Delta h_f \quad (5)$$

$$Q_{f \rightarrow l} = m_l c_{p\ l} (T_w - T_f) = \rho_l \pi (r_w^2 - r_f^2) c_{p\ l} (T_w - T_f) \quad (6)$$

where $m_{PCM\ s}$ is the mass of the solid PCM (kg), $c_{p\ s}$ is the specific heat of the solid PCM (kJ/kg.K), T_f is the fusion temperature of the PCM ($^{\circ}C$), T_i is the initial temperature of the solid PCM ($^{\circ}C$), Q_f is the total heat of fusion of the phase of the PCM (kJ), m_l is the mass of the liquid PCM (kg), Δh_f is the heat of fusion (kJ/kg), ρ_l is the density of the liquid PCM (kg/m³), r_w is the inside radius of the cylinder (m), r_f is the solid–liquid interface radius of fusion of the PCM (m), and T_w is the temperature of the CTB ($^{\circ}C$).

Combining Eqs. (4-6), the radius of fusion may be expressed as

$$r_f = \sqrt{r_w^2 - \frac{Q_1 - (Q_2 + m_{tot} c_{p\ s} (T_f - T_i))}{\rho_l \pi H (c_{p\ l} (T_w - T_f) + \Delta h_f)}} \quad (7)$$

where m_{tot} is the total mass of the PCM (kg).

At the melt interface, the heat transfer can be expressed as

$$Q_3 = 2\pi r_w H h (T_w - T_f) \quad (8)$$

where h is the convection heat transfer coefficient (W/m².K). The convection heat transfer coefficient is directly related to the Nusselt number based on the cylinder height as [4]

$$Nu_H = \frac{hH}{k_l} \quad (9)$$

where H is the height of the tank, and k_l is the conduction heat transfer coefficient of the liquid. Table 1 shows the parameters and dimensions of the melting experiment.

Table 1. Parameters and dimensions of the experiment [2]	
$H = 0.4536 \text{ m}$	$T_i = 10^\circ\text{C}$
$r_w = 0.07778 \text{ m}$	$T_f = 36.5^\circ\text{C}$
$m_{\text{tot}} = 6.8 \text{ kg}$	$T_w = 50^\circ\text{C}$
$\rho_l = 774.01 \frac{\text{kg}}{\text{m}^3}$	$c_{ps} = 2108 \frac{\text{J}}{\text{kg}\cdot\text{K}}$
$\Delta h_f = 239.94 \frac{\text{kJ}}{\text{kg}}$	$C_{p1} = 2236 \frac{\text{J}}{\text{kg}\cdot\text{K}}$

We can solve Eq. (8) for the convection heat transfer coefficient and substitute into Eq. (9). The result is

$$Nu_H = \frac{Q_3}{2\pi r_w (T_w - T_f) k_l} \quad (10)$$

SCALE ANALYSIS

As the PCM in a cylinder melts, the shape of the frozen eicosane changes, the amount of heat transfer into the solid PCM changes, and the melt behavior changes. In our analysis, we recognized four distinct melt behaviors based on the shape of the solid PCM. We will refer to these different melt behaviors as the melting regimes [5]. Figure 2, from previous research performed at SUU [2], shows the four melting regimes and their main characteristics.

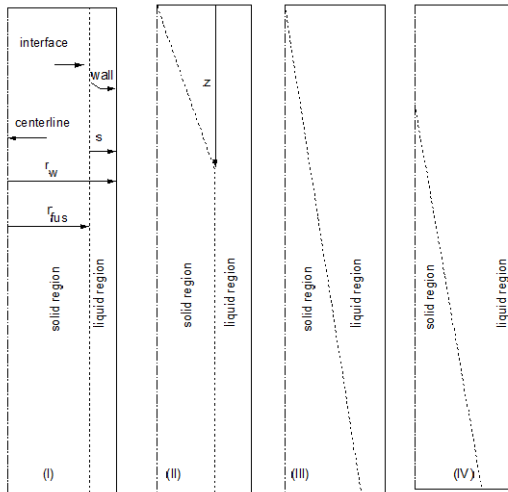


Figure 2. Four regimes of the scale analysis.

In this figure, the dashed lines represent the melt interface. To the right of each dashed line is the liquid region and on the left is the solid region. The melt front progresses from the right side of each image to the left (centerline of the cylinder). Each regime is described in detail in the following sections.

Regime I: Conduction

To simplify our analysis, we assumed the PCM is at fusion temperature at the beginning of the analysis (no convection heat transfer in liquid). For a short period of time, there is only pure conduction heat transfer in the very thin liquid boundary layer. The heat flux across the thin liquid film is absorbed by the latent heat of fusion at the melting interface. This heat balance can be expressed as [6]

$$2\pi r_f k_l H \frac{T_w - T_f}{r_w - r_f} \approx \frac{dm}{dt} \Delta h_f \quad (11)$$

The $\frac{dm}{dt}$ may be expressed as

$$\frac{dm}{dt} = \frac{d}{dt} (\rho_l \pi (r_w^2 - r_{fus}^2) H) \quad (12)$$

Substituting Eq. (12) into Eq. (11) and integrating gives the solution for the radius of fusion in the conduction regime as

$$\begin{aligned} s = r_w - r_f &\approx H\theta^{\frac{1}{2}} \\ \text{or} & \\ r_f &\approx r_w - H\theta^{\frac{1}{2}} \end{aligned} \quad (13)$$

where s is the thickness of the liquid PCM (m), and θ is dimensionless time defined as

$$\theta = \frac{k_l (T_w - T_f)}{\rho_l \Delta h_f H^2} t = St_1 Fo \quad (14)$$

where St_1 is the liquid Stefan number, and Fo is the Fourier number (non-dimensional time). The Stefan number is defined as [7]

$$St_1 = \frac{c_{p,l} (T_w - T_f)}{\Delta h_f} \quad (15)$$

and the Fourier number is defined as [4]

$$Fo = \frac{\alpha t}{H^2} \quad (16)$$

where α is the thermal diffusivity of the liquid PCM defined as [4]

$$\alpha = \frac{k_1}{c_{p1} \rho_1} \quad (17)$$

At the interface, the heat transfer (conduction balances convection) can be expressed in terms of the heat transfer coefficients as [5]

$$2\pi r_f H(T_w - T_f)h \approx 2\pi r_f H(T_w - T_f) \frac{k_1}{s} \quad (18)$$

Simplifying Eq. (18), for the Regime (I), the scale of the convection heat transfer coefficient may be expressed as

$$h \approx \frac{k_1}{s} \quad (19)$$

Substituting the h value from Eq. (17) into the Nusselt number Eq. (9), the scale of the Nusselt number in the conduction regime may be expressed as

$$Nu_1 \approx \frac{H}{s} \quad (20)$$

Regime II: Transition/Mixed

This regime is defined by a transition from pure conduction to convection heat transfer as the liquid layer thickness increases. For Regime (II) analysis, we will assume the height of the upper region (z) is dominated by convection and the remainder of the height ($H - z$) continues to be controlled by conduction.

In the upper zone that is dominated by convection, the boundary layer δ_z is less than the width of the liquid layer at that height. In the lower zone, the boundary layer is in the same order as the thickness of the gap between the wall of the solid PCM.

$$\delta_z \approx s \quad (21)$$

To find the relationships used in the scale analysis, combine conservation of mass, Eq. (22), conservation of momentum in the z direction, Eq. (23), and conservation of energy, Eq. (21). Considering the heat transfer to be symmetric with respect to the angular direction (θ), they may be expressed as [4]

$$\frac{\partial u}{\partial r} + \frac{u}{r} + \frac{\partial w}{\partial z} = 0 \quad (22)$$

$$\frac{\partial w}{\partial t} + u \frac{\partial w}{\partial r} + w \frac{\partial w}{\partial z} = -g\beta\Delta T + \nu \left(\frac{1}{r} \frac{\partial w}{\partial r} + \frac{\partial^2 w}{\partial r^2} + \frac{\partial^2 w}{\partial z^2} \right) \quad (23)$$

$$\frac{\partial T}{\partial t} + u \frac{\partial T}{\partial r} + w \frac{\partial T}{\partial z} = \alpha \left(\frac{1}{r} \frac{\partial T}{\partial r} + \frac{\partial^2 T}{\partial r^2} + \frac{\partial^2 T}{\partial z^2} \right) \quad (24)$$

where u is the velocity in the radial direction (m/s), w is the velocity in the axial z direction (m/s), g is the acceleration due to gravity (m/s^2), β is the coefficient of thermal expansion ($1/\text{K}$), ν is the kinematic viscosity (m^2/s), and α is the thermal diffusivity (m^2/s).

In the thermal boundary layer, $r \approx \delta$, and $z \approx H$, then, the scales of mass, z momentum, and energy equation become [6]

$$\frac{u}{\delta}, \frac{u}{\delta} \approx \frac{w}{H} \quad (25)$$

$$u \frac{w}{\delta}, \frac{w^2}{H} \approx g\beta\Delta T, \nu \left(\frac{w}{\delta^2}, \frac{w}{\delta^2}, \frac{w}{H^2} \right) \quad (26)$$

$$u \frac{\Delta T}{\delta}, w \frac{\Delta T}{H} \approx \alpha \left(\frac{\Delta T}{\delta^2}, \frac{\Delta T}{\delta^2}, \frac{\Delta T}{H^2} \right) \quad (27)$$

where $\Delta T = T_w - T_f$ is the scale of $T - T_f$. Since $\delta \ll H$, the terms w/H^2 and $\Delta T/H^2$ will be insignificant compared to w/δ^2 and $\Delta T/\delta^2$ and may be ignored.

From the continuity equation, Eq. (25), we find

$$\frac{u}{\delta} \approx \frac{w}{H} \quad (28)$$

Substituting Eq. (28) into the scale of the z momentum equation, Eq. (26), yields

$$\frac{w^2}{H} \approx g\beta\Delta T, \nu \frac{w}{\delta^2} \quad (29)$$

Substitution of Eq. (28) into the scale of the energy equation, Eq. (27) yields

$$\frac{w}{H} \approx \frac{\alpha}{\delta^2} \quad (30)$$

Combining Eq. (29) and (30) will allow us to eliminate the vertical velocity component, and dividing both sides by the buoyancy term ($g\beta\Delta T$) allows us to simplify using the nondimensional Rayleigh (Ra) and Prandtl (Pr) numbers as

$$\left(\frac{H}{\delta}\right)^4 \text{Ra}_H^{-1} \text{Pr}^{-1} \approx \left(\frac{H}{\delta}\right)^4 \text{Ra}_H^{-1}, 1 \quad (31)$$

where Rayleigh's number and Prandtl number are, respectively, defined as [4]

$$\text{Ra}_H = \frac{\beta g \Delta T H^3}{\alpha \nu} \quad (32)$$

$$\text{Pr} = \frac{\nu}{\alpha} \quad (33)$$

For eicosane (slow melting), the Prandtl number is much greater than one ($\text{Pr} \gg 1$) [3]; therefore, the term on the lefthand side of Eq. (31) can be ignored because it is insignificant when compared with the righthand side. Simplifying Eq. (29), the boundary layer thickness scale may be expressed as

$$\delta \approx H \text{Ra}_H^{-\frac{1}{4}} \quad (34)$$

For the upper convection region, Eq. (34) can be used to show the scale of the convection thermal boundary layer thickness (δ_z) as

$$\delta_z \approx z \text{Ra}_z^{-\frac{1}{4}} \quad (35)$$

where Ra_z is the Rayleigh number based on z , and is expressed as

$$\text{Ra}_z = \left(\frac{z}{H}\right)^3 \text{Ra}_H \quad (36)$$

Combining Eqs. (13), (21), (35), and (36) yields an expression for z .

$$z \approx H \text{Ra}_H \theta^2 \approx s \text{Ra}_H \theta^{\frac{3}{2}} \quad (37)$$

Next, we focus on the heat transfer in the transition/mixed regime, Regime (II). The total heat transfer in this regime, Q_{II} , has two components, the heat transfer by convection in the upper region with a height of z , and heat transfer by conduction in the remainder of the height of the cylinder ($H - z$). The scale of convection heat transfer is the same as the scale of conduction heat transfer. The total scale of heat transfer in Regime (II) is expressed as [6],

$$Q_{II} \approx 2\pi r_w \left(k_1 z \frac{T_w - T_f}{\delta_z} - k_1 (H - z) \frac{T_w - T_f}{s} \right) \quad (38)$$

Substituting the heat transfer into the solid PCM, Eq. (38), into the expression for the Nusselt number Eq. (10) and utilizing Eqs. (13), (35), and (37) will result in the scale of the Nusselt number for the transition regime as

$$\text{Nu}_{\text{II}} \approx \theta^{-\frac{1}{2}} + \text{Ra}_H \theta^{\frac{3}{2}} \quad (39)$$

The Nusselt number in the transition regime, Eq. (39), is made up of two components, one due to conduction, the first term on the right side of the equation, and one due to convection, the second term on the right of the equation.

The transition regime ends when the heat transfer in the entire height of the PCM is dominated by convection ($z \approx H$). Eq. (37) suggests that the transition regime ends at a time order of (θ_{II})

$$\theta_{\text{II}} \approx \text{Ra}_H^{-\frac{1}{2}} \quad (40)$$

Regime III: Quasi-steady Convection Regime

At nondimensional times greater than θ_{II} , Eq. (40), the entire height of the liquid region is filled by the quasi-steady convection heat transfer zone. The end of Regime (II) is the beginning of Regime (III). Utilizing Eq. (39) and recognizing the conduction term from Regime (II) is not present, we arrive at the equation for the Nusselt number in Regime (III).

$$\text{Nu}_{\text{III}} \approx \text{Ra}_H \theta^{\frac{3}{2}} \quad (41)$$

Substituting the time at the beginning of Regime (III), Eq. (40), into Eq. (39) yields the minimum Nusselt number scale of Regime (III).

$$\text{Nu}_{\text{min-III}} \approx \text{Ra}_H^{\frac{1}{4}} \quad (42)$$

The Nusselt number for this regime is time dependent but does not vary significantly. Most of the fluid is relatively stagnant and thermally stratified [5].

To evaluate the heat transfer, we will utilize a height-averaged melt-front location (r_f). At the interface, the convection heat transfer rate (Q_{conv}) balances the latent heat of fusion (Q_{fus}) released from the interface. We can evaluate the convection heat transfer by using the heat transfer at the melt interface, Eq. (18). Substituting the Nusselt number based on the height of the cylinder, Eq. (9), the minimum Nusselt number in Regime (III), Eq. (42), and the convection equation expressed in Eq. (8), yields the scale of the convection heat transfer as

$$Q_{\text{conv}} \approx \frac{k_1}{H} \text{Ra}_H^{\frac{1}{4}} (H \times 1) (T_w - T_f) \quad (43)$$

where $H \times 1$ is the unit area perpendicular to the heat transfer direction. The righthand side of Eq. (11) is an expression for the latent heat of fusion. Substituting Eq. (12) into Eq. (11) yields the scale of the heat of fusion as

$$Q_{\text{fus}} \approx \Delta h_f \rho_1 \pi H (-2r_f) \frac{dr_f}{dt} \quad (44)$$

Equating and integrating Eqs. (43) and (44) result in an expression for the position of the melt front with respect to dimensionless time.

$$r_f \approx \sqrt{r_w^2 - \frac{1 \times H}{\pi} \text{Ra}_H^{\frac{1}{4}} \theta} \quad (45)$$

Eqs. (45) and (42) are valid until the melt front, r_f , reaches the centerline. When $r_f = 0$, the convection regime ends, and dimensionless time θ_{III} will be

$$\theta_{\text{III}} \approx \frac{\pi r_w^2}{1 \times H} \text{Ra}_H^{-\frac{1}{4}} \quad (46)$$

Regime IV: Variable-Height Regime

Regime (IV) begins as the uppermost height H of the solid PCM and descends along the center line. The heat transfer to the solid PCM continues by the convection heat transfer, but the heat transfer and melting rates are dependent on the size of the remaining solid PCM. Bejan [6] made assumptions about how the shape of the solid PCM in this regime changes as it melts to determine the scales of the regime. He assumed that early on in Regime (IV), the fusion radius of the solid region is fixed and the height of the solid region (h_{IV}) decreases. In our analysis, we refer to this first stage as Regime (IV) stage A (IV-A). In the next stage of Regime (IV), h_{IV} and r_f of the solid region decrease at the same rate such that the melting interface will advance in a manner that it remains parallel to itself, this portion of Regime (IV) is referred to as Regime (IV) stage B (IV-B). Once the PCM is nearly melted ($h_{\text{IV}} \ll H$), the solid PCM is left in a near horizontal zone ($r_f \gg h_{\text{IV}}$) where the shape change is almost completely in the radius of fusion rather than height. This final portion is insignificant in terms of heat transfer and will not be analyzed.

We will begin our analysis by exploring the first stage of this regime where the fusion radius is fixed. The scale of the Nusselt number

in this stage is the order of $Ra_{h_{IV}}^{\frac{1}{4}}$ (Rayleigh number is based on the height of solid PCM h_{IV}) because the interface resistance controlled the heat transfer rate that melted the solid. The Rayleigh number is based on the height of the solid PCM such that

$$Ra_{h_{IV}} \approx \left(\frac{h_{IV}}{H}\right)^3 Ra_H \tag{47}$$

Applying an energy balance at the interface yields

$$\left(\frac{h_{IV}}{H}\right)^{\frac{3}{4}} Ra_H^{\frac{1}{4}} k_l \times 1(T_w - T_f) \approx \Delta h_f \frac{dm}{dt} \tag{48}$$

where $\frac{dm}{dt}$ is defined by a modified Eq. (12)

$$\frac{dm}{dt} = \frac{d}{dt}(\rho_l \pi(r_w^2 - r_{fus}^2)h_{IV}) = \rho_l \pi(r_w^2 - r_{fus}^2) \frac{dh_{IV}}{dt} \tag{49}$$

By modifying Eq. (14), we can define dt in terms of θ as

$$dt = \frac{\rho_l \Delta h_f H^2}{k_l(T_w - T_f)} d\theta \tag{50}$$

Substituting Eq. (50) into Eq. (49), then substituting the result into Eq. (48) yields the energy balance at the melting interface as

$$\int_{\theta_{III}}^{\theta} \frac{Ra_H^{\frac{1}{4}} H^{\frac{5}{4}} \times 1}{\pi(r_w^2 - r_f^2)} d\theta \approx - \int_H^{h_{IV}} h_{IV}^{-\frac{3}{4}} dh_{IV} \tag{51}$$

Integrating Eq. (51) yields the rate of the height decrease in Regime (IV) as

$$\left(\frac{h_{IV}}{H}\right)^{\frac{1}{4}} \approx 1 - \frac{1}{4} \frac{Ra_H^{\frac{1}{4}} H^{\frac{5}{4}} \times 1}{\pi(r_w^2 - r_f^2)} (\theta - \theta_{III}) \tag{52}$$

This equation is only valid during Regime (IV) ($\theta > \theta_{III}$). This regime ends when the solid disappears entirely at $\theta_{IV}(h_{IV} \ll H)$. Using Eq. (52), we can determine the time θ_{IV} as

$$\theta_{IV} - \theta_{III} \approx 4 \frac{\pi(r_w^2 - r_f^2)}{H \times 1} Ra_H^{-\frac{1}{4}} \tag{53}$$

The Nusselt number in this regime is on the order of $Ra_{h_{IV}}^{\frac{1}{4}}$. When Eq. (52) is substituted into Eq. (47), the result is the scale of the Nusselt number in the first stage of Regime (IV).

$$Nu_{IV-1} \approx Ra_H^{\frac{1}{4}} \left[1 - \frac{1}{4} \frac{Ra_H^{\frac{1}{4}} H \times 1}{\pi(r_w^2 - r_f^2)} (\theta - \theta_{III}) \right]^3 \tag{54}$$

The second stage of Regime (IV) is characterized by the parallel recession of the melt interface. The energy balance at the interface, Eq. (48), can still be applied, but $\frac{dr_f}{dt} \approx \frac{dh_{IV}}{dt}$. Solving the energy balance for the radius of fusion, r_f , the result is

$$r_f^{\frac{5}{4}} \approx r_w^{\frac{5}{4}} - \frac{5}{8} \frac{H^{\frac{5}{4}}}{\pi} Ra_H^{\frac{1}{4}} (\theta - \theta_{III}) \tag{55}$$

Utilizing Eq. (47) and the scale of the Nusselt number (on the order of $Ra_{h_{IV}}^{\frac{1}{4}}$), we can determine the Nusselt number in the second stage of Regime (IV).

$$Nu_{IV-2} \approx \frac{Ra_H^{\frac{1}{4}}}{r_w^{\frac{3}{4}}} \left[r_w^{\frac{5}{4}} - \frac{5}{8} \frac{H^{\frac{5}{4}}}{\pi} Ra_H^{\frac{1}{4}} (\theta - \theta_{III}) \right]^{\frac{3}{5}} \tag{56}$$

RESULTS AND DISCUSSION

We will compare the Nusselt numbers found in the scale analysis to the Nusselt number evaluated experimentally. Figure 3 shows the Nusselt number from the experiment plotted with the Nusselt number determined throughout each of the melt regimes.

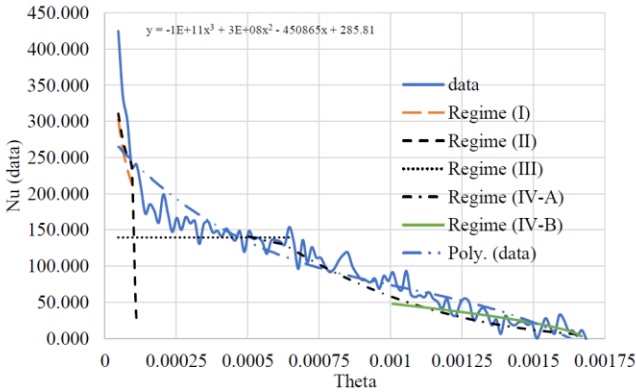


Figure 3. The Nusselt number for the experiment results and the scale analysis.

As it may be observed, the experimental data were not “smooth.” The data to record temperature were collected every 5 minutes. Because the process was slow melting, the result would have been better if the data were recorded every 15 minutes. Therefore, a polynomial degree 3 was fitted to data and all regimes were compared with the fitted data.

The Nusselt evaluated from data shows that the melting behavior of the eicosane changes throughout the experiment as seen in Figure 3. In the beginning portion of the experiment, the Nusselt number declines rapidly, which transitions to an asymptote around a Nusselt number of 140. After a period of time, the Nusselt number begins a much gentler decline until reaching near 0.

Comparing the Nusselt number found in the Regime (I) of the scale analysis, Eq. (20), to the Nusselt number found by analyzing the data, Eq. (10), we see that the Nusselt number predicted by the scale analysis quickly begins to deviate from the data. After about 15 minutes, the data are better described by Regime (II) as the regions where the heat transfer is dominated by convection begin to develop.

The transition regime, Regime (II), lasted a very short period of time compared with the total length of the experiment. Comparing the Nusselt number found in Regime (II), Eq. (39), to the Nusselt number evaluated from the data, Eq. (10), the plots begin to deviate almost immediately as it began to level out into Regime (III).

Comparing the Nusselt number as predicted in Regime (III), Eq. (42), with the Nusselt number found by analyzing the data, Eq. (10), we can see that both the predicted the Nusselt number and the Nusselt number from the data are nearly steady. Figure 4 compares the radius of fusion as determined by scale analysis to the radius of fusion evaluated from data, Eq. (7).

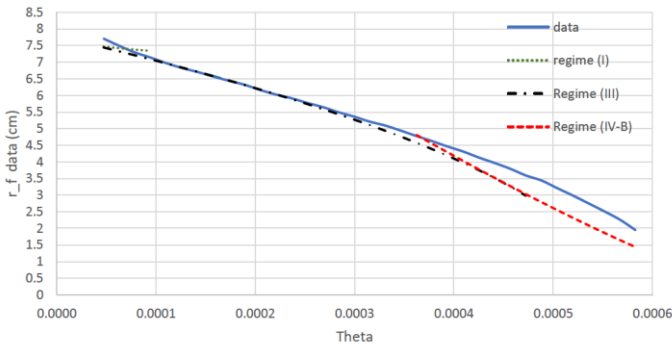


Figure 4. The radius of fusion data vs. scale analysis.

This figure shows that the scale of the average fusion radius matches the prediction for a portion of Regime (III) exactly, and we can use this model for both regimes. The r_{fus}/r_w ratio decreases almost linearly, which is confirmed also by the shape of the data in this figure. This scale matches the data almost to the end of the experiment ($\text{Nu} \approx 0$), and it is valid to assume that there is no need to explore the last stage of the Regime (IV) to express the scale of the fusion radius.

Comparing the Nusselt numbers in Regime (IV-1), Eq. (54), and Regime (IV-2), Eq. (56), with the Nusselt number determined by the data, Eq. (10), we see that we can effectively describe the melting behavior of the PCM through the scale analysis.

Figure 5 compares the height of the remaining solid PCM as predicted by Eq. (52) compared with the height extracted based on temperatures from the thermocouple data. This shows that the first stage of Regime (IV) has correctly predicted the height and there is no need to evaluate the height for the latter stages.

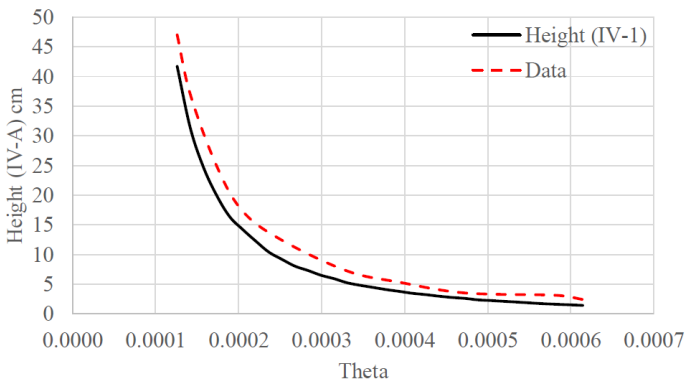


Figure 5. The height of the remaining solid PCM in Regime (IV) as measured by the data and scale analysis.

CONCLUSION

We have evaluated the heat transfer performance of a solid–liquid phase change thermal energy storage system. The PCM is contained in a vertically oriented test cylinder that is heated at its outside boundary (inward interface motion). Detailed quantitative time-dependent volumetric temperature distributions and melt-front motion and shape data were obtained. Under idealized conditions, the PCM behaves as a thermal lumped capacitance, providing heating for a wide range of heat transfer rates at a single temperature corresponding to its melting-point

temperature. In practice, this temperature exists only at the solid–liquid interface. As the PCM melts, the interface moves away from the surface of the heat source/sink, and a thermal resistance layer is built up, resulting in a reduced heat transfer rate and/or increased temperature difference between the system to be heated and the PCM.

The PCM employed in this work was 99% pure eicosane paraffin having a melting point of 36.5°C. Data acquisition included direct measurement of temperatures at numerous locations inside the tank, at several locations on the tank wall, on the acrylic lids, and at the cooling/heating water inlet and outlet. In addition, the CTB flow rate and ΔT of the cooling/heating water were continuously monitored. These measurements yielded quantitative results for both the net energy transfer associated with the PCM as well as the physical patterns of melting and freezing. Also, quantitative results for the temperature distribution and the solid–liquid interface position during freezing and melting have been obtained.

The following conclusions and observations were made:

1. Initial subcooling of the solid decreased the rate of melting and, correspondingly, the rate of sensible heat storage in the liquid.
2. The melting problem is characterized by a conduction heat transfer regime (“Conduction Regime”) at early times followed by a transition (“Transition/Mixed Convection and Conduction Regime”) to a natural convection dominated regime (“Quasi-Steady Natural Convection Regime”). Finally, the arrival of the liquid–solid interface at the centerline marks the beginning of the “Variable Height Regime.” From this time, the height of the liquid–solid interface decreases steadily until the solid region disappears entirely.
3. An examination of the experimentally observed pattern of melting confirmed the progression through the four regimes of melting. For very short melting times, vertical near-wall isotherms indicated that conduction was the sole means of heat transfer. However, the upward flow of fluid, due to the natural convection that accompanied melting, caused the solid material to take on a curvature near its top. The accumulation of liquid atop the solid caused a downward melting in addition to inward melting. This type of melting was perpetuated by natural convection, which developed in the liquid region. Melt shapes corresponding to the completion of selected tests were measured and reported. The inverted bell shape of the cavities demonstrated the dominant role of natural convection in the melting problem.

4. The model presented here to predict melting was based on a scale analysis that considers conduction and convection heat transfer with zero superheat contained in the liquid eicosane. Predictions obtained from model results have been compared with the experimentally measured radius of fusion values, evaluated utilizing a volume-averaged technique. The results were within 10% of the data measurements in the worst case. It was shown that the melting of the entire PCM passes through a sequence of four regimes, and each regime has its Nusselt number and melting location scaling rules.

Based on the scale analysis of all four regimes, it is clear that Regimes (I) and (II) occupy relatively a short period of time, and they disappear quickly into Regime (III). These two regimes do not contribute significantly to the scale of the fusion radius and may easily be ignored. On the other hand, the Nusselt number of Regimes (I) and (II) cannot be disregarded. The Nusselt numbers of the Regimes (I) and (II) started at infinity at the beginning of the experiment. As time progressed, the Nusselt numbers decreased proportionally to the dimensionless time ($\theta^{1/2}$). As conduction gradually disappeared, convection appeared and its effect eventually dominated the heat transfer. In Regime (III), the Nusselt number is quasi-steady. When the Regime (IV) started, in stage one of Regime (IV), the Nusselt number rapidly decreased as a function of $[1 - (\theta - \theta_{III})]^3$, but toward the very end of the experiment, intermediate stage of Regime (IV), the Nusselt number changes as a function of $[1 - (\theta - \theta_{III})]^{3/5}$. The complete history of the scale of the Nusselt numbers of all four regimes is shown in Figure 3.

The analytical scale heat transfer results demonstrated good agreement with the experimental results and confirmed the existence of four melting regions.

REFERENCES

- [1] Tomaru, T., Suzuki, T., Haruyama, T., and Shintomi T., Vibration analysis of cryocoolers, *Cryogenics*, Vol. 44, Iss. 5, pp. 309-317, 2004.
- [2] Kim, S., Maxwell B., and Siahpush A., Heat transfer analysis of eicosane during melting, *J. Utah Acad. Sci. Arts Letts.*, Vol. 98, pp. 143-156, 2021.

[3] Siahpush A., (2001), "Performance enhancement of solid/liquid phase-change thermal energy storage systems through the use of a high conductivity porous metal matrix," Ph.D. Dissertation, University of Idaho, Idaho Falls, ID.

[4] Çengel, Y.A., and Ghajar, A.J., *Heat and Mass Transfer: Fundamentals & Applications* Fifth Edition, McGraw-Hill, New York, NY, 2015.

[5] Bejan, A., *Convection Heat Transfer*, Second Edition, John Wiley, NY, 1995.

[6] Jang, P., and Bejan, A., Scaling theory of melting with natural convection in an enclosure, *Int. J. Heat Mass Transfer*, Vol. 31. No. 6, pp. 1221–1235, 1988.

[7] Viskanta, A.R., Bathelt, A.G., and Hale, N.W., "Latent heat-of-fusion energy storage: experiments on heat transfer during solid-liquid phase change, *Proceedings, Third Miami Conference on Alternative Energy Sources*, December 1980.

Inward Melting in Cylindrical Coordinate System: Analytical Solution (Derivations)

Jordan Whitlock and Ali Siahpush
Southern Utah University

ABSTRACT

This research is the continuation of last year's undergraduate research concerning the experimental and analytical solution to the inward melting in the cylindrical coordinate system at Southern Utah University. The phase change material is eicosane (paraffin, $C_{20}H_{42}$) with a melting point of $36.5^{\circ}C$. Up to this point, the experiment has been performed to collect melting data from $50^{\circ}C$ to $1^{\circ}C$. Previously, we evaluated the performance of eicosane for releasing thermal energy (melting). The scope of this project includes (I) analytical solution of the inward melting, which includes the conservation of mass, momentum, and energy; and (II) applying the scale analysis to validate the experimental results. In part (I), we successfully derived the analytical solution for the conservation equations.

INTRODUCTION

When we are performing analysis on melting, conservation of mass, momentum, and energy has to be considered. In any heat transfer textbook [1, 2], the conservation equations start with the detailed derivation in the cartesian coordinate system. The cartesian analysis starts with stress terms, then presented as a function of displacements. Next, the results are briefly discussed for the cylindrical and spherical coordinate systems. Quite often, a simple drawing of the system with unit vectors is presented, and the final form of the conservation equations are then presented in terms of displacements.

To the best of our knowledge, there is not a complete derivation of the conservation equations in cylindrical or spherical coordinate systems [1-4].

The focus of this paper is to derive the analytical symbolic solution of the inward melting, which includes the conservation of mass, momentum, and energy. In the accompanying paper (Melting Scale Analysis), the scale analysis method is utilized to predict the behavior of the system.

CONSERVATION OF MASS

The law of conservation of mass states matter cannot be created or destroyed. In this section, we will focus on deriving the continuity equation based on the conservation of mass for a differential volume element of a cylinder in a steady-state of an incompressible flow where the density (ρ) of the Newtonian fluid is constant. A typical element in a cylindrical coordinate system is shown in Fig. 1.

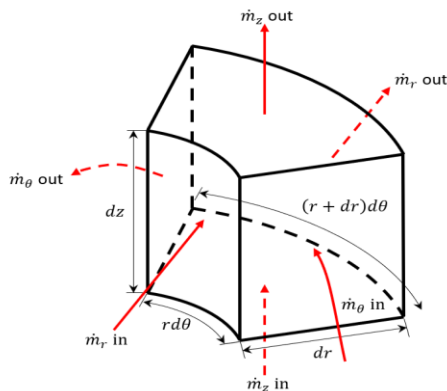


Figure 1. Control volume in cylindrical coordinates.

To satisfy the conservation of mass (continuity equation), the mass into the control volume must be equal to the mass out of the control volume as

$$\dot{m}_{in} = \dot{m}_{out} \quad (1)$$

To derive the continuity equation, the mass flow in and out of the control volume in each direction will be considered in the form of a change in mass flow rate through the control volume in the radial (r), circumferential (θ), and axial (z) directions.

The change in mass flow rate across the control volume in the radial direction is expressed as

$$\Delta \dot{m}_r = \rho(r d\theta dz) u_r - \rho(r + dr)(d\theta dz) \left(u_r + \frac{du_r}{dr} dr \right) \quad (2)$$

where $\Delta \dot{m}_r$ is the change in mass flow rate in the radial direction, r is the inner radius of the volume element, $d\theta$ is the angle of the differential element, dz is the change in height across the differential element, dr is the change in radius across the differential, and u_r is the velocity of the mass in the radial direction.

Assuming that the value of dr is small, then dr^2 is zero. The mass flow rate in the radial direction can be simplified as

$$\Delta \dot{m}_r = -\rho \frac{d}{dr} (u_r r) dr dz d\theta \quad (3)$$

The change in mass flow rate across the control volume in the θ direction is expressed as

$$\Delta \dot{m}_\theta = \rho u_\theta (dr dz) - \rho \left(u_\theta + \frac{du_\theta}{d\theta} \right) (dr dz) \quad (4)$$

where $\Delta \dot{m}_\theta$ is the change in mass flow rate across the control volume in the θ direction, and u_θ is the velocity in the θ direction. Equation (4) is simplified as

$$\Delta \dot{m}_\theta = -\frac{\rho}{r} \left(\frac{du_\theta}{d\theta} \right) (r dr dz) \quad (5)$$

The change in mass flow rate across the control volume in the z direction is expressed as

$$\Delta \dot{m}_z = \rho u_z (r d\theta dr) - \rho \left(u_z + \frac{du_z}{dz} dz \right) (r d\theta dr) \quad (6)$$

where $\Delta \dot{m}_z$ is the change in mass flow rate across the control volume in the z direction, and u_z is the velocity in the z direction.

Equation (6) is simplified to

$$\Delta \dot{m}_z = -\rho \frac{du_z}{dz} (rd\theta dr dz) \quad (7)$$

Combining the change in mass flow rate in each of the directions, the conservation of mass may be presented as

$$\Delta \dot{m} = \Delta \dot{m}_r + \Delta \dot{m}_z + \Delta \dot{m}_\theta = 0 \quad (8)$$

Combining Eqs. (3), (5), and (7) and simplifying yields

$$\frac{du_r}{dr} + \frac{du_z}{dz} + \frac{1}{r} \frac{du_\theta}{d\theta} + \frac{u_r}{r} = 0 \quad (9)$$

Equation (9) presents the conservation of mass (continuity equation) in the cylindrical coordinate system. Quite often, the θ direction is considered symmetric and consequently, the angular term of Eq. (9) may be ignored.

CONSERVATION OF MOMENTUM

The convective form of the Cauchy momentum equation is shown as [5]

$$\rho \frac{Du}{Dt} = \nabla \cdot \sigma + f \quad (10)$$

where u is the flow velocity vector field, ρ is the density, $\nabla \cdot \sigma$ is the divergence of the stress tensor (surface forces) with units of pressure per unit length, and f is the body forces.

To derive Cauchy momentum equation in a cylindrical coordinate system, the left side of the equation will first be expanded followed by the right side.

The $\frac{Du}{Dt}$ on the left side of Eq. (10) may be expanded as [5]

$$\frac{Du}{Dt} = \frac{\partial u}{\partial t} + \frac{\partial u}{\partial r} \frac{dr}{dt} + \frac{\partial u}{\partial \theta} \frac{d\theta}{dt} + \frac{\partial u}{\partial z} \frac{dz}{dt} \quad (11)$$

Considering $u = u_r e_r + u_\theta e_\theta + u_z e_z$, each of the terms of the expanded equation can be expanded further. The first term on the right side of Eq. (11) expands as [5]

$$\frac{\partial u}{\partial t} = \frac{\partial u_r}{\partial t} e_r + \frac{\partial u_\theta}{\partial t} e_\theta + \frac{\partial u_z}{\partial t} e_z \quad (12)$$

where e is the unit vector in r , θ , and z directions, respectively. The second term on the right side of Eq. (11) expands and simplifies to

$$\frac{\partial u}{\partial r} \frac{dr}{dt} = u_r \left[\frac{\partial u_r}{\partial r} e_r + \frac{\partial u_\theta}{\partial r} e_\theta + \frac{\partial u_z}{\partial r} e_z \right] \quad (13)$$

The third term on the right side of Eq. (11) expands and simplifies to

$$\frac{\partial \underline{u}}{\partial \theta} \frac{d\theta}{dt} = \frac{u_\theta}{r} \left[\left(\frac{\partial u_r}{\partial \theta} - u_\theta \right) e_r + \left(\frac{\partial u_\theta}{\partial \theta} + u_r \right) e_\theta + \frac{\partial u_z}{\partial \theta} e_z \right] \quad (14)$$

The fourth term on the right side of Eq. (11) expands and simplifies to

$$\frac{\partial \underline{u}}{\partial z} \frac{dz}{dt} = u_z \left[\frac{\partial u_r}{\partial z} e_r + \frac{\partial u_\theta}{\partial z} e_\theta + \frac{\partial u_z}{\partial z} e_z \right] \quad (15)$$

Substituting the expanded terms of Eqs. (12-15) into Eq. (11) yields the Cauchy momentum equation in a cylindrical coordinate system as

$$\begin{aligned} \frac{D\underline{u}}{Dt} = & \left[\frac{\partial u_r}{\partial t} + u_r \frac{\partial u_r}{\partial r} + \frac{u_\theta}{r} \frac{\partial u_r}{\partial \theta} - \frac{u_\theta^2}{r} + u_z \frac{\partial u_r}{\partial z} \right] e_r + \\ & \left[\frac{\partial u_\theta}{\partial t} + u_r \frac{\partial u_\theta}{\partial r} + \frac{u_\theta}{r} \frac{\partial u_\theta}{\partial \theta} + \frac{u_\theta u_r}{r} + u_z \frac{\partial u_\theta}{\partial z} \right] e_\theta + \\ & \left[\frac{\partial u_z}{\partial t} + u_r \frac{\partial u_z}{\partial r} + \frac{u_\theta}{r} \frac{\partial u_z}{\partial \theta} + u_z \frac{\partial u_z}{\partial z} \right] e_z \end{aligned} \quad (16)$$

Radial Stresses

Figure 2 shows the stresses in the radial direction. In this figure, the stress tensor is symbolically expressed as σ , the first subscript denotes the face that the stress is applied to, and the second subscript denotes the direction of the stress. For example, $\sigma_{\theta r}$ refers to the stress on the plane perpendicular to the θ direction that acts in the r direction. Also, it is worth noting that $\frac{\partial e_r}{\partial r} = \frac{\partial e_\theta}{\partial \theta} = \frac{\partial e_z}{\partial z} = 0$.

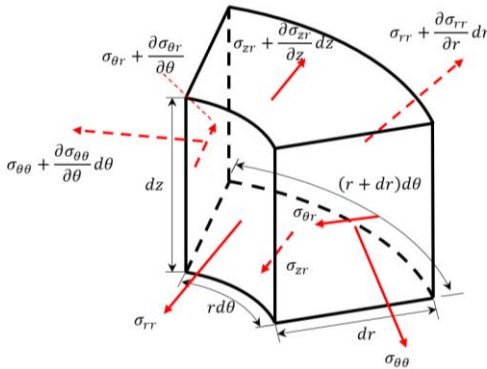


Figure 2. Control volume with the stresses in the radial direction.

The σ_r components of the stress tensor are

$$\sigma_{rr} r d\theta dz - \left(\sigma_{rr} + \frac{\partial \sigma_{rr}}{\partial r} dr \right) (r + dr) d\theta dz \tag{17}$$

where σ_{rr} is the stress in r direction on the face perpendicular to r direction, and dr is the change in radius across the differential element. The $\sigma_{\theta r}$ components are defined as

$$-\sigma_{\theta r} dr dz + \left(\sigma_{\theta r} + \frac{\partial \sigma_{\theta r}}{\partial \theta} d\theta \right) dr dz \tag{18}$$

where $\sigma_{\theta r}$ is the stress in r direction on the face perpendicular to θ direction. The σ_{zr} components may be expressed as

$$-\sigma_{zr} r d\theta dr + \left(\sigma_{zr} + \frac{\partial \sigma_{zr}}{\partial z} dz \right) r d\theta dr \tag{19}$$

where σ_{zr} is the stress in r direction applied on the face perpendicular to z direction. Next, $\sigma_{\theta\theta}$ contribution to r direction may be expressed as

$$-\sigma_{\theta\theta} dr dz \sin\left(\frac{\theta}{2}\right) - \left(\sigma_{\theta\theta} + \frac{\partial \sigma_{\theta\theta}}{\partial \theta} d\theta \right) dr dz \sin\left(\frac{\theta}{2}\right) \tag{20}$$

Where $\sigma_{\theta\theta}$ is the stress in θ direction on the face perpendicular to θ direction.

Combining all of the stresses in the r direction, Eq. (17-20) yields the total stress in the r direction as

$$\left(\frac{1}{r} \sigma_{rr} + \frac{\partial \sigma_{rr}}{\partial r} + \frac{1}{r} \frac{\partial \sigma_{\theta r}}{\partial \theta} + \frac{\partial \sigma_{zr}}{\partial z} - \frac{\sigma_{\theta\theta}}{r} \right) r dr d\theta dz \tag{21}$$

Angular (θ) Stresses

Figure 3 shows the control volume with the stresses in the θ (angular) direction.

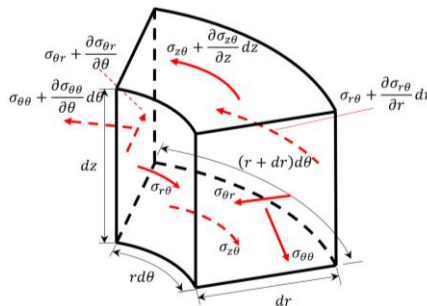


Figure 3. Control volume with the stresses in the θ direction.

The $\sigma_{\theta\theta}$ contribution in the θ direction is expressed as

$$-\sigma_{\theta\theta} dr dz + \left(\sigma_{\theta\theta} + \frac{\partial \sigma_{\theta\theta}}{\partial \theta} d\theta \right) dr dz \quad (22)$$

where $\sigma_{\theta\theta}$ is the stress in the θ direction on the face perpendicular to the θ direction. The $\sigma_{z\theta}$ contribution in the θ direction may be expressed as

$$-\sigma_{z\theta} r d\theta dr + \left(\sigma_{z\theta} + \frac{\partial \sigma_{z\theta}}{\partial z} dz \right) r d\theta dr \quad (23)$$

where $\sigma_{z\theta}$ is the stress in θ direction on the face perpendicular to the z direction. The $\sigma_{r\theta}$ contribution in the θ direction is expressed as

$$-\sigma_{r\theta} r d\theta dz + \left(\sigma_{r\theta} + \frac{\partial \sigma_{r\theta}}{\partial r} dr \right) (r + dr) d\theta dz \quad (24)$$

where $\sigma_{r\theta}$ is the stress in the θ direction on the face perpendicular to the r direction. The $\sigma_{\theta r}$ contribution in the θ direction is expressed as

$$\sigma_{\theta r} \sin \left(\frac{d\theta}{2} \right) dr dz + \left(\sigma_{\theta r} + \frac{\partial \sigma_{\theta r}}{\partial \theta} d\theta \right) \sin \left(\frac{d\theta}{2} \right) dr dz \quad (25)$$

where $\sigma_{\theta r}$ is the stress in the r direction on the face perpendicular to the θ direction. Combining the stresses in the θ direction, Eq. (22-25), yields

$$\left(\frac{1}{r} \frac{\partial \sigma_{\theta\theta}}{\partial \theta} + \frac{\partial \sigma_{z\theta}}{\partial z} + 2 \frac{\sigma_{r\theta}}{r} + \frac{\partial \sigma_{r\theta}}{\partial r} \right) r dr d\theta dz \quad (26)$$

Figure 4 shows the control volume with the stresses in the z direction.

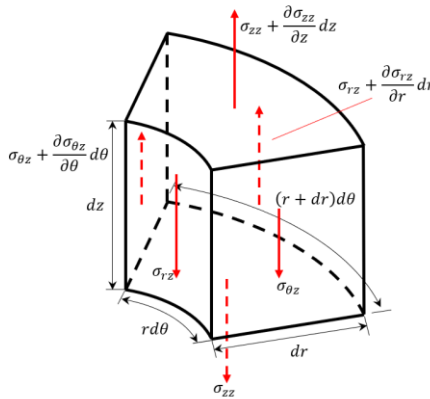


Figure 4. Control volume with the stresses in the z direction.

The σ_{zz} contribution in the z direction is expressed as

$$-\sigma_{zz}r d\theta dr + \left(\sigma_{zz} + \frac{\partial \sigma_{zz}}{\partial z} dz \right) r d\theta dr \quad (27)$$

where σ_{zz} is the stress on the fluid element in z direction on the face perpendicular to the z direction. The $\sigma_{\theta z}$ contribution in the z direction is expressed as

$$-\sigma_{\theta z} dr dz + \left(\sigma_{\theta z} + \frac{\partial \sigma_{\theta z}}{\partial \theta} d\theta \right) dr dz \quad (28)$$

where $\sigma_{\theta z}$ is the stress in the z direction on the face perpendicular to the θ direction. The σ_{rz} contribution in the z direction is expressed as

$$-\sigma_{rz} r d\theta dz + \left(\sigma_{rz} \frac{\partial \sigma_{rz}}{\partial r} dr \right) (r + dr) d\theta dz \quad (29)$$

where σ_{rz} is the stress in the z direction on the face perpendicular to the r direction. Combining all stresses in the z direction, Eqs. (27-29) yields

$$\left(\frac{\partial \sigma_{zz}}{\partial z} + \frac{1}{r} \frac{\partial \sigma_{\theta z}}{\partial \theta} + \frac{\sigma_{rz}}{r} + \frac{\partial \sigma_{rz}}{\partial r} \right) r dr d\theta dz \quad (30)$$

Combining the stresses in each direction, Eqs. (21), (26), and (30), yields the full gradient of stress as

$$\begin{aligned} \nabla \sigma = & \left[\left(\frac{\sigma_{rr}}{r} + \frac{\partial \sigma_{rr}}{\partial r} + \frac{1}{r} \frac{\partial \sigma_{\theta r}}{\partial \theta} + \frac{\partial \sigma_{zr}}{\partial z} - \frac{\sigma_{\theta\theta}}{r} \right) r dr d\theta dz \right] e_r + \\ & \left[\left(\frac{1}{r} \frac{\partial \sigma_{\theta\theta}}{\partial \theta} + \frac{2}{r} \sigma_{r\theta} + \frac{\partial \sigma_{r\theta}}{\partial r} + \frac{\partial \sigma_{z\theta}}{\partial z} \right) r dr d\theta dz \right] e_\theta + \\ & \left[\left(\frac{\partial \sigma_{zz}}{\partial z} + \frac{1}{r} \frac{\partial \sigma_{\theta z}}{\partial \theta} + \frac{\sigma_{rz}}{r} + \frac{\partial \sigma_{rz}}{\partial r} \right) r dr d\theta dz \right] e_z \end{aligned} \quad (31)$$

To relate the right and left sides of Eq. (31), it is useful to express stress in terms of velocity and absolute viscosity. The stress tensor is defined as [6]

$$\sigma = \mu(\nabla u + \nabla u^T) \quad (32)$$

where μ is the absolute viscosity of the fluid, ∇u is the gradient of velocity, and ∇u^T is the transpose of the velocity gradient matrix.

To derive the velocity gradient in cylindrical components, we will transform the cartesian equations using the following relationships

$$\begin{aligned} x &= r \cos \theta \\ y &= r \sin \theta \\ z &= z \end{aligned} \quad (33)$$

To evaluate $\frac{\partial u}{\partial r}$, the change in velocity with respect to the r , $\frac{\partial u}{\partial \theta}$ the change in velocity with respect to the θ , and $\frac{\partial u}{\partial z}$ the change in velocity with respect to z , the following relationship may be used. This equation shows the transformation from the Cartesian to cylindrical coordinate systems.

$$\begin{bmatrix} \frac{\partial u}{\partial r} \\ \frac{\partial u}{\partial \theta} \\ \frac{\partial u}{\partial z} \end{bmatrix} = \begin{bmatrix} \frac{\partial x}{\partial r} & \frac{\partial y}{\partial r} & \frac{\partial z}{\partial r} \\ \frac{\partial x}{\partial \theta} & \frac{\partial y}{\partial \theta} & \frac{\partial z}{\partial \theta} \\ \frac{\partial x}{\partial z} & \frac{\partial y}{\partial z} & \frac{\partial z}{\partial z} \end{bmatrix} \begin{bmatrix} \frac{\partial u}{\partial x} \\ \frac{\partial u}{\partial y} \\ \frac{\partial u}{\partial z} \end{bmatrix} \quad (35)$$

The unit vectors in the cylindrical coordinate system may be expressed in terms of unit vectors in the Cartesian coordinate system as

$$\begin{aligned} e_r &= \cos(\theta) e_x + \sin(\theta) e_y \\ e_\theta &= -\sin(\theta) e_x + \cos(\theta) e_y \\ e_z &= e_z \end{aligned} \quad (36)$$

The gradient of velocity, ∇u , in the Cartesian coordinate system is defined as [7]

$$\nabla u = \frac{\partial u}{\partial x} e_x + \frac{\partial u}{\partial y} e_y + \frac{\partial u}{\partial z} e_z \quad (37)$$

To transform from the cartesian to a cylindrical system, some constants (a, b, and c) are introduced [8].

$$\nabla u = a \frac{\partial u}{\partial r} e_r + b \frac{\partial u}{\partial \theta} e_\theta + c \frac{\partial u}{\partial z} e_z \quad (38)$$

Values of a, b, and c are determined as [8]

$$\begin{aligned} a &= 1 \\ b &= \frac{1}{r} \\ c &= 1 \end{aligned} \quad (39)$$

Then, the gradient of velocity ∇u in the cylindrical system may be presented as

$$\nabla u = \frac{\partial u}{\partial r} e_r + \frac{1}{r} \frac{\partial u}{\partial \theta} e_\theta + \frac{\partial u}{\partial z} e_z \quad (40)$$

Noting that

$$u = u_r e_r + u_\theta e_\theta + u_z e_z \quad (41a)$$

$$\frac{\partial e_r}{\partial r} = \frac{\partial e_\theta}{\partial r} = \frac{\partial e_z}{\partial r} = \frac{\partial e_z}{\partial \theta} = \frac{\partial e_z}{\partial z} = \frac{\partial e_r}{\partial z} = \frac{\partial e_\theta}{\partial z} = 0 \quad (41b)$$

and

$$\frac{\partial e_r}{\partial \theta} = e_\theta \text{ and } \frac{\partial e_\theta}{\partial \theta} = -e_r \quad (41c)$$

Using Eq. (41a-c), it is an easy task to show how Eq. (40) is converted to

$$\nabla u = = \begin{bmatrix} \frac{\partial u_r}{\partial r} & \frac{1}{r} \left(\frac{\partial u_r}{\partial \theta} - u_\theta \right) & \frac{\partial u_r}{\partial z} \\ \frac{\partial u_\theta}{\partial r} & \frac{1}{r} \left(\frac{\partial u_\theta}{\partial \theta} + u_r \right) & \frac{\partial u_\theta}{\partial z} \\ \frac{\partial u_z}{\partial r} & \frac{1}{r} \frac{\partial u_z}{\partial \theta} & \frac{\partial u_z}{\partial z} \end{bmatrix} \quad (42)$$

Considering stresses and pressure terms, substituting Eq. (42) into Eq. (32), the stress tensor in the cylindrical coordinate system may be expressed as

$$\begin{aligned} & \sigma \\ & = \mu \begin{bmatrix} 2 \frac{\partial u_r}{\partial r} & \frac{1}{r} \left(\frac{\partial u_r}{\partial \theta} - u_\theta \right) + \frac{\partial u_\theta}{\partial r} & \frac{\partial u_r}{\partial z} + \frac{\partial u_z}{\partial r} \\ \frac{\partial u_\theta}{\partial r} + \frac{1}{r} \left(\frac{\partial u_r}{\partial \theta} - u_\theta \right) & \frac{2}{r} \left(\frac{\partial u_\theta}{\partial \theta} + u_r \right) & \frac{\partial u_\theta}{\partial z} + \frac{1}{r} \frac{\partial u_z}{\partial \theta} \\ \frac{\partial u_z}{\partial r} + \frac{\partial u_r}{\partial z} & \frac{1}{r} \frac{\partial u_z}{\partial \theta} + \frac{\partial u_\theta}{\partial z} & 2 \frac{\partial u_z}{\partial z} \end{bmatrix} \\ & + \begin{bmatrix} -P & 0 & 0 \\ 0 & -P & 0 \\ 0 & 0 & -P \end{bmatrix} \end{aligned} \quad (43)$$

It should be noted that the normal pressure terms are added to the stress tensor. Substituting Eq. (31) into Eq. (10) yields

$$\begin{aligned} \frac{D\underline{u}}{Dt} = & \frac{1}{\rho} \left(\left[\left(\frac{\sigma_{rr}}{r} + \frac{\partial \sigma_{rr}}{\partial r} + \frac{1}{r} \frac{\partial \sigma_{\theta r}}{\partial \theta} + \frac{\partial \sigma_{zr}}{\partial z} - \frac{\sigma_{\theta\theta}}{r} \right) r \, dr \, d\theta \, dz \right] e_r \right. \\ & + \left[\left(\frac{1}{r} \frac{\partial \sigma_{\theta\theta}}{\partial \theta} + \frac{2}{r} \sigma_{r\theta} + \frac{\partial \sigma_{r\theta}}{\partial r} \right. \right. \\ & \left. \left. + \frac{\partial \sigma_{z\theta}}{\partial z} \right) r \, dr \, d\theta \, dz \right] e_\theta \\ & + \left[\left(\frac{\partial \sigma_{zz}}{\partial z} + \frac{1}{r} \frac{\partial \sigma_{\theta z}}{\partial \theta} + \frac{\sigma_{rz}}{r} \right. \right. \\ & \left. \left. + \frac{\partial \sigma_{rz}}{\partial r} \right) r \, dr \, d\theta \, dz \right] e_z \end{aligned} \quad (44)$$

This equation shows the momentum equation as a function of stresses in the cylindrical coordinate system. Next, substitute the values of each stress component as a function of displacement (u). The final result is the momentum equation in the cylindrical coordinate system for an incompressible, Newtonian flow as

$$\begin{aligned}
 r_{comp} &= \frac{1}{\rho} \left[-\frac{\partial P}{\partial r} + \mu \left(-\frac{u_r}{r^2} + \frac{1}{r} \frac{\partial}{\partial r} \left(r \frac{\partial u_r}{\partial r} \right) + \frac{\partial^2 u_r}{\partial z^2} + \frac{1}{r^2} \frac{\partial^2 u_\theta}{\partial \theta^2} \right. \right. \\
 &\quad \left. \left. - \frac{2}{r^2} \frac{\partial u_\theta}{\partial \theta} \right) \right] e_r \\
 \theta_{comp} &= \frac{1}{\rho} \left[-\frac{\partial P}{\partial \theta} + \mu \left(-\frac{u_\theta}{r^2} + \frac{1}{r} \frac{\partial u_\theta}{\partial r} + \frac{\partial^2 u_\theta}{\partial r^2} + \frac{1}{r^2} \frac{\partial^2 u_\theta}{\partial \theta^2} + \frac{\partial^2 u_\theta}{\partial z^2} \right. \right. \\
 &\quad \left. \left. + \frac{2}{r^2} \frac{\partial u_r}{\partial \theta} \right) \right] e_\theta \quad (45) \\
 z_{comp} &= \frac{1}{\rho} \left[-\frac{\partial P}{\partial z} + \mu \left(\frac{\partial^2 u_z}{\partial z^2} + \frac{1}{r^2} \frac{\partial^2 u_z}{\partial \theta^2} + \frac{1}{r} \frac{\partial u_z}{\partial r} + \frac{\partial^2 u_z}{\partial r^2} + \rho g \right) \right] e_z
 \end{aligned}$$

where the last term is the buoyancy term. The buoyancy is the same for cylindrical as in the cartesian coordinates since it is part of the z component of the momentum equation [1-2].

CONSERVATION OF ENERGY

The conservation of energy in the Cartesian coordinate systems are available in any heat transfer book [1-2]. The emphasis of this section is to derive the energy equation in the cylindrical coordinate system. For a steady-state heat transfer, the first law of thermodynamics states [9]

$$\dot{E}_{in} - \dot{E}_{out} = 0 \quad (46)$$

where \dot{E}_{in} is the energy entering the control volume and \dot{E}_{out} is the energy leaving the system.

The energy into the system may be defined as

$$\dot{E}_{in} = \dot{m}e_i + \dot{Q}_i \quad (47)$$

where \dot{m} is the mass flow rate into the control volume (CV), e_i is the specific energy of into the CV, and \dot{Q}_i is the heat transfer through the CV. The terms on the right side of the Eq. (47) may be expressed as

$$\dot{m}_i = \rho A u_i \quad (48a)$$

$$e_i = c_p T \quad (48b)$$

$$\dot{Q}_i = -kA \frac{dT}{dr} \tag{48c}$$

where ρ is the density, A is the cross-sectional area, u is the velocity, cp is the specific heat, T is the temperature, and k is the thermal conductivity.

In the radial direction, terms of Eqs. (47-48a-c) maybe expressed as

$$\begin{aligned} \dot{m}_{i_r} &= \rho r d\theta dz u_r \\ \dot{Q}_{i_r} &= -k r d\theta dz \frac{dT}{dr} \end{aligned} \tag{49}$$

Substitute Eq. (49) into Eq. (47). The result is

$$\dot{E}_{in_r} = \rho r d\theta dz u_r c_p T - k r d\theta dz \frac{dT}{dr} \tag{50}$$

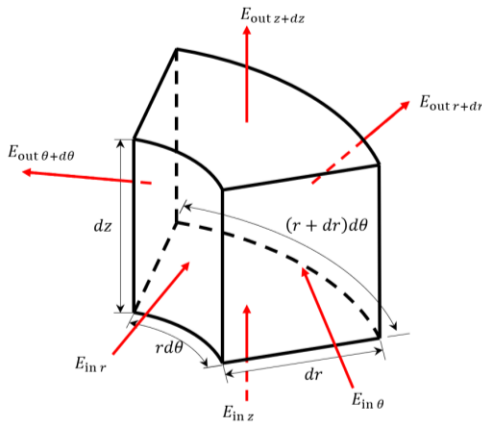


Figure 5. Control volume showing the energy transfer on each face.

Using the same approach, the \dot{E}_{out} maybe expressed as

$$\begin{aligned} \dot{E}_{out_r} = & \left[\rho r d\theta dz u_r c_p T + \frac{\partial(\rho r d\theta dz u_r c_p T)}{\partial r} dr \right] + \left[-k r d\theta dz \frac{\partial T}{\partial r} + \right. \\ & \left. \left(\frac{\partial(-k r d\theta dz \frac{dT}{dr})}{\partial r} \right) dr \right] \end{aligned} \tag{51}$$

Substituting Eqs. (50) and (51) into Eq. (47) yields the energy balance in the radial direction as

$$\begin{aligned}
 -\rho c_p \left(\frac{\partial u_r}{\partial r} T + \frac{1}{r} u_r T + u_r \frac{\partial T}{\partial r} \right) r d\theta dr dz \\
 + k \left(\frac{1}{r} \frac{\partial T}{\partial r} + \frac{\partial^2 T}{\partial r^2} \right) r d\theta dr dz = 0
 \end{aligned} \quad (52)$$

Next, consider the energy balance (in and out of the control volume) in the θ direction. Considering $\dot{m}e_i$ and \dot{Q}_i definition in the θ direction as

$$\dot{E}_{in \theta} = \rho dr dz u_\theta c_p T - k dr dz \frac{\partial T}{r \partial \theta} \quad (53)$$

$$\begin{aligned}
 \dot{E}_{out \theta} = & \left[\rho dr dz u_\theta c_p T - \frac{\partial(\rho dr dz u_\theta c_p T)}{\partial \theta} \right] \\
 & + \left[-k dr dz \frac{\partial T}{r \partial \theta} - \frac{\partial(-k dr dz \frac{\partial T}{r \partial \theta})}{\partial \theta} d\theta \right]
 \end{aligned} \quad (54)$$

The final form of the θ energy balance is

$$-\rho c_p \left(\frac{1}{r} \frac{\partial u_\theta}{\partial \theta} T + \frac{u_\theta}{r} \frac{\partial T}{\partial \theta} \right) r dr d\theta dz + k \frac{1}{r^2} \frac{\partial^2 T}{\partial \theta^2} r dr d\theta dz = 0 \quad (55)$$

Finally, consider the axial (z) direction. Defining $\dot{m}_z = \rho dr r d\theta u_z$, the final result may be expressed as

$$-\rho c_p \left(T \frac{\partial u_z}{\partial z} + u_z \frac{\partial T}{\partial z} \right) r dr d\theta dz + k \frac{\partial^2 T}{\partial z^2} r dr d\theta dz \quad (56)$$

Combining $r\theta z$ and considering the continuity equation, the final energy equation combined in all directions are

$$\begin{aligned}
 \rho c_p \left(u_r \frac{\partial T}{\partial r} + \frac{u_\theta}{r} \frac{\partial T}{\partial \theta} + u_z \frac{\partial T}{\partial z} \right) \\
 = k \left(\frac{1}{r} \frac{\partial T}{\partial r} + \frac{\partial^2 T}{\partial r^2} + \frac{1}{r^2} \frac{\partial^2 T}{\partial \theta^2} + \frac{\partial^2 T}{\partial z^2} \right)
 \end{aligned} \quad (57)$$

In many cases, there is no change in the θ direction. In this case, the final result may be simplified as

$$\rho c_p \left(u_r \frac{\partial T}{\partial r} + u_z \frac{\partial T}{\partial z} \right) = k \left(\frac{1}{r} \frac{\partial T}{\partial r} + \frac{\partial^2 T}{\partial r^2} + \frac{\partial^2 T}{\partial z^2} \right) \quad (58)$$

CONCLUSION

After studying many fluid mechanics and heat transfer books and articles to fully understand the derivation of the conservation equations

[1-8], we judged that to the best knowledge of our knowledge, there is not a complete derivation of the conservation equations in cylindrical or spherical coordinate systems.

This research is the continuation of last year's undergraduate research concerning the experimental and analytical solution to the inward melting in the cylindrical coordinate system at Southern Utah University. The scope of this project included (I) analytical solution of the inward melting which includes the conservation of mass, momentum, and energy and (II) application of the scale analysis to validate the experimental results. In part (I), we successfully derived the analytical solution for the conservation equations.

The focus of this paper was to derive the analytical symbolic solution of the inward melting, which includes the conservation of mass, momentum, and energy. In the accompanying paper, the scale analysis method is utilized to predict the behavior of the system.

REFERENCES

[1] Cengel, Y.A., Ghajar, A.J., *Heat and Mass Transfer: Fundamentals & Applications* Fifth Edition, McGraw-Hill, New York, 2015.

[2] Bergman, T.L, Lavine, A.S., Incropera, F.P., *Fundamental of Heat and Mass Transfer*, Seventh Edition, John Wiley, Hoboken, 2011

[3] Mott, R.L., J.A., Untener, *Applied Fluid Mechanics*, Seventh Edition, London, UK, 2015.

[4] Sengel, Y.A., Cimbala, J.M., *Fluid Mechanics, Fundamental and Applications*, Fourth Edition, McGraw-Hill, New York, 2018.

[5] Acheson, D.J., *Elementary Fluid Dynamics*. p. 205. Oxford University Press. New York, 1990.

[6] Burnley, P., "Tensors: stress, strain and elasticity." Retrieved July 20, 2021, from https://serc.carleton.edu/NAGTWorkshops/mineralogy/mineral_physics/tensors.html.

[7] Rosen, A., "Fluid mechanics." Retrieved July 20, 2021, from https://sites.tufts.edu/andrewrosen/files/2016/10/grad_fluids.pdf.

[8] Engineering at Alberta. “Calculus: vector calculus in cylindrical coordinate systems.” Retrieved July 20, 2021, from <https://engcourses-uofa.ca/books/introduction-to-solid-mechanics/calculus/vector-calculus-in-cylindrical-coordinate-systems/>

[9] Cengel, A., *Thermodynamics: An Engineering Approach*, Ninth Edition, McGraw-Hill, New York, 2015.

Cavitation Demonstration Trials

Owen Telford and Ali Siahpush

Southern Utah University

ABSTRACT

In this paper, multiple experiments were conducted on various types of pumps. Pumps varied in size and function to explore a suitable cavitation demonstration for a fluid mechanics laboratory. It was intended to compare experimental results with analytical methods and discuss discrepancies. Four different pumps were tested: submersible pump, circulation pump, diaphragm pump, and centrifugal pump. Based on its classification, each pump was used differently to generate cavitation and each pump gave various results. Each pump was discussed along with recommendations for how to create a proper system that can be used for students to learn and experience cavitation in a fluid mechanics laboratory.

INTRODUCTION

Cavitation in pumps is the rapid creation and subsequent collapse of air bubbles in a fluid due to the low pressure. Cavitation causes pump performance deterioration, mechanical damage, noise, and vibration,

which can ultimately lead to pump failure. Vibration is a common symptom of cavitation, and many times the first sign of an issue. Vibration causes problems for many pump components, including the shaft, bearings, and seals [1].

Cavitation is caused when the net positive suction head available ($NPSH_a$) is lower than the net positive suction head required ($NPSH_r$). When the flow before the pump is restricted enough, net positive suction head available ($NPSH_a$) is less than $NPSH_r$ [2]. $NPSH_r$ is commonly provided by the pump manufacturer by empirical methods and using standards and specifications from the Hydraulic Institute (HI). $NPSH_r$ values are normally reported on the performance curves for the pump [3].

If the pressure of the fluid at any point in a pump is lower than its vapor pressure, it will form vapor within the pump. When the bubbles pass on into a section of the pump at higher pressure, the vapor condenses back into liquid and the bubbles implode, causing severe erosion of pump components.

The internet is saturated with pump cavitation materials that discuss the most common causes of cavitation, avoidance, detection, and evaluations [4-8]. The purpose of this paper is to make demonstrations for undergraduate fluid mechanics laboratories to properly show how cavitation occurs in a pump and how to prevent it. Four pumps were tested to explore cavitation possibility: a submersible pump, a circulation pump, a diaphragm pump, and a centrifugal pump.

Only one of the pumps tested uses metal components (impeller); the other three pumps used are made of plastic material. Plastics are less brittle than metal. The plastic components of the pump will bend and deform unlike metal, which will break into fragments; this is called pitting. For each pump, we provided a detailed procedure on how the system was constructed and tested, as well as an explanation of whether this was an adequate way of demonstrating the phenomenon for learning purposes.

THEORY

The four pumps selected for experimentation are different, but conceptually, the equations necessary to understand cavitation are the same. $NPSH_r$ is determined by the manufacturer of the pump. Equation (1) shows the relationship between $NPSH_a$ and $NPSH_r$ that causes cavitation in the system [2].

$$NPSH_a > NPSH_r \quad (1)$$

To avoid cavitation, typically, the system is designed to have $NPSH_a$ greater than 1.1 of $NPSH_r$ [2]. Equation (2) presents the $NPSH_a$ as [2]

$$NPSH_a = \frac{p_{sp}}{\gamma} \pm h_s - h_f - \frac{p_{vp}}{\gamma} \quad (2)$$

where p_{sp} is the atmospheric pressure (absolute) above the fluid in the reservoir (82.5 kPa in Cedar City, UT), γ is the specific gravity of water ($9.81 \frac{kN}{m^3}$), h_s is the elevation difference from the top of the fluid in the reservoir to the centerline of the inlet on the pump (m), h_f is the head loss in the suction pipe due to friction and minor losses (m), and p_{vp} is the vapor pressure of water (approximately 2.33 kPa). The value of $NPSH_a$ can then be compared with the $NPSH_r$ that is typically provided by the manufacturer (pump performance).

There are many sources and charts available to determine the $NPSH_r$, but most of these references are related to only centrifugal pumps with the minimum impeller size of 6 in [2].

Figures 1 and 2 show the suction line of the pump system configurations for the tests. Three of the tests used the first configuration (Fig. 1) and one of the tests used the second configuration because the pump needed to be primed (Fig. 2).

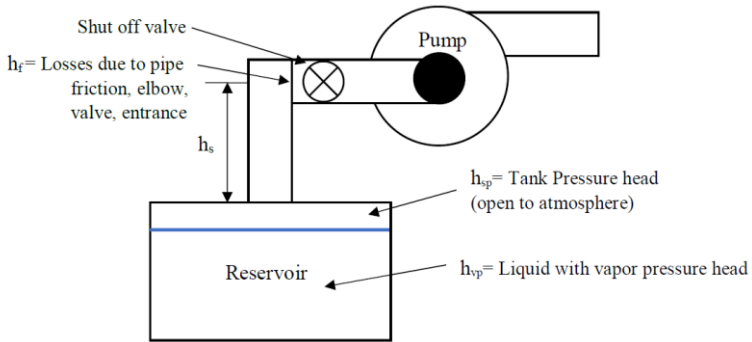


Figure 1. Pump suction-line diagram with reservoir below the pump.

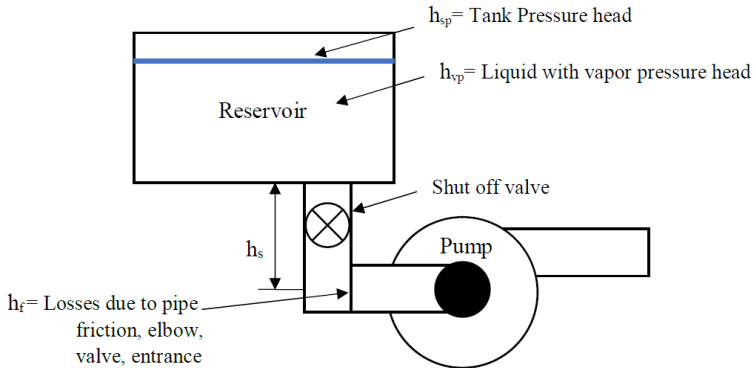


Figure 2. Pump suction-line diagram with reservoir above the pump.

SUBMERSIBLE PUMP

A video on YouTube is posted about cavitation that demonstrates cavitation using a small bucket and a submersible pump. In the video, it was unclear how Larry Bachus (“The pump guy”) makes the pump cavitate or what kind of pump he used [9-10]. We contacted Mr. Bachus, and he was extremely helpful by sending us a detailed procedure on how he performed his cavitation demonstration, including the exact pump he used. A test was conducted to explore whether the cavitation could be replicated at the Southern Utah University (SUU) fluids laboratory.

The small pump (‘Little Giant’ model #P-AAA [11]) was submerged in water. In the video, the water was pumped from the bucket out and back into the same one, so the water was circulating with only one reservoir. In this process, the water is slowly taken out of the bucket until bubbles form in the discharge line. Figure 3 shows the pump and tubing system assembled at SUU inside of the bucket.

After multiple tests were performed by decreasing the water level very low, no cavitation was observed. It appeared that the video cavitation demonstration is not typical cavitation in the suction port of the pump system because it had no suction line. It is possible that the water level decreases in the bucket until the pump starts pulling air into the system; however, this is simply speculation from the observations of the test we conducted. His approach is a brilliant way of explaining the idea of cavitation. The full conversation with Larry Bachus is in the Appendix.

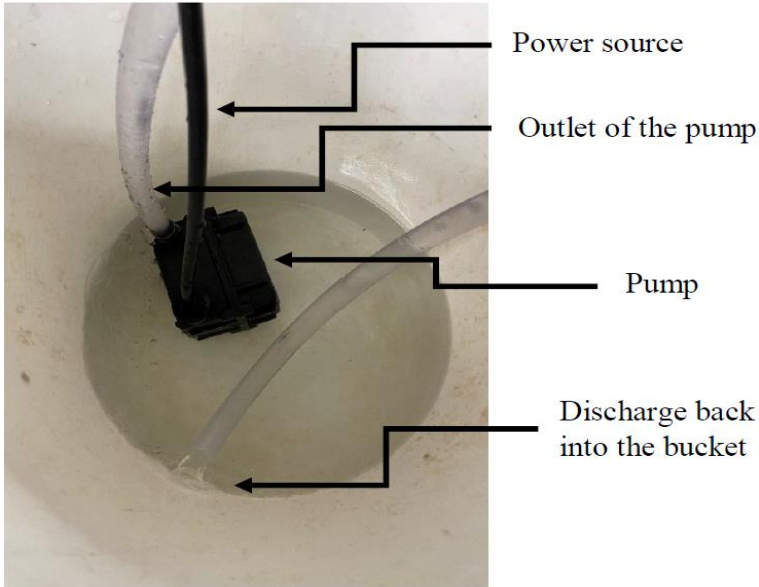


Figure 3. Submersible pump system.

We discussed how we could make the pump cavitate by increasing the suction capacity of the pump. Figure 4 shows a 3D-printed attachment that goes over the small impeller on the pump. The pump impeller and attachment on the pump are also shown. In this configuration, the pump does not need to be submerged.

The original submersible pump used an open vent with a small impeller that moves the water into the discharge tube (Fig. 4A). The printed part was attached to the pump, and a test was conducted to cause the pump to cavitate (Fig. 4B,C). The impellers were small and had little power, causing limited function when connected to a hose. This opposed the functionality when the pump was submerged. Impellers on centrifugal pumps are designed with angles in the blade to efficiently move water out of the pump. This submersible pump has impellers with no angle and is small relative to the size of the motor. It behaves correctly when submerged because the weight of the water on top of the pump is helping push the water through the system.

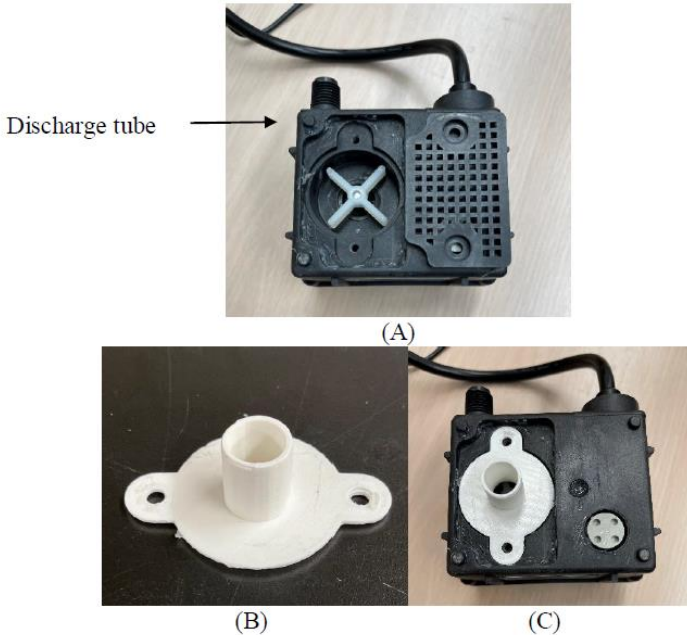


Figure 4. 3D-printed adapter to connect a tube on the inlet side of the pump.

CIRCULATION PUMP

The circulation pump is typically used for appliances in the home. This model is a Bayite Solar Circulation Pump [12]. This kind of pump needs to be primed, and water needs to be in the entire suction system before the pump is turned on. Figure 5 shows the setup of the experiment.

The pump is on top of the cabinet to increase the h_s of the system. The ball valve on the inlet tube restricted the flow and increased the h_f of the system. These restrictions decreased the overall $NPSH_a$ of the system.

The pump documentation did not provide $NPSH_r$. Without the published $NPSH_r$, cavitation may not be predicted. It appeared that manufacturers of these pumps do not publish their calculations of $NPSH_r$, or that the pumps were not used to run experiments to detect cavitation.

Nonetheless, an experiment was conducted on the system. The pump was primed, and the flow ran smoothly. The pump was then raised (9 ft above the discharge tank), and the flow continued throughout the system. The valve was then closed incrementally, and the flow decreased dramatically until completely stopped. The $NPSH_a$ was too high. With

our observations, it is possible that if the pump was raised higher or another valve was put on the inlet tube, the pump may have cavitated. However, this experiment was constrained by the height of the room and limited time. Cavitation is possible with further research and experimental trials.

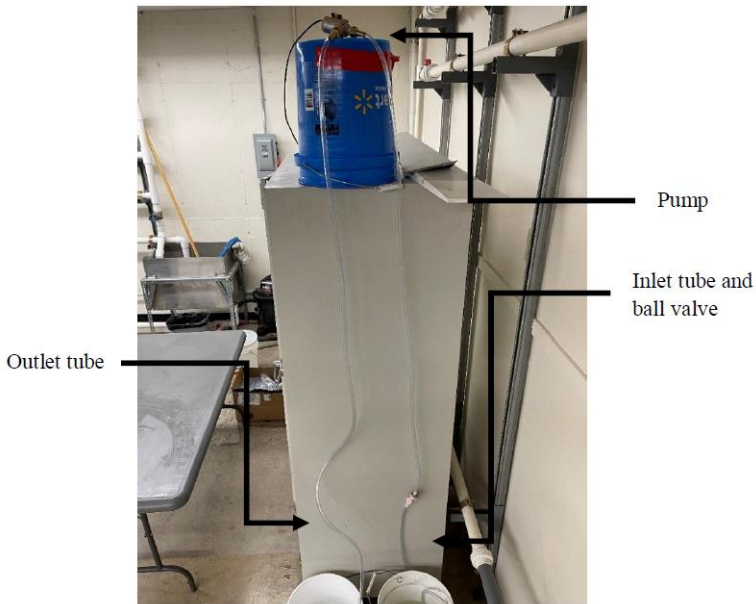


Figure 5. Circulation pump experiment setup.

DIAPHRAGM PUMP

The diaphragm pump is a unique way of pumping a liquid through a system. A piston moves against a flexible membrane, pushing and pulling it to bring the liquid through the pump. The Seaflow 33 Series Diaphragm pump was used for this test [13]. The pump was a double-acting diaphragm pump. There are two membranes inside doubling the production of the pump. Figure 6A shows the double action of the pump. Figure 6B is an image of the pump as used.

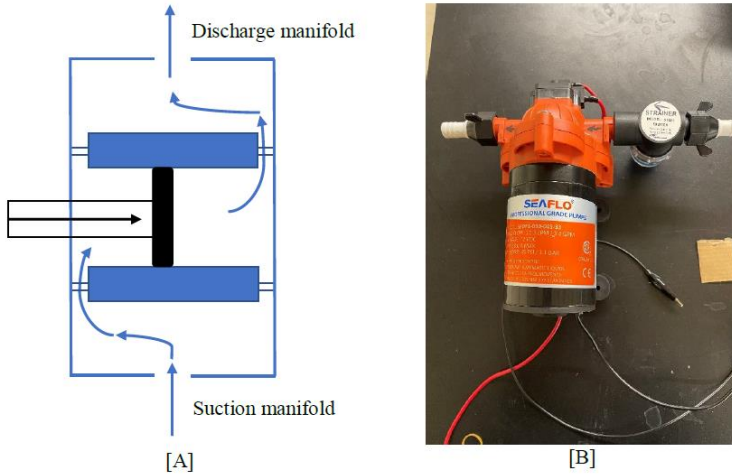


Figure 6. Cross-section of a double-acting diaphragm pump.

The set-up for this test was the same as that used for the circulation pump; however, this pump did not need to be primed. The pump was raised to increase head loss. The valve was then partially closed, and the pump showed signs of cavitation. Bubbles began to form on the discharge side of the pump, and a rough, rocky noise was heard and the pump vibrated. Figure 7 shows the bubbles that were formed from the pump. The bubbles seen in the image are from the discharge side of the pump. Cavitation started on the intake side of the pump. A majority of the bubbles collapsed inside the pump while others remained and are seen in the discharge.

The valve used in this system was a plastic ball valve. No information was available to predict energy losses in the valve. Similar to the circulation pump, the $NPSH_r$ was not provided by the pump manufacturer, which was located in China, making it very difficult to find technical information about the pump.

CENTRIFUGAL PUMP

For the last attempt to demonstrate cavitation, we selected a larger pump. A Hoteche 3/4HP [14] Water Pump was used for this experiment. This pump is the most similar to a traditional centrifugal pump among those involved in this experiment. It has a spinning disk that moves the water, but instead of individual impellers, the disk is made up of small

channels with an inlet and an outlet opening. This pump needed to be primed.

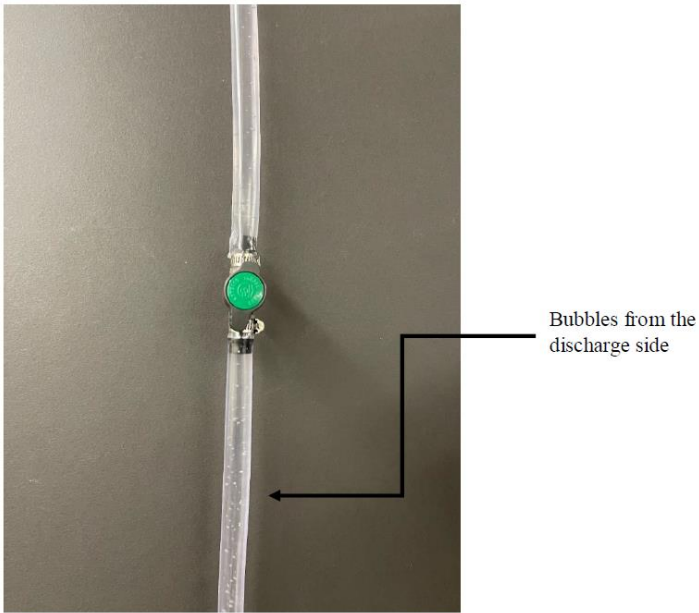


Figure 7. Discharge tube and bubbles on both sides of the valve.

A thin-walled (with a nominal diameter of 1 in.) tubing was used for the testing, along with a gate valve. The pump proved to be too powerful for the 0.04-in (1-mm) wall thickness of the suction tubing. It flattened and restricted the flow to the system. A new reinforced clear braided tubing with 0.15 in (3.75 mm) wall thickness was trialed next to replace the previous tubing. The wall thickness and braided reinforcement were able to keep the tube from collapsing the suction line of the system. Figure 8 shows the pump during steady-state condition. At the inlet of the pump, the braided tubing experiences a large amount of vacuum, almost to the point of closing off the system, but it was just strong enough for the system to function properly.



Figure 8. Pump shown during steady-state flow.

The pump proved to be very powerful for our in-house experiment, and the intake reservoir (bucket) needed to be filled continuously using a water faucet to keep the system at a steady flow. The gate valve was put on the end of the inlet tube. Figure 9 shows the inlet portion of the system.



Figure 9. Inlet tube with a portion of the gate valve shown.

After the system reached steady-state, the gate valve was slowly closed to increase the head loss of the system to try to cavitate the pump. The pump withstood the flow restriction of the valve closing without noticeable cavitation in the suction line of the pump. Some bubbles were formed in the discharge. This might be a sign of cavitation in the system, but the pump never sounded differently (loudly) as the diaphragm pump did. This suggests that the $NPSH_a$ was close to the $NPSH_r$ but never surpassed that value. Figure 10 shows the bubbles that were formed when the gate valve was $3/4^{\text{th}}$ closed.



Figure 10. Bubbles at the outlet of the pump.

Again, the $NPSH_r$ was not provided by the manufacturer. It appears that the $NPSH_r$ is not typically included for any pump that is not a traditional large industrial-sized centrifugal pump. Further tests must be performed on this pump to explore more apparent cavitation. Elevating the pump and making it a closed loop system could solve the problem.

CONCLUSION AND RECOMMENDATIONS

The conducted tests were worthy lessons to produce cavitation in pumps. Because there were no calculations done in these tests, there is no reason for any of these tests to be performed for a fluid mechanics laboratory course. Documentation of $NPSH_r$ is the prime issue to not being able to theoretically predict the cavitation of any of the systems.

Future tests should not be performed until the proper value for the $NPSH_r$ is provided by the manufacturer. Contacting the manufacturer or finding a pump that has proper documentation is necessary.

We recommend the following guidance when undertaking similar tests: (1) soft PVC tubing is very difficult to work with. We recommend that an acrylic clear piping system be used for future systems because they are much stronger than the regular tubing and, because the material is transparent, cavitation would be very easy to detect; (2) an actual self-priming centrifugal pump should be used to get accurate predictions for cavitation. Centrifugal pumps are the most common type of pump, and manufacturers are more likely to provide $NPSH_r$ for them; and (3) a pressure differential system should be put on the inlet side of the system. If two pressure gauges were placed on both sides of the gate valve and another two were placed on the sides of the pump, the pressure drop can be calculated to detect the pressure the cavitation starts. Theoretical predictions could also be made to compare to the results when the trials are conducted.

ACKNOWLEDGMENTS

This project would not have been possible without the help and support of the Department of Engineering and Technology at Southern Utah University. Their contributions included providing the equipment and assistance from faculty. Also, the undergraduate research funding was partially provided by the NASA Utah Space Grant Consortia.

REFERENCES

- [1] Xylem Applied Water Systems. (2015). Pump Cavitation and How to Avoid It. Retrieved December 2, 2021, from https://www.xylem.com/siteassets/support/case-studies/case-studies-pdf/cavitation-white-paper_final-2.pdf
- [2] Mott, R.L. & Untener, J.A. (2019). *Applied Fluid Mechanics*. Pearson Education, London.
- [3] Elsey, J. (2018). NPSH Calculation: A Step-by-Step Guide, Retrieved December 2, 2021, from <https://www.pumpsandsystems.com/centrifugal-pumps/nps-h-calculation-step-step-guide>

- [4] Central States Industrial. (n.d.). What is pump cavitation? And four ways to prevent it. Retrieved on December 2, 2021 from <https://www.csidesigns.com/blog/articles/what-is-pump-cavitation-and-how-to-prevent-it>
- [5] Peters, S. (2020). What is pump cavitation and how do I avoid it? Retrieved December 2, 2021, from <https://blog.craneengineering.net/what-is-pump-cavitation>
- [6] Kelton, S. (2018). What are the most common causes of cavitation in pumps? Retrieved December 2, 2021 from <https://empoweringpumps.com/what-causes-cavitation-triangle-pump-components/>
- [7] Motlani, A. (2021). Learn the symptoms of pump cavitation and solutions to correct it. Retrieved December 2, 2021, from <https://www.pumpsandsystems.com/how-detect-pump-cavitation>
- [8] Michael Smith Engineers Ltd. (n.d.). Useful information on pump cavitation. Retrieved December 2, 2021 from <https://www.michael-smith-engineers.co.uk/resources/useful-info/pump-cavitation>
- [9] Bachus, L. (2013). Cavitation demonstration. Retrieved December 5, 2021, from <https://www.youtube.com/watch?v=FJnX6gR-JNo>.
- [10] Telford, O. (2021). Pump Cavitation Media. Retrieved December 4, 2021, from <https://drive.google.com/drive/folders/14FTrXxvr6JI9hfexYUDk0u3fdYaJMP7F?usp=sharing>.
- [11] Franklin Electric. (n.d.). P-AAA Series Oil-Filled Submersible Pump. Little Giant. Retrieved December 16, 2021, from <https://www.littlegiant.com/products/specialty-pumps/small-submersible-pumps/oil-filled/p-aaa-series/>
- [12] Bayite byt-7a015 DC 12V solar hot water heater circulation pump with DC power supply adapter low noise 3M head 8LPM 2.1GPM. (n.d.). Retrieved December 16, 2021, from <https://www.amazon.com/bayite-BYT-7A015-Heater-Circulation-Adapter/dp/B01G305PK0>

[13] XIAMEN DOOFAR OUTDOOR. (n.d.). SEAFLO 33 series DC diaphragm pump 12V/24V 3.0-13.2LPM 17-60PSI. Retrieved December 16, 2021, from <http://www.seaflo.com/en-us/product/detail/604.html>

[14] Hoteche. (n.d.). 3/4 hp Centrifugal Electric Water Pump Pool Farm Pond Biodiesel Hoteche 1". Retrieved December 16, 2021, from <https://www.amazon.com/Centrifugal-Electric-Water-Biodiesel-Hoteche/dp/B0176XILRC>

APPENDIX

TRANSCRIPTION OF EMAILS FROM LARRY BACHUS

From: Owen Telford
To: Larry Bachus
Cc: Ali Siahpush
Fri, Sep 17, 2021 at 1:36 PM

Hello Mr. Bachus,

My name is Owen Telford and I am an undergraduate researcher for the engineering department at Southern Utah University. Along with my mentor Dr. Ali Siahpush, we are trying to create an effective demonstration of cavitation for a lab setting at the university. We know that you have extensive knowledge of the subject and have seen the videos you have created about cavitation. We would like to talk to you about the system that you have created and know how we could replicate a system similar to yours. Specifically, we have had trouble finding a sufficient pump for our system. If you could possibly point us in the right direction of where we could purchase a similar pump that was used in your videos that would help us tremendously.

Thank you for your time,
Owen Telford

From: Larry Bachus
To: Owen Telford
Sun, Sep 19, 2021 at 11:29 AM

Hello Owen,

Let me offer a couple of suggestions:

Before COVID, I traveled to many process facilities (oil refineries, chemical plants, etc.) around the globe to lecture on pumps. When

traveling, I demonstrate cavitation with a small submersible fish tank pump. You can see this in some of my videos on You Tube.

The brand of the pump is “Little Giant”. The model (I believe) is: P-AAA. The pump/motor unit is about 4-inches square with a 6 foot power cord.

On arrival in the seminar city, I go to a Home Depot, Menards, or Lowes and buy two plastic buckets (3 or 5 gallon buckets in the paint dept.) and about 8 feet of plastic tubing.

I can pump from one bucket to the other, or pump around in a circle, back into the same bucket. I put cold water in the bucket and submerge the pump and motor unit. The electrical cord plugs into a power strip and the power strip plugs into the wall socket. The on/off button on the power strip activates the pump.

I can demonstrate cavitation by reducing the water level in the bucket, or by partially blocking the pump suction screen with a piece of paper, or cloth. The students can hear the rumbling and stress on the pump caused by the cavitation. And, the students can see the cavitation bubbles (voids) passing through the plastic tubing.

I normally invite one of the students to help with the demonstration. I explain that cavitation results from an energy imbalance... either an ‘energy deficit’ at the suction side of the pump, or an ‘energy surplus’ on the discharge side of the pump.

I let the student resolve the cavitation by balancing the energy. The energy will balance by increasing the energy entering into the pump (removing the blockage at the suction screen, or increasing the water level (head) in the bucket), or by reducing the energy surplus (pinching the plastic tubing) on the discharge side of the pump.

When the energy balances, the rumbling, stress and bubbles disappear.

When the class ends, I donate the paint buckets to a student who might be planning on painting his bedroom or house, and get onto the airplane with my plastic pump.

The plastic buckets, plastic tubing and plastic pump don’t offer the best demonstration of cavitation. You can’t really hear the violent energy (snapping, popping and implosions) of cavitation with plastic components. Because you are a university, you can produce a better demonstration with a permanent metal pump, and metal pipe loop from, and back into, a metal holding tank, with metal valves on the suction and discharge pipe.

You don’t have to pay list price for a new pump and motor. Go to a pump rebuild shop in your city. Most pump shops will have a used pump that no one has claimed or paid for after repair. The pump shop

might donate the pump or sell the pump for pennies on the dollar just to get rid of the pump.

I hope this helps. Good luck.

Larry

From: Larry Bachus

To: Owen Telford

Thu, Sep 30, 2021 at 11:01 AM

Owen,

I don't know the type or size of pump you are using, so I can't really say what might be going wrong.

The Cavitation noise and damage is easy to produce by starving a stainless steel industrial pump with a 20-inch (diam.) impeller rotating at 3,600 rpm on a 100-hp motor. The noise (clicking, snapping, popping) is loud enough to require hearing protection (ear plugs or headphones).

The plastic pump I use in my on-sight demonstrations has a 1.5-inch impeller on a fractional horsepower motor. It isn't the best demonstration. But the pump passes through the security sensors at the airport without alerting the guards or sounding the alarm.

Also, let me say that producing cavitation with a plastic fish tank pump requires some time, patience, practice and finesse. It is like learning to ride a bicycle. You fall off the first few times you try. You must first find your balance. Once you find your balance, riding a bicycle is easy.

When I was a child, my grandfather made a whistling sound by blowing on the lip of an empty coke bottle. It took me weeks and a gallon of spit to learn how to do it. But I eventually learned.

There isn't enough energy in a fish-tank pump to reproduce classic industrial cavitation. But you can hear the stressed, vibrating pump (if everyone in the room is quiet), and see the bubbles (voids) moving through the tubing.

Keep working at it.

Regarding the videos, I use one length of about 8 feet of plastic tubing. Sometimes I pump from one bucket to another bucket. Sometimes I recirculate the flow back into the first bucket.

The NPSHr on a fish tank pump is miniscule. Besides, the NPSHr is an absolute value and the fish tank is exposed to atmospheric pressure. So, it isn't a consideration. However, the NPSHr is a standard feature at different flows on the performance curve of an industrial pump.

I hope this helps.

Larry

From: Larry Bachus
To: Owen Telford
CC: Ali Siapush
May 24, 2022, 1:44 PM

Hello Ali and Owen,

I read the attached paper. I didn't see anything to change with your text.

I saw something I would like to revise in my text. I said:

The students can hear the rumbling and stress on the pump caused by the cavitation.

I want to change this to say, "The students can hear the rumbling and stress on the pump caused by the energy starvation." A plastic fish tank pump with a fractional HP motor, can't really display true cavitation.

Because you survive and thrive in academic circles, you might never have seen an industrial pump curve showing NPSHr at different flows. This is revealed a few times in your text.

The pump documentation did not provide NPSHr. Without the published NPSHr, cavitation may not be predicted. It appeared that manufacturers of these pumps don't publish their calculations of NPSHr, or were not used to run experiments to detect cavitation.

Similar to the circulation pump, the NPSHr- was not provided by the pump manufacturer. Unfortunately, these pumps are made in China, making it very difficult to find technical information about the pump.

Again, the NPSHr was not provided by the manufacturer. It appears that the NPSHr for small pumps are not included for any pump that is not a traditional large industrial sized centrifugal pump.

Another problem we are having is finding a value for the NPSHr for pumps, theoretically, they are given by the manufacturer but none of the documentation we have found has given us a value.

NPSHr is a standard metric on the pumps I work with, and the NPSHr appears on the performance curve. I am attaching performance curves of 2 industrial pumps.

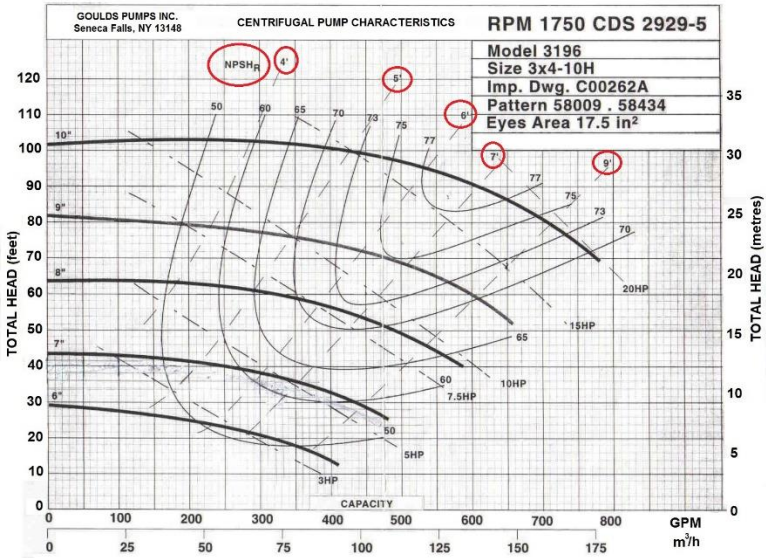
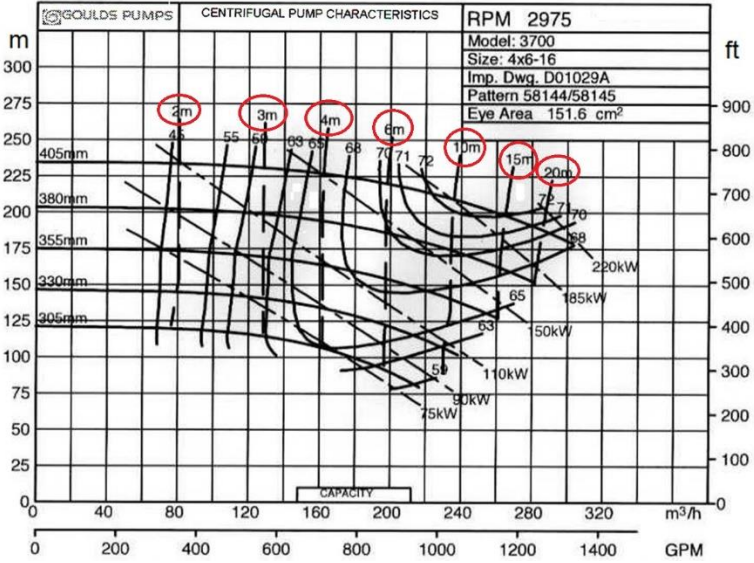
One curve is a chemical process pump (meeting the ANSI spec) and shows the NPSHr in feet.

The other curve is an oil and gas refinery pump (meeting the API spec) shows the NPSHr in metres.

Remember: NPSHr readings are absolute. A NPSHr reading less than 34-ft or 10-m is less than atmospheric pressure at sea level and 70°F or 20°C. These pumps can pull a vacuum.

I hope this helps.

Regards,
Larry Bachus



Exploring Correlates of Domestic Violence and Homelessness: A Review of the Literature

Linnette Wong

Weber State University

Abstract

Domestic violence is a serious issue our society is facing. While trying to recover from this trauma, victims of domestic violence may experience related difficulties. Homelessness has been observed as a trend among those impacted as they are trying to escape an abusive situation. This literature review is an examination of the impact of domestic violence on an individual's life. The keywords 'domestic violence' and 'homelessness' were used to screen the available literature to identify articles pertinent to the topic. The initial searches captured 53 unique articles. Eight articles were selected based on keywords and relevance to the topic studied. The results suggested positive correlations between domestic violence and homelessness. The findings have important implications for the design of health and social programs targeting homelessness such as transitional housing, patient-centered care, and health care financing.

Introduction

Homelessness is increasingly recognized as a serious social problem. There were around 554,000 homeless individuals in the United States with homeless families accounting for approximately 40% of the total homeless population (U.S. Department of Housing and Urban Development [HUD], 2017; National Coalition for the Homeless, 2005). Researchers who study homelessness have noted areas of concern such as drug and alcohol use, physical and mental health, sexual practices, and sexual health and violence and victimization (Mallett et al., 2009). Those who are homeless have poorer health and well-being and higher levels of substance use and are at greater risk of contracting sexually transmitted infections (STIs) and of victimization (Mallett et al., 2009). There are concerns about the mental health and emotional well-being of adults experiencing homelessness. High rates of mental health problems have been reported with a prevalence of anxiety and depression, and feelings of powerlessness and loss (Flatau et al., 2010; Meadows-Oliver, 2005; Tischler et al., 2004; Walters and East, 2001).

The road to homelessness is often complex and varied but usually involves some form of crisis (Mallett et al., 2009; Tischler et al., 2007). A crisis may involve housing, drugs and alcohol, mental health, relationships, and individual choice (Tischler et al. 2007). It is also widely reported that homelessness follows a cycle that often repeats itself; therefore, individuals may find themselves homeless on more than one occasion (University of York Center for Housing Policy, 2003).

Domestic violence is defined as any pattern of abusive or violent behavior used by a partner in a relationship to gain or maintain power and control (U.S. Department of Justice, 2007). Domestic violence includes physical assault, threats, harassment, humiliation, and sexual, emotional, or economic abuse (Brewster, 2002). Homeless adults experience high exposure to lifetime trauma and victimization caused by domestic violence (McWhirter, 2006). A previous study with the sample size of 220 individuals found domestic violence was a major predictor of homelessness (Bassuk et al., 1998). Additionally, exposure to violence is associated with an increased risk of homelessness for adolescent mothers (Kennedy, 2007).

Given the critical role of domestic violence in homelessness, it is important to gain a better understanding of the relationship between the two. The purpose of this literature review was to provide a comprehensive report of the published research regarding the correlation between domestic violence and homelessness. Articles were selected using the keywords “domestic violence” and “homelessness” to assess the amount of articles that were available.

Methods

A search for relevant articles was conducted by utilizing the keywords 'domestic violence' and 'homelessness.' Multiple databases were searched including Academic Search Premier, ERIC, CINAHL Complete, PsycINFO, and MEDLINE. The search focused on peer-reviewed scholarly articles that dated from 2007 to 2017. Dissertations, books, magazines, and articles that did not match the specified keywords were not included in the results list. In addition, to be included in the literature review, articles were required to have samples drawn from only the U.S., consisted of only adult subjects, and had to include analyses of the relationship between domestic violence and homelessness. The initial searches captured 53 unique articles. Of these, eight articles were selected based on keywords and relevance to the topic studied.

Results

The eight articles are listed in Table 1. Four of the articles reviewed concerned the extent of domestic violence among homeless individuals. Tyler and Schmitz (2013) conducted a study among 40 homeless young adults and revealed that 31 (77.5%) experienced physical abuse. Thirteen homeless young adults (32.5%) reported sexual abuse experiences. Thirty-eight homeless young adults (95%) indicated experiencing sexual abuse, a physically violent household, and/or conflict that caused them to run away. Kim et al. (2010) reported that more than half their sample reported childhood physical abuse (68.2%); 71.1% reported adulthood physical abuse; more than half reported childhood sexual abuse (55.6%); and 53.1% reported adulthood sexual abuse.

Iyengar and Sabik (2009) focused on the demands incurred by homeless shelters and reported that on a single night, 14,518 domestic violence victims required emergency homeless shelter nationwide. Clevenger and Roe-Sepowitz (2009) found domestic violence victims who had children at the time of the incident were more likely to use homeless shelter services [$X^2(1, N=283)=3.87; p<.05$]. Domestic violence victims were more likely than expected to use shelter services [$X^2(1, N=283)=4.19; p<.05$] (Clevenger & Roe-Sepowitz, 2009).

Three of the articles suggested domestic violence may be predictive or causative of homelessness in women. Moe (2007) found all of the 19 homeless women had suffered severe and multiple forms of battery. Eighteen of them (95%) had been physically assaulted, 7 (37%) had been sexually assaulted, 16 (84%) described instances of emotional or psychological abuse, and 13 (68%) recounted experiences of financial and/or property abuse (Moe, 2007).

Table 1: Summary of reviewed articles			
Authors	Aims/objectives of study	Methods	Major findings
Tyler & Schmitz, 2013	To explore the early family histories of homeless young adults, the types and number of transitions they experienced, and their pathways to the street.	Qualitative study N=40	31 homeless young adults (77.5%) experienced physical abuse. Sexual abuse experiences were also quite extensive and reported by 13 young adults (32.5%). 38 homeless young adults (95%) indicated that it was abuse, a physically violent household, and/or conflict that caused them to run away.
Kim et al., 2010	To examine the impact of physical and sexual trauma on a sample of homeless men.	Quantitative study N=239	More than half the sample reported childhood physical abuse (68.2%), and 71.1% of the sample reported adulthood physical abuse. More than half the sample reported childhood sexual abuse (55.6%), and 53.1% reported adulthood sexual abuse.
Clevenger & Roe-Sepowitz, 2009	To examine service utilization among adult victims of domestic violence identified by crisis responders as being in need of crisis services.	Quantitative study N=283	Domestic violence victims who had children at the time of the incident were more likely to use homeless shelter services [$X^2(1, N=283)=3.87$; $p<.05$]. Victims without an order of protection were more likely than expected to use shelter services [$X^2(1, N=283)=4.19$; $p<.05$].

Iyengar & Sabik, 2009	To determine the extent of domestic violence victims' needs and the resources necessary to address them.	Quantitative study N=48,350	On a single night, 14,518 domestic violence victims required emergency homeless shelter.
Moe, 2007	To examine the various aspects of help seeking, and the social and institutional responses to such efforts, through the narratives of women in a domestic violence shelter.	Qualitative study N=19	All 19 women had suffered severe and multiple forms of battery: 18 (95%) stated that they had been physically assaulted, 7 (37%) reported having been sexually assaulted, 16 (84%) described instances of emotional or psychological abuse, and 13 (68%) recounted experiences of financial and/or property abuse.
Lewinson et al., 2014	To present traumatic experiences among women residing in budget hotels after housing displacement.	Qualitative study N=19	All women in the sample (N=19) described troubled or violent home environments prior to hotel living. In their narratives, physical and emotional abuse were common trauma themes causing their homelessness.

Hamilton et al., 2011	To provide a grounded description of veterans' pathways into homelessness.	Qualitative study N=29	15/29 participants (52%) described pre-military adversity (including child abuse and domestic violence) that either resulted in homelessness pre-military or sowed "seeds of homelessness" that occurred post-military. Four participants described abusive relationships that ultimately resulted in homelessness.
Gültekin et al., 2014	To explore the experiences of homelessness families in Detroit, Michigan, and to determine whether the perceptions of needs and services were in alignment.	Qualitative study N=28	85% of the homeless women reported involvement in abusive relationships.

Results from Lewinson et al. (2014) indicated that all the homeless women in the sample (N=19) described prior troubled or violent home environments and found physical and emotional abuse were common trauma themes causing their homelessness. Additionally, in a self-report collection, Gültekin et al. (2014) observed that 85% of the 28 homeless women reported involvement in abusive relationships.

One study conducted on homeless veterans was located among databases concerning the relationship of homelessness to domestic violence among veterans. Hamilton et al. (2011) found that 15 of the 29 participants (52%) described pre-military adversity (including child abuse and domestic violence) that either resulted in homelessness pre-military or sowed “seeds of homelessness” that occurred post-military.

Four participants (13.8%) described abusive relationships that ultimately resulted in their homelessness.

Discussion

With only eight articles uncovered related to the correlates of domestic violence and homelessness, there remains an apparent paucity of information. Limitations to the existing studies' sample populations included location, demographic areas, self-reporting, race, small sample sizes, and the reliability of participants' report, particularly those with possible mental illnesses. A large portion of the surveys used women as the only source of data, limiting the information about male homeless domestic violence victims. This may be attributed to the biased assumption that men are less likely to report their abuse history or be identified as domestic violence victims (Tyler & Melander, 2009). A limited amount of research has been recorded regarding the correlation between homelessness and military victims of domestic violence. There is lack of existing information on the relationship between domestic violence treatment and the likelihood of recovering from homelessness.

Studies on the topic of homelessness and domestic violence have been conducted for the past few decades, and the existing results provide a wide variety of options for assisting the homeless population who are also the victims of domestic violence. The options vary depending on the specific population that is being studied. The most popular assistance options were transitional housing, patient-centered care, and health care financing (Koh & O'Connell, 2016; Schinka et al., 2015). These services can help homeless people get their lives back on track.

Some concerns exist with improving the options for homeless adults to deal with their trauma. It is imperative domestic violence victims are informed of and referred to health services within their community; however, there is some concern as to how these costs will be covered. There are many adults on the streets with mental and emotional issues. Community facilities able to offer counseling, self-esteem awareness classes, and group therapy would be beneficial to the adults on the streets. Because of the long-lasting effects of abuse and trauma, homeless adults may lack the trust and self-confidence needed to recover from their physical and psychological damage (Whitbecket et al., 2015). Offering options such as psychological treatment and safe places could decrease the amounts of domestic violence and abuse, thus, decreasing risky and dangerous behaviors with which they would normally be involved.

References

Bassuk, E.L., Perloff, J.N., & Bassuk, S.S. (1998). Prevalence of mental health and substance use disorders among homeless and low-income housed mothers. *American Journal of Psychiatry*, 155(11), 1561-1564. doi: 10.1176/ajp.155.11.1561

Brewster, M.P. (2002). Domestic violence theories, research, and practice implications. In A.R. Roberts (Ed.), *Handbook of Domestic Violence Intervention Strategies: Policies, Programs, and Legal Remedies*. New York: Oxford University Press

Clevenger, B.J.M., & Roe-Sepowitz, D. (2009). Shelter service utilization of domestic violence victims. *Journal of Human Behavior in the Social Environment*, 19(4), 359-374. doi: 10.1080/10911350902787429

Flatau, P., Conroy, E., Clear, A., Burns, L. (2010). *The integration of homelessness, mental health and drug and alcohol services in Australia*. AHURI Positioning Paper (132). Retrieved March 18, 2022 from <http://www.ahuri.edu.au/publications/projects/p80568>

Gültekin, L., Brush, B.L., Baiardi, J.M., & VanMaldeghem, K. (2014). Voices from the street: exploring the realities of family homelessness. *Journal of Family Nursing*, 20(4), 390-414. doi: 0.1177/1074840714548943

Hamilton, A.B., Poza, I., & Washington, D. L. (2011). "Homelessness and trauma go hand-in-hand": Pathways to homelessness among women veterans. *Women's Health Issues*, 21(4), 203-209. doi: 10.1016/j.whi.2011.04.005

Iyengar, R., & Sabik, L. (2009). The dangerous shortage of domestic violence services. *Health Affairs*, 28(6), 1052-1065. doi: 10.1377/hlthaff.28.6.w1052

Kennedy, A.C. (2007). Homelessness, violence exposure, and school participation among urban adolescent mothers. *Journal of Community Psychology*, 35(5), 639–654. doi: 10.1002/jcop.20169

Kim, M.M., Ford, J.D., Howard, D.L., & Bradford, D.W. (2010). Assessing trauma, substance abuse, and mental health in a sample of homeless men. *Health Social Work*, 35(1), 39-48. 10.1093/hsw/ 35.1.39

Koh, H.K., & O'Connell, J.J. (2016). Improving health care for homeless people. *Journal of the American Medical Association*, 316(24), 2586-2587. doi: 10.1001/jama.2016.18760

Lewinson, T., Thomas, M.L., White, S. (2014). Traumatic transitions: Homeless women's narratives of abuse, loss, and fear. *Affilia: Journal of Women and Social Work*, 29(2), 192-205. doi: 0.1177/0886109913516449

Mallett, S., Rosenthal, D., Keys, D., & Averill, R. (2009). *Moving Out, Moving On. Young People's Pathways In and Through Homelessness*. London: Routledge

McWhirter, P. (2006). Community therapeutic intervention for women healing from trauma. *Journal for Specialists in Group Work*, 31(4), 339-351. doi: 10.1080/01933920600918857

Meadows-Oliver, M. (2005). Social support among homeless and housed mothers: An integrative review. *Journal of Psychosocial Nursing*, 43(2), 40-47. doi: 10.3928/02793695-20050201-02

Moe, A.M. (2007). Silenced voices and structured survival. *Violence Against Women*, 13(7), 676-699. doi: 10.1177/1077801207302041

National Coalition for the Homeless. (2005). *Family Homelessness*. Retrieved March 18, 2022 from <http://www.nationalhomeless.org/families>

Schinka, J.A., Casey, R.J., Kaspro, W., & Rosenheck, R.A. (2015). Requiring sobriety at program entry: Impact on outcomes in supported transitional housing for homeless veterans. *Psychiatric Services*, 62(11), 1325-1330. doi: 10.1176/ps.62.11.pss6211_1325

The U.S. Department of Housing and Urban Development. (2017). *The 2017 Annual Homeless Assessment Report (AHAR) to Congress*. Retrieved March 18, 2022 from <https://www.hudexchange.info/resources/documents/2017-AHAR-Part-1.pdf>

Tischler V., Karim K., Gregory P., & Vostanis P. (2004). A family support service for homeless children and parents: users' perspectives and characteristics. *Health and Social Care in the Community*, 12(4), 327-335. doi: 10.1111/j.1365-2524.2004.00502.x

Tischler, V., Rademeyer, A., & Vostanis, P. (2007). Mothers experiencing homelessness: mental health, support and social care needs. *Health and Social Care in the Community*, 15(3), 246-253. doi: 10.1111/j.1365-2524.2006.00678.x

Tyler, K.A., & Melander, L.A. (2009). Discrepancies in reporting of physical and sexual abuse among homeless young adults. *Journal of Child Sexual Abuse*, 18(5), 513-531. doi: 10.1080/10538710903183360

Tyler, K.A., & Schmitz, R.M. (2013). Family histories and multiple transitions among homeless young adults: pathways to homelessness. *Child and Youth Service Review*, 35(10), 1719-1726. doi: 10.1016/j.childyouth.2013.07.014

University of York Centre for Housing Policy. (2003). *A Feasibility Study on the Causes, Impacts and Costs of Family Homelessness*. Retrieved March 18, 2022 from <https://www.kcl.ac.uk/kcmhr/publications/assetfiles/veterans/Dandeker2005-feasabilitystudyhomeless.pdf>

United States Department of Justice. (2007). *About Domestic Violence*. Retrieved March 18, 2022 from <http://www.usdoj.gov/ovw/domviolence.htm>

Walters S., & East L. (2001). The cycle of homelessness in the lives of young mothers: the diagnostic phase of an action research project. *Journal of Clinical Nursing*, 10(2), 171-179. doi: 10.1111/j.1365-2702.2001.00458.x

Whitbeck, L.B., Armenta, B.E., & Gentzler, K.C. (2015). Homelessness-related traumatic events and PTSD among women experiencing episodes of homelessness in three U.S. cities. *Journal of Traumatic Stress*, 28(4), 355-360. doi: 1002/jts.22024.

Rhetorics of Advocacy in Disability Accommodation

Rachel Bryson and Peter Call

Utah State University

Abstract

Students with less-apparent disabilities in higher education frequently have accommodation needs that can complicate existing institutional practices. Using a disability studies methodology, this article articulates possibilities for students and faculty to partner in the accommodation process in ways that increase opportunities for advocacy, mutual understanding, and student success.

Students with disabilities represent an increasingly large share of the student population in higher education. According to the National Center for Education Statistics, nearly 20% of college students identify as having a disability, defined as one or more of the following conditions: “blindness or visual impairment that cannot be corrected by wearing glasses; hearing impairment (e.g., deaf or hard of hearing); orthopedic or mobility impairment; speech or language impairment; learning, mental, emotional, or psychiatric condition (e.g., serious learning disability, depression, ADD [attention deficit disorder], or ADHD [attention deficit hyperactivity disorder]); or other health impairment or problem”

(National Center for Education Statistics 2018). While each of these impairments and conditions is protected under the 1990 Americans with Disabilities Act (ADA), as well as the 2008 ADA Amendments Act, students with less-apparent disabilities—such as learning or mental health disabilities, ADHD, or autism spectrum disorder—remain less likely to seek or receive necessary accommodations.

Understanding the reasons students with less-apparent disabilities are less likely to receive classroom accommodations is a complex endeavor. Yet awareness of barriers students encounter when seeking accommodations can help faculty have a greater awareness of how to advocate for their disabled students.¹ Current accommodation practices, particularly for students with less-apparent disabilities, may lead to disconnects between pedagogy and accommodation requests; distance between instructors and students; and the assumption that accommodation requests are simply checklists to be completed rather than opportunities for dialogue and advocacy. We explore these problems through the lens of Margaret Price's disability studies methodology (Price 2012) to address how faculty and students can actively collaborate to create sites of advocacy for students with disabilities.

Literature Review

Students with less-apparent disabilities encounter a variety of barriers in their pursuit of higher education. Disability studies scholar Christopher Toutain compiled a literature review identifying many of these barriers (Toutain 2019). Among the barrier types his research identifies are a lack of student and faculty awareness about accommodations resources; student inability to secure accommodations; faculty refusing to implement accommodations; student or faculty dismissal of accommodations as nonfunctional or unhelpful; and a lack of student desire to use accommodations. These barrier types are not discrete, nor are they abstract; rather, they highlight affective and material challenges faced by disabled students as they seek to achieve academic goals.

¹ In this essay, we use a blend of person-first and identity-first language. While most references are person-first, we want to acknowledge that linguistic practices surrounding disability, including less-apparent disability, are contested and in flux (Price 2012). Person-first language and similar linguistic strategies, while intended to be inclusive, may in fact increase stigma and unintentionally overlook the preferences of individuals and groups in defining their own identities and relationships with disability (Gernsbacher 2017; Gutsell & Hulgin 2013).

A 2020 survey from the advocacy organization Mental Health America found that 70% of students with mental health disabilities—arguably the most common of all less-apparent disabilities—were not registered with their respective campus disability services offices and thus did not receive institutional accommodations (Davis 2021). Only 20% of such students said that they were not registered because they did not want accommodations. According to the survey, “Students’ top reason [for not registering] was that they did not feel ‘sick enough’ for accommodations” (7). In addition, such students believe “they should ‘suck it up’—and may feel that their challenges are personal failures or indications that they do not belong in their school or in higher education more broadly” (7). Such self-reproaching sentiments are echoed in other research as well. Kain et al. (2019, 412) explained that students with mental health disabilities may experience “low self-esteem, feelings of inadequacy, lack of confidence, inability to concentrate, and lack of trust”—exacerbating factors of their impairments that may also lead to increasing stigmatization from self and others.

The experience of students with mental health disabilities is mirrored, in many ways, by students with other less-apparent disabilities such as learning or attention impairments. Stigma remains a powerful force in dissuading students with less-apparent disabilities from disclosing their disability status to institutional offices or individual faculty. According to Kranke et al. (2013), students with less-apparent disabilities experience both extrinsic and intrinsic stigma, meaning that they experience both the social discrimination leveraged against disabled persons as well as self-stigma, the “internalizing [of] negative social responses” (36). Kranke et al. note that a student’s desire to be “normal” or autonomous or to conform to faculty expectations made the student reluctant to disclose less-apparent disabilities. One of the key predictors of student unwillingness to disclose was the perceived lack of professorial support (43). Disabled students may also be hesitant to disclose if they fear their impairments make them appear less qualified to participate in college or university life—to engage a culture that “thrives on and rewards stamina, ability, independence, and mental fitness” (Hibbs and Pothier, qtd. in Matthews 2009, 233).

The rhetorical implications of labeling disabled individuals as “abnormal” or “deviant” are significant—and pervasive. In explaining how ableism functions within higher education to marginalize students, faculty, and staff with mental illness, Price (2011) argues that “persons with mental disabilities are presumed not to be competent, nor understandable, nor valuable, nor whole” (26). In terms of what she calls “rhetorical functionality,” or the ability to be taken seriously, to be valued and perceived as reliable by others, Price insists that a

presumption of competence is absolutely vital. Given that the disabled student is often presumed to be incompetent, Price argues that such a student is confined by “rhetorical disability.” This lack of what Price, Prendergast (2001), and others term *rhetoricity*, or the “ability to be received as a valid human subject” (Price 2011, 26), is a clear consequence of ableism, which Cherney (2019) defines as an orientation that “involves ways of knowing, valuing, and seeing the so-called ‘abnormal’ body as inferior” (8). Jay Dolmage (2017) argues that ableism is the means by which “academia powerfully mandates able-bodiedness and able-mindedness as well as other forms of social and communicative hyperability” (7), thereby underscoring how disabled university students—including those with less-apparent disabilities—are situated outside the preferential norms of the academy and restricted by its codes and expectations. If such students are to fairly engage in university classrooms and programs with their abled peers, they must be protected by law and accommodated by faculty who understand their roles in enabling the advancement of all students. Otherwise, accommodation will exist in theory only, and the stigmatization and marginalization of disabled students will be perpetuated.

Disability Studies Methodology Overview

Disability Studies (DS), as a field, is a “big tent.” Scholars from multiple disciplines are drawn to DS as a way to broaden considerations of disability and related issues of equity and inclusion within their fields and to add specific disciplinary perspectives or approaches to broader discussions within DS. Price (2012) asserts that the multidisciplinary makeup of DS is highly advantageous because its collective research “represents a great range of methods and beliefs” (159); its multidisciplinary nature is simultaneously problematic, she says, creating challenges in “identify[ing] common definitions, questions, and practices” (159). In response to such challenges, Price articulates a DS methodology that focuses on four “contact zones” in DS scholarship: access, activism, identification, and representation (160).

The concept of contact zones comes from Mary Louise Pratt (1991), who defines the zones as “social spaces where cultures meet, clash, and grapple with each other, often in contexts of highly asymmetrical relations of power” (34). In context of student–faculty interactions surrounding disability and accommodation, Pratt’s contact zones are evident. The classroom itself is a contact zone of meetings and clashes characterized by expectations and assumptions linked to ability and power. Within the classroom hierarchy, students typically have less power than faculty, and the stigma and misunderstanding accompanying

impairment or disability often compound the complexities surrounding contact zones.

Central to Price's methodology is the social model of disability, which Price describes as disability "constructed through social, political, historical, and other contexts" (164), given that—as she claims—"people with any form of accredited impairment are disabled by an unjust and uncaring society" (214). Those familiar with DS will recognize that Price's social model exists in contrast to medical or individual models, which "define disability in terms of individual deficit" (Shakespeare 2017, 197). While the social model does not *replace* the individual or medical model, it focuses on external social barriers as the true source of perceived disability rather than on things inherent to the "disabled" individual. Indeed, it repositions "disability" as a source of pride, affinity, and community. The social model also works to identify and disrupt unequal power relationships that label and oppress disabled people. Price's DS methodology thus "aims at a radical reshaping of relations of power" (164). As we build on Price's model and articulate ways for students and faculty to dialogue and collaborate, we seek to reshape power relations in classroom spaces. We do this through presenting our own assessment of and work in the four contact zones comprising Price's DS methodology: access, activism, identification, and representation.

Access

The rhetoric of access for disabled university students currently rests on legal frameworks for delineating and securing accommodations for medically or clinically defined disability. However, such legal frameworks may be inadequate means for understanding or meeting the needs of disabled individuals. At its best, the medical model does not accommodate faculty challenges in facilitating student accommodations, nor does it allow for necessary flexibility in faculty implementation of one-size-fits-all stipulations.

Furthermore, although accommodations are critical in improving access to learning for students with less-apparent disabilities, they are not the only means for understanding or enabling access. Citing Jay Dolmage, Price defines access as "working within and toward a mindset that continually explores, re-maps, and revises built [existing] contexts in ways that reflect the needs and values of the people who use them" (2012, 165). These "built contexts" include more than the physical spaces of learning; they also include "metaphorical spaces, such as attitudes, institutions, or social groups" (165). Faculty–student negotiations in these spaces can improve student accommodation and

access if the negotiations are motivated by student–faculty commitments to action.

However, if disabled-student access is met *only* through specified medical accommodations, and if such access ignores the roles of student self-advocacy and faculty-student dialogues within contact zones, such access will be less than ideal and may not meet true student needs.

Put differently, there are two general types of accommodations for students with disabilities. *Formal accommodations* are required by law, arranged with students by disability services offices, and implemented by faculty. *Informal accommodations* are not enforceable by law and are generally negotiated between student and instructor; they may be established with any student, regardless of institutional disability disclosure or participation in a formal process. It is important to note that both types of accommodation restrict collaboration: formal accommodations ostensibly privilege student input; informal accommodations are likely shaped by the perspectives and priorities of the instructor. But because instructors are ultimately responsible for implementing accommodations, and because instructors may not fully understand disabled students' perspectives and needs (or related legal obligations), instructors may “be resistant toward providing legally mandated accommodations” (Love et al. 2015, 28). Although imperfections exist in any system, opening up both formal and informal accommodation discussions to genuine collaboration can allow for mutual advocacy for both students and instructors.

To include a social model for accommodations, the rhetoric surrounding access needs to address the perspectives of both students with disabilities and faculty responsibilities and approaches. Current institutional practices can be inadvertently self-limiting because not all accommodations offered to a student apply to every course situation. This may leave some faculty with the assumption that if no listed accommodations are easily adaptable to their pedagogies or curricula, their courses are accessible and they do not need to offer accommodations.

Such assumptions are problematic for two reasons. First, formal processes sometimes leave little room for faculty to legally adapt mandated accommodations to classrooms that don't appropriately fit them. Second, many disabled students would benefit from policies or practices—from accommodations—that have not been formally granted them through institutional processes. In fact, if faculty learned to dialogue with disabled students (in ways that preserved student confidentiality regarding disability details), collaborative access beneficial to both students and faculty could be established.

Put another way, if access is met only through accommodation, it is often inadequate and may, in some cases, fail the student. Ideally, as Hong (2015) advocates, “Programs on faculty development should seek to increase disability awareness, rights, and obligations instead of changing attitudes” (222). Such programs could be offered through new faculty training or ongoing professional development—and might appropriately focus on creating spaces for students with disabilities to self-advocate and for faculty to initiate dialogue and increase responsiveness.

Activism

As a field, DS grew from the disability rights movement of the 1960s, a wide-ranging, inclusive movement modeled after the broader Civil Rights movement and focused on increasing access and rights for people with disabilities. The ADA of 1990 and the subsequent 2008 ADA Amendments Act prohibited discrimination based on ability. Consequently, disabled individuals who had previously been denied access to public spaces, integrated educational opportunities, and other forms of equal representation were guaranteed access to the spaces and support previously denied them. One result of this increased access was that students with disabilities enrolled in higher education in increasingly greater numbers. As mentioned previously, the National Center for Education Statistics reports that nearly 20% of undergraduates in the United States identify as disabled; the actual percentage is likely higher (Toutain 2019, 297), especially among students with less-apparent disabilities. These students likely remain underserved in terms of classroom accommodations.

It is because of such underserved students—according to Price (2012)—that “activism is regarded as a necessary component of a DS research agenda, and a theory of ‘emancipatory disability research’ was formulated and debated soon after the development of DS as a discipline” (168). Kimball et al. (2016) assert that “by witnessing parents demand accommodations and access, students with disabilities learned that advocacy skills were essential life skills” (251). Sensitive faculty on university campuses can continue to supplement parental activism by advocating for their students, encouraging self-advocacy in their students, and helping normalize disability through working to destigmatize it.

Identification

How do we understand the identity of disability in the world of academics, especially in contexts of accommodations? Our concerns

here are the manifold relations² for those who identify as disabled. As we have already emphasized, and as Sophia Mitra (2006) asserts, the medical model of student accommodations “is strongly normative: people are considered disabled on the basis of being unable to function as a ‘normal’ person does” (237). In addition, *disability* may have very different meanings for students and faculty, leading to disconnects or miscommunications when students seek formal or informal accommodations. According to Price, “positioning oneself in relation to disability is not a simple announcement, it is part of a complex web of discourses” (2012, 172); in addition, the manifold relations of disability present themselves only when they are communicated, not guessed at.

If accommodations are to meet needs of students with disabilities, faculty must recognize how their personal understanding of disability relates to the lived experiences of disabled students. Such understanding may be cultivated through formative assessments where disabled students are invited to share their lived experiences—and not always those specifically related to disability. Such faculty–student dialogues can enhance trust and invite disclosures leading to additional dialogue and understanding.

Price admits that, when reading DS scholarship, “I have been puzzled by the frequent failure on the part of researchers to discuss their own positions, identifications, or other alliances with respect to the topic they research” (2012, 171). This failure of researchers to self-identify is often shared by faculty and students as well. Faculty can and must advocate for their disabled students regardless of their own disability status. Explicitly identifying as a nondisabled ally or as a disabled faculty advocate is a powerful boon to disabled students in understanding, claiming, or communicating their own disability identities. Claiming and communicating disability identity can lead to meaningful representation.

Representation

Disability representation has a complicated history in popular culture and academics. DS scholar Rosemarie Garland-Thomson discusses the long and often problematic history of disability representation in literature and film, noting how “the blind, mad, lame, crippled, and unusually embodied have fired the imagination and underwritten the metaphors of classic Western literature” (2005, 523).

²The word manifold is a mathematical description in which the idea of a smaller area is related to the whole of a structure. More specifically, the complexity of something is readily simplified to a smaller proportion without loss of generality of said complexity. These facts govern our use of the term here.

Codifying such metaphors, Dolmage points to myths perpetuated by disability representation in popular media, especially myths constructing disability as pathology, weakness or pitifulness, deformity, abnormality, or even immorality (2014, 3-37). Such myths, Dolmage asserts, induce disability drift or disability hierarchy, where the physically disabled—especially in academic settings—are also perceived as mentally disabled and where “physical disabilities are situated as less stigmatizing than cognitive disabilities” (2014, 46). It is precisely because of such stigmatization that students with less-apparent mental health disabilities resist disclosure. As Kain et al. (2019) report, students tend to see faculty responding to mental health disabilities in ways that are “judgmental, discriminatory, [or] lacking compassion”; faculty themselves seem “suspicious of a student’s need for accommodations” while “acting dismissively toward the student and their concerns” (415).

Of course, disability representation can also work to create productive contact zones for teachers and students. Price discusses the role of narrative in disability representation, using examples from her own research with students. She confesses that she wrestled with what representation meant to her work as she engaged with multiple, even contradictory, narratives from her students. As she invited one student to respond to narratives of “overcoming,” Price recognized that while she herself found such narratives problematic, her disabled student strongly resonated with them. In the end, Price learned that her student’s adherence to the concept of “overcoming” disability—which Price saw as “an old chestnut in DS discourse, an eye-roller on a level with ‘tragic’ or ‘inspiring’” (2012, 179)—was an important part of the student’s own identity formation and personal narrative. Price could encourage, but not force, her student to accept a reading of disability that aligned with Price’s own—but she did so at the risk of undermining her student’s self-concept and thus stunting or blocking subsequent growth.

In short, opening room for students to claim their own disability identity and frame their own disability narrative is a key component in representation. As students and instructors dialogue together about how self-representation informs self-advocacy, they create opportunities to collaborate on classroom policies and practices that benefit disabled students as well as their nondisabled peers.

Conclusion

A well-known slogan of the disability rights community is “Nothing about us without us,” which in many ways brings together the methodological concepts of access, activism, identity, and representation we have discussed in this paper. In writing about disability oppression

and empowerment, James Charlton argues that “Nothing about us without us” is “a demand for self-determination and a necessary precedent to liberation” (1998, 25). We would add to this framing a key concept within contemporary disability studies: the push to recognize “human interdependence and reciprocal responsibility” (Kasnitz & Block 2012 197) as counterpoints to the binary of independence–dependence. The blended concept of *interdependence* necessarily rests on two assumptions: that interdependence is desirable and that the term itself describes how human beings naturally live within a given society. Garland-Thompson argues that to *value* disability is to “more fully recognize interdependence rather than independence by becoming more aware that all people rely on one another for life tasks and survival” (2011, 603). In higher education, interdependence can be framed in many ways, but the fundamental interdependent academic relationship is the relationship between faculty and students. As instructors and students recognize and embrace their interdependence, they are more likely to pursue collaboration and flexibility in teaching and learning—and, more crucially, in genuinely accommodating needs of those who are disabled.

In spite of supportive laws and policies, classroom disability accommodation remains complex. Faculty may sometimes feel more confident enacting accommodations for students with physical and sensory disabilities than for those with mental health or other less-apparent disabilities. Accommodations for physical disability tend to be more specific and concrete—and often more congenial with faculty teaching and evaluation. Students with less-apparent disabilities may be granted more nebulous sets of accommodations; they may also encounter faculty and peer stigmas about perceived capabilities in academic settings. The lack of concrete accommodations for students with less-apparent disabilities can be confusing and frustrating to students and instructors alike, emphasizing the need for flexibility and dialogue when enacting accommodations.

Because nonformalized accommodation enactment is a complex challenge, it defies simple solutions. Yet these basic principles of a nonformalized accommodation rhetoric create a sound beginning. First, students and faculty should construct accommodation as something at the heart of educational theory, not something outside it. Second, students and faculty should be committed to collaboration—to dialogue and mutual advocacy—as they consider accommodations and how to implement them. Third, such collaboration should shape disability accommodation as a dialogic and recursive (and thus more effective) process. As Mia Mingus writes, “Access for the sake of access is not necessarily liberatory, but access for the sake of connection, justice, community, love, and liberation *is*” (Mingus 2017). Finally, as faculty

seek out perspectives of students with less-apparent disabilities and as students with less-apparent disabilities self-advocate while attempting to understand the constraints and perspectives of their instructors, they can solve issues of access, solidify disability identity, and negotiate issues of representation in the classroom to supplant “able-bodied supremacy” and “exclusion” (Mingus 2017).

Works Cited

Charlton, James I. *Nothing About Us Without Us: Disability Oppression and Empowerment*. Berkeley: U of California P, 1998.

Cherney, James L. *Ableist Rhetoric: How We Know, Value, and See Disability*. University Park, PA: Pennsylvania State UP, 2019.

Davis, K. “Supporting college students: mental health and disability in higher education.” Mental Health America. 2021. Accessed April 15, 2022 from www.mhanational.org/collegereport.

Dolmage, Jay. “Mapping composition: inviting disability in the front door.” In *Disability and the Teaching of Writing: A Critical Sourcebook*, edited by Cynthia Lewiecki-Wilson and Brenda Jo Brueggemann, Boston: Bedford/St. Martin’s, 2008, pp. 14-27.

Dolmage, Jay Timothy. *Disability Rhetoric*. Syracuse: Syracuse UP, 2014.

Dolmage, Jay T. *Academic Ableism: Disability and Higher Education*. Ann Arbor: U of Michigan P, 2017.

Garland-Thomson, Rosemarie. “Disability and representation.” *PMLA*, vol. 120, no. 2, 2005, pp. 522-27.

Garland-Thomson, Rosemarie. “Misfits: a feminist materialist disability concept.” *Hypatia*, vol. 26, no. 3, 2011, pp. 591-609.

Gernsbacher, Morton Ann. “Editorial perspective: the use of person-first language in scholarly writing may accentuate stigma.” *Journal of Child Psychology and Psychiatry*, vol. 58, no. 7, 2017, pp. 859-61.

Gutsell, Margaret, and Kathleen Hulin. "Supercrrips don't fly: technical communication to support ordinary lives of people with disabilities." *Rhetorical Accessibility: At the Intersection of Technical Communication and Disability Studies*, edited by Lisa Meloncon, Milton Park, Abingdon-on-Thames: Routledge, 2013, pp. 84-94.

Hong, Barbara. "Qualitative analysis of the barriers college students with disabilities experience in higher education." *Journal of College Student Development*, vol. 56, no. 3, 2015, pp. 209-26.

Kain, Suanne, Christina Chin-Newman, and Sara Smith. "'It's all in your head...': students with psychiatric disability navigating the university environment." *Journal of Postsecondary Education and Disability*, vol. 32, no. 4, 2019, pp. 411-25.

Kasnitz, Devva, and Pamela Block. "Participation, time, effort and speech disability justice." *Politics of Occupation-Centred Practice: Reflections on Occupational Engagement Across Cultures*, edited by Nick Pollard and Dikaivos Sakellariou, New York: Wiley, pp. 197-216. 2012

Kimball, Ezekiel W., Adam Moore, Annemarie Vaccaro, Peter F. Troiano, and Barbara M. Newman. "College students with disabilities redefine activism: self-advocacy, storytelling, and collective action." *Journal of Diversity in Higher Education*, vol. 9, no. 3, 2016, pp. 245-60.

Kranke, Derrick, Sarah E. Jackson, Debbie A. Taylor, Eileen Anderson-Fye, and Jerry Floersch. "College student disclosure of non-apparent disabilities to receive classroom accommodations." *Journal of Postsecondary Education and Disability*, vol. 26, no. 1, 2013, pp. 35-51.

Love, Tyler S., Nicole Kreiser, Elsa Camargo, Michael E. Grubbs, Eugin Julia Kim, Penny L. Burge, and Steven M. Culver. "STEM faculty experiences with students with disabilities at a land grant institution." *Journal of Education and Training Studies*, vol. 3, no. 1, 2015, 27-38.

Matthews, Nicole. "Teaching the 'invisible' disabled students in the classroom: disclosure, inclusion and the social model of disability." *Teaching in Higher Education*, vol. 14, no. 3, 2009, pp. 229-39.

Mingus, Mia. "Access intimacy, interdependence and disability justice" [blog post]. 2017. Accessed March 12, 2022 at <https://leavingevidence.wordpress.com/2017/04/12/access-intimacy-interdependence-and-disability-justice/>

Mitra, Sophie. "The capability approach and disability." *Journal of Disability Policy Studies*, vol. 16, no. 4, 2006, pp. 236-47.

National Center for Education Statistics. "Table 311.10. Number and percentage distribution of students enrolled in postsecondary institutions, by level, disability status, and selected student characteristics: 2015-2016 [Data table]." *Digest of Education Statistics*. U.S. Department of Education, Institute of Education Sciences, May 2018. Accessed March 20, 2022 at <https://nces.ed.gov/fastfacts/display.asp?id=60>.

Pratt, Mary Louise. "Arts of the contact zone." *Profession*, 1991, pp. 33-40.

Prendergast, Catherine. "On the rhetorics of mental disability." In *Embodied Rhetorics: Disability in Language and Culture*, edited by James C. Wilson and Cynthia Lewiecki-Wilson, Carbondale, IL: Southern Illinois UP, 2001, pp. 45-60.

Price, Margaret. *Mad at School: Rhetorics of Mental Disability and Academic Life*. Ann Arbor: U of Michigan P, 2011.

Price, Margaret. "Disability studies methodology." In *Practicing Research in Writing Studies: Reflexive and Ethically Responsible Research*, edited by Katrina Powell and Pamela Takayoshi, New York: Hampton, 2012, pp. 159-86.

Shakespeare, Tom. "The Social Model of Disability." *The Disability Studies Reader*, 5th ed., edited by Lennard Davis, Milton Park, Abingdon-on-Thames: Routledge, 2017, pp. 195-203.

Toutain, Christopher. "Barriers to accommodations for students with disabilities in higher education: a literature review." *Journal of Postsecondary Education and Disability*, vol. 32, no. 3, 2019, pp. 297-310.

Investigation of Manganese Nanoparticles with Various Capping Ligands and Their Effects on *Raphanus sativus*

Taytum Stratton,^{1,2} Elizabeth Pierce,¹ Christopher F. Monson¹

¹Southern Utah University, ²SUCCESS Academy

Abstract

*Nanoparticles have been studied in agriculture for their potential to mitigate abiotic stress in crops. Here, the use of manganese nanoparticles to increase stress tolerance in *Raphanus sativus* was investigated. Few studies have been conducted on the synthesis and uses of manganese nanoparticles. This study was among the first to synthesize manganese nanoparticles using a microfluidic device. Fluorescence spectroscopy and scanning electron microscopy were used to confirm that the particles synthesized were in the nanoscale size range. When foliarly applied to *R. sativus* that had been exposed to stress, the nanoparticles significantly increased growth rate, indicating an increase in stress tolerance. In addition, several other capping ligands were used for the manganese nanoparticles. FusionRed protein was expressed and purified in *Escherichia coli*. This protein, along with a Texas-Red labeled*

BSA protein, were successfully used as capping ligands for the manganese nanoparticles.

Introduction

Nanoparticles have physical and chemical properties that differ from those in bulk material and are therefore of great interest in many fields.¹⁻³ Although many studies work with copper, silver, and gold nanoparticles,^{1,2,4-7} there are few studies that have successfully synthesized manganese nanoparticles (MnNPs).⁸ This research investigated using a microfluidic device to synthesize MnNPs.

Microfluidic devices are instruments in which the flow regime can be controlled; they commonly take advantage of this property to use laminar and turbulent flow to precisely mix fluids.⁹⁻¹¹ Using a microfluidic device to synthesize nanoparticles is often more efficient than other methods of synthesis because small amounts of reagents are used, making it more cost effective, and it can create more uniform nanoparticles. There are several techniques that are commonly employed to fabricate microfluidic devices. The most common techniques use masters that are copied to form the microfluidic device.¹²⁻¹⁴ However, the microfluidic device used in this research was fabricated using a sacrificial method, which involves removing a prepositioned material to form channels in the device.¹³⁻²¹

Different capping ligands were used for synthesizing the MnNPs, including fluorescent proteins. Fluorescent proteins have a variety of uses and applications.²² FusionRed protein has been shown to be strongly monomeric and has low cytotoxicity, while other fluorescent proteins have a tendency to oligomerize and aggregate.²³ In this research, FusionRed protein was used as a capping ligand for MnNPs.

Nanoparticles have recently been applied to agricultural studies as a preventative measure against abiotic stresses in crops.²⁴ Manganese is an essential micronutrient found in crops because of its key role in photosynthesis²⁵ and in the antioxidant defense system.²⁶ In addition, use of nanoparticles for drug delivery²⁷ and delivery of gene editing technologies has been increasing.²⁸ In this paper, the ability of MnNPs to deliver Mn to plants was investigated.

Methods

Protein Expression and Purification

FusionRed protein was expressed in *Escherichia coli* (*E. coli*) from the plasmid FusionRed-pBAD, a gift from Michael Davidson (Addgene

plasmid #54677).²³ A glycerol stock of DH10 β *E. coli* transformed with FusionRed plasmid was made. An overnight liquid culture was grown, and the plasmid was recovered using GeneJET Miniprep Kit from Thermo Fisher. Restriction digest then gel electrophoresis were used to verify the plasmid. DH10 β *E. coli* colonies with FusionRed plasmid were grown on ampicillin plates, and flasks of LB medium with 1% arabinose were prepared and inoculated with *E. coli*. The cells were lysed, and the cell-free extract was collected. Nickel nitrilotriacetic acid chromatography was used to purify the protein.

Three buffer exchanges were performed. The buffers used were 20 mM tris-HCl and 50 mM NaCl (pH \approx 7.5), 20 mM tris-HCl (pH \approx 7.5), and 20 mM sodium phosphate (NaPi) and 50 mM NaCl (pH \approx 7.5). UV-vis spectroscopy was used to determine concentration, and gel electrophoresis was performed to determine purity.

In addition to the expression and purification of FusionRed, bovine serum albumin protein (BSA) labeled with Texas Red (TR) was prepared. BSA was labeled using TR-sulfonyl chloride, then purified using a size exclusion column.

Nanoparticle Synthesis and Characterization

MnNPs were synthesized using a microfluidic device. Manganese acetate (10 mM) was used as an ion source, sodium dithionite (15 mM) was used as source of oxide, and various capping agents were used including 20 mM oleic acid with 0.1 M NaOH, FusionRed in the three buffers, and TR-labeled BSA (TRBSA).

The nanoparticles were characterized using fluorescence spectroscopy, fluorescence microscopy, scanning electron microscopy (SEM), energy dispersive x-ray spectroscopy (EDS), and a titration. For the titration, 1 M HCl was used to titrate the MnNPs. HCl was added in 1- μ L additions, and the pH was measured with each addition of HCl.

Foliar Application of Manganese Nanoparticles to Raphanus sativus

The MnNPs capped with oleic acid were diluted with water and foliarly applied to *Raphanus sativus*. The plants were then put under a five-day drought stress. Stress tolerance of the plants was measured using growth rate and chlorophyll content.

The ability of MnNPs to deliver fluorescent proteins into the cell of the plant was also investigated. After foliarly applying the MnNPs to *R. sativus*, two samples from each plant were taken (control and plants treated with MnNPs capped with oleic acid (MnNP-oleic acid), MnNPs

capped with TRBSA (MnNP-TRBSA), and MnNPs capped with FusionRed (MnNP-FusionRed)), and one leaf from each plant was sonicated to rinse off any nanoparticles on the outside of the plant leaf. The other leaves were not rinsed to allow the comparison of the fluorescent proteins on the surface of the leaf versus the proteins in the inside of the cell. After washing (if applicable), the leaves were crushed in water using a mortar and pestle. The solution was filtered, then viewed under a fluorescence microscope with a three-second exposure using TR and fluorescein (FI) filters. The red fluorescence was measured over several days to determine if the protein made it into the plant cell.

Results and Discussion

The left panel of Figure 1 shows the gel of the purified plasmid. The restricted sample was about 5,000 bp, as expected. The right panel shows the gel for the purified protein. Three bands appeared for this protein. The protein was expected to be about 25 kDa, which is shown in the first band in lane 10. When the protein is expressed in *E. coli*, the protein can be cleaved forming two smaller proteins. This is likely where the 18-kDa band the 7-kDa band are coming from. Using UV-vis, it was determined that the protein was about 0.25 mg/mL.

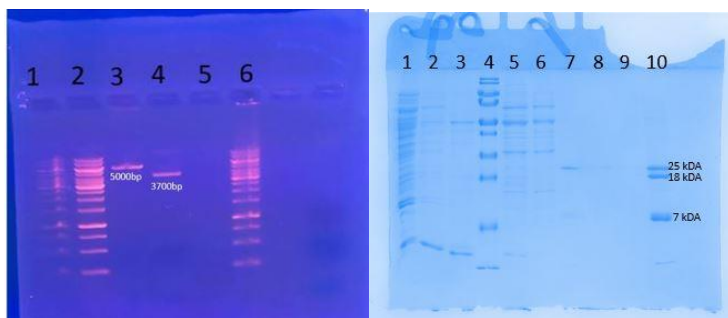


Figure 1: Gel of purified plasmid (left). Lane 1, 2, and 6 contain a DNA ladder. Lane 3 contains a sample after restriction digest. Lane 4 contains a sample before restriction digest. Gel of purified protein (right). Lane 4 contains a protein ladder, and lane 10 contains the protein that came off of the Ni-NTA column. The other lanes contain samples coming off the Ni-NTA column.

The first confirmation of nanoparticle formation was observed when the MnNPs were capped with oleic acid. In this case, none of the components used to make the nanoparticles were fluorescent, so the observation of fluorescence (Fig. 2A) strongly suggests the presence of nanoparticles. With these nanoparticles, because they were diluted

with water, the fluorescence blue shifted (Fig. 2A). This is likely because at high concentrations agglomerates of the nanoparticles formed, so the nanoparticles were acting as larger nanoparticles. As the MnNPs were diluted with water, the agglomerates broke up and a shift in fluorescence was seen. For the MnNPs capped with TRBSA, the fluorescence peaks of the protein were different than the peaks of the nanoparticles, suggesting that nanoparticles are present as shown in Figure 2B.

The MnNPs were also synthesized using FusionRed as a capping ligand, with the FusionRed suspended in three different buffers. Figure 2C shows the fluorescence spectra of the MnNPs capped with FusionRed. The 450-nm peak suggests that nanoparticles are present because the peaks in fluorescence of the FusionRed protein occur at about 400 nm and 610 nm. Because the fluorescence spectra were similar for all three buffers and the peaks occurred in the same places, the buffer did not appear to have an effect on nanoparticle formation.

SEM was used to characterize the nanoparticles. The left panel in Figure 3 shows the MnNPs capped with oleic acid. The nanoparticles formed were about 70 nm across and spherical in shape. The middle panel shows the MnNPs capped with TRBSA. A greater variety of shapes was observed, including nanosheets, with each sheet approximately 2- to 3- μm long and about 80- to 90-nm wide. As can be seen in the center panel of Figure 3, the nanosheets tended to aggregate into desert rose-like clusters. The right panel shows the MnNPs capped with FusionRed. FusionRed-capped MnNPs also formed sheets, which aggregated into larger and more complex desert rose-like clusters, approximately 10-20 μm across.

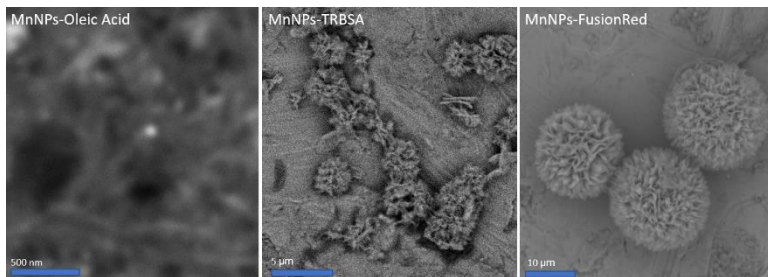


Figure 3: MnNPs capped with oleic acid (left), MnNPs capped with TRBSA (middle), and MnNPs capped with FusionRed (right) imaged on SEM.

Although we had confirmed the presence of nanoparticles, we had not yet determined the composition of these nanoparticles. The MnNPs could have been made of either manganese metal or manganese salt. If it

was a manganese salt, it could have been made of manganese dithionite, manganese oxide, manganese sulfide, or manganese sulfate (the latter anions can be produced by dithionite reactions). EDS data obtained using oleic acid-coated MnNPs (not shown) suggest that the MnNPs are composed of manganese oxide. There was a negligible amount of sulfur present, so the nanoparticles could not have been manganese dithionite, manganese sulfide, or manganese sulfate. According to EDS measurements, the manganese accounted for approximately $32.4 \pm 8.17\%$ (by mole) and the oxygen accounted for about $38.4 \pm 7.27\%$ (by mole) of the material on the surface. The approximately 1:1 manganese-to-oxygen ratio and the correlated location of the manganese and oxygen both suggest manganese oxide nanoparticles. Although the oxygen could have been present because of the oleic acid, this is likely not the case because little to no carbon was present, implying that the bulk of the nanoparticle was being measured and not a thin surface coating of oleic acid. Therefore, it is likely that the nanoparticles are composed of manganese oxide, most likely manganese(II) oxide, perhaps with some manganese(III) oxide.

MnNPs capped with both TRBSA and FusionRed protein were also analyzed by EDS (Fig. 4). As can be seen in the SEM image (top left), two types of features were present—desert rose shapes (center of SEM image) and other aggregates (left of SEM image). The desert rose shapes were determined to be MnNPs based on their containing significant amounts of manganese. The other aggregates contained carbon, oxygen, and nitrogen, but no manganese, and were thus identified as protein aggregates. The MnNPs were found to contain significant amounts of carbon (13%), oxygen (56%), and phosphorus (11%), and small amounts of sulfur (~1%), along with around 18 mole percent manganese.

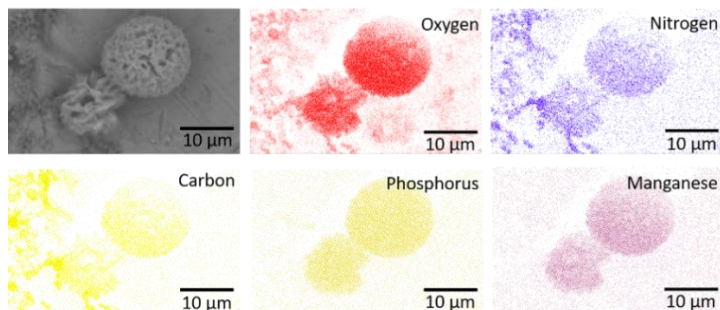


Figure 4: EDS data for FusionRed MnNPs. Top left, SEM image of desert rose clusters. Other panels: elemental data for the image. The desert rose clusters are MnNPs, while the other features to the left of the desert roses are protein aggregates.

Figure 5 further suggests that the MnNPs are made of manganese oxide. In the titration, two buffer regions were seen. The first buffer region occurred around pH 9.5, which was likely due to manganese oxide being present, suggesting that the nanoparticles are made of a manganese salt. The second buffer region occurred around pH 5.5, which likely occurred because oleate and acetate were present, as that is the approximate pKa of the carboxylic acid groups in those compounds.

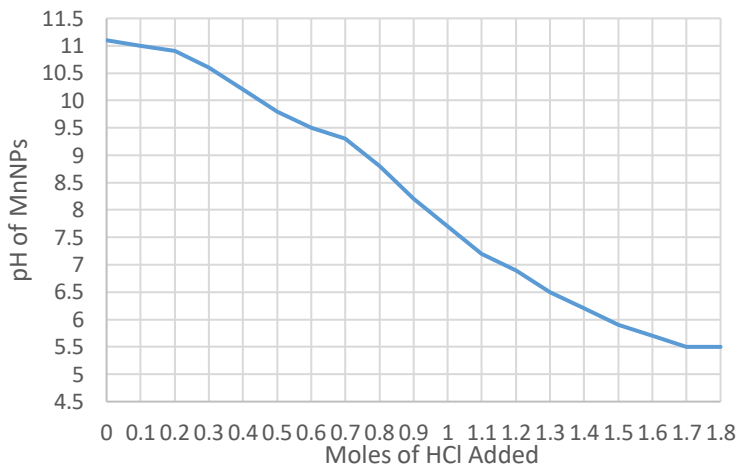


Figure 5: Titration curve of MnNPs capped with oleic acid.

The chlorophyll content was inconclusive in showing a change of stress tolerance in the radish plants after the MnNPs were foliarly applied. There was no significant increase or decrease in chlorophyll content. However, the radishes that were put under a drought and treated with MnNPs had a significantly higher growth rate than the control group of radishes put under drought stress, indicating that the MnNPs increased the stress tolerance of the radish plants, as shown in Figure 6.

The ability of MnNPs to deliver the fluorescent proteins into the plant cells was also evaluated. Over the course of four days after the nanoparticles were applied to the plants, there was no significant increase or decrease in red fluorescence in the leaves. Additionally, there were no significant differences in red fluorescence between the leaves that were rinsed and not rinsed. Finally, there was also no significant difference in red fluorescence in the plants treated with nanoparticles and the plants treated without nanoparticles. Thus, there was no observation of any

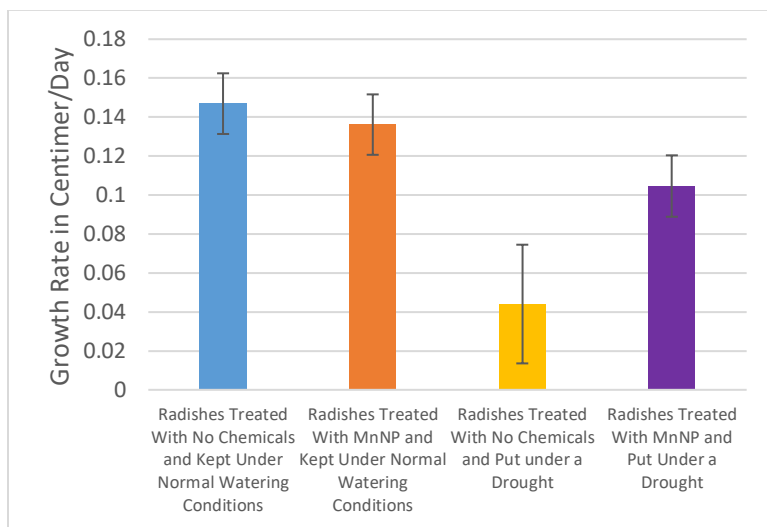


Figure 6: Average rate of change in height of radishes.

transport of proteins into plant cell using MnNPs, although it is possible that this was due to a relatively small sample size or protein degradation in the plant.

Conclusions

FusionRed protein was successfully expressed in *E. coli*, and manganese nanoparticles were successfully synthesized using FusionRed, TRBSA, and oleic acid as capping ligands. These manganese nanoparticles were found to be composed of manganese oxide. When they were applied to *R. sativus*, the growth rate of the plants increased, suggesting an increase in stress tolerance. In addition, the nanoparticles were applied to *R. sativus* to see whether the nanoparticles could be used to deliver the fluorescent proteins into a plant cell, and the data for this is currently inconclusive.

Acknowledgments

We thank the SUU College of Science, Physical Science Department, and Biology Department, who allowed us to use their facilities. We thank Dr. Matt Ogburn and Angela Patino-Acevedo, who assisted with the experimental work with plants. We also thank

Mackenzie Stratton and Kirby Stratton, who assisted with the experimental work with plants and nanoparticle synthesis.

References

- (1) Valodkar, M.; Modi, S.; Pal, A.; Thakore, S. Synthesis and anti-bacterial activity of Cu, Ag and Cu-Ag alloy nanoparticles: a green approach. *Mater Res Bull* **2011**, *46* (3), 384–389. <https://doi.org/10.1016/j.materresbull.2010.12.001>.
- (2) Li, Y.; Wu, Y.; Ong, B.S. Facile synthesis of silver nanoparticles useful for fabrication of high-conductivity elements for printed electronics. *J Am Chem Soc* **2005**, *127* (10), 3266–3267. <https://doi.org/10.1021/ja043425k>.
- (3) Chahar, M. A Review: The uses of various nanoparticles in organic synthesis. *J Nanomed Nanotechnol* **2020**, *11* (2), 543. <https://doi.org/10.35248/2157-7439.20.11.543>.
- (4) Yang, C.H.; Wang, L.S.; Chen, S.Y.; Huang, M.C.; Li, Y.H.; Lin, Y.C.; et al. Microfluidic assisted synthesis of silver nanoparticle–chitosan composite microparticles for antibacterial applications. *Int J Pharm* **2016**, *510* (2), 493–500. <https://doi.org/10.1016/j.ijpharm.2016.01.010>.
- (5) Hameed, M.; Panicker, S.; Abdallah, S.H.; Khan, A.A.; Han, C.; Chehimi, M.M.; Mohamed, A.A. Protein-coated aryl modified gold nanoparticles for cellular uptake study by osteosarcoma cancer cells. *Langmuir* **2020**, *36* (40), 11765–11775. <https://doi.org/10.1021/acs.langmuir.0c01443>.
- (6) Mariam, J.; Dongre, P.M.; Kothari, D.C. Study of interaction of silver nanoparticles with bovine serum albumin using fluorescence spectroscopy. *J Fluor* **2011**, *21* (6), 2193–2199. <https://doi.org/10.1007/s10895-011-0922-3>.
- (7) Wang, R.; Xu, Y.; Sors, T.; Irudayaraj, J.; Ren, W.; Wang, R. Impedimetric detection of bacteria by using a microfluidic chip and silver nanoparticle based signal enhancement. *Microchimica Acta* **2018**, *185* (3), 184. <https://doi.org/10.1007/s00604-017-2645-x>.

- (8) Bondi, J.F.; Oyler, K.D.; Ke, X.; Schiffer, P.; Schaak, R.E. Chemical synthesis of air-stable manganese nanoparticles. *J Am Chem Soc* **2009**, *131* (26), 9144–9145. <https://doi.org/10.1021/ja901372q>.
- (9) Raj M,K.; Chakraborty, S. PDMS microfluidics: a mini review. *J Appl Polym Sci* **2020**, *137* (27), 46958. <https://doi.org/10.1002/app.48958>.
- (10) Ma, J.; Lee, S.M.Y.; Yi, C.; Li, C.W. Controllable synthesis of functional nanoparticles by microfluidic platforms for biomedical applications—a review. *Lab Chip* **2017**, *17*, 209–226. <https://doi.org/10.1039/C6LC01049K>.
- (11) Hung, L.-H.; Lee, A.P. Microfluidic Devices for the Synthesis of Nanoparticles and Biomaterials. *J. Med Biol Eng* **2007**, *27* (1), 1-6.
- (12) Kim, B.; Oh, S.; You, D.; Choi, S. Microfluidic pipette tip for high-purity and high-throughput blood plasma separation from whole blood. *Anal Chem* **2017**, *89* (3), 1439–1444. <https://doi.org/10.1021/acs.analchem.6b04587>.
- (13) Eves, D.J.; Woolley, A.T. Phase-changing sacrificial layers in microfluidic devices: adding another dimension to separations. *Anal Bioanal Chem* **2009**, *393* (2), 431–435. <https://doi.org/10.1007/s00216-008-2408-y>.
- (14) Zhou, L.; Zhuang, G.; Li, G. A facile method for the fabrication of glass-PDMS-glass sandwich microfluidic devices by sacrificial molding. *Sens Actuators B* **2018**, *261*, 364–371. <https://doi.org/10.1016/j.snb.2018.01.158>.
- (15) Barney, J.; Torgersen, T.; Monson, C.F. A diffusion-limited titration using microfluidics. *J Utah Acad Sci Arts Lett* **2018**, *95*, 235–249.
- (16) Bellan, L.M.; Pearsall, M.; Crokek, D.M.; Langer, R. A 3D interconnected microchannel network formed in gelatin by sacrificial shellac microfibers. *Adv Mater* **2012**, *24* (38), 5187–5191. <https://doi.org/10.1002/adma.201200810>.
- (17) Golden, A.P.; Tien, J. Fabrication of microfluidic hydrogels using molded gelatin as a sacrificial element. *Lab Chip* **2007**, *7* (6), 720–725. <https://doi.org/10.1039/B618409J>.

- (18) Metz, S.; Jiguet, S.; Bertsch, A.; Renaud, Ph. Polyimide and SU-8 microfluidic devices manufactured by heat-depolymerizable sacrificial material technique. *Lab Chip* **2004**, *4* (2), 114–120. <https://doi.org/10.1039/B310866J>.
- (19) Kelly, R.T.; Li, Y.; Woolley, A.T. Phase-changing sacrificial materials for interfacing microfluidics with ion-permeable membranes to create on-chip preconcentrators and electric field gradient focusing microchips. *Anal Chem* **2006**, *78* (8), 2565–2570. <https://doi.org/10.1021/ac0521394>.
- (20) Peeni, B.A.; Lee, M.L.; Hawkins, A.R.; Woolley, A.T. Sacrificial layer microfluidic device fabrication methods. *Electrophoresis* **2006**, *27* (24), 4888–4895. <https://doi.org/10.1002/elps.200600399>.
- (21) Nguyen, D.T.; Leho, Y.T.; Esser-Kahn, A.P. Process of making three-dimensional microstructures using vaporization of a sacrificial component. *JoVE* **2013**, *81*, e50459. <https://doi.org/10.3791/50459>.
- (22) Chudakov, D.M.; Matz, M.V.; Lukyanov, S.; Lukyanov, K.A. Fluorescent proteins and their applications in imaging living cells and tissues. *Physiol Rev* **2010**, *90* (3), 1103–1163. <https://doi.org/10.1152/physrev.00038.2009>.
- (23) Shemiakina, I.I.; Ermakova, G.V.; Cranfill, P.J.; Baird, M.A.; Evans, R.A.; Souslova, E.A.; et al. A monomeric red fluorescent protein with low cytotoxicity. *Nat Comm* **2012**, *3*, 1204. <https://doi.org/10.1038/ncomms2208>.
- (24) Fraceto, L.F.; Grillo, R.; de Medeiros, G.A.; Scognamiglio, V.; Rea, G.; Bartolucci, C. Nanotechnology in agriculture: which innovation potential does it have? *Front EnvSci* **2016**, *4*, 20. <https://doi.org/10.3389/fenvs.2016.00020>.
- (25) Messant, M.; Hennebelle, T.; Guérard, F.; Gakière, B.; Gall, A.; Krieger-Liszkay, A. Manganese excess and deficiency affects photosynthesis and metabolism in *Marchantia polymorpha* bioRxiv <https://doi.org/10.1101/2022.01.24.477552>.

- (26) Morgan, M.J.; Lehmann, M.; Schwarzländer, M.; Baxter, C.J.; Sienkiewicz-Porzucek, A.; Williams, T.C.R.; et al. Decrease in manganese superoxide dismutase leads to reduced root growth and affects tricarboxylic acid cycle flux and mitochondrial redox homeostasis. *Plant Physiology* **2008**, *147* (1), 101–114. <https://doi.org/10.1104/pp.107.113613>.
- (27) Patra, J.K.; Das, G.; Fraceto, L.F.; Campos, E.V.R.; Rodriguez-Torres, M.D.P.; Acosta-Torres, L.S.; et al. Nano based drug delivery systems: recent developments and future prospects. *J Nanobiotech* **2018**, *16*, 71. <https://doi.org/10.1186/s12951-018-0392-8>.
- (28) Duan, L.; Ouyang, K.; Xu, X.; Xu, L.; Wen, C.; Zhou, X.; et al. Nanoparticle delivery of CRISPR/Cas9 for genome editing. *Front Genet* **12**, 673286. <https://doi.org/10.3389/fgene.2021.673286>.

Creating a Map for Quantum Teleportation Protocols

Aidan Gillam and Jean-François Van Huele
Brigham Young University

Abstract

Quantum teleportation is a powerful example of current quantum technology. It allows a quantum state to be communicated from one location to another without physically transporting the physical system that encodes the state. Since the original conception of quantum teleportation, many protocols that utilize different resources have been designed to teleport quantum information. We present a map of teleportation protocols that organizes them by five degrees of freedom. By searching this map, we find and then present a new teleportation protocol, namely the teleportation of a three-qubit state with two Bell pairs under short-distance scenarios.

Introduction to Quantum Information

Quantum information is the information that is contained within a quantum state. Quantum information science seeks to understand, analyze, and process this information using the laws of quantum mechanics. The simplest quantum state that contains quantum

information can produce one of two outcomes when a measurement is performed on it. Quantum computers are devices built to store, manipulate, and measure such simple quantum states.

The theory and techniques of quantum computation differ substantially from how traditional computers process information. These traditional computers use laws of classical physics—especially electricity and magnetism—to analyze and process information. Quantum computers use quantum mechanics as well to process information, incorporating the superposition of states found in quantum systems as well as the phenomenon of entanglement—a type of correlation to which there is no true classical analog—to solve specific problems in a fashion which traditional computers cannot imitate efficiently. The state of maximum entanglement between two quantum states is the most commonly used entanglement resource in quantum computing and is called a Bell state.

Where classical computers use bits as the basic unit of information processing, quantum computers use quantum bits, or qubits. Qubits differ from classical bits in some important ways. Classical bits can have one of two states: 0 or 1. Operations, or gates, can be performed on a bit to change it from one state to the other, but a bit only ever exists as either 0 or 1. Laws of uncertainty and superposition in quantum mechanics cause the qubit to behave differently. One can only know the probability that measuring a qubit will result in a 0 or a 1. These two outcomes correspond to the computational basis states $|0\rangle$ and $|1\rangle$ for qubits. A qubit $|\varphi\rangle$ in a linear vector space can be expressed mathematically as $|\varphi\rangle = a|0\rangle + b|1\rangle$, where the complex numbers a and b satisfy $|a|^2 + |b|^2 = 1$.

Within a quantum computer we can manipulate the state of a qubit with quantum operators, also known as quantum gates. Qubits can also be made to change conditionally on the current state of another qubit. The most widely used model for the representation of the operations of a quantum computer is the quantum circuit model (Nielsen & Chuang 2011).

Some of the possible single qubit operations are the Pauli-X gate (X), the Pauli-Z gate (Z), and the Hadamard gate (H). The Pauli-X gate swaps the coefficients a and b in the state of a qubit $a|0\rangle + b|1\rangle$. It is sometimes called the quantum NOT gate, or just the NOT gate when referring to quantum circuits. The Pauli-Z gate has the effect of introducing a negative sign in front of the b in the qubits state $a|0\rangle + b|1\rangle$, causing the state to become $a|0\rangle - b|1\rangle$.

The Hadamard gate H plays an important role in quantum computers. It transforms each of the basis states into a superposition:

$$H : |0\rangle \rightarrow \frac{1}{\sqrt{2}} (|1\rangle + |0\rangle), \quad H : |1\rangle \rightarrow \frac{1}{\sqrt{2}} (|1\rangle - |0\rangle)$$

The only two-qubit gate that is needed for any quantum circuit is the Controlled-NOT (C-NOT) gate. The C-NOT gate performs the Pauli-X operation on the target qubit if and only if the control qubit is $|1\rangle$ and leaves the target qubit unchanged otherwise. There are other multi qubit quantum gates, but they can all be decomposed using a series of single qubit gates and the C-NOT gate. For this reason, the C-NOT gate is known as the universal two-qubit gate.

In Fig. 1, we illustrate an important quantum circuit. Each horizontal line represents a qubit, and time passes as you move from the left to the right. The input states for each qubit are shown on the left of the circuit, and the final combined output state is shown at the right. It is standard protocol for the input states to be the same, usually the computational basis state of $|0\rangle$. Boxes that appear on individual lines represent quantum gates that cause a change to occur for the qubit whose line it is on. The C-NOT gate is represented by a vertical line with circles on both ends that connects two qubits. One qubit has a dark circle on it; this is the control qubit. The other qubit has a reticle; this is called the target qubit. When the Hadamard gate is applied to a qubit and followed by a C-NOT gate where the qubit that just had the Hadamard gate applied to it is the control qubit, a Bell state is created between the two qubits. This is the combined state that is shown at the right of the circuit diagram. A two-qubit system has four computational basis states, constructed from the basis states of the one-qubit states and denoted as $|00\rangle, |01\rangle, |10\rangle, |11\rangle$. Alternatively, one can use four Bell states to construct the Bell basis for two-qubit systems.

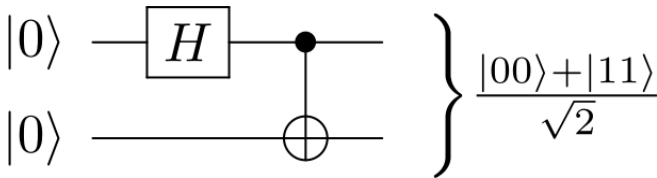


Figure 1. A simple quantum circuit consisting of a Hadamard gate and a C-NOT gate. This circuit creates a Bell state.

We can also include a measurement in a quantum circuit diagram. Measurements appear as a meter with an arrow, as in Fig. 2. A measurement of a qubit results in the superposition of states of the qubit to collapse, ending the life of the qubit and resulting in one of the qubits computational basis states being measured. The double lines associated

with a measurement that are seen in Fig. 2 represent a classical bit of information being sent that encodes the result of the measurement; whether a $|0\rangle$ or a $|1\rangle$ was measured.

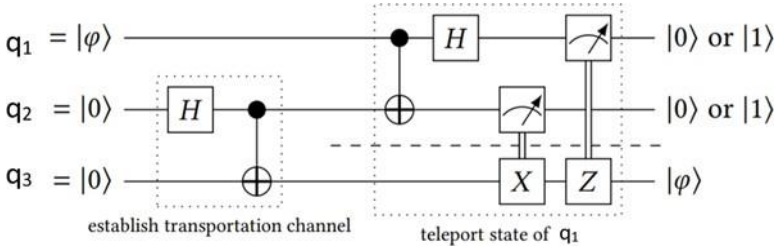


Figure 2. Circuit diagram for quantum teleportation. Adapted from Hillmich et al. (2020).

There are other ways for quantum states to be entangled that are qualitatively different from the entanglement associated with Bell states. The Greenberger–Horne–Zeilinger (GHZ) state (Greenberger et al. 1989) generalizes the type of entanglement for a two-qubit entangled state to n states. So, the GHZ state represents the state of maximal entanglement that an n -particle system can be in.

The Teleportation Protocol

A means of communicating quantum information known as quantum teleportation was discovered by Charles Bennett in the 1990s (Bennett et al. 1993). Quantum teleportation allows any quantum state to be communicated from one location to another without physically transporting the physical system that encodes this information. The following resources are required to accomplish quantum teleportation: a qubit to be teleported; the ability to create and distribute a Bell state; the ability to perform Bell measurements (Nielsen & Chuang 2011) on the joint state of 1) one half of the Bell pair and 2) the state to be developed; a way to send two bits of classical information; and the ability to apply quantum gates—or operations that change the state of a quantum system in a predictable way—on the other qubit in the Bell pair.

With these resources, the protocol for quantum teleportation can be broken down into four steps.

1. A Bell state is created between two qubits. One of each of the members of this Bell state is given to the sending party (called Alice) and the receiving party (called Bob).

2. Alice performs a Bell measurement on her half of the Bell pair and the quantum state that she would like to teleport to Bob. The Bell basis has four possible outcomes to this joint measurement; the result can thus be encoded in two bits of classical information to be sent to Bob. At this point, the measured qubits have no more use and can be discarded.
3. The two bits of classical information are sent to Bob.
4. Because of the entangled nature of the Bell state, after Alice performs her measurement, Bob's half of the Bell state is now in one of four possible states that are related to the original quantum state. One of these possible states is identical to the original; the other three are related to it by a known transformation. Using the information sent from Alice as to which state she measured, Bob can know the identity of the qubit that is in his possession and apply the appropriate transformation to retrieve the state that Alice wished to teleport to him.

It is important to differentiate quantum teleportation from the type of teleportation that has become popularized from TV and movies. Quantum teleportation cannot be used to send matter or energy but only to send the quantum information attached to a quantum state. In this way, teleportation is more of a form of communication than it is a form of transportation. The speed of teleportation is also limited by the speed of light because of the need to send two bits of classical information.

Shown in Fig. 2 is the circuit diagram for standard quantum teleportation. The input states are shown on the left. The qubit q_1 is being sent from Alice to Bob. This quantum state has the form

$$q_1 = |\varphi\rangle = a|0\rangle + b|1\rangle \quad (2)$$

The other qubits, q_2 and q_3 , are used to create a Bell state and are initialized in the $|0\rangle$ computational basis state. There is a dotted square around the Hadamard gate and C-NOT gate that connects q_2 and q_3 . These operations create a Bell state between those two qubits, which allows for a quantum channel to be established between the two parties. One half of this Bell pair goes with Alice and the other with Bob. The dotted line in the circuit diagram illustrates a separation in space between Alice and Bob. This separation in space is a physical distance long enough that a C-NOT gate cannot be applied between qubits on opposite sides of the dotted line. The second dotted box contains the gates and measurements that constitute the Bell measurement performed by Alice and the sending of classical bits of information to Bob. This is the step in which the teleportation of the state of q_1 is accomplished. The resulting output states are shown at the right of the circuit. We can see that q_3 , which has always

remained in Bob’s possession, now has the state of the qubit that was originally in Alice’s possession.

The most complete description of the system before Alice’s Bell measurement is

$$|\phi_{123}\rangle = \frac{1}{2} [|\Psi_{12}^-\rangle (a|1_3\rangle - b|0_3\rangle) + |\Psi_{12}^+\rangle (a|1_3\rangle + b|0_3\rangle) + |\Phi_{12}^-\rangle (a|0_3\rangle - b|1_3\rangle) + |\Phi_{12}^+\rangle (a|0_3\rangle + b|1_3\rangle)] \tag{3}$$

where $|\Psi^{+/-}\rangle$ and $|\Phi^{+/-}\rangle$ are the Bell states given by

$$|\Phi^+\rangle = \frac{1}{\sqrt{2}} (|00\rangle + |11\rangle) \tag{4}$$

$$|\Phi^-\rangle = \frac{1}{\sqrt{2}} (|00\rangle - |11\rangle) \tag{5}$$

$$|\Psi^+\rangle = \frac{1}{\sqrt{2}} (|01\rangle + |10\rangle) \tag{6}$$

$$|\Psi^-\rangle = \frac{1}{\sqrt{2}} (|01\rangle - |10\rangle) \tag{7}$$

and the indices 1, 2, and 3 refer to the three qubits of the teleportation circuit.

From Eq. (3), we can see what state Bob will have. The state in Bob’s possession q3 is correlated with the state that Alice measures; that is, the joint Bell state for qubits q1 and q2. For example, if Alice’s joint measurement leaves her with $|\Phi_{12}^-\rangle$, then the state of the qubit in Bob’s possession will be $|\phi_3\rangle = a|0_3\rangle - b|1_3\rangle$. This differs from the original state just by a negative sign in front of the b, which corresponds to the matrix transformation in the first row of Table 1.

Table 1 Teleportation transformations for teleportation with a $\Phi^+\rangle$ Bell state	
Alice’s measurement	Transformation
$ \Psi^-\rangle$	$\begin{bmatrix} 1 & 0 \\ 0 & -1 \end{bmatrix}$
$ \Phi^-\rangle$	$\begin{bmatrix} 0 & 1 \\ -1 & 0 \end{bmatrix}$
$ \Phi^-\rangle$	$\begin{bmatrix} 0 & 1 \\ 1 & 0 \end{bmatrix}$
$ \Phi^+\rangle$	$\begin{bmatrix} 1 & 0 \\ 0 & 1 \end{bmatrix}$

Alice will measure one of the four Bell states from her joint measurement. The result will correspond to the transformations shown. If decided beforehand what matrix corresponds to what measurement outcome, Alice can inform Bob what transformation to apply to his state with just two classical bits.

Table 1 shows the transformations needed for all four possible outcomes of the joint measurement. With two bits of classical information, four messages can be sent (00, 01, 10, and 11). Since there are four outcomes, if Alice and Bob agree beforehand which message corresponds to which measurement outcome, then Bob can obtain the information needed to perform the appropriate transformation on his state and come into possession of the state $|\varphi\rangle$ that was initially in Alice's possession if he is sent two classical bits of information from Alice. Thus, the state has been teleported from Alice to Bob by utilizing both classical and entanglement channels.

We have just illustrated the standard teleportation protocol. From here a variety of new teleportation protocols have been proposed. These protocols involve varying numbers of qubits to be teleported and various entanglement resources to enable the teleportation. Each also comes with its own possibilities of circuitry design. The common feature among these protocols is the teleportation of at least one qubit from one physical particle to another without the need to physically move the particle to which the qubit is attached.

A way has been found to teleport an arbitrary two-qubit state via a single Bell pair given short-distances (Tan & Han 2021). "Short-distances" in this protocol references how Bob needs to take into his possession a qubit on which Alice performs a C-NOT operation with one of her qubits. Therefore, both Alice and Bob must be able to interact with this qubit, which limits the distance they can be from each other.

What makes each teleportation protocols unique? Why were they not all uncovered in the first decade after the discovery of quantum teleportation? It is in part the fact that each has particular conditions or circumstances under which they can be incorporated. For example, distance limitations exist for the accomplishment of the teleportation of a two-qubit state with a single Bell pair. One is left to wonder if there isn't a more systematic way of discovering teleportation protocols.

Teleportation Degrees of Freedom

One way to facilitate discovery is to map out what is already known. Maps and charts play an important role in organizing scientific facts and deriving new properties. As an example, in chemistry, the periodic table of the elements was formulated to organize a large amount of data relating to existing atoms. As the periodic table was developed, gaps were found where yet undiscovered elements were suspected to exist. The prime example is the element gallium, which Dmitri Mendeleev predicted in 1871 after publishing the first early prototype of the modern periodic table of the elements.

Mendeleev considered what degrees of freedom (DOFs)—independent pieces of information—uniquely identified the elements. An understanding of these could motivate the organization of the elements into a table or chart. He first organized the elements by mass. He also found that some of the elements had chemical similarities and reacted similarly to other elements and that there was a pattern in the occurrence of these trends. He was the first to organize the elements into a table with gaps left for predicted elements that had not yet been discovered. By doing so, he helped chemistry advance significantly.

An attempt to organize existing teleportation protocols into a table or map gives further insight into what possibilities exist in quantum teleportation. The relevant question in creating a map of teleportation is thus “what DOF exist that uniquely identify teleportation protocols?” By identifying these DOF, we can construct a map that illustrates trends and may reveal insights to the science of quantum teleportation in a similar fashion as the periodic table did for chemistry.

The number of qubits teleported is our first DOF (DOF1). Each protocol could always be repeated to teleport a multiple number of qubits. But this is simply a matter of repetition. However, some unique methods of teleportation involve the teleportation of multiple qubits, such as the protocol that involves the short-distance teleportation of a two-qubit state with a single Bell pair. The minimum number of qubits teleported for a unique protocol is therefore the first piece of information that qualifies as a DOF.

A second DOF (DOF2) is how many quantum computer qubits are needed to accomplish the teleportation. For example, both teleportation with a Bell state and with a GHZ state involve the teleportation of a single qubit, but the GHZ state teleportation involves four quantum computer qubits compared with the three that are needed in the standard teleportation protocol that uses a Bell state. Also the short-distance teleportation of a two-qubit state with a single Bell pair protocol teleports two qubits with a total of five quantum computer qubits. Not all teleportation types are as efficient given the amount of qubits they require, but they all have other unique attributes that could make them useful.

The amount of classical information that must be communicated through a classical channel for the teleportation to take place is a third important DOF (DOF3) that varies from protocol to protocol. In general, for every joint measurement of two qubits that Alice performs, she must convey two bits of classical information to Bob to complete the teleportation. But there is at least one protocol that promises teleportation with less than perfect probability while only conveying a single bit of classical information (Parakh 2021).

The number of single-qubit quantum gates, the number of multi-qubit quantum gates, and their organization in a quantum circuit to accomplish teleportation are all important DOF to consider. Some teleportation protocols belong to the same classification according to the previously mentioned DOF (qubits teleported, number of quantum computer qubits, and number of classical bits of information sent), but vary considerably in their use of quantum gates. This use and organization of quantum gates can be grouped into a single DOF (DOF4), which we can call the “specifics of the quantum circuitry” for the protocol.

Our last two DOFs for teleportation are the type of entanglement resource used in the teleportation protocol (DOF5) and the number of that entanglement resource needed (DOF6). The types of entanglement resources include, but are not limited to, Bell states and GHZ states.

All of the teleportation protocols can be uniquely identified and described using the DOF described in this section. The question becomes: “Having found the degrees of freedom, can we organize or map teleportation protocols to present the information in a way that reveals trends and undiscovered teleportation protocols?”

The Map of Teleportation

In this section, we present a map of teleportation that categorizes teleportation protocols by their DOFs. We present in Fig. 3 a first attempt of organizing teleportation protocols. We use five of the six DOFs for teleportation described in the previous section. The DOF that is not included is that for the specifics of the quantum circuitry. This DOF is the most difficult to convey on a two-dimensional map, because each space could require a quantum circuit diagram to illustrate its quantum circuitry design. Because all of the teleportation protocols we consider can be uniquely identified without considering this DOF, it is not included at present.

Fig. 3 contains a lot of information, so we will walk the reader through its interpretation and use. In Fig. 3, there are two DOF on the x -axis and three on the y -axis. The primary x -axis records the total number of qubits that will be teleported (DOF1). The sub x -axis records how many quantum computer qubits are needed to teleport the number of qubits indicated by the primary x -axis (DOF2). The primary y -axis tells the type of quantum resource used (DOF5), the sub y -axis tells the number of the quantum resource needed (DOF6), and the sub-sub y -axis tells the total number of classical bits of information needed (DOF3). Note again that there is no description of the specifics of the quantum circuitry design (DOF4).

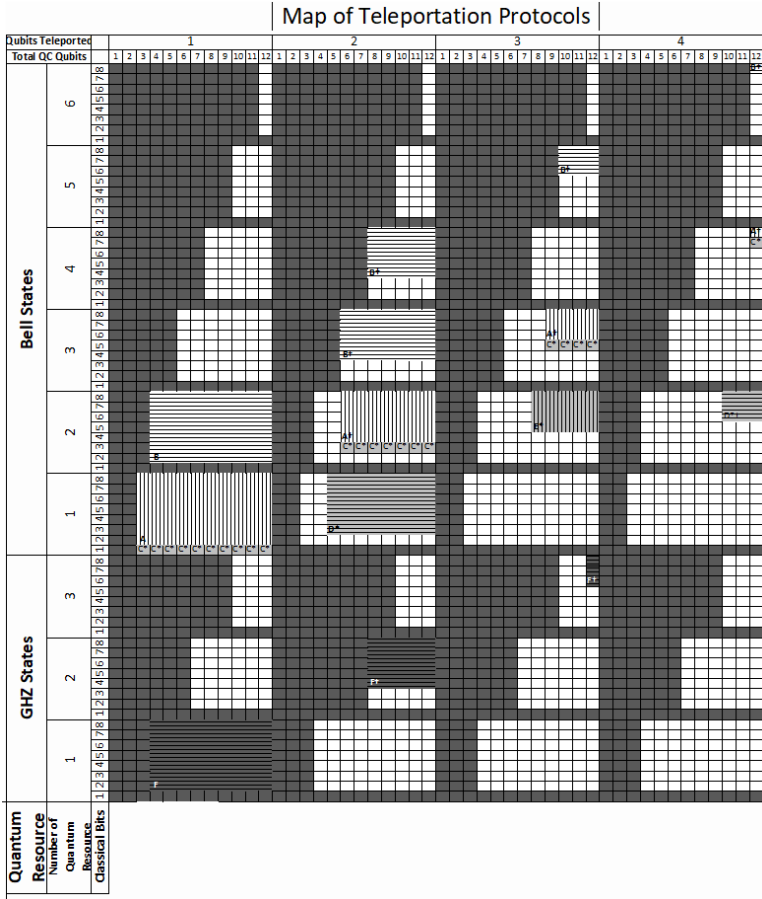


Figure 3. Map of teleportation protocols.

After the layout of this table was designed, some spaces were quickly identified as being illogical spaces for teleportation to take place. The number of qubits teleported must not be more than the total number of quantum computer qubits needed. Also, the number of classical bits of information needed to perform a teleportation must (in general) be greater than or equal to the number of qubits that a measurement is performed on at the end of the protocol. These illogical spaces were filled in with a patternless dark gray color, as no useful protocol can arise from them.

Now we place the original teleportation protocol onto the map. This protocol will be placed and described thoroughly here to aid the

reader in interpreting the map. The letter “A” placed on the map indicates the standard teleportation protocol. We can confirm this by checking the values given by the x and y axes. We see from the x axes that one qubit is teleported and three quantum computer qubits are needed. We see from the y axes that the quantum resource is a Bell state, one Bell state is required, and two bits of classical information are needed. These correctly identify Bennett’s teleportation protocol. The dagger ‘†’ attached to all but the leftmost “A” as well as on other letters indicate that the protocol is duplicated more than one time to fill that space on the table. So, by checking the resources needed for the first A† further to the right of “A” on the x axis than “A,” we will see that all the resources needed for “A” are doubled for it. Patterned spaces without a letter represent spaces in which the teleportation protocol of the same pattern that is marked with a letter can occur there with some leftover resources. These might be called the “inefficient” spaces. For example, standard teleportation can of course be used to teleport a single qubit with three quantum computer qubits, one Bell pair, and three classical bits of information. But one of these bits of classical information is not needed at all to accomplish the task, and so within that space it is possible with unused and leftover resources.

Next, some existing teleportation protocols were placed in their appropriate positions on the table. “B” indicates a type of standard teleportation, where part of a Bell pair is teleported. The protocol is the same as for “A,” but the result is the teleportation of part of a Bell pair. “C” is where teleportation with a single classical bit exists (Parakh 2021). The asterisk * indicates that special conditions, not indicated explicitly on the chart, apply. “D” places the protocol from “Short-Distance Teleportation of an Arbitrary Two-Qubit State via a Bell State” (Tan & Han 2021). “E” is the protocol of “short-distance teleportation of an arbitrary three-qubit state via two Bell states,” which is proposed in this paper and described in the next section. “F” indicates teleportation of a quantum state via a GHZ state. The legend that identifies these teleportation protocols is shown in Fig. 4.

Symbol and Pattern Legend For Teleportation Map		
†	Indicates the protocol has been done a multiple number of times to fill those spaces	B: A type of classical teleportation, where part of a Bell pair is teleported
*	Indicates special conditions not shown by the chart may apply	C*: Teleportation with 1 classical bit
White cells	White cells indicate teleportation may be feasible, but hasn't been searched.	D*: Short distance teleportation of an arbitrary two-qubit state via a Bell State.
Dark gray cells	Dark gray cells indicate teleportation is unfeasible	E*: Short distance teleportation of an arbitrary three-qubit state via two Bell-states
A	Classical teleportation	F: Teleportation of an unknown state via a GHZ state

Figure 4. Legend for Fig. 3.

One objective of creating this map of teleportation is to identify spaces for teleportation that can be filled but for which a protocol has not yet been proposed. Identifying trends in the map could aid in accomplishing this objective. By considering the trends for “A” (standard teleportation), “B” (standard teleportation of Bell pair members), and “F” (teleportation using a GHZ state), we investigate whether a trend could exist with less triviality among any of the other protocols.

Protocol “D” (short-distance teleportation of a two-qubit state with a single Bell pair) falls within the domain of the map (Bell state or GHZ quantum resources) where the patterns in “A,” “B,” and “F” are observed. This protocol teleports a two-qubit state with just one Bell pair, given short-distance scenarios. Duplicating this protocol could be done, but a unique teleportation protocol possibility is also identifiable; the teleportation of a three-qubit state with two Bell pairs. We discuss this in the next section.

Teleportation of a Three-qubit State With Two Bell Pairs Under Short-distance Scenarios

The paper “Short-Distance Teleportation of an Arbitrary Two-Qubit State Via a Bell State” (Tan & Han 2021) showed how under short-distance scenarios a two-qubit state can be teleported by utilizing a single Bell pair. Short-distance protocols use an auxiliary qubit that is to be shared between Alice and Bob. Whether this protocol could be extended to teleport larger numbers of qubits while minimizing quantum resources was not presented in this paper. We decided to investigate the question “can a three-qubit state be teleported with two Bell pairs under short-distance conditions?” where short-distance indicates the ability for both Alice and Bob to be within reach of certain qubits throughout the entire process. This means they both can perform C-NOT operations on those qubits that are close to both of them with qubits that are in their own possession.

With the map of teleportation appropriately organized, we considered whether there are spaces within the map in which a three-qubit state could be teleported with just two Bell pairs under short-distance conditions. To be possible, the total number of quantum computer qubits would have to increase from the five that are needed to teleport a two-qubit state with a single Bell pair to eight. One additional qubit is needed for the third qubit in the three-qubit state, and two more qubits are needed to accommodate the second Bell pair. So within the map of teleportation, one knows to look for this space on the x-axis at the two qubits teleported column and at the eight qubits or more location

on the sub x-axis. One also knows that they are looking at a space where two Bell pairs are used. One could logically guess that five classical bits of information will be needed to complete this teleportation. From this, we could create a schematic for the protocol that teleports a three-qubit state with two Bell pairs. Fig. 5 illustrates that Alice is in close proximity to the qubits 1, 2, 3, 4, 6, and 8. Bob is in close proximity to qubits 5, 7, and 8. This is what the two large ovals indicate. They group together the qubits that are close to Alice and those that are close to Bob. Qubits 1, 2, and 3 denote the qubits that are to be teleported from Alice to Bob. The dots with dotted lines connecting them denote the Bell pairs. Qubit 8 represents an auxiliary qubit, shared by Alice and Bob. After the teleportation is accomplished, qubits 5, 7, and 8 will now be identical to what qubits 1, 2, and 3 originally were.

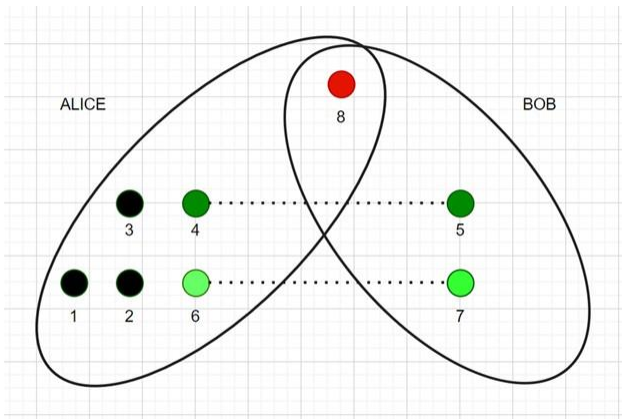


Figure 5. Schematic for the teleportation of a three-qubit state with two Bell pairs under short-distance scenarios. Shaded circles indicate qubits. The large ovals indicate which qubits are close to the two parties (Alice and Bob). The black qubits indicate the three-qubit state to be teleported from Alice to Bob. The qubits attached by a dotted line are Bell pairs (different shades of for different Bell pairs). Qubit 8 represents the auxiliary qubit, which is close to both Alice and Bob. After the teleportation is accomplished qubits 5, 7, and 8 will contain the three-qubit state initially held by 1, 2, and 3.

From this schematic and reasoning from the previous paragraph, one can place this protocol onto the map of quantum teleportation. It is marked with the letter “E” and shaded light gray with vertical lines going through its spaces. Like all the protocols that have come before, this protocol can be described by a quantum circuit diagram, and one should be able to show mathematically that the circuit is physically possible.

The quantum circuit diagram for the short-distance teleportation of a three-qubit state with just two Bell pairs is presented in Fig. 6. One can show that the circuit does indeed lead to the desired teleportation and is an extension of the circuit discussed in Tan & Han (2021).

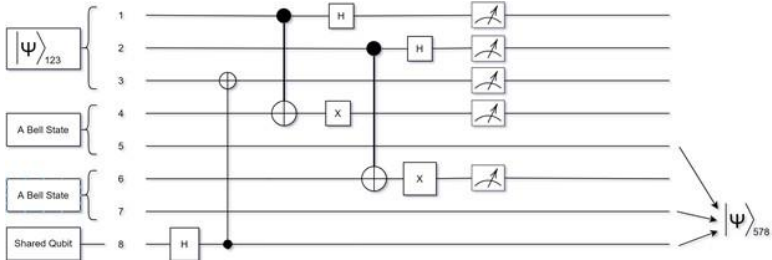


Figure 6. The circuit diagram for the teleportation of a three-qubit state with two Bell pairs under short-distance scenarios.

This is the first instance of the map of teleportation in Fig. 3 having predictive power to identify yet unidentified spaces where teleportation can take place.

Discussion, Further Work, and Conclusion

A viable space for the teleportation of a three-qubit state under short-distance situations was discovered, in part by the consideration of its possible placement on the map of teleportation. A quantum circuit was proposed, and checking the circuit gives promising results that the circuit is valid for the teleportation of a three-qubit state using two Bell pairs under short-distance scenarios. The discovery of this protocol indicates that by considering the DOF of teleportation for particular protocols, new spaces for teleportation can be discovered.

The discovery of the three-qubit state teleportation with two Bell states under short-distance scenarios immediately motivates the question as to whether a four-qubit state could be teleported with three (or even with two) Bell pairs. From the map of teleportation, it is obvious that a duplication of the two-qubit state teleportation protocol would result in the teleporting of two two-qubit states with two Bell pairs under short-distance scenarios. But is this different from teleporting a four-qubit state, rather than two two-qubit states? Further research is needed to give an unambiguous answer to this question.

The map from Fig. 3 has the strength of showing trends for individual teleportation protocols. It has the weakness of containing no information concerning the particulars of each specific protocols,

including the quantum gates needed for each protocol and the circuitry design. Additionally, many existing quantum teleportation protocols have not been considered and placed on this map yet. Many more could be included, and as this is done, more patterns may emerge and more intuitive or appealing design schemes may become apparent. Just as the periodic table changed over the course of 100 years as discoveries were made and appropriate changes were implemented, we imagine that this teleportation map will evolve into a more complete and useful version. In particular, one might consider developing an interactive or dynamical version of this map.

The map of Fig. 3 describes theoretically perfect protocols. No noise enters through the use of quantum gates and teleportation fidelity is 100%, save the protocols, which themselves have a less than unitary probability of occurring (as in teleportation using a single classical bit). It could be a useful project to consider the real world cases where noise exists, and consider whether the map would change in these instances.

Just as the periodic table of the elements aided scientists and students within the field of chemistry, a map of teleportation like the one presented herein could aid those interested in quantum teleportation topics. Patterns are revealed that show resources needed to teleport multiple qubits with varying teleportation protocols. Experimentalists could also see what minimum resources are needed to accomplish different teleportation protocols in the laboratory. The map gives a bird's-eye view of the possibilities and extend of teleportation and may inspire others to develop new protocols and enhance the applicability and reach of teleportation technology.

Bibliography

Bennett, C.H., Brassard, G., Crepeau, C., Jozsa, R., Peres, A., & Wootters, W.K. 1993, *Physical Review Letters*, 70(13), 1895-1899

Greenberger, D.M., Horne, M.A., & Zeilinger, A. 1989, In *Bell's Theorem, Quantum Theory, and Conceptions of the Universe* (ed. M. Kafatos). Kluwer Academic (Dordrecht, The Netherlands), 73-76

Hillmich, S., Zulehner, A., & Wille, R. 2020, arXiv:2011.07314

Nielsen, M.A., & Chuang, I.L. 2011, *Quantum Computation and Quantum Information: 10th Anniversary Edition*. Cambridge University Press (New York)

Parakh, A. 2021, arXiv:2110.11254

Tan, X.-D., & Han, J.-Q. 2021, International Journal of Theoretical Physics, 60(4), 1275-1282

Tupac Shakur and Kendrick Lamar: A Legacy of Hip Hop Resistance

Theresa A. Martinez

University of Utah

Abstract

From its very beginnings in the 1970s, rap music has reflected the profound disenfranchisement of African Americans living in the nation's neglected and abandoned inner cities. Rap was only one aspect of hip hop that emerged in the South Bronx in that time period—along with graffiti and breakdancing, among others. Rap could be playful, catchy, sexy, and humorous, but it also intoned a forceful cultural critique of ongoing and horrendous disparities facing Black communities, including police violence, systemic inequity in the criminal justice system, housing discrimination, and educational disparity. This paper focuses on a lyrical and thematic analysis of the work of two hip hop artists—one legendary artist from the 1990s and one contemporary hip hop artist who is already making a sizable mark on the genre—as they reflect on and unpack the sociohistorical contexts of their times. The paper unpacks the lyrics of our two hip hop artists through a theoretical lens that evokes oppositional cultures or cultures of resistance within distinct social locations or cultural formations—a nuanced response to appalling structural disparity then and now.

INTRODUCTION

In February 2012, an African American youth—only 17 years old—was shot and killed in Sanford, Florida. His name was Trayvon Martin and the man who murdered him was George Zimmerman. There is disagreement on both sides of the case, but some of the facts are indisputable. Trayvon Martin had just purchased a few items from a convenience store and was walking back to the home of a family friend (Fulton and Martin 2017: 29). George Zimmerman followed the young man despite being told by a police dispatcher *not* to follow and to wait until an officer arrived (2017: 109). Zimmerman described the young man he was following as “a black male” who “looks like he’s up to no good” and wearing a “gray hoodie,” adding the revealing caveat, “[t]hese assholes, they always get away” (2017: 109). In the end, Trayvon Martin died, only yards from his friends’ home, of a gunshot wound to the chest (2017: 112). It was the murder of Trayvon Martin that catalyzed a movement—Black Lives Matter—which is so much the culmination of a disgraceful history and an atrocious contemporary reality with the police and civilian murders of so many Black citizens, including Michael Brown, Tamir Rice, Eric Garner, Sandra Bland, Freddie Gray, Ahmaud Arbery, Breonna Taylor, and George Floyd, who was pinned to the ground in handcuffs with the weight of a police officer on his neck for an estimated 8 minutes and 46 seconds (Bogel-Burroughs 2020, Vinson 2021).

Trayvon Martin’s murder and these many tragic deaths foreground our analysis of hip hop legacies past and present as our artists grapple with issues of police violence in Black communities, but also many other forms of immiseration facing Black people—from mass incarceration to educational inequity, and from healthcare to housing. This paper is an exploration of the lyrics of two hip hop artists as formidable oppositional voices who delineate their particular social locations both in the past and in the present. The paper contributes to our understanding of hip hop music from the 1990s as well as our contemporary times. This analysis is conducted through a theoretical lens that evokes what Bonnie Mitchell and Joe Feagin (1995) introduced as “oppositional cultures” and what Raymond Williams (1989) described as “cultural formations.” In this way, we will uncover how our selected hip hop artists voice messages of resistance as they simultaneously speak to the sociohistorical location of Black people in America.

SITUATING HIP HOP: OPPOSITIONAL AND CULTURAL FORMATION

Bonnie Mitchell and Joe Feagin describe *oppositional cultures* or *cultures of resistance* as cultural forms that arise specifically among the disenfranchised (Mitchell and Feagin 1995: 68). Disenfranchised peoples, Mitchell and Feagin suggest, draw on their own rich knowledge bases and cultural traditions to resist subjugation. This resistance takes on several distinct forms including kinship networks, social movements, and artistic mediums (Mitchell and Feagin 1995: 73). Specifically, Mitchell and Feagin (1995: 69) suggest that communities of color frame art and music to describe and resist oppression, thereby helping “to preserve dignity and autonomy, to provide an alternative construction of identity (one not based entirely on deprivation), and to give members of the dominant group an insightful critique of their own culture.”

The work of Raymond Williams (1989) resonates with Mitchell’s and Feagin’s assertions, particularly with respect to the significance of the social location in which art and music emerges. Williams (1989: 174) asserts that the interrelationship between artistic forms and societal relations are “cultural formations”—the remarkable combination of art and social location. For Williams, art is essentially in constant and dynamic relationship to the place where it arose and its societal milieu—its point of origin as well as its social location. Williams (1989: 176) further describes a particular distinction of cultural formations “where the cultural and artistic intention is shaped, from the outset, by the acceptance and the possibility of broader common relationships, in a shared search for emancipation.”

The central argument of this paper is that our selected hip hop artists have crafted oppositional messages of resistance—artistic expressions reflecting on disenfranchisement and systemic disparity. In addition, these rap artists are crafting messages of emancipation within the sociohistorical location of 1990s American society and contemporary American society as they describe the experience of African American people within the artists’ own unique social structure. The lyrics of our selected hip hop artists are oppositional cultures as well as cultural formations—voices of dissent to societal disenfranchisement.

FRAMING A GENRE AND A SOCIAL LOCATION

From its inception in the South Bronx in the early 1970s, hip hop has reflected a post-industrial urban sociohistorical context—a social location Tricia Rose describes as characterized by “social isolation, economic fragility, truncated communications media, and shrinking

social service organizations” (Rose 1994: 33-34). Notably, Robin D. G. Kelley (1994: 208) describes voices of resistance in 1990s hip hop when he asserts that the “criminalization, surveillance, incarceration, and immiseration of black youth in the postindustrial city have been the central theme in gangsta rap.” Felicia Angeja Viator (2020) resoundingly echoes Kelley’s work, unraveling the political economy of 1990s gangsta rap within a South L.A. notorious for profound levels of disinvestment, unemployment, and poverty. This environment predominantly impacted Black and Latino youth, turning “relatively benign neighborhood social cliques and lowrider car clubs into criminal street gangs” (Viator 2020: 13).

As we move into the 21st century, the scholarly literature focuses once again on the relevance of hip hop to the sociopolitical context. Todd Boyd (2002: 132) describes hip hop as a social movement situated squarely in a post-civil rights America “where racism is still rampant and now deeply embedded in the collective psyche of America” and “where ‘driving while Black or Brown’ is considered a crime by many law enforcement officials.” Like Boyd, Nelson George (2005: 43) asserts that hip hop arose as a “product of post-civil rights America”—a discourse that speaks to the mass incarceration of Black men, growing de facto segregation, and “the eroded economic base for urban America.” Reiland Rabaka (2013: 333) is emphatic in his description of hip hop’s relevance as voicing realities for African Americans both past and present—“enslaved and shackled and chained by antiblack racism, poverty, poor housing, horrid health care, unabated unemployment, ongoing substandard education...and penal escalation.”

At the same time, the literature specifically notes the contradictory nature and complexities represented within contemporary hip hop (Martinez 1997; Kitwana 2004; Peoples 2008). S. Craig Watkins (2005: 50) describes the contradictory nature of the genre, which includes “deeply ingrained misogyny and sexual violence.” Rose (2008: 3) concedes that hip hop’s mainstream has devolved into “a breeding ground for the most explicitly exploitative and increasingly one-dimensional narratives of black ghetto life.” Rabaka (2013: 5) revealingly describes the “nihilism, materialism, misogyny, and homophobia” that track from “commercial, pop, and gangsta rap.”

Still, scholars seek and uphold the best of the genre. For Watkins (2005: 4, 255), “an intense struggle for the soul of the hip hop movement” has been part of its evolution, and he notes that “hip hop continues to inspire young people to believe they matter and can change the world.” Rose’s work is also framed as a “struggle for the soul” of hip hop, and she asserts that the haters of the genre fail to acknowledge the devastating realities in black urban communities, including “police

targeting, racially motivated escalations of imprisonment, and reductions in support for what are still mostly segregated and deeply unequal schools” (Rose 2008: 11). More than that, Rose (2008: 262) proposes six principles as “a starting place for encouraging all who love black music to create a progressive community around it.” For Rabaka (2013: 337), conscious and political hip hop are consistently relevant voices—a “beacon of light” in the struggle for social justice.

In all, the scholarly literature demonstrates an acute awareness of hip hop’s complex and contradictory character, but recognizes hip hop’s tremendous potential for growth and transformation as it remains genuinely concerned with the brutal realities facing Black and Brown communities to the present day. Hip hop, then and now, has continued to express the stories of the disenfranchised in “a committed politics of action and loyalty” (Harrison and Arthur 2019: 49).

A WORD ON METHODS

The foregoing discussion of the literature pronounces hip hop as one of the most influential and complex artistic forms of this and the last century. The current study frames a thematic and lyrical analysis of the work of Tupac Shakur and Kendrick Lamar—a hip-hop artist from the 1990s and a contemporary hip hop artist, respectively. Each reflects on their social location with messages of resistance to their specific sociohistorical context—cultural formations that are markedly oppositional to the status quo. These artists were selected because of their particular relevance to their times and with regard to the political nature of their work (Stanford 2011; Popple 2015; Love 2016; Ralph et al. 2017; Linder 2017; Allen and Randolph 2019).

The present study unpacks the lyrics of these artists within an analytical rubric whereby “analysis is conceived as an emergent product of a process of gradual induction...very much a creative act” (Lofland and Lofland 1995:181-182). Specifically, the analysis will unpack common themes and tropes that emerge from exploring the lyrics of selected songs. As Shulamit Reinharz (1992: 159) asserts, “qualitative sociologists apply an inductive, interpretive framework to cultural artifacts. What differentiates sociologists from historians is simply the use of sociological theory as an aid in the explanation.” In this regard, our theoretical lens will serve as a guide to explore the songs of our selected hip-hop artists, unpacking their oppositional lyricism within a sociohistorical location of disenfranchisement in contemporary America. The cultural formation of these revolutionaries of beats and rhymes speak oppositional poniards to the powers that be.

BEATS AND RHYMES ACROSS GENERATIONS

The hip hop artists selected for this analysis—Tupac Shakur and Kendrick Lamar—express a particular focus on the sociohistorical context of their generations. Drawing on our theoretical lenses, we will find that songs by these artists are profound messages of resistance that “give members of the dominant group an insightful critique of their own culture” (Mitchell and Feagin 1995: 69). Their lyrics are also a testament to the social location of inner-city disenfranchisement—a cultural formation attuned to the lived experience of oppression (Williams 1989; Mitchell and Feagin 1995).

PRISON CELL BLUES

Since its inception, rap music has served as “an articulate cry to the world about the insufferable poverty, relentless police brutality, and frustrated hopes of the black urban scene... It presented its own clear black understanding of the inner city’s economic and political abandonment” (Baker 1993: 46). Anthony Kwame Harrison and Craig E. Arthur (2019: 49) assert that hip hop was created in some of the “most marginalized communities in urban America” and became a consistent challenge to “historical and ongoing inequities.” Just so, our selected artists have reflected on life through the prism of violence, brutality, neglect, and decay, offering strident critiques of the immiseration found in their sociohistorical context—voices of opposition within a particular social location.

In the song, “Changes,” Tupac Shakur is straightforward in his assessment of how inner-city Black communities are treated in a 1990s sociohistorical context of systemic racism—a scathing critique of a social location charged with violence and misery. The lyrics unequivocally state that police perceive violence toward Black people as worthy of reward—“Cops give a damn about a Negro/pull the trigger, kill a nigga, he’s a hero.” Moreover, the violence toward Black communities is framed as a conscious decision, as crack cocaine and guns are introduced into the community for the ultimate purpose of annihilation—“First ship ‘em dope and let ‘em deal to brothers/Give ‘em guns, step back, watch ‘em kill each other.” Black children are part of this destructive equation, and drugs are deliberately given to children without compunction—“Give crack to the kids, who the hell cares/One less ugly mouth on the welfare.” Note the description of children’s mouths as “ugly”—a wrenching description that in one word horrifically negates the beauty and worth of Black children. This further evokes older racist imagery that depicts Black children as lesser and even savage, and therefore deserving of violent threats. This imagery is bluntly described

by Patricia Turner in the documentary *Ethnic Notions* when she states that "...there was a need to imagine black children as animal-like, as savage. If you do that, if you make that step and say that these children are really like little furry animals then it's much easier to rationalize and justify the threat..." (Riggs 1987). Further, the lyrics state that fighting back is not an option in this context, because those in power will find a way to eliminate any resistance such as that of Huey Newton—cofounder of the Black Panther Party (Newton 1972)—"It's time to fight back, that's what Huey said/Two shots in the dark now Huey's dead." More than this, the lyrics call out a criminal justice system that disproportionately incarcerates Black people—"The penitentiary's packed and it's filled with blacks"—and a government that fights "a war in the Middle East/Instead of a war on poverty." Shakur is insistent that the country is not "ready to see a black president" given all these signs of immiseration and on-going issues with structural disparity.

This harrowing critique of the appalling treatment of Black people in the 1990s is clearly mirrored in the song "Hood Politics" by Kendrick Lamar within a 21st century social location—an inner-city sociohistorical context. The song suggests that violence haunts the Black community with a slow-motion "ambulance" caught on tape in a heavily surveilled area—"the project filled with cameras." Police make an appearance in the song, looking shady and corrupt—"The LAPD gamblin', scramblin', football numbers slanderin'/Niggas names on paper"—perhaps referring to various scandals within LAPD but also arrests of and prison sentences for Black people (The Lost Tapes 2015). The lyrics go on to suggest that those in power are nothing more nor less than gang members who only serve to afflict struggling people—"They tell me it's a new gang in town/From Compton to Congress...Ain't nothin' new but a flu of Demo-Crips and Re-Blood-icans." Whichever party is in power doesn't really matter, as the lyrics suggest that neither Democrats nor Republicans care about the issues facing Black people in the inner cities, as those in power ravage the poor by giving them "guns and drugs" while stigmatizing the people—"call us thugs." Moreover, the politicians make it their mission to "fuck with you," doing damage to the people in any number of ways with "no condom"—a self-serving, shortsighted, and reckless approach to governing (Podgist 2016). In one insightful interlude in the song, the lyrics state the same line three times, "Obama say, 'What it do?'" implying that although the country has a Black president, he is part of the aforementioned political gang that doesn't actually bring changes that would concretely support Black people living in the inner city—"Red state versus a blue state—which one you governin'?"

WALKING BLUES

Nelson George (2005) situates contemporary hip hop within a post-civil rights American discourse that sheds light on brutal urban realities such as mass incarceration, growing segregation, and an erosion of urban infrastructure. George (2005: 43) goes further to describe a “profound sense of hopelessness” that follows in the wake of these realities. S. Craig Watkins (2005: 204) similarly describes decades of urban crisis that have devastated Black urban communities, noting that after 9/11, “the issues confronting urban America are no longer on the nation’s radar. Simply put, they do not matter.” This urban abandonment, the immiseration it heralds, and the relentless hopelessness that follows is painfully reflected in the work of our selected artists then and now.

In the song “Keep Ya Head Up,” Tupac Shakur is searing in his discussion of what the future holds for Black people—a standpoint and critique rooted in his own 1990s context and social location. In a blunt reminder that America does not care for everyone equitably, the lyrics state that there is always enough funding to wage wars, but somehow never enough to “feed the poor.” This line leads into a frank and agonizing statement on the ultimate ends when you come from the standpoint of wars over people—“it ain’t no hope for the youth and the truth is it ain’t no hope for the future.” This ferocious truth is followed by a fascinatingly insightful point—“and then they wonder why we crazy.” This observation resonates with the words of Hannah Nelson, “an elderly Black domestic worker” discussed in the work of Patricia Hill Collins (2000: 24) who had been interviewed by John Langston Gwaltney (1980). Hannah Nelson states, “I have grown to womanhood in a world where the saner you are, the madder you are made to appear” (Gwaltney 1980: 7). The song suggests that Shakur had at first blamed his mother for such a bleakly dealt hand, but then eventually recognized the facts—“We ain’t meant to survive cause it’s a set up.” The ramifications of these terrible truths eventually filter down to the children—“And now my son’s gettin’ older and older and cold from havin’ the world on his shoulders.”

This gutting discussion of the experiences of Black people in the 1990s, which Tupac Shakur speaks to so compellingly, is taken to new levels of rage and despair in the work of Kendrick Lamar. The song “The Blacker the Berry” takes the devastating certainties of inner-city Black experience in contemporary times and delivers a ferocious diatribe against the white establishment for an abundance of corruptions. The song suggests that Black people are judged and hated for their skin color and their physical appearance as the lyrics intone “I’m African American, I’m African, I’m black as the moon.../My hair is nappy, my

dick is big, my nose is round and wide/You hate me, don't you?" These lines are followed by an unequivocal reference to a commitment by the white establishment to the annihilation of Black people—"You hate my people, your plan is to terminate my culture/You're fuckin' evil." Lamar here eerily resonates with Watkins's discussion of the appalling neglect and abandonment of Black people in an America where "[s]imply put, they do not matter" (Watkins 2005: 204). This theme is also continued with the line "You sabotage my community, makin' a killin'," suggesting that the dominant group not only profits from the destruction of Black communities, but even seeks the eradication of Black people. These references to the devastation and demolition of the Black community occur again later in the song along with the suggestion that incarceration is the inevitable outcome for Black people with the lines "I mean, it's evident that I'm irrelevant to society/That's what you're tellin' me, penitentiary would only hire me." Lamar here echoes the work of Angela Davis (1997: 266) who tellingly critiques an "out of control" prison industrial complex in America that disproportionately incarcerates Black men. Amazingly, these harshly critical rebukes of the white establishment are small change to the ultimate critique in the song, which is the suggestion that the immiseration of Black people has created and encouraged Black on Black crime and ultimately bastardized Black pride into hypocrisy—a nod to George's discussion of a "profound sense of hopelessness" in the Black community (George 2005: 43).

So don't matter how much I say I like to preach with the
Panthers
Or tell Georgia State "Marcus Garvey got all the answers"
Or try to celebrate February like it's my B-Day...
Or watch BET 'cause urban support is important
So why did I weep when Trayvon Martin was in the street
When gang-banging make me kill a nigga blacker than me?
Hypocrite!

STONES IN MY PASSWAY

In her examination of hip hop from the first decade of the 21st century, Rose (2008: ix) painfully acknowledges that "[h]ip hop is not dead, but it is gravely ill." She unpacks a struggle for the soul of hip hop, proposing a set of principles that stand up to and reject the very worst of the genre—"the gangsta-pimp-ho trinity" and "the trade in destructive images and visions of black people" (Rose 2008: 261). In this regard, Rose is calling for a "transformational love" with regard to the genre—one that "sets boundaries in the interests of change, growth, and health"

(Rose 2008: 262, 271-272). Tennille Nicole Allen and Antonia Randolph (2019) as well as Bettina L. Love (2016) include Kendrick Lamar in their analyses of the “quiet” found within the songs of hip hop artists whose lyrics offer “subtle, quotidian challenges to oppression, dehumanization, and objectification” in American society (Allen and Randolph 2019: 49). Love (2016), in particular, “explores the idea that an act of resistance can occur simply by focusing on one’s interior self.” Both of these strands of research resonate with the work of our selected artists as they grapple with a response to all the hatred and horror that they witness.

For Tupac Shakur, a particular response is to call on his community to hold on and step up. In the song “Keep Ya Head Up,” Shakur speaks with a profound sense of honor and integrity to Black women, who struggle with poverty and racism but also misogyny in the Black community itself.

I give a holler to my sisters on welfare
 2Pac cares if ain’t nobody else care
 And, uh, I know they like to beat you down a lot
 When you come around the block, brothers clown a lot
 But please don’t cry, dry your eyes, never let up
 Forgive, but don’t forget, girl, keep ya head up

Moreover, Shakur is blunt and unflinching in calling out damaging behavior, very much in keeping with Rose’s call for a transformational love that sets boundaries and rejects destructive visions of Black people (Rose 2008). Shakur calls out Black men who abandon their children and the Black women in their lives—“You know what makes me unhappy?/When brothers make babies and leave a young mother to be a pappy.” Further, in harsh and strident terms, he calls out Black men for violently preying on Black women—“I wonder why we take from our women/Why we rape our women, do we hate our women?” Patricia Hill Collins (2000: 124) suggests that implicating Black men in any discussions of misogynist practices and the rape of Black women has historically been silenced as “it violates norms of racial solidarity.” Shakur’s taking on of this taboo subject is remarkable on its face. The lyrics go so far as to foster an egalitarian ethic even to the point of committing homicide for the women in the community, which in many ways speaks to the levels of danger in these women’s neighborhoods and “the eroded economic base for urban America” (George 2005: 43)—“I think it’s time to kill for our women/Time to heal our women, be real to our women.” In the end, Shakur is clear on a man’s responsibility to the woman in his life—“So will the real men get up?/I know you’re fed up, ladies, but keep ya head up.”

For Kendrick Lamar, the focus of resistance seems to center on navigating out of the morass of disparity and despair all around him, and the journey is both communal and personal. In Lamar's song "Alright," the lyrics state that Black people have been wounded and low with very few avenues of recourse—"We been hurt, been down before/Lookin' at the world like, 'Where do we go?'" In the song, much of the struggle to survive is laid at the door of the police, who, according to the lyrics, think nothing of taking Black lives—"Nigga, and we hate the po-po/Wanna kill us dead in the street for sho'." Beyond the police, the song shifts into a discussion of interiority and struggles with personal demons—a nod to the work of Allen and Randolph (2019) and Love (2016). The lyrics even suggest an evil presence in the form of "Lucy," who like Lucifer, tempts Lamar and perhaps the community with vices—"What you want you, a house? You, a car? Forty acres and a mule? A piano, a guitar?/Anything, see my name is Lucy, I'm your dog"—and at times he succumbs—"Where pretty pussy and Benjamin is the highlight.../Drown inside my vices all day." Yet, in owning and facing his failures that are all too human—"I'm fucked up, homie, you fucked up"—he finds solace and self-acceptance, particularly a need to trust in a higher power with the line, "My rights, my wrongs; I write 'til I'm right with God." The chorus of the song reads like a litany of hope for a community haunted by grief and immiseration.

Nigga, we gon' be alright
 Nigga, we gon' be alright
 We gon' be alright
 Do you hear me, do you feel me?
 We gon' be alright

The lyrics include a nod to Shakur's "Keep Ya Head Up" by embracing that very counsel though with the clear acknowledgement of on-going struggle, painful truths, and human frailty—"I keep my head high/I cross my heart and hope to die/Lovin' me is complicated." Finally, the lyrics close with a commitment to continue the struggle with the "evils of Lucy" by seeking truth—"I didn't want to self-destruct.../So I went runnin' for answers."

CONCLUSION

This analysis has focused on the work of two hip hop artists from very different historical timeframes—Tupac Shakur was performing and writing music in the 1990s, and Kendrick Lamar is very much a 21st century hip hop artist. Yet, our lyrical and thematic analysis uncovers

quite a bit of resonance and parallelism between their work as they speak to unconscionable realities for marginalized Black urban communities. Each artist powerfully articulates their generational and sociohistorical reality in shades of rage and despair, but also tellingly, abandonment and annihilation. In fact, their work in many ways resembles tragic mirror images of oppression in our past and in our present. Their profound and insightful critiques of systemic racism and the utter disenfranchisement of inner-city Black communities endure as messages of resistance—blistering assessments of the dominant white establishment as they give “members of the dominant group an insightful critique of their own culture” (Mitchell and Feagin 1995: 69). More than that, they each speak to cultural formations across generations—to the social location of inner-city disenfranchisement (Williams 1989).

In Rabaka’s (2013: 335-336) nuanced and exhaustive exploration into the contested soul of the hip hop movement, he insists that “conscious, political, and message rap...remain a beacon of light, boldly illuminating the cold and corrupt, dark and discontent world we inherited.” Moreover, he suggests that not only hip hop artists but we *all* must contribute to the “struggle for freedom and social justice,” for “[w]hat we do right here and right now will have an impact on the future: our individual future and our collective future” (Rabaka 2013: 337). Tupac Shakur and Kendrick Lamar illuminate so much that is damaged and disheartening in our world, but their words also call for the courage to change and to seek the truth—voices in the struggle then and now.

ACKNOWLEDGMENTS

Many thanks to Raymond Williams as well as Bonnie Mitchell and Joe Feagin for the wealth of their ideas. Profound thanks go to the many hip hop artists who continue to question authority in our time.

REFERENCES

- Allen, Tennille Nicole and Antonia Randolph. 2019. “Listening for the Interior in Hip-Hop and R&B Music.” *Sociology of Race & Ethnicity* 6(1): 46-60.
- Baker, Houston. 1993. “Scene...Not Heard.” Pp. 38-48 in *Reading Rodney King/Reading Urban Uprising*, edited by Robert Gooding-William. New York: Routledge.

Bogel-Burroughs, Nicholas. 2020, June 18. "8 Minutes, 46 Seconds Became a Symbol in George Floyd's Death. The Exact Time is Less Clear." *The New York Times*.

Boyd, Todd. 2002. *The New H.N.I.C. (Head Niggas in Charge): The Death of Civil Rights and the Reign of Hip Hop*. New York: NYU Press.

Collins, Patricia Hill. 2000. *Black Feminist Thought*. 2nd ed. New York: Routledge.

Davis, Angela Y. 1997. "Race and Criminalization: Black Americans and the Punishment Industry." Pp. 264-279 in *The House That Race Built*, edited by Wahneema Lubiano. New York: Pantheon.

Fulton, Sybrina and Tracy Martin. 2017. *Rest in Power: The Enduring Life of Trayvon Martin*. New York: Spiegel & Grau.

George, Nelson. 2005. *Hip Hop America*. New York: Penguin Books.

Gwaltney, John Langston. 1980. *Drylongso, A Self-Portrait of Black America*. New York: Vintage.

Harrison, Anthony Kwame and Craig E. Arthur. 2019. "Hip-Hop Ethos." *Humanities* 8(1): 39-53.

Kelley, Robin D.G. 1994. *Race Rebels: Culture, Politics, and the Black Working Class*. New York: Free Press.

Kitwana, Bakari. 2004. "Hip-Hop Studies and the New Culture Wars." *Socialism and Democracy* 18(2): 73-77.

Linder, Matthew. 2017. "'Am I Worth It?': The Forgiveness, Death, and Resurrection of Kendrick Lamar." *Toronto Journal of Theology* 33(1): 107-112.

Lofland, John and Lyn H. Lofland. 1995. *Analyzing Social Settings: A Guide to Qualitative Observation and Analysis*. 3rd ed. Belmont, CA: Wadsworth.

Love, Bettina L. 2016. "Good Kids, Mad Cities: Kendrick Lamar and Finding Inner Resistance in Response to FergusonUSA." *Cultural Studies ↔ Cultural Methodologies* 16(3): 1-4.

Martinez, Theresa A. 1997. "Popular Culture as Oppositional Culture: Rap as Resistance." *Sociological Perspectives* 40(2): 265-286.

Mitchell, Bonnie L. and Joe R. Feagin. 1995. "America's Racial-Ethnic Cultures: Opposition within a Mythical Melting Pot." Pp. 65-86 in *Toward the Multicultural University*, edited by B. Bowser, T. Jones, and G.A. Young. Westport, CT: Praeger.

Newton, Huey P. 1972. *To Die for the People: The Writings of Huey P. Newton*. New York: Random House.

Peoples, Whitney A. 2008. "'Under Construction': Identifying Foundations of Hip-Hop Feminism and Exploring Bridges between Black Second-Wave and Hip-Hop Feminisms." *Meridians* 8(1): 19-52.

Podgist. 2016. "S1E12—Hood Politics by Kendrick Lamar." Retrieved January 22, 2022 from <https://www.podgist.com/dissect/s1e12-hood-politics-by-kendrick-lamar/index.html>

Popple, Naomi. "Imagining Freedom in a Post-Emancipation 'Pigmentocracy': Wallace Thurman, Toni Morrison, and Tupac Shakur." *Journal of Black Studies* 46(4): 404-414.

Rabaka, Reiland. 2013. *The Hip Hop Movement: From R&B and the Civil Rights Movement to Rap and the Hip Hop Generation*. New York: Lexington Books.

Ralph, Michael, De Jesús, Aisha Beliso, and Stephan Palmié. 2017. "Saint Tupac." *Transforming Anthropology* 25(2): 90-102.

Reinharz, Shulamit. 1992. *Feminist Methods in Social Research*. New York: Oxford University Press.

Riggs, Marlon. 1987. *Ethnic Notions*. California Newsreel.

Rose, Tricia. 1994. *Black Noise: Rap Music and Black Culture in Contemporary America*. Middletown, CT: Wesleyan University Press.

_____. 2008. *The Hip Hop Wars*. New York: Basic Books.

Stanford, Karin L. 2011. "Keepin' It Real in Hip Hop Politics: A Political Perspective of Tupac Shakur." *Journal of Black Studies* 42(1): 3-22.

The Lost Tapes. 2015. "Narrative Fidelity in Kendrick Lamar's 'Hood Politics.'" Retrieved January 22, 2022 from <https://blog.mcdaniel.edu/caarap/2015/04/23/narrative-fidelity-in-kendrick-lamars-hood-politics/>

Viator, Felicia Angeja. 2020. *To Live and Defy in LA: How Gangsta Rap Changed America*. Cambridge, MA: Harvard University Press.

Vinson, Liz. 2021, May 28. "His Last Breath: A year after George Floyd's murder, nation reckons with history of racism, police brutality." Retrieved May 22, 2022 from <https://www.splcenter.org/news/2021/05/28/his-last-breath-year-after-george-floyds-murder-nation-reckons-history-racism-police>

Watkins, S. Craig. 2005. *Hip Hop Matters: Politics, Popular Culture, and the Struggle for the Soul of a Movement*. Boston, MA: Beacon Press.

Williams, Raymond. 1989. "The Uses of Cultural Theory." Pp. 163-176 in *Politics of Modernism: Against the New Conformists*. London: Verso.

MUSIC REFERENCES

Lamar, Kendrick. 2015. "Alright." To Pimp a Butterfly. TDE, Aftermath, Interscope.

_____. 2015. "Hood Politics." To Pimp a Butterfly. TDE, Aftermath, Interscope.

_____. 2015. "The Blacker the Berry." To Pimp a Butterfly. TDE, Aftermath, Interscope.

Shakur, Tupac. 1993. "Keep Ya Head Up." Strictly 4 My N.I.G.G.A.Z. Interscope, Jive.

_____. 1998. "Changes." Greatest Hits. Amaru, Death Row, Interscope.

Understanding Us: Undergraduate Research to Support a Community Partner Working on Homelessness

Kambry Woodbury and Daniel Poole
Salt Lake Community College

Abstract

Understanding Us is a non-profit organization that provides several programs focusing on individuals experiencing homelessness in Salt Lake City, Utah. Currently, they run a Tai Chi program at the downtown city library four days a week. We collected preliminary demographic survey data to help the organization better understand the population they are serving, so that they may best meet the needs of participants. In addition to the demographic survey data, we have also included anecdotal examples and insight from participants in the Tai Chi Program.

Introduction

The purpose of this study was to collect data from participants in the Street Tai Chi program of the non-profit Understanding Us to inform best practices for the organization and to create a better understanding of homelessness in our community. In addition to learning more about the

participants' experiences and identifying their social connectedness, we also sought to highlight the participants' individual strengths and struggles as members of the homeless community. From this information, we provided Understanding Us with valuable participant feedback that may be used to promote opportunities for the non-profit to expand its programs. This also provides an opportunity for undergraduate students at Salt Lake Community College (SLCC) to conduct and publish research that not only benefits their community but also contributes to the academic literature on a local issue.

It has been noted that Salt Lake City is home to the majority of Utah's growing homeless population. This attention has pressured Salt Lake City officials and homeless service providers to discover effective means of supporting our expanding homeless population. In recent years, Salt Lake City has altered its approach to sheltering people experiencing homelessness (PEH) and cracked down on crime in response to the increasing demand for services (typically crime relating to drugs, loitering, and panhandling). In 2017, the city launched Operation Rio Grande, a three-phase plan to restore public safety and order, enroll PEH into treatment, and provide them with employment opportunities. Over 80% of this operation budget was allocated to law enforcement from August 2017 to July 2019, resulting in 1,442 felony arrests and 3,322 misdemeanor arrests (Rodgers and Stevens 2020). This resulted in a significant portion of the homeless population being displaced, coerced into treatment, and trapped in the revolving door of incarceration and homelessness. This operation has shown to have a lasting impact on the homeless community of Salt Lake City through further normalizing the stigmatization, displacement, and harassment of impoverished populations (Brown 2021:47–51). Unfortunately, these harsh tactics and their unforgiving consequences have become all too socially and politically acceptable.

Not having a stable place to live is a dangerous health condition. PEH typically experience numerous afflictions that are frequently a complex mix of serious physical, mental, social, and substance use problems. These can include poor health, high stress, unhealthy and dangerous environments, and an inability to control food intake (National Health Care for the Homeless Council 2019).

For the PEH, finding professional medical healthcare, mental healthcare, and self-care opportunities is challenging. A local non-profit organization, Understanding Us, was created in part to help understand the challenges experienced by PEH and to work to create solutions. Bernie and Marita Hart founded this organization and developed the Street Tai Chi program in an effort to supplement the physical, mental, and social treatment needs of PEH that local service providers fail to

address. Understanding Us contacted faculty at SLCC to request research in support of these efforts. The first phase of research aimed to provide Understanding Us with demographic data as well as basic information about its program participants.

Participants of the Street Tai Chi program self-identify as members of the street community (the program's preferred terminology for the homeless community). The program occurs four times each week, with an average of 30–40 participants. In addition to a burrito and coffee, participants in Street Tai Chi are offered two dollars or an eight-pack of cigarettes if they remain and participate in the exercises. Each session begins with time for participants to socialize, drink coffee, and eat burritos. This time before practice allows participants to arrive intermittently. Participants then form a large circle and engage in tai chi warm-up exercises, the primary tai chi form, and finally chi gong. These exercises are led by people who are currently experiencing homelessness or who have in the past. Understanding Us does not have any exclusions or criteria to become a participant in the program. One value the program holds is that no one should ever be asked to leave. The program is a place that one can always come back to, be welcomed, and feel safe. The program is specifically targeted towards people who are typically excluded by other homeless service providers, who are considered to be treatment-resistant, and who are chronically experiencing homelessness.

The tai chi exercise comes from an ancient Chinese martial art that consists of slow, continuous, fluid movements, while maintaining a meditative state of mind and controlled breath for total self-development. Tai chi interventions take on a mind–body approach: bringing awareness to the relationship of the mind, body, and surrounding environment and how they all affect one another (Abdi 2019:88). The wide range of benefits from practicing tai chi can extend to people with various health conditions, particularly those that have chronic health conditions such as asthma, HIV, and cardiovascular disease. When practiced in a group, tai chi can have a beneficial social impact. Participants of tai chi interventions have described experiencing a renewed social role. Some explain this feeling as redefining social roles in a new way that offers them new purpose or returning to social roles that were previously meaningful to them but, at some point, lost meaning. There is a body of academic research that has shown practicing tai chi can have a positive effect on balance, cognitive function, and overall self-esteem (Wu et al. 2013:202; Fetherston and Wei 2011:160; Hosseini et al. 2018:1029).

Improvements in these areas have the potential to improve self-efficacy and quality of life by providing people a sense of control over their body and the environment in which they live (Fetherston and Wei 2011:160). Tai chi can be applied as a self-management and care practice

that is accessible to people with disabilities, people that are in low-resource settings, or people that are resistant to conventional care. A tai chi program targeted towards a community of people that are experiencing homelessness has potential to mitigate the harms they face.

Research Question

In addition to international research on the effects of tai chi programs, as well as a significant amount of student research going on in Salt Lake City on the topic of homelessness, there is now research being conducted on the potential impact that a long-standing, community-led tai chi program can have on people who have experienced or are currently experiencing homelessness. For this first phase of research, we focused on the following research questions:

- Who are the participants of the Street Tai Chi program?
- What are their feelings of connection to social groups?
- What effects does the program have, and why do participants choose to participate in the program?

Research Methods

The first phase of research focuses on collecting demographic survey data to help Understanding Us better understand the needs of its participants. We also want to give voice to a vulnerable population of people to better alleviate societal-wide issues, specifically homelessness. Understanding Us will use the data we collect to inform local and state policy as well as their own programming. To avoid causing harm to an already vulnerable group, a well-considered research strategy is crucial not only for the people from whom we collect information but also for the reliability of the results. Our research team carefully thought about the risks and benefits of each survey question, as well as how to ask the questions in a way that respected participants' identities and experiences without making assumptions about them. Before conducting research, it was fundamental that we familiarize ourselves with participants and that they felt comfortable with us. We did not want participants to feel as though they were our test subjects that we poked and prodded for data. Researchers spent session after session during the entirety of our research process participating in tai chi with everyone else in the group. This helped us establish rapport with participants, allowing them to feel safe in our presence and while completing the questionnaire. The researcher conducting the survey informed respondents that there is no incentive or harm that could come to them from participating in the survey and that they have the right to refuse to answer any question on

the survey. Participants were assured that their information would be kept private and only shared anonymously. To ensure that everyone who wished to participate in the survey and share their story had an equal opportunity to do so, the survey was read aloud to those who would have been unable to participate because of blindness, language barriers, or other barriers, and their responses were recorded in a secure environment. In all interactions with this population, we respect their identity and experiences as members of the street community, while recognizing that their character and their narratives extend beyond the label of “homeless.”

This survey is intended to be a starting point for Understanding Us as well as future research and to be updated periodically as the results inform practices and the group evolves over time. The survey questionnaire contains both qualitative and quantitative questions. After receiving Institutional Review Board approval, the surveys were printed and distributed at Street Tai Chi sessions. The responses were then digitized for analysis. Questions on the surveys can be categorized into three research sections:

1. Demographic information of the participants of the program, includes their identified gender, race, age, and other factors.
2. Participants’ levels of connection and safety. Using a 1–10 scale, participants rate their level of connection to different social groups and their feelings of safety on the streets.
3. Feedback about the program. Participants answer questions regarding their thoughts, experiences, and strengths/ weaknesses of the program.

Participants were approached and asked whether they would take part in a short questionnaire to provide Understanding Us with a deeper awareness of the people in the tai chi program and its impacts. If participants were willing to participate, they received a pen and clipboard with the survey attached, and they were informed of the purpose of the survey and their rights, as well as the fact that there was no incentive for completing the survey and no risk involved. Participants taking the survey were able to ask the present researchers any questions they had about the survey and, if necessary, request accommodations. When they had completed the survey, they returned it to the researchers who placed it in a secure location where no other participant could view or alter it. From there, the data were collected from the paper surveys and transferred to a digital datasheet for analysis. To date, we have collected responses from 48 participants.

Results

Including two optional questions at the end, the survey comprises 23 questions total. The majority of survey questions are short-answer response questions, for which participants have the option to elaborate. There are, however, four rating-scale response questions and one yes-or-no response question. Resulting data of the survey is presented in the relevant research sections.

Research Section 1: Demographic Information

Respondents were asked to self-identify their age, gender, employment status, whether or not they identify as a Utah native, and if they are currently experiencing homelessness (Table 1).

Table 1. Demographic information of tai chi class members	
Characteristic	Number (%)
Age in years (n=48)	Mean 46.7, median 48 range 24-75
Gender identity (n=47)	
Female	8 (17%)
Male	37 (79%)
Other	2 (4%)
Utah native (n=48)	
Yes	20 (42%)
No	28 (58%)
Employment status (n=48)	
Employed	11 (23%)
Unemployed	37 (77%)
Housing status (n=48)	
Housed	16 (33%)
Not housed	32 (66%)
Highest education (n=48)	
No high school diploma	4 (8%)
High school diploma/GED	22 (45%)
Some college	10 (21%)
Associates degree	10 (21%)
Bachelors degree	2 (4%)
Arrest record (n=45)	
Never been arrested	15 (33%)
Been arrested once	5 (11%)
Been arrested more than once	18 (40%)
Been arrested >10 times	7 (16%)

The majority of survey respondents were between the ages of 40 and 59 years old. Males comprised a significant proportion of the research participants (79%). There were eight respondents that identified as females (17%) and two respondents that identified outside of the male–female binary (4%). Of the 48 participants who responded, 77% were unemployed and 23% employed. Thirty-two (66%) of the participants identified as currently experiencing homelessness. Of those not currently housed, 6 (38%) had been on the street for more than a year. All program participants who completed the survey identified as either a PEH currently or as having experienced homelessness in the past.

Participants were asked to identify their highest level of education: 92% of respondents identified a GED/high school diploma or higher as their highest level of education, whereas only 8% have no high school diploma. Participants were also asked the number of times they have been arrested. This question elicited both qualitative and quantitative responses; to include and represent all of the responses in a manner that is accurate and respectful of the participants' experiences, the data were organized into the four categories shown in Table 1. Of the respondents, 67% identified as having been arrested at least once. Participants were given the option of responding to two additional questions regarding their relationship with society and the perceived circumstances that led to their experiencing homelessness. From the question regarding their relationship with society, all responses could be classified as neutral or negative. Neutral responses included: "participator," "okay," and "need to know more about society." Negative responses included: "not good," "strained due to misinformation about who most of us really are and ignorance about why we ended up here," and "sometimes I feel like a second class citizen." Responses to the question of what experiences they think led to them to become homeless included experiences relating to substance use, incarceration, mental health, unemployment, and lack of affordable housing.

Table 2 shows the responses to questions about participants' biggest obstacles and their greatest strengths. Physical, mental or emotional, and social characteristics were mentioned in the majority of responses to both questions.

Table 2: Sample of participant responses: biggest obstacles	
Observed Categories	What are your biggest obstacles at the moment?
Physical health	Legs not working Blindness Physical problems (cannot stand for long) Feeling tired Being abused physically

Mental health	Living Maintaining my sobriety Anxiety My life is against a rock Mental health issues Substance use Being abused mentally
Social	Being social Getting out in public Making more friends Re-entering society after incarceration Difficulty communicating
Finance/ employment	Money Unemployment/can't work
Other	A secure place to leave my belongings to work Everything being closed Cold weather Accessing taxes
Observed Categories	What are your greatest strengths?
Emotional strengths	Confident Perseverance To distance myself from extreme hatred issues I am a survivor Never lose hope for a better quality of life
Interpersonal strengths	A good support system That people care about me True friends Family I made for myself
Intellectual strengths	Intelligent An open mind A willingness to learn
Physical strengths	Health Broad Strong
Interests/hobbies	Art Working out Tai chi
Other	Motivated Being myself Cautious Spirituality Love to work Love life

Research Section 2: Levels of Connection and Safety

Nineteen participants were asked to rate their feeling of connection to PEH, their family, and society using a 1-10 scale where 1 represents a weak connection and 10 represents a strong connection (Figures 1-3).

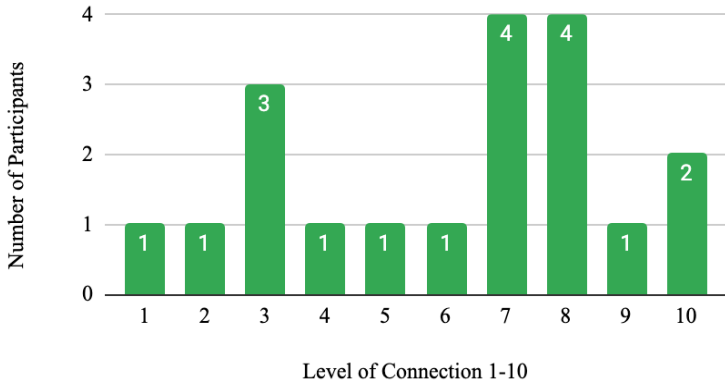


Figure 1: Participants’ level of connection to society.

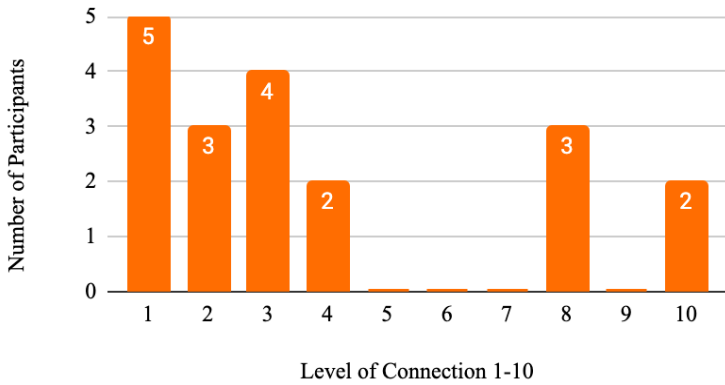


Figure 2: Participants’ level of connection to family.

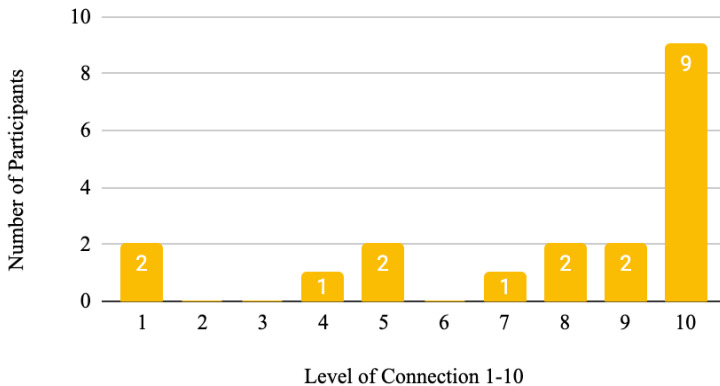


Figure 3: Participants' level of connection to PEH

The figures above show that there is a significant number of respondents that had strong connection to PEH (68.4% rating their connection 8 or higher) and a significant number of respondents feeling a weak connection to family (63.2% rating their connection 3 or lower).

Participants were also asked to rate their feelings of safety on the streets using the same 1-10 scale, but with 1 representing feeling not safe at all and 10 representing feeling very safe (Figure 4).

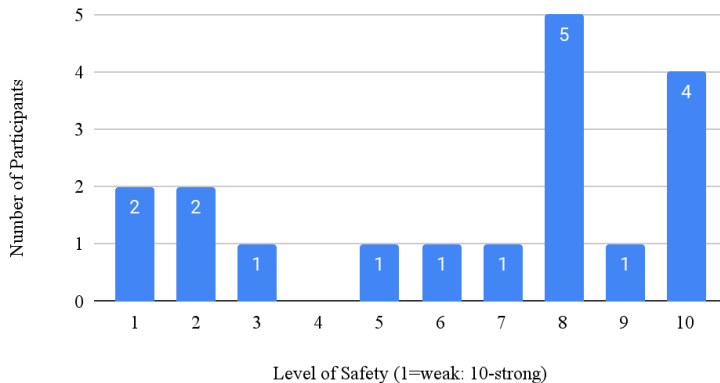


Figure 4: Participants' perceived level of safety on the streets.

These data demonstrate a relatively high feeling of safety while on living on the streets among the respondents.

Research Section 3: Program Feedback

Table 3 presents respondents’ perceived benefits and motivations of attending the tai chi sessions, which are organized by the observed categories. Responses that are categorized as self-efficacy and empowerment correspond with an individual’s belief in themselves, their ability to complete tasks, and their capacity to exercise control. Social support category responses mention motivation from others, shared understanding, and camaraderie. The mindfulness and awareness category includes responses relating to being in control of one’s body or mind, being attentive to the present moment, and letting go of stress. The incentives category includes responses that mention the rewards received for taking part. Responses that are represented in the routine category are those that mention a positive, consistent routine, i.e., something that the participants may include in their day on a regular basis.

Table 3: Participants’ self-identified benefits of the tai chi program and their motivation for attending		
Categories	Benefits of Program	Motivations for Attending
Self-Efficacy/ empowerment	Being able to get out of my place Spend some time outside Learning something new Helps me learn new people skills Bettens my mental and social health I don’t feel as bad after coming It has physical benefits for my disabilities Stretching Exercise helps	Strengthen both physically and mentally It is enjoyable to do Stretching Cause I can Done with physical therapy and this is a good exercise Helps with mental health
Social support	Being supported at tai chi I can support my homeless friends You can talk to others that face the same issues that we all have had Companionship	Together-ness Come for family/friends Camaraderie Nice to be part of something To connect with others and do something productive with my time Trying to communicate It’s a great group

Mindfulness/ awareness	Serenity Humility Hope Slowing my mind as well as smoothing my soul Breathing	Helps with nervous feelings A healthy positive refocus to overwhelming situations Clears my mind Relaxing Good meditation
Incentives	Burritos Couple of dollars when I need it Coffee Cigs	The coffee Cigarettes Smokes
Routine	Having a place to be at a set time It helps me to get motivated and focused on the day ahead	Because I have been coming for 4 years To get into a routine again

Discussion and Recommendations

These results showed that the larger part of respondents identified as sharing multiple experiences such as having been arrested at least once, being unemployed, and not feeling connected to their families. In addition to those experiences, all of the respondents identified as PEH or as having experienced homelessness in the past. Because of the commonalities of the group, it was not surprising to find that a majority of the sample felt a strong connection to PEH. The results also demonstrated that participants were coming to tai chi for camaraderie, togetherness, and to connect with others who face the same issues. Participants experienced the benefits of being able to support their homeless friends while also feeling supported themselves at tai chi.

Regarding the program's benefits and why participants come to tai chi, social support and self-efficacy were the most emergent themes of the responses. These themes were consistent with other studies that explored the effects of tai chi interventions (Fetherston and Wei 2011; Hosseini et al. 2018), especially one study for people with heart failure conditions (Yeh et al. 2016:7–12). These health outcomes are similar to impacts of homelessness characterized by increased stress, feelings of helplessness, and social role dysfunction (Yeh et al. 2016:7–12). Overall results from the survey have shown that the Street Tai Chi program is a space where many of the participants share difficult experiences with

each other, creating an environment of connection, support, and social inclusion.

Future Research

There should be further studies to investigate the potential role and benefits of this program for the street community. Researchers attending the sessions observed participants providing each other with helpful resources and other forms of aid. Future research could be done investigating the impacts that participants of the program have in each other's success and survival as PEH. This could include tracking new participants at a baseline and assessing the benefits and role that the program has over time. Preliminary demographic information will be compiled into a longitudinal dataset to track participants' experiences over several years. We will measure changes in behavior and attitude as well as social interactions, housing status, health outcomes, and other aspects of well-being.

Limitations

This preliminary data has only started to shed light on the experience of Street Tai Chi participants. There have been several hundred participants involved with the program, and we have only captured responses from 48 so far. As we work to collect more data and implement new phases of the broader research agenda, we will gain a better-informed perspective. Much of the data relies on self-reporting from individuals. This leaves room for error, and our data would be stronger if we were able to corroborate arrest, education, and health records with the self-reported survey responses. As mentioned earlier in the paper, responses to the surveys were short-answer format. This meant that for some questions we had both qualitative and quantitative responses, including responses that were difficult to compare or analyze. Although providing short-answer response-type questions on the survey added limitations for some questions, it also strengthened and validated others by allowing participants to self-identify their responses based solely on their own experiences without any external assumptions. The limitations of our research, like many other undergraduate research projects, could be mended or reduced significantly through access to resources such as a larger research team, technology, funding, and time.

Conclusion

Participation in the Street Tai Chi program is completely voluntary. Participants report feeling more connected and having a better sense of

identity and belonging when interacting with the group. This appears to be an important factor in explaining why so many individuals living on the street continue to show up and engage with Understanding Us. A common narrative among participants is that “the system” has pushed them to the margins of society, and that law enforcement and the courts continue to ensure they are locked into an undesirable status. There is a common misconception that people living on the street are lazy, uneducated, or lacking determination to succeed in society. Our preliminary results show that the participants in the Street Tai Chi program are educated, with more than 90% having at least a GED/high school diploma. Many of the individuals are also working and earning a paycheck, but they cannot afford housing. Structural barriers such as being arrested for being on the street create a cyclical process of locking individuals into a situation that is nearly impossible to overcome. Once an arrest record is attached to a person, it is much more difficult to find jobs and housing. Understanding Us continues to work to understand homelessness in our community and to create awareness about the flaws in the current system. The data collected for this study will inform future research and help the Understanding Us organization to better serve its participants with refined program goals.

Acknowledgments

We would like to acknowledge all the participants of the Street Tai Chi program for their willingness to participate and entrust us with their responses regarding their experiences as people in the street community. We would also like to acknowledge Bernie and Marita Hart, the founders of Understanding Us, for giving SLCC students the opportunity to conduct meaningful research that will go on to benefit them and their community. The last acknowledgment is to the past SLCC students that had previously conducted research with Understanding Us: Bianca Dellapenta, Marie Ellis, Mackenzie Hughes, Tyler Jamieson, Kristen Kessler, Zahary Naylor, Jennifer Salazar, Kymberly Simons, and Celeste Suite.

Disclaimer

Tai chi can sometimes be referenced as an alternative to traditional therapies and care. Although practicing tai chi has many longstanding, known, and proven health and physical benefits, it cannot and should not be used as a replacement for professional medical or mental healthcare. Rather, tai chi should be viewed and used as something along the lines of what the World Health Organization defines as self-care practice, that is, within the ability and access “of individuals, families and

communities to promote health, prevent disease, maintain health, and cope with illness and disability with or without the support of a health-care provider” (WHO 2019).

In addition to that, the contents of this report do not necessarily reflect the views of Understanding Us as a nonprofit but the views of the authors. Understanding Us provided SLCC students with an opportunity to collect data from their program’s participants in the interest that they may also use that information to expand opportunities and learn more about the program’s participants. Understanding Us is not responsible for the accuracy of the material and information presented in this paper.

References

Abdi, Meghdad. 2019. “Making sense of an ancient discipline in a modern time: how tai chi (太极) practice benefits the body–mind.” *Chinese Medicine and Culture* 2(2):88. doi: 10.4103/cmac.cmac_16_19.

Brown, Lauren, and Jeff Rose. 2021. “Slow violence and homelessness: activating public space and amplifying displacement.” *Lo Squaderno: Explorations in Space and Society* 59:47–51.

Fetherston, Catherine M., and Li Wei. 2011. “The benefits of tai chi as a self management strategy to improve health in people with chronic conditions.” *Journal of Nursing and Healthcare of Chronic Illness* 3(3):155–64. doi: 10.1111/j.1752-9824.2011.01089.x.

Hosseini, et al. 2018. “Tai chi chuan can improve balance and reduce fear of falling in community dwelling older adults: a randomized control trial.” *Journal of Exercise Rehabilitation* 14(6):1024–31. doi: 10.12965/jer.1836488.244.

National Health Care for the Homeless Council. 2019, February. “Homelessness & health: what’s the connection?” Accessed 6/1/2022 at <https://nhchc.org/wp-content/uploads/2019/08/homelessness-and-health.pdf>.

Rodgers, Bethany, and Taylor Stevens. 2020, December 13. “Nearly 80% of the money budgeted for Operation Rio Grande was used for policing, jail beds and court costs.” *The Salt Lake Tribune*.

World Health Organization. 2019, April 2. "Self-Care Can Be an Effective Part of National Health Systems." *World Health Organization: WHO*. Accessed 6/1/2022 at <https://www.who.int/news/item/02-04-2019-self-care-can-be-an-effective-part-of-national-health-systems>.

Wu, Yin, Yongtai Wang, Elisabeth O. Burgess, and Jerry Wu. 2013. "The effects of tai chi exercise on cognitive function in older adults: a meta-analysis." *Journal of Sport and Health Science* 2(4):193–203. doi: 10.1016/j.jshs.2013.09.001.

Yeh, Gloria Y., Caroline W. Chan, Peter M. Wayne, and Lisa Conboy. 2016. "The impact of tai chi exercise on self-efficacy, social support, and empowerment in heart failure: insights from a qualitative sub-study from a randomized controlled trial." *PLOS ONE* 11(5):e0154678. doi: 10.1371/journal.pone.0154678.

Smoke Season: Exploring the Geographies of Transient Wildfire Smoke on the Wasatch Front

Jeremy Bryson and Jeff Montague
Weber State University

ABSTRACT

Wildfire seasons around the American West have been intensifying as the effects of climate change are reshaping the region. Smoke seasons in Utah are also intensifying because when places like California and Oregon experience massive wildfires, the smoke from those fires can descend on the Wasatch Front for weeks during the late summer. This transient smoke from cross-border wildfires can cause the air quality in Utah's predominant urban region to become among the worst in the world. How are urban places along the urbanized Wasatch Front experiencing transient wildfire smoke? What efforts are state leaders making to alleviate the negative impacts of the smoke? Which residents are most impacted? What specific challenges do the smoke incursions create for the Wasatch Front's human, environmental, and economic health? How is the smoke changing the way we live in the places we live? In this paper, we explore the contested human geographies of transient wildfire smoke along the urban corridor of the Wasatch Front.

In 2015, Envision Utah, a statewide planning organization, asked more than 50,000 residents about their values and priorities concerning the current state of Utah and the prospects for the future. Among all of the areas of concern, air quality stood out. “For Utahns, poor air quality is the greatest negative attribute of their quality of life and one of their strongest concerns,” the organization wrote after evaluating the findings of their survey. Utah residents, they continued, complained that “poor air quality constrains their freedom to enjoy Utah’s beautiful outdoors and affects the state economy by discouraging businesses and employees from locating in Utah” (Envision Utah 2016). Indeed, over the last decade, Utah residents, particularly the majority of the state that lives along the urbanized Wasatch Front, might have read headlines that highlight the air quality challenge. These residents might recall the winter of 2013 when *The New York Times* claimed, “Seen as a nature lover’s paradise, Utah struggles with air quality” (Frosch 2013), and the winter of 2020 when a *Salt Lake Tribune* headline reported that “Salt Lake City’s air quality is nation’s 7th worst among large metro areas” (Maffly 2020). These and other articles highlighted the Wasatch Front’s struggles with seasonal inversions in which the region’s topography can trap automobile exhaust, heating emissions, and industrial pollution along the front. Although this wintertime seasonal air quality problem remains difficult to curb, it is largely solvable. Through a combination of cleaner fuels, regulations on types of winter heating, and industrial standards, there are potential solutions to the challenge of winter air quality.

Moreover, the Wasatch Front has another air quality challenge: summertime smoke from distant wildfires. For much of the late summer in 2021, the cities along the Wasatch Front were blanketed by persistent and sometimes very heavy smoke from wildfires burning in California and the Pacific Northwest. The smoke impacted public health outcomes and quality of life for residents and prompted news coverage that mirrored the winter headlines. *The New York Times* noted, “Booming Utah’s weak link: surging air pollution” and claimed that “wildfire smoke from California [is] making Utah’s alarming pollution even worse” (Romero, 2021). Similarly, a summer 2021 headline from *The Salt Lake Tribune* proclaimed, “Salt Lake has the worst air in the world as wildfire smoke moves in” (Pierce 2021). These headlines (and of course the lived experience of millions of Wasatch Front residents) suggest that seasonal, transitory wildfire smoke often from faraway places is a growing problem along the Wasatch Front.

The problem of late summer wildfire smoke incursions is only likely to *grow* as the Wasatch Front, and the larger American West, struggle to adapt to our changing climate. Climate research suggests that

an increase in wildfire will be one of the results from global warming in the American West (Abatzoglou and Williams 2016). The smoke from wildfires in states like California, Oregon, or Washington can travel with prevailing winds and settle along heavily populated urban centers in the American West, including the Wasatch Front. Research by Kalashnikov and associates confirmed that “in recent years, millions of people across the western US have been affected by hazardous air quality conditions caused by wildfire smoke” (2022). Other research by Wilmot et al. again confirmed the urban challenge, stating that an “expanding number of Western US urban centers face declining summertime air quality due to enhanced wildland fire activity” (2021). Indeed, in recent years, the summer season in Utah has increasingly seen its air become burdened with pollution from the transient smoke of distant wildfires. Such wildfires are becoming more common as a result of higher temperatures, increased drought, lower soil moisture, and subsequently longer fire seasons brought on by anthropogenic climate change (National Integrated Drought Information System, 2022).

Scholars have recently begun to explore how urban residents experience smoke. Urban smoke blurs human-made/natural boundaries, as we inhale and effectively embody the airborne natural waste products. As urban environmental historian Frank Uekoetter (2009, 1) observed: “one [does] not simply live with the problem of smoke, but literally in it.” The act of being immersed in smoke, as well as the act of ingesting smoke shapes the human urban experience. “As in the smoke-filled industrial cities of 19th-century Europe,” landscape architect Stephen Graham argued when comparing historic cities with contemporary cities, “these airs also inevitably shape the atmospheric, aesthetic and affective experiences of place” (Graham 2015, 201). The power of smoke to shape urban life is perhaps made more jarring when instead of coming from local industrial sources, the smoke comes from non-local rural places. Geographer Phil McManus discussed the urban experience with wildfire smoke after the 2019 fires in eastern Australia: “bushfire smoke is perceived as intrusive because it transgresses boundaries such as an urban/rural divide” (2021, 245). Thus, smoke that travels from a distant location and descends on a city temporarily has the power to disrupt the lived urban experience of residents. In this way, the geography of wildfire smoke in cities is a useful topic to reflect on.

This paper seeks to provide a framework for understanding seasonal, transitory wildfire smoke in cities—along the Wasatch Front specifically—with applications that can help us understand other western cities. Our motivating question is: How does seasonal, transitory wildfire smoke shape the urban human geography of the Wasatch Front? In this paper, we discuss a few key topics that can help us to understand how

transient smoke is impacting our urban geography: public health impacts, landscape and policy resilience, smoke nativity, and environmental justice.

Public Health Impacts

Public human health impacts are perhaps the most fundamental topic to consider when exploring the urban geography of transient wildfire smoke. Wildfire smoke is a chemically complex gaseous solution made up of the incompletely burned carbon of wood and other foliage (McManus 2021, UN Environment Programme 2022). This unburned material takes the form of particulate matter, which, when gathered together in large smoke clouds, can negatively affect visibility. The smoke-filled skies that are characteristic of wildfires contain particulates that have been shown to cause cardiovascular, neurological, and, most significantly, respiratory harm. Larger particulates of 10 microns or less (PM10) can be harmful irritants in the eyes, nose, and throat, but these larger particles can readily be eliminated through coughing or sneezing. Smaller particles of 2.5 microns or less (PM2.5) are the smoke product of most concern. These smaller particles can penetrate deep into and impact the respiratory system through asthma and chronic obstructive pulmonary disease (COPD). Additionally, wildfire smoke contains hydrocarbons, aldehydes, polyacrylic, and carbon monoxide, all of which are hazardous to human health (McManus 2021). Thus, exposure to the toxic makeup of smoke clouds can have immediate short-term health impacts, including coughing, stinging eyes, irritated sinuses, shortness of breath, chest pain, headaches, elevated heart rate, tiredness, and trouble breathing or asthma attacks, but it can also have long-term health impacts such as cardiovascular disease and neurological disorders (Centers for Disease Control 2022).

The Centers for Disease Control (CDC) and most state air quality authorities, including Utah's, observe that the health risk posed by smoke is greater for those with pre-existing conditions, such as asthma, COPD, and heart disease, which can become aggravated. People with such chronic conditions are termed "vulnerable groups" or "sensitive groups." It is worth noting that there is a growing medical recognition that there are no so-called "insensitive groups" because there are no truly safe levels of air pollution like wildfire smoke (Errigo et al., 2020).

In addition to the already problematic formulation of smoke clouds, smoke events along the Wasatch Front can trigger increased production of ground-level ozone (Horel et al., 2016). Ozone is typically already found in higher concentrations during the summer months in Utah (Maffly 2021). Ozone can exacerbate the harmful effects of particulate

matter because it causes reduced mucus production in the respiratory system, thereby allowing particulate matter to penetrate more deeply into the lungs (Maffly 2021).

As mentioned at the beginning of this paper, transient wildfire smoke is only a part of Utah's larger experience with air pollution, but it is important to keep in mind the larger context of the costs of air pollution generally in the state. An interdisciplinary group of researchers at Brigham Young University recently estimated that air pollution in the state causes between 2,480 to 8,000 premature deaths per year and reduces average life expectancy by 1.1 to 3.6 years. Additionally, this research group estimated the economic cost of air pollution to be \$750 million to 3.3 billion annually, which is roughly 1.7% of the state GDP (Errigo et al., 2020). Although transient wildfire smoke only represents a portion of these public health and economic impacts, it is likely going to become a larger portion of these impacts as wildfires increase while our climate continues to change.

Landscape and Policy Resilience

Over their long history, cities have typically proven to be adaptable and resilient to changing environmental conditions. Urban residents tend to find a way to adapt their landscapes, lifestyles, and laws to protect themselves and their communities from threats. Seasonal, transitory wildfire smoke incursions represent one of these changing environmental conditions along the urban Wasatch Front. What, then, are Utah's communities doing to adapt their landscapes and policies to meet the environmental and public health challenge of the seasonal smoke? Although it is still very early in this emerging challenge to make sure statements, the early evidence suggests that the communities are doing relatively little. There is little evidence of urban landscape change in response to this challenge: housing patterns or construction patterns have not changed, transportation systems remain as they have been, and we have not yet seen even the creation of a network of emergency shelters for severe smoke days. And while landscape changes may be slow in emerging, the policy response is also slow to emerge. Public health challenges often require some sort of community response, but to this point there appears to be an emphasis on individual rather than collective solutions for dealing with transient smoke.

In its tips for dealing with smoke, the Utah Department of Environmental Quality (DEQ) (2021) recommends that "vulnerable populations" maintain contact with their personal healthcare provider, be stocked up on medicine for at least 5 days of any smoke event, have a supply of N-95 or P-100 masks on hand, and consider purchasing indoor

air purifiers. The high cost of air purifiers, starting at about \$200, can limit the ability of individuals and families to acquire them. Notably, the Utah DEQ does not provide information on cheaper alternatives.

Further advice provided by the Utah DEQ was disseminated via Twitter by then Utah Governor Gary Herbert on September 18, 2018. This specific DEQ publication recommended individuals avoid outdoor activity, close doors and windows, not rely on standard dust masks, avoid indoor activities that increase air pollution, e.g. vacuuming and candle burning, and recirculate air in personal automobiles. The governor's tweet ended by directing concerned residents to the Utah DEQ homepage for more information. This language suggests that the state's level of concern was focused on the individual rather than the environmental conditions affecting the collective.

During smoke events it is also recommended that the fresh air intake on air conditioners be closed and that the use of evaporative coolers, like swamp coolers, be limited (Utah County Health Department, 2021). Families and individuals who do not have central air may be caught in a bind where they must endure either hot summer temperatures indoors or increased exposure to smoke.

As shown above, in their proposed solutions, Utah authorities rely heavily on individuals making choices and having access to personal resources, such as central air purification, to reduce the contribution to and impacts from smoke pollution. These recommendations depend on the public being *aware* of the current air quality to make those choices.

To spread public awareness of current air quality conditions, the Utah DEQ publishes information based on the Utah Division of Air Quality's (UDAQ) Wasatch Front Air Quality Alert System. This system uses an air quality index (AQI) score to delimit its three categories of air quality: green (0-50 AQI), yellow (51-73 AQI), Red (74+AQI). Tribby et al. (2013) determined that air quality alerts along the Wasatch Front corresponded with increases in automobile traffic, especially along mountain roads leading to areas perceived to have better air quality. This increased automobile traffic further increases local air pollution. Tribby et al. concluded that the individual health risk of being exposed to air pollution conflicted with the public responsibility to reduce contributions to air pollution, such as exhaust from automobiles. Further research into *how* air quality advisories and recommendations actually *manifest* at the individual level could prove useful for understanding current air policy shortcomings and for formulating more robust air policy in the future.

Smoke Nativity

To understand how wildfire smoke from distant places is impacting Utah and the Wasatch Front, it is important to know where the smoke comes from, a concept known as smoke nativity. At the most obvious level, the smoke is coming from wildfires. The fact that the smoke is from wildfires impacts the policy response because wildfires are an “exceptional event” under federal Clean Air Act regulations. “Exceptional events,” the Utah Department of Environmental Quality (2019) states, “are unusual or naturally occurring events that can affect air quality but are not reasonably controllable.” States, therefore, are not accountable to minimize these smoke events to meet the National Ambient Air Quality Standards. The Utah DEQ continues to explain that because the US Environmental Protection Agency defines a “natural event” as “an event in which human activity plays little or no direct causal role,” then surely wildfires in other western states, which are exacerbated by anthropogenic climate change, should not be something with which state regulators need to concern themselves.

Smoke nativity matters in other ways as well. Most of the summertime wildfire smoke that descends on the Wasatch Front during the late summer months travels along wind currents from states like Washington, Oregon, and California. The fact that the smoke travels across state lines dramatically impacts the possibility for any type of smoke management. What, after all, can state leaders do when the noxious pollutant is coming from outside the state? It seems that in addition to putting the responsibility for staying safe from wildfire smoke squarely on the shoulders of citizens, state lawmakers can also point fingers at the states with the fires, most notably California. On September 16, 2020, US Senator Mike Lee of Utah argued that the wildfires of California and Oregon were not caused by climate change, but by mismanagement of California’s forests (Davidson 2020). The historic fire suppression practices undertaken by the US Forest Service have in fact led to the immense buildup of fuel in federally managed forests, which enables the formation of large uncontrollable crown fires (Lozano, 2020). A few weeks prior to Lee’s comments in August 2020, then-President Donald Trump blamed the state of California for its wildfires, *despite* most of the burning occurring in federally managed forests (White 2020). Utah residents, in response to an August 2020 tweet from Utah Governor Spencer Cox echoed this commentary, recommending that someone apply pressure to California to “fix their idiotic forest management” (@DaleARex 2021), asking whether Utah could “sue California for incompetent fire prevention practices” (@dinopontino 2021), and suggesting that the smoke was another way

that “California invades and makes challenges for us” (@MeestaMilla, 2021). Knowing that that much of the smoke is coming from states like California shapes the way that Utah responds to the smoke incursions.

Environmental Justice

It is tempting to say that once the wildfire smoke comes from California, it blankets the Wasatch Front equally and so it impacts all residents equally. After all, all residents breathe the same air. Indeed, although smoke does not discriminate by age, sex, income, or race, the distribution of the smoke’s impacts affects some Wasatch Front residents more than others. As such, transient wildfire smoke is an important and emerging environmental justice issue in urban settings in the American West.

A generation of environmental justice literature has proven again and again that low-income residents tend to experience more negative environmental conditions than their neighbors in higher income neighborhoods (Brulle and Pellow 2006, Pulido 2017). Environmental justice is similarly a socioeconomic problem along the Wasatch Front as well (Collins and Grineski 2019, Jones 2021). Consider the challenge of indoor smoke exposure on the heaviest wildfire smoke days. The best way to avoid smoke inhalation is to stay indoors with air conditioning and an air purifier. Low-income residents are less likely to have central air conditioning and more likely to have evaporative cooling in their homes. Evaporative cooling systems do not filter air nearly as effectively as central air systems. Likewise, the cost of purchasing, maintaining, and powering a standalone air purification unit can be prohibitive to lower-income residents. Additionally, lower-income housing is more likely to have a leaky building envelope, which allows the smoky air to penetrate the house, regardless of other measures that the residents might take.

Another especially vulnerable group to smoke pollution is children (Holm et al. 2021). Holm et al. noted that exposure to wildfire smoke can result in decreased lung development and an increased likelihood of asthma, exposure to particulate matter is increasingly shown to be associated with ADHD and autism, and ultra-fine particles can potentially cross the blood-brain barrier, which can result in worse memory and decreased school performance. Because of these health and education implications, the organization Utah Physicians for Healthy Environment (UPHE) called on the Utah State Legislature to fund the \$30-40 million dollar acquisition of individual room air purifiers for the state’s classrooms (Utah Physicians for Healthy Environment 2021). State Representative Doug Owens took up this campaign, but the call was not heeded by the legislature, and no such air purifier procurement

was passed. The failure of the State of Utah to acquire pollution-removing air purifiers for its public schools is characteristic of its flawed strategy for mitigating the harmful effects of smoke pollution.

Conclusion

As climate change continues to impact the American West, transient wildfire smoke will endure as a significant part of late summer along the urban Wasatch Front. There are many pressing questions to consider about how these seasonal smoke incursions are changing and will continue to change life in the urban region. As a starting point, it is important to consider the variety of public health impacts created by the temporary smoke, the potential for landscape and policy resilience at the community level, and the important role of smoke nativity, all while remaining sensitive to the environmental justice questions surrounding smoke exposure. Only if scholars, residents, and decision-makers consider these and other topics will we be able to adapt in such a way that we can avoid the most negative consequences of transient smoke on the Wasatch Front.

References

- Abatzoglou, J.T., & Williams, A.P. (2016). Impact of anthropogenic climate change on wildfire across western US forests. *Proceedings of the National Academy of Sciences*, 113(42), 11770–11775. <https://doi.org/10.1073/pnas.1607171113>
- Brulle, R., & D. Pellow. (2006). Environmental justice: human health and environmental inequalities. *Annual Review of Public Health* 27, 103–24. doi: 10.1146/annurev.publhealth.27.021405.102124
- Centers for Disease Control and Prevention. (2022). Protect yourself from wildfire smoke. Retrieved March 9, 2022, from <https://www.cdc.gov/air/wildfire-smoke/default.htm>
- Collins, T.W., & Grineski, S.E. (2019). Environmental injustice and religion: outdoor air pollution disparities in metropolitan Salt Lake City, Utah. *Annals of the American Association of Geographers*, 109(5), 1597–1617. doi: 10.1080/24694452.2018.1546568

@DaleARex. Dale Rex. Maybe it's time to apply some pressure to California and their idiotic forest management. Posted August 6, 2021. Accessed February 10, 2022. <https://twitter.com/DaleARex/status/1423716404721635328?t=YCmLXYDQwG8Eb4COmJeP0A&s=19>

Davidson, L. (2020, September 17). Utah Sen. Mike Lee says California wildfires caused by mismanagement, not climate change. *The Salt Lake Tribune*. Retrieved March 10, 2022, from <https://www.sltrib.com/news/politics/2020/09/16/utah-sen-mike-lee-says/>

@dinopontino. Can we sue California for incompetent fire prevention practices? Posted August 6, 2021. Accessed February 10, 2022. <https://twitter.com/dinopontino/status/1423690626134994949?t=09D1T5xGcjMTZT60leXhNg&s=19>

Envision Utah. (2016, January 5). Background: air quality in Utah. Retrieved May 20, 2022, from <https://yourutahyourfuture.org/topics/air-quality/item/44-background-air-quality-in-utah>

Errigo, I.M., Abbott, B.W., Mendoza, D.L., et al. (2020). Human health and economic costs of air pollution in Utah: an expert assessment. *Atmosphere*, 11(11), 1238. doi: 10.3390/atmos11111238

Frosch, D. (2013, February 26). Utah, a nature lover's haven, is plagued by dirty air. *The New York Times*. Retrieved May 20, 2022, from <https://www.nytimes.com/2013/02/24/us/utah-a-nature-lovers-haven-is-plagued-by-dirty-air.html>

Graham, S. (2015). Life support: The political ecology of urban air. *City*, 19:2-3, 192-215. DOI: 10.1080/13604813.2015.1014710

Holm, S.M., Miller, M.D., & Balmes, J.R. (2021). Health effects of wildfire smoke in children and public health tools: a narrative review. *Journal of Exposure Science and Environmental Epidemiology*, 31(1), 1-20. doi: 10.1038/s41370-020-00267-4

Horel, J., Crosman, E., Jacques, A., et al. (2016). Summer ozone concentrations in the vicinity of the great salt lake. *Atmospheric Science Letters*, 17(9), 480-486. doi: 10.1002/asl.680.

Jones, E.N. (2021). Environmental racism in a growing city: investigating demographic shifts in Salt Lake City's polluted neighborhoods. Utah State University Undergraduate Honors Capstone Projects. 699. <https://digitalcommons.usu.edu/honors/699>.

Kalashnikov, D.A., Schnell, J.L., Abatzoglou, J.T., Swain, D.L., Singh, D. (2022). Increasing co-occurrence of fine particulate matter and ground-level ozone extremes in the western United States. *Science Advances*, 8(1): eabi9386. doi: 10.1126/sciadv.abi9386.

Lozano, A.V. (2020, October 18). Decades of mismanagement led to choked forests—now it's time to clear them out, fire experts say. NBC News. Retrieved March 10, 2022, from <https://www.nbcnews.com/news/us-news/decades-mismanagement-led-choked-forests-now-it-s-time-clear-n1243599>.

Maffly, B. (2020, January 31). Salt Lake City's air quality is nation's 7th worst among large metro areas. *The Salt Lake Tribune*. Retrieved May 20, 2022, from <https://www.sltrib.com/news/environment/2020/01/28/salt-lake-citys-air/>.

Maffly, B. (2021, August 7). Air quality remains poor as West Coast smoke continues to linger over much of Utah. *The Salt Lake Tribune*. Retrieved March 10, 2022, from <https://www.sltrib.com/news/environment/2021/08/07/air-quality-remains-poor/>.

McManus, P. (2021) A more-than-urban political ecology of bushfire smoke in eastern Australia, 2019–2020. *Australian Geographer*, 52(3), 243-256. doi: 10.1080/00049182.2021.1946244.

@MeestaMilla. In some way or shape, California invades and makes challenges for us. Posted July 11, 2021. Accessed February 10, 2022. <https://twitter.com/MeestaMilla/status/1414325868357324800?t=RftgaAvl5IxOe4PpLVd8oQ&s=19>.

National Integrated Drought Information System. (2022). Wildfire Management. *Drought.gov*. Retrieved March 10, 2022, from <https://www.drought.gov/sectors/wildfire-management>.

Pierce, S. (2021, August 7). Salt Lake has the worst air in the world as wildfire smoke moves in. *The Salt Lake Tribune*. Retrieved May 20, 2022, from <https://www.sltrib.com/news/2021/08/06/west-coast-wildfire-smoke/>.

Pulido, L. (2017). Geographies of race and ethnicity II: Environmental racism, racial capitalism and state-sanctioned violence. *Progress in Human Geography*, 41(4), 524-533. doi: 10.1177/030913251664649.

Romero, S. (2021, September 8). Utah's air quality is worsening during drought. *The New York Times*. Retrieved May 20, 2022, from <https://www.nytimes.com/2021/09/07/us/great-salt-lake-utah-air-quality.html>.

Tribby, C.P., Miller, H.J., Song, Y., Smith, K.R. (2013). Do air quality alerts reduce traffic? An analysis of traffic data from the Salt Lake City metropolitan area, Utah, USA. *Transport Policy*, 30, 173-185. doi: 10.1016/j.tranpol.2013.09.012.

Uekotter, F. (2009). *The Age of Smoke: Environmental Policy in Germany and the United States, 1880–1970*. University of Pittsburgh Press, Pittsburgh, PA.

UN Environment Programme. (2022, February 23). Spreading like wildfire: the rising threat of extraordinary landscape fires. Retrieved May 20, 2022, from <https://www.unep.org/resources/report/spreading-wildfire-rising-threat-extraordinary-landscape-fires>.

Utah County Health Department. (2021, August 6). Wildfire smoke. Retrieved March 10, 2022, from <https://health.utahcounty.gov/2021/08/06/wildfire-smoke/>.

Utah Department of Environmental Quality. (2019, June 25). Exceptional Events Program. Retrieved May 20, 2022, from <https://deq.utah.gov/air-quality/exceptional-events-program>.

Utah Department of Environmental Quality. (2021, August 25). Health Impacts of Wildfire Smoke. Retrieved March 10, 2022, from <https://deq.utah.gov/air-quality/health-impacts-of-wildfire-smoke>.

Utah Physicians for Healthy Environment. (2021, August 12). An urgent necessity: classroom air purifiers for Utah's school children. Retrieved March 10, 2022, from <https://www.uphe.org/2021/08/12/classroom-air-purifiers-for-utahs-school-children-is-now-an-urgent-necessity/>.

White, J. (2020, August 20). Trump blames California for wildfires, tells state “you gotta clean your floors.” POLITICO. Retrieved March 10, 2022, from <https://www.politico.com/states/california/story/2020/08/20/trump-blames-california-for-wildfires-tells-state-you-gotta-clean-your-floors-1311059>.

Wilmot, T.Y., Hallar, A.G., Lin, J.C., Mallia, D.V. (2021). Expanding number of Western US urban centers face declining summertime air quality due to enhanced wildland fire activity. *Environmental Research Letters*, 16(5), 054036. doi: 10.1088/1748-9326/abf966.

Abstracts

ARTS

Novel: *Witchstead* Chapter 1

Kayla Todd

Weber State University

Witchstead is a work of fiction that draws influence from authors such as J. R. R. Tolkien and J. K. Rowling, and it is meant for young adult audiences. The book takes place in a fictitious world and is set in a time period similar to our 1700s. In the first chapter, the main character, who is the daughter of a small town farmer, is summoned to take part in the annual Testing, along with the rest of her age group. When she unexpectedly passes the Test, she finds herself forcibly separated from her family and everything she knows to attend *Witchstead Academy*, where she will grow in her newfound abilities.

ARTS

Yankee Doodle Dandy: The Role of Yankee Doodle in the American Revolution

Ethan Walton

Brigham Young University

Every kindergartener throughout America is familiar with the timeless tune known as “Yankee Doodle.” However, most adults do not recognize the significant role this song played before, during, and after the Revolutionary War. A simple children’s song was once an anthem of triumph. Although originally written by Richard Schuckburg in the 1750s to mock untrained colonial militiamen, “Yankee Doodle” converted into a strong political statement against British oppression. The Americans took an insult and turned it into a weapon of morale warfare used against enemy forces. The American soldiers of the Revolutionary War set a valuable precedent regarding the power of music, the influence of attitude, and the vitality of resilience. By the end

of the American Revolution, “Yankee Doodle” had converted into a manifestation of American determination. Without “Yankee Doodle” and the pattern it demonstrated, American victory may not have been possible. If a group of untrained, unprofessional militiamen could defeat the world’s greatest superpower nation with the appropriate actions and reactions, what are their successors capable of? The proper attitudes and resilience can turn the worst circumstances into the most beneficial scenarios. Perspective is everything.

ARTS

Immigrants and Indigeneity in the Original “West Side Story” Film

Thomas Jenson

Brigham Young University

The 1961 film version of “West Side Story” at first glance presents a dichotomy between immigrant Sharks and native Jets, the two gangs battling for turf on the West Side of Manhattan in the 1950s. The film goes on to unsettle that dichotomy by emphasizing the Sharks’ origins in Puerto Rico, a territory of the United States, and by exposing the foreignness of the Jets, whose parents immigrated from Eastern Europe. While most of the critical discussion around “West Side Story” focuses on the film’s exoticization of the Sharks, my analysis points out how the systems of power do not endorse the Jets as fully American either. As the Sharks and the Jets grapple with contradictory standards of ethnic citizenship, “West Side Story” unravels what it means to be native to America. Ultimately, I argue that the film makes two moves. First, it establishes a hierarchy of ethnic groups with native Anglo-Americans on top followed by European immigrants and then Puerto-Rican immigrants. The second move is to use that ethnic hierarchy to justify the displacement of foreigners under the banner of urban renewal. While the Sharks and the Jets fight over the streets amongst themselves, bickering over who is more American than the other, a more sinister force lurks behind them in the form of city planners. The rumble between the gangs, which leaves them in pieces, opens the door for an outside force to enter and “clean up” the streets; the death of so many characters suggest the dysfunction of immigrant communities and the necessity of slum clearance.

ARTS

Haunting Shadows

Jenessa Trimble

Weber State University

Ian Holmes, an Army veteran, suffers from PTSD that is mediated by the presence of his psychiatric service dog, Sasha. Sasha's skills are tested when Ian, thrown off balance by a difficult morning, is triggered during a seemingly simple trip to the mall. A polyphonic short story, "Haunting Shadows" alternates between the perspectives of Ian, his therapist, his friend Kylie, and Sasha.

BIOLOGICAL SCIENCES

Hand Dryers Serve as a Reservoir for Antibiotic-Resistant Bacteria

Ashlynd Greenwood, Colette Mortensen, Michele Culumber, and Craig Oberg

Weber State University

Automatic hand dryers at Weber State University were installed in most restrooms to improve convenience, decrease paper waste, and increase hygiene. However, previous research has shown hand dryers act as a reservoir for pathogenic bacteria. The purpose of this experiment was to isolate bacteria from hand dryers, characterize their antibiotic resistance profiles, and then identify these bacteria. Hand dryers from 32 high-traffic restrooms in four buildings were sampled. A 10-cm² area at the bottom of the drying chamber was sampled using a 3M Quickswab. Swabs were used to inoculate MSA, TSA, EMB, and SBA plates, which were incubated at 37°C for 24–48 h with 73 isolates selected. Isolates were transferred to TSB broth and grown at 37°C for 24 h and then screened for resistance to five antibiotics—ampicillin, vancomycin, tetracycline, penicillin, and chloramphenicol—utilizing the Kirby-Bauer method. Isolates that showed antibiotic resistance were identified using 16S rRNA gene sequence analysis. Forty-four isolates showed resistance to one antibiotic, with 42 resistant to at least two antibiotics. The majority of the isolates were resistant to penicillin, but a few were also resistant to vancomycin. The most common isolates among the penicillin-resistant organisms were common human commensal *Staphylococcus* sp. including, *S. warneri*, *S. intermedius*, *S. saprophyticus*, and *S. aureus*.

We also found representatives of environmental bacteria including *Bacillus pumilus*, *B. velezensis*, and *B. subtilis*. Less common were Gram-negative bacteria including *Enterobacter hormaechei* and *Mixta calida*. All identified species have the potential for opportunistic infections. We have shown that antibiotic-resistant bacteria are present in electric hand dryers and may represent a significant source of community-acquired antibiotic-resistant infections. To prevent bacterial contamination and the spread of antibiotic resistance during hand drying, the hand dryers' inner chamber should be thoroughly cleaned with a disinfectant on a daily basis.

BIOLOGICAL SCIENCES

Amino acid decarboxylation is a potential source of CO₂ production in cheese by *Paucilactibacillus wasatchensis* WDC04

Kate Sorensen, George Barrera, Michele Culumber, Matthew Domek, Craig Oberg, Taylor Oberg, and Donald McMahon
Weber State University

Paucilactobacillus wasatchensis (WDC04) is a non-starter lactic acid bacterium that is linked to unwanted late gas production in cheddar cheese. Recent research has shown that this organism has the capability of utilizing the pentose phosphate pathway, following the removal of CO₂ from a 6-carbon sugar, such as galactose. However, WDC04 has still been known to produce splits and cracks in cheddar cheese in the absence of these sugars. In cheese production trials, more CO₂ is released than can be accounted for by added carbon substrates. One possible source of gas production could be the decarboxylation of free amino acids with the formation of biogenic amines. The ability of lactic acid bacteria to decarboxylate amino acids varies greatly but can be used to generate proton motive force. Putrescine and cadaverine, the decarboxylation products of ornithine and lysine, respectively, have been detected in cheese inoculated with WDC04. The purpose of this study was to determine if lysine and ornithine could be utilized for growth by WDC04 and if decarboxylation would lead to gas production. The incomplete *P. wasatchensis* WDC04 genome (GenBank accession number GCF_000876205.1) was analyzed for decarboxylation enzymes. In this research, an ornithine decarboxylase was found, but a lysine decarboxylase was not. Carbohydrate-restricted MRS (CR-MRS) with 100-700 mM of lysine or ornithine was inoculated with *P. wasatchensis*

WDC04 in 24-well plates and incubated at 30°C. Oxyrase (2%) was added to create anaerobic conditions. Growth curves were monitored by measuring turbidity over 72 h on a Tecan Infinite M200 plate reader. Without the addition of ribose (1%), neither amino acid supported growth above the media alone. However, amino acid decarboxylation may still be the source of excess CO₂ production without the amino acids being used as a growth substrate. Further culture-based analysis will determine if the amino acids contribute to gas release by *P. wasatchensis* WDC04.

BIOLOGICAL SCIENCES

Physiochemical basis of high salinity tolerance in an obligate halophyte *Suaeda fruticosa*

Abdul Hameed¹, Bilquees Gul¹, and Brent L. Nielsen²

¹Dr. Muhammad Ajmal Khan Institute of Sustainable Halophyte Utilization, University of Karachi; ²Brigham Young University

A thorough understanding of salinity tolerance mechanisms of halophytes, the natural flora of saline habitats, could benefit efforts to breed salinity-tolerant crops. This is important for crop production in saline soils and is an uphill task as there are still many unanswered questions about salinity tolerance. We examined growth, water relations, ion homeostasis, photosynthesis, and oxidative-stress mitigation responses of an obligate halophyte *Suaeda fruticosa* to increasing salinity. Most growth parameters increased in moderate salinity (300 mM NaCl) with effective osmotic adjustment and accumulation of Na⁺, which did not accompany nutrient deficiency, damage to photosynthetic machinery, or oxidative damage. In contrast, high salinity (900 mM NaCl) caused some reduction in growth, which coincided with a decline in sap osmotic potential and higher Na⁺ accumulation. However, Na⁺ buildup under high salinity did not cause a decline in relative water content or maximum quantum yield of PSII or an increase in oxidative damage (H₂O₂ and MDA). Hence, it appears that physiochemical modulations enable *S. fruticosa* to grow optimally under moderate salinity, while growth reduction in high salinity might be the result of increased energetic costs rather than ionic toxicity.

BIOLOGICAL SCIENCES

A Longitudinal Study of Acceptance of Evolution in a University Setting from 2011-2021

Sawyer T. Baum and T. Heath Ogden

Utah Valley University

Acceptance of evolution has been growing among the general population in the United States over the last decade (2010-2020), increasing from 40% to 54%, or even 80%, depending upon the format of the question. Many factors influence the acceptance of evolution, including education, role models, religion, age, and the format of the question. The objective of this study was to evaluate the long-term trends of evolution acceptance of students in a public open-enrollment university (as an overall representation of the general public). This study used surveys taken from Introductory Biology classes (non-majors) at a large public university in Utah from 2011 through 2021. Students were asked to fill out the survey prior to the semester's instruction and towards the end of the semester. We found that the proportion of students who accept evolution increased from 25% in 2011 to 44% in 2021 prior to any instruction. Using a forecast model, if current conditions and trends were to remain the same, the positive trend would continue with an estimated 53% of the participants accepting evolution in 2025.

BIOLOGICAL SCIENCES

Maintenance and Expression of Redundant Carbapenem Resistance Mechanisms in the Prolonged Absence of Antibiotic Pressure

Taalín Hoj, Allison Brower, and Richard Robison

Brigham Young University

Constant exposure to antibiotics in a hospital setting creates an environment that encourages bacteria to acquire and maintain antibiotic resistance mechanisms. The most difficult to treat of these resistant bacteria are carbapenem-resistant enterobacteriaceae (CRE), which are resistant to last-resort antibiotics such as carbapenems. Previous studies have indicated that a prolonged absence of antibiotic pressure will reduce antibiotic resistance in resistant strains, as bacteria are extremely efficient at maintaining and expressing only necessary genes. This raises

the question as to whether strains with multiple resistance mechanisms will maintain redundant mechanisms in the prolonged absence of antibiotic pressure. We aim to answer if and how quickly strains lose resistance and to identify the mechanism by which such loss occurs. Two clinical CRE isolates with multiple resistance mechanisms (Strain 1: NDM, CMY, OXA-2, TEM, ompF; Strain 2: NDM, CTX, CMY, OXA-2, ompF) were grown from April to October 2021 in the absence of antibiotic pressure. During this time, minimum inhibitory concentrations (MICs) to doripenem and aztreonam were performed to measure loss of resistance. PCR was performed to measure either loss or downregulation of resistance mechanisms. MIC data indicated that both isolates gradually lost resistance over time but never became fully susceptible to either antibiotic. qPCR data from strain 1 indicated an 8.71-fold drop in the number of CMY DNA copies from April to July 2021 and a 22.69-fold drop from April to August 2021. This presents a possible explanation of the loss of the resistance phenotype, in that fewer gene copies were present during prolonged absence of antibiotic pressure. PCR data indicated no downregulation or loss of ompF, which may explain the incomplete return to a fully susceptible resistance phenotype.

BIOLOGICAL SCIENCES

Exploring Environmental Reservoirs for *Paucilactobacillus wasatchensis*

Niharika Mishra, Michele Culumber, Karen Mann, and Craig Oberg

Weber State University

Paucilactobacillus wasatchensis is a NSLAB preferentially utilizing ribose sugar, which can liberate carbon dioxide from six carbon sugars such as galactose. This organism is a primary cause of late gas defect in cheese resulting in post-processing problems and consumer rejection. *P. wasatchensis* is a contaminant in the cheese industry, but its environmental source is unknown. Previous work showed *P. wasatchensis* does not survive pasteurization, and microbial surveys of cheese-manufacturing facilities have not detected *P. wasatchensis*, yet closely related organisms have been isolated from silage and compost. We hypothesize that *P. wasatchensis* resides in the environment around the dairy cows and contaminates milk during the milking process. Samples of corn silage, hay silage, pre-compost manure, post-compost manure, and sugar beetroot pulp were collected at the USU Caine Dairy

Farm. Samples were homogenized, diluted, and plated on two agar media (MRS + 1% ribose and MRS + 1% ribose + 10 µg/ml vancomycin) and incubated anaerobically at 25°C. Visible colonies were marked on plates after 2 d, and then plates were incubated for 7 d. Unmarked colonies were selected and incubated in gas detection broth (MRS + 0.3% ribose + 0.7% galactose) containing a Durham tube for 72 h to identify gas-producing isolates. The 16S rRNA gene from these isolates was analyzed using BLAST. While *P. wasatchensis* was not found in the samples, isolate PCR/V2 from pre-compost samples was 94.98% similar. API 50CHL results for PCR/V2 indicate the organism was a closely related species. Analysis of DNA extracted directly from the same environmental samples using 16S rRNA gene sequencing also showed negative results for *P. wasatchensis*. Our results did not find *P. wasatchensis* in any silage or compost samples, which have been suggested as the source of this organism based on the previous isolation of closely related species (*P. hokkaidonensis* and *P. vaccinostercus*).

BUSINESS

Seasonality of Frequency and Intensity in Consumer Complaints: A Sentiment Analysis Approach

Reagan Siggard, Yong Seog Kim

Utah State University

Is there a time of year when consumers are more intense in their complaints regarding financial products and services? Consumer complaints and reviews are pervasive in current competitive digital marketplaces as they provide consumers with valuable information about services and products. Consumers may refrain from purchasing items when they find strong negative reviews more frequently than positive reviews. At the same time, consumer behavior is known to be affected by seasonal changes and events. This temporal imbalance phenomenon of consumer shopping behavior is often expressed in total sales or other key performance indicators. This phenomenon forces many business entities to develop their marketing and operational strategies around shifts in consumers' seasonal needs. This abstract presentation focuses on detecting the seasonality of frequency and intensity in consumer complaints of financial products and services over multiple years using data obtained from the Consumer Financial Protection Bureau (CFPB). Our research focuses on temporal patterns and their potential relationship with seasonal dynamics by measuring the change in the number of

positive and negative complaints and the emotional intensity of the complaint narratives. Our analysis finds that seasonal patterns of frequency of consumer complaints differ from the intensity of the narratives. We also observed twice as many positive narratives as negative ones; however, the overall sentiments of the narratives on temporal checkpoints (e.g., monthly and quarterly) were negative because of many strong negative complaints. Additionally, we identify root causes across all quarterly dimensions that affect the frequency and intensity of complaint narratives. The purpose of our abstract presentation is to provide an overview of the data collection process used to retrieve and store the 160,490 consumer complaint narratives from the CFPB, demonstrate our text mining and sentiment analysis processes, and provide insight and recommendations into seasonal dynamics and consumer complaints in the financial product sector.

BUSINESS

Graduate School Admission Webpages: Analysis of Marketing Messages for Gendered Marketing Themes

Paige Gardiner, Madison Johnson, Dalton Droubay

Southern Utah University

Great strides have been made by American graduate business and law schools to recruit and graduate competitive female students. Increasing marketing messages about program format options, positive career outcomes for women, and programs that bridge the gap between undergraduate programs and graduate programs have persuaded more female students to apply to graduate school. As the number of female students attending graduate business and law schools is reaching parity with male students, will these female-gendered marketing messages continue to be used to recruit female students? Our research aims to understand how business and law schools in the Western United States market to female students through the graduate school admission webpage. To understand gendered marketing messages for business and law graduate students, we provide a review of the literature regarding female graduate school choice model, perceived influence of the graduate website admissions page, and gendered marketing messages. Next, using a qualitative media analysis, we examined 25 business and law schools in the Western United States for frequency and type of gendered college choice marketing messages. As the number of female and male graduate business and law school students reaches parity, we

offer conclusions, implications, and ideas for future research that will continue to market and promote prospective female students to apply to graduate business and law school.

BUSINESS

Business Ethics Education in Utah: A Look at Higher Education

Chelsea Dye, Dara Hoffa, Ron Mano (posthumously)

Westminster College

Utah suffers from the dubious nickname of “The Fraud Capital of the World” time and again. Utahans have fallen prey to the unethical practices of fake practitioners and suspicious swindlers. In recent years, the State of Utah implemented several different programs to shed that moniker, working mainly from the consumer angle. This paper takes a preventative approach, through the examination of business ethics education in Utah’s colleges and universities. This paper examines the importance of ethics education and the unique situation of higher education in Utah and provides a detailed breakdown of how ethics are taught in the state, concluding with recommendations on how to move forward.

BUSINESS

Elderly Abuse Fraud—A Forensic Accounting and Legal Case

Jeff Davis and Hal Davis

Weber State University and Davis & Sanchez, PLLC

Fraud is a challenge in the world today. One of the most heinous ways to commit fraud is by elderly abuse. This article explains an actual elderly abuse fraud case of a man who suffered from short-term memory loss likely from some level of dementia. The article tells the actual story of the people (no real names), events, transactions, financial and legal issues, and outcome of the case. The article also discusses the events that led to the investigation. The article provides the investigative processes that were used to obtain forensic evidence in support of the legal facts and issues of the case and that led to the final outcome from a legal

standpoint. The article lays out the fraud as related to the fraud triangle, which includes (1) an opportunity or access to assets and or accounting records, (2) a perceived need, and (3) rationalization of the fraudulent actions. Finally, the article presents some suggestions as to how the elderly might be protected from some financial abuse.

BUSINESS

Data Science and Analytics: A Data-Driven Decision-Making Approach for Business

Amar Sahay

Salt Lake Community College

Data science—a data-driven decision-making approach—is the most desired field in driving business decisions. Using data science, decision makers extract insights and knowledge from structured and unstructured data, develop algorithms and models that help improve processes, and make key business decisions. The models are widely used in data-driven decisions, machine-learning, and predictive analytics to predict future outcomes. This paper explores the key topics in data science and analytics and provides an overview of (i) data science’s scope, its evolution, and its relationship with other disciplines, (ii) the field of business intelligence, which investigates historical data to better understand business performance, thereby improving performance, and creating new strategic opportunities for growth, (iii) business analytics and the three major categories of business analytics, the descriptive, predictive, and prescriptive analytics, along with advanced analytics tools explained using flow diagrams outlining the tools of each of the descriptive, predictive, and prescriptive analytics, (iv) the most widely used predictive analytics models including regression, classification, forecasting, data mining and machine learning–based models and applications, (v) business analytics, business intelligence and their relation to data science, (vi) data science and software tools in data science and analytics, (vii) data visualization using Excel and other software, (viii) statistical tools in data science’s inferential and probability concepts, and (ix) machine learning and R-statistical software in data science. the paper is motivated by the booming interest in data science and business analytics. It explores the key models and applications in both areas.

BUSINESS

Investigating Bracketed Difference-in-Difference Estimation: A Simulation Study

Anthony Frazier, Julian Chan

Weber State University

Difference-in-difference (DiD) estimation is a commonly used and widely known statistical method of estimating causal effects of a particular treatment over time. Unfortunately, regular DiD estimation often neglects unmeasured confounding variables that bias the treatment effect (TE) estimate. To adjust for possible confounders, Hasegawa et al. proposed Bracketed DiD estimation, which provides an interval of possible DiD estimates. In this paper, we simulate a multitude of scenarios to test the effectiveness of Bracketed DiD estimation. We also propose and investigate several DiD estimators that utilize Bracketed DiD estimates. First, we find the interval generated by Bracketed DiD estimation correctly captures the true TE at varying rates, depending on violations of DiD assumptions or other changes in data characteristics. Second, we find the DiD estimator that adjusts for variances in control groups generally predicts the true TE most accurately. We conclude by discussing in what circumstances Bracketed DiD estimation is most effective and comparing the accuracy of different DiD estimators.

BUSINESS

Bracketed Difference-in-Differences Estimation to Measure the Effect of Medical Marijuana Laws on Violent Crime

Julian Chan, Gavin Roberts, Anthony Frazier

Weber State University

The difference-in-differences (DiD) model is a popular statistical model in economics that can estimate the effect of a policy on an outcome variable. It is often difficult for researchers to assess the validity of the assumptions of the DiD model when using observational data. Hasegawa et al. introduced a bracketed DiD approach that provides an unbiased interval estimate of the treatment effect in some such cases when the influence of the confounder in certain situations. We implement these DiD approaches to estimate the effect of medical marijuana legislation

on violent crime rates. Recent estimates of the effect of medical marijuana legislation on violent crime rates vary significantly.

BUSINESS

Desired Leadership Traits in First Bosses: A Study of Extant Leadership Theories Using Generation Z College Students

James Brau, Jameson Brau

Brigham Young University, Gonzaga University

In this paper, we document the extant theories of business leadership and partition them into main threads (e.g., great man theory, trait theory, contingency theory) Next, we examine the sociocognitive literature on Generation Z and formulate hypotheses of desired leadership traits in first bosses. We then conduct a comprehensive survey gathering data from 700+ undergraduate college students, asking them what preferred traits they would like to have in their first boss upon graduating from college. Empirical analyses are then conducted to test the various hypotheses pertaining to the extant leadership theoretical camps.

BUSINESS

Setting Context and Expectations in Adult Education

Todd J. Wentz

Ensign College

Malcolm Knowles's insights into how adults prefer to be engaged in instructional environments are well known, but some opportunities for application of these insights are missed because of an emphasis on pedagogical techniques in teacher and instructor training programs. Although vital, pedagogical approaches may be insufficient to engage the most driven or demanding of adult learners. A simple three-question exercise has been demonstrated to open the student to the context of a course of information and to provide a framework of respect and inclusion for all participants regardless of previous educational or professional exposure. This presentation will walk through some real-life examples of how this process has benefited educators and students

and successfully set the stage for better engagement and learning for university-level students.

BUSINESS

An Econometric Analysis of Inventory Turnover: Expanding the Gaur, Fisher, and Raman (2005) Three-Factor Model Up and Down the Supply Chain

James Brau, Rebekah Brau, Joe Henry, Peter Christensen

Brigham Young University, Rowan University

Gaur, Fisher, and Raman presented a three-factor model to explain inventory turnover within firms. To the three factors of gross margin ((sales – COGS / sales), capital intensity (GFA / [AvInv + GFA]), and sales surprise (sales / expected sales)), we add factors for the inventory turnover of firms above and below each firm in the supply chain. We test two hypotheses, the JIT displacement hypothesis, specifically that suppliers and customers have negatively correlated inventory turns [$\rho(\text{ITC}, \text{ITS}) < 0$] and the JIT integration hypothesis, that suppliers and customers have positively correlated inventory turns [$\rho(\text{ITC}, \text{ITS}) > 0$]. Our empirical evidence provides general support for the JIT integration hypothesis, although with some intertemporal nuance.

BUSINESS

Global Commercial Civilization

Edward G. Engh

Salt Lake Community College

Earth operates under a single global commercial civilization (GCC), which continually evolves, growing as the roots of a tree weaving around obstacles. Humanity is a social organism sustained by commerce. Traditional national and institutional systems are becoming obstacles to commerce. National, political, social, and ideological institutions struggle to find a useful way to contribute, while some show signs of decay and obsolescence. A de-facto world state exists as a GCC, not as a traditional nation-state or aggregation of states. Commerce is a global process of attraction within and between communities, drawing them together, whereas war and ideology tend to repel. Commerce attracts

from a distance, while fostering civic-virtue, formation of democratic institutions. War infects with the urge to use violence, and ideology often infects with intolerance and animosity. Commerce fosters democratic and republican forms of political discourse. Trade fosters intellectual commerce of knowledge, technology, civility, and liberal education, challenging ideologies and nations who would otherwise resort to war. Commerce becomes a teacher of the world, engendering trust. Commercial republics and democracies form new institutions to protect trade, by which the commercial civilization survives. Commerce becomes decadent through centralization and privatization of interests, when former trading communities are alienated from each other. Communities and institutions struggle to catch up with facts. GCC is a physical and social reality. Commerce may have had greater evolutionary influence than either war or religion. Physical and social facts of global commerce and civilization are described.

BUSINESS

Academic Success and Comparison of Beginning, Intermediate, Senior, and Graduate Accounting Students: Self-Assessment of Self-Efficacy, Emotional Intelligence, Self Determination, and Regulation

Jeff Davis

Weber State University

A rich history of research in self efficacy (SE), emotional intelligence (EI), self-determination (SD), self-regulated learning (SRL) indicates students have better academic success when they perceive that they have higher levels of SE, EI, SE, and SRL. Some of this research also indicates professionals in the workplace also benefit from having perceived higher levels of these same cognitive constructs. This article explains and analyzes the results of a survey given to accounting students in different class levels (beginning (B), intermediate (I), senior (S), and graduate (G)) as they prepare for a career in accounting and business. The survey questions provide a measure of a respondent's levels for each of these cognitive constructs. As students gain more experience in college, their levels of SE, EI, SD and SRL should typically improve as they navigate their college training. The course grades are analyzed in relation to students' measures of SE, EI, SD, and SRL at each class level (B, I, S, G). A 4×4 ANOVA ($\{SE, EI, SD, SRL\} \times [B, I, S, G]$) is proposed as to predicting course grade. Understanding the relationships of SE, EI, SD,

and SRL to grades can help instructors suggest ways that students can navigate more successfully their college preparation for a career. More research needs to be done to isolate any confounding variables in relation to improved grades or lack of improved grades as a measure of academic success.

BUSINESS

The (Non-existent) Effect of Video Gaming and Social Media on Academic Performance

Heber Brau, Jim Brau, James Gaskin

Brigham Young University

Prior research by Brau et al. identified factors that correlate with university student course grades. We employ the same research structure as Brau et al., with the innovation of adding dozens of questions that deal with video game and social media usage. Extant research argues that time spent on video gaming and using social media can: 1) hurt student grades; 2) help student grades; or 3) have no impact on student grades. We test the video game and social media impact hypotheses using a survey of over 500 college students in an Introduction to Information Systems course at a large, private, US university. Methodologically, we employ univariate and multivariate testing with course grade as the dependent variable and a set of video game, social media, and control variables as independent variables. Our results indicate that for this sample period (2019-2020), neither video game usage nor social media usage significantly impacted course grades.

BUSINESS

A Framework for Incorporating CFA and CFP Preparation Courses in an Undergraduate Finance Major

James Brau, Taft Dorman, Peter Marshall, Stephen Owen

Brigham Young University, Brigham Young University-Idaho, University of North Texas

Academic research on the chartered financial analyst (CFA) and the certified financial planner (CFP) programs spans from Hamilton and

Marshall (1987) through Grieb, Noguera, and Trejo-Pech (2021). In this paper, we extend this thread of literature by presenting a framework for providing a CFA prep program and a registered CFP program at the university level without a heavy professor burden. We highlight two programs that exist at a large, US university located in the west. The first program started in 2010 when Dr. Andrew Holmes began a CFA Level 1 prep course as an advanced finance elective. The school pass rates range from 56% to 100%, with the national pass rates ranging from 38% to 43%. Annual differences between school pass rates and national pass rates range from 18% to 57%. The university prep program outperforms the national pass rate in every year. The first part of our paper discusses the CFA prep program and how it can be applied at the MBA and/or the undergraduate level. The second part of the paper discusses the CFP program, which began in January 2021 at the university when Dr. Jim Brau obtained registered status for the CFP curriculum. Unlike the CFA, which can be taken without completing a registered educational program, the CFP requires a CFP Board–approved registered program. The university officially became CFP-registered in December 2020. No student has taken the CFP exam for record, so we do not have a table of results. The last section of the paper covers the professional development activities at three separate universities in the context of the CFA and CFP. Activities such as Meet the Advisors Night, NetTreks, Case Competitions, and student-managed funds are discussed. We present student job placement data that results, at least in part, from these professional development activities.

BUSINESS

An Econometric Analysis of Diversity: Perceptions of College Students towards Corporate Social Responsibility Metrics

James Brau, Jameson Brau

Brigham Young University, Gonzaga University

The focus of this study is to examine college student perceptions of diversity issues in a business setting. We use a sample of 1,149 students and ask questions pertaining to how important diversity is in their ideal first job. The dependent variables are derived from a corporate social responsibility database and focus on diversity issues. We employ a set of econometric tests to find correlations between demographic independent variables and six dependent variables as well as an aggregate diversity

index dependent variable. The tests show that gender and political affiliation are robustly correlated with the dependent variables.

EDUCATION

Story in the Stars

Belinda 'Ofakihevahanoa Fotu

Utah State University

Past, present, and future stories are important devices for transferring culture and knowledge while connecting communities. Narratives of self are apparent in the types of stories we tell each other as well as the venues in which we tell them. In this autoethnography, I investigate specifically through a Tongan-American lens the community built through stories: ancestors ancient and living as well as those outside of the Tongan-American culture. This is especially relevant for members of the Tongan-diasporic community born into or living within land-locked states. Situated spaces and storytelling play an important role in the success of a Tongan-American storytelling: the diasporic execution and reception of generational stories, parental advice (*akonaki*), or reciprocal conversations (*talanoa*). Contexts of audience and venues disrupt those spaces. This disruption is the most true space for Tongan-American learning, as we navigate generational promises and expectations that cross continents, mingling with the immediate demands of westernized systems of knowledge reproduction. Online learning and family separation due to the ongoing Covid-19 pandemic further complicate and redefine these interactions. I develop the concept of *vahano* as an important liminal destination and throughway Tongan-Americans constantly navigate using wayfinding techniques that include storytelling over stages, at kitchen counters, across pillows, and through the internet. It is the space Tongan-Americans constantly cross in learning pathways that pay credence to both family and state demands. Implications of this study include the need for educators to adjust learning spaces to better integrate epistemologies and learning strategies that feature strengths of community and genres of literacy building centered in Polynesian epistemologies of respect, sacrifice, and humility. With the opportunity to create new digital spaces in online learning, educators can restructure curriculums to better include access to storytelling platforms that magnify the literacy strengths of students often marginalized in traditional classrooms.

EDUCATION

Policies and Practices for Supporting Secondary Multilingual Learners—Teacher Perspectives

Marilee Coles-Ritchi and Alondra Miranda

Westminster College

This study explores the perspectives of secondary public school teachers whose primary responsibility is supporting multilingual learners (MLs). Approximately 10% of all students in the United States are MLs or English learners. There is a gap around the literature focusing on the experiences and issues teachers face when teaching MLs in a secondary school environment. Available research points to inequitable policies and practices that result in lower graduation rates and achievement gaps for secondary MLs. To better understand these phenomena, the researchers used qualitative methods to explore the perspectives of English Language development (ELD) teachers within secondary schools based on research of effective practice and policy. Data were collected through in-depth, semi-structured interviews with secondary teachers in a metropolitan area of the western United States. By analyzing the data with the constant comparison method, the following findings arose: 1) content teachers often do not have the background knowledge and/or take the time to learn teaching strategies that support MLs; 2) tension arises when planning programs with courses specifically designed for MLs for fear of separating MLs from mainstream classrooms; 3) requiring standardized testing as the sole instrument for MLs program placement can result in long-term ELD placement and a lack of support. Based on the data collected, the authors suggest specific policies and administrative support for teachers of MLs.

EDUCATION

An Exploratory Tribal-Crit Analysis of Educators Rising's Role in Teacher Recruitment

William J. Davis

Southern Utah University

Utah consistently contends with teacher staffing challenges, which have made teacher recruitment a pressing issue in the state. In recent years, Utah's grow-your-own initiative has been expanded into high schools,

through the development of curriculum standards for the state's secondary-level Teaching as a Profession (TAP) courses as well as through the involvement of Educators Rising. A nationwide nongovernmental entity that claims to promote a community-based model of teacher recruitment, Educators Rising partners with state career and technical education offices, marketing itself in Utah as a career and technical organization for TAP students (akin to Future Farmers of America and students interested in agricultural education). Separating TAP from Educators Rising is difficult. TAP teachers must complete Educators Rising New Advisor Training to obtain an endorsement, and the summer TAP conference involves several training modules on establishing chapters and participating in Educators Rising. For indigenous people to enter the teaching profession through Educators Rising is to subject themselves to a (re)colonization into white Euro/Americentric thinking, knowledge, and power structures. In this paper, I analyze Educators Rising through its publicly available documents and web sites using Tribal Critical Race Theory (TribalCrit). TribalCrit includes nine tenets, three of which can easily be illustrated using Educators Rising. By promoting microcredentials' skill certificates awarded in exchange for a review of documents and a fee, Educators Rising uses secondary students by transforming their teacher learning into material gain. The Educators Rising standards and microcredentials require assimilation to Euro/Americentric forms of teaching like the data-driven plan-teach-assess-reflect cycle and anti-bias instruction. Although Educators Rising's standards cast students as change agents, it is difficult to see how paying for credentials and teaching using assessment data will affect change. To pursue teaching the Educators Rising way is to submit to colonization, assimilation, and a sterile view of culture and diversity.

ENGINEERING

Thermodynamics Experiment: Adiabatic Compression of Air

Toby McMurray and Ali Syed Siahpush

Southern Utah University

Thermodynamics concepts are complicated and hard to understand. In the undergraduate mechanical engineering lab, we studied and built a thermodynamic cycle of ideal gases. In this study, air was considered as the working fluid. The experiment was conducted by compressing and

expanding air in a sealed container (two-liter pop bottle). This process is complicated, but breaking down the ideal gas processes as adiabatic and isometric will simplify it to demonstrate the concept. This simplified model was applied to predict the ratio of specific heats of air (cp/cv). The results for the air were very close to the published value of air specific heat ratio.

ENGINEERING

Scale Analysis of a Solid/Liquid Phase Change Thermal Energy Storage System

Jordan Whitlock , Ali Syyed Siahpush

Southern Utah University

A detailed scale analysis study has been carried out to evaluate the heat transfer performance of a solid/liquid phase change thermal energy storage system. The phase change material (PCM), 99% pure eicosane with a melting temperature of 36.5°C , was contained in a vertically oriented test cylinder that was heated at its outside boundary, resulting in radially inward melting. Detailed quantitative time-dependent temperature distributions and melt front motion and shape data were obtained in previous research. A heat transfer scale analysis was used to help interpret the data and development of heat transfer correlations. In this scale analysis, conduction and natural convection heat transfer were considered. Experimental data with scale analysis predictions of the solid liquid interface position and temperature distribution were compared. The analytical scale heat transfer results demonstrated good agreement with the experimental results and confirmed the existence of four melting regions.

ENGINEERING

Inward Melting in Cylindrical Coordinate System. Part 1 – Analytical Solution (Derivations)

Jordan Whitlock and Ali Syyed Siahpush

Southern Utah University

This research is the continuation of last year's undergraduate research concerning the experimental and analytical solution to the inward

melting in the cylindrical coordinate system at Southern Utah University. The phase change material is eicosane (paraffin, $C_{20}H_{42}$) with a melting point of 36.5°C . Up to this point, the experiment has been performed to collect melting data from 50°C to 1°C . Previously, we evaluated the performance of eicosane for releasing thermal energy (melting). The scope of this project includes (I) analytical solution of the inward melting, which includes the conservation of mass, momentum, and energy, and (II) application of the scale analysis to validate the experimental results. In part (I), we successfully derived the analytical solution for the conservation equations.

ENGINEERING

Transient and Steady-State Heat Transfer Analysis of Long Aluminum Fin

Lee Lorimer, Alicyn Astle, Ali Syyed Siahpush

Southern Utah University

There are several important concepts in heat transfer, including conduction, convection, and radiation. Most heat transfer analysis is assumed to be one-dimensional, steady-state, and uniform, if possible. These simplifications make solving complicated problems easier. Convection heat transfer is enhanced by enlarging the surface area and exposing it to the surrounding fluid, air. This can be done by adding fins. Fins are often used to cool down or heat devices over a broad range of industries. Fins are highly conductive and made from various materials like aluminum. The purpose of this experiment was to analyze the heat transfer throughout a fin, an aluminum rod suspended in air, assumed to be infinitely long (the end of the rod is at room temperature). This was done by using experimental data and known transient and steady-state heat transfer equations for a fin to predict the temperature profiles. To get an accurate heat transfer coefficient, the value can be found by changing the value until the temperature curves match. The value found for the natural convection heat transfer coefficient was $10 \text{ (W/(m}\cdot\text{K))}$. The temperature profiles between the theoretical and measured steady-state were compared and the average difference between them was 1.34. The transient state was also compared and the average difference between all the nodes was 0.2912. The difference values between both the steady and transient states are extremely small and show that the data gathered was correct.

ENGINEERING

Transient and Steady-State and Transient Analysis of a Fin Under Water

Mitchell Halverson, Kobe Potter, Floyd K Kimber, Jordan Whitlock, Jathen Chaffin, Cameron Dix, Ali Syyed Siahpush
Southern Utah University

This paper describes an analysis that was performed on a fin underwater to better understand the convective coefficient of heat transfer, h , while giving experience into real-life engineering projects. The experiment was set up by making an aluminum fin using an aluminum plate and rod, where the rod was submerged in a plastic tub filled with water and the plate was heated via a heating pad outside of the tub of water. The plate and heat pad were insulated, so that heat from the heat pad was not lost to the environment. Thermocouples attached at specified distances from the heat source measured the temperature throughout the rod. To analyze the heat transfer through the rod, steady-state and transient conditions were considered, with models created on MATLAB to predict how the rod would lose heat and compare it with the data collected through experimentation. To collect the data, two 8-channel thermocouple data loggers were used. There also exists a general solution for finding the temperature and heat flux throughout the fin. This solution proves useful under conditions where the fin is assumed to be very long.

ENGINEERING

Cavitation Demonstration Trials

Owen Telford, Ali Syyed Siahpush
Southern Utah University

In this paper, multiple experiments were conducted on various types of pumps. Pumps vary in size and function to explore a suitable cavitation demonstration for a fluid mechanics lab. It was intended to compare experimental results with analytical methods and discuss discrepancies. Four different pumps were tested: a submersible pump, a circulation pump, a diaphragm pump, and a centrifugal pump. Based on its classification, each pump was used differently to generate cavitation, and each pump gave various results. Each pump was discussed along with recommendations for how to create a proper system that can be used for students to learn and experience cavitation in a fluid mechanics lab.

ENGINEERING

Making a Big Impact with a Small Design

Taylor Perry, Guelord Mirindi, Alexandra Hutchinson

Southern Utah University

Cities and counties across the United States are restricting new construction because of the limited nature of life-sustaining resources (e.g., water, electricity). What we are proposing with this project is a solution that goes against tradition to provide the safety and security of homeownership, while implementing ecofriendly technology to meet the needs of a growing population. This design challenges the square footage of a traditional single-family home by reducing it to less than 200 square feet. Along with the benefits of a small footprint, this design utilizes advanced solar technology, high-efficiency appliances, and purposeful architecture. With the rising cost of homes, and high-density dwellings taking over residential zones, tiny homes provide an alternative opportunity for homeownership. Furthermore, this design would help conserve life-sustaining resources in growing communities. This proposal expands beyond the suburban environment as we explore the potential of placing ecofriendly tiny homes in areas that historically have not had access to traditional housing. Specifically, we will be looking at the process of building these ecofriendly tiny homes in the Democratic Republic of the Congo.

ENGINEERING

Developing and Implementing Traffic Control Plans for Road Work Zones: Case Study on SR-130, North Cedar to MP 9

Tyson Prince, Sean Carr, Tavish Darger, Mohamed Askar, Jared Baker

Southern Utah University

Any construction project has its share of challenges; however, when it comes to road construction, there are various things to consider and address that are unique to road work. During the planning and construction phase of a roundabout project, a temporary traffic control system must be designed and implemented to provide an acceptable margin of safety to personnel within the work zone and keep the natural

flow of traffic to the minimum extent possible during the construction phase. Because of the limited but growing incorporation of roundabouts in the US, an inadequate amount of information is available for definitive guidance on the design and operation of such temporary traffic control systems. This paper seeks to understand what rules and considerations could have been utilized to manage such traffic better in the project case study: N. Minersville Hwy. and E. Midvalley Rd as the I-15 offramp, exit 62. When looking at traffic control, the intent is to provide a traffic control plan that would include materials, equipment, labor, flagging, pilot car, variable message boards, temporary pavement, markings, and all quality required. In addition to these considerations, the Utah Department of Transportation standards should be maintained as necessary, as located in section 00555M of the Special Provisions. Regarding the considerations placed on exit 62 offramp, all work being done on the offramps must allow for the interchange ramps to remain open at all times. The research concluded a traffic control plan with more detail as the job gets closer to the start date, with all traffic plans to be approved 14 days prior to start.

ENGINEERING

Developing a Quantitative Quality Control System for Road Construction: Case Study On SR-130, North Cedar To MP 9

Wade Schmid, Jaden Black, Duo Chen

Southern Utah University

Construction is a significant contributor to the USA economy. The industry has more than 680,000 employers with over 7 million employees and creates nearly \$1.3 trillion worth of structures each year. Unfortunately, the outbreak of COVID-19 has changed some of that, disrupting the construction industry's pace. Construction laborers are required to work while maintaining social distance, resulting in reduced productivity and poor quality. This research's primary goal is to develop a quantitative quality control system to improve the quality of construction projects. A secondary objective is to focus on the regular monitoring of the construction site conditions of a heavy civil construction project, SR-130, North Cedar to MP 9, and effectively solve the quality problems of the main work items, such as materials, subbase, base, concrete, pavement, and testing. The methodology of this research is to outline the best practices for using application software and quality

checklists to discover, raise, and solve problems of the construction process. A quality dashboard and statistical analyses were developed to measure the quality of the construction work items and the general quality index. The developed model will be used for monitoring each problem and scheduling solutions. More complete checklists and management methods have been considered, ensuring that the project meets a certain quality level with practical strategies, solutions and safe communication methods. The research concluded several ideas to identify, resolve, and report project quality issues in a timely manner to protect workers' safety and ensure project quality, such as improving the quality checklists, online monitoring, and spot-checking the quality of the project.

ENGINEERING

Application of Value Engineering Technique on Tall Wood Building Structural Design

Jacob Rollins, Tony Olsen, Mohamed Askar

Southern Utah University

Value engineering is a combination of technical and economic subjects. It is committed to the lowest life-cycle cost and reliable completion of the functions required by the client. Value engineering is an intensive, interdisciplinary problem-solving technique that focuses on improving the value of the required functions to accomplish the goals. It is essentially a process that uses function analysis, teamwork, and creativity to enhance value. The International Code Council (ICC) has approved 17 changes to the 2021 editions of the International Building Code (IBC) and International Fire Code, allowing mass timber buildings up to 18 stories with the addition of three new mass timber construction types (Type IV-A, IV-B, and IV-C). These new types are based on the previous Heavy Timber construction type (renamed Type IV-HT) but with additional fire-resistance ratings. This is the first time in the modern building code history that significantly new construction types have been added. The main objective of this undergraduate research is to develop a structural design and analysis of an 18-story timber building considering a rational performance-based design approach such as sustainability, environmentally friendly, economy, fire and safety testing, and constructability. The structural systems of the study building are composed of cross-laminated timber (CLT) shear walls, CLT floors, glulam columns, and reinforced-concrete link cores. Numerical

simulations, such as 3-D finite element model development and non-linear time history analysis, have been used in the design analysis. The application of value engineering to structural design in various design phases has been applied. Further, an analysis of these performance indicators and suggestions of design alternatives have been considered during the value engineering workshops. Finally, the workshop results will be taken into consideration in the design.

ENGINEERING

Comparative Study of Structural Systems for Tall Mass Timber Buildings

Khevar McLeod, Braden Madsen, Mohamed Askar

Southern Utah University

A comparative study has been carried out to examine the most common structural systems that are used for tall mass timber buildings. These systems include rigid frame, shear wall, core system, and braced frame. This comparative analysis has been aimed to select the optimal structural system for an 18-story mass timber building. The structural efficiency is measured by the time frame, fire resistance factor, ease of design, sustainability, maintainability, and constructability. Relative weight is created for each selection criteria. A quantitative measurement method/formula is designed to measure the score of each criterion. The recommendations for each structural system are based upon reducing the timeframe of the design and construction, minimizing the cost of the construction, simplifying the design process, eliminating the negative environmental impacts, allowing safe, quick and easy replacement of the component parts, and using construction knowledge and experience in planning, design, procurement, and field operations to achieve overall project objectives. Combinations of systems were also considered for comparison, such as the shear wall lateral system, which seems to have excellent acoustic and fire insulators between rooms in a high rise and appeared to be more cost-effective for high-rise buildings in areas of seismic zones II and III. The conclusion of the study shows that the core system structural method and the combination between the core system and shear walls have the highest values.

HUMANITIES, PHILOSOPHY, FOREIGN LANGUAGE

Social Justice in the Languages

Lucia Taylor

Dixie State University

Languages, ethnicities, and races have been part of the discussion of identities for a long time. When looking into languages with gender differentiations, the new non-binary status has entered the classroom. What do we do when a non-binary student is learning gendered language? Beyond these issues, society is changing moving into looking at social justice from all perspectives in academia. In this presentation, I will discuss my own experience as a Spanish teacher. I will dive into myths in languages, language in the media, and the importance of linguistic diversity in global justice. Attendees will reflect on their own biases and their own constructs of what language and identity is for each of them.

HUMANITIES, PHILOSOPHY, FOREIGN LANGUAGE

Instant Out of Time: Mathew Brady's Photographs of the First and Second Ladies, 1844-1896

Thomas C. Terry

Utah State University

Mathew Brady is the most famous photographer in American history. People who do not know the name of any other photographer know Brady. His career stretched from 1844 to 1896, and over that period Brady photographed 18 of the 45 presidents—40%—from the 6th to the 25th (counting Cleveland only once). Only the 9th president, William Henry Harrison, escaped Brady's lens by dying within a month of his March 1841 inauguration. Brady also photographed 17 of the 49 vice presidents—roughly 35%—from the 7th through the 23rd. Only Richard Mentor Johnson (1780-1850), the 9th vice president from 1837 to 1841, never sat for Brady. However, there are only five Brady photographs of First Ladies, out of a possible 13 during his career and just two Second Ladies of a potential 10. They are First and Second Lady Abigail Powers Fillmore (1798-1853), wife of Millard Fillmore; First Lady Mary Todd Lincoln (1818-1882), wife of Abraham Lincoln; Second Lady Ellen Maria Wade Colfax (1836-1911), wife of Schuyler Colfax; First Lady Julia Dent Grant (1826-1902), wife of Ulysses Grant; First Lady Lucy

Webb Hayes (1831-1889), wife of Rutherford Hayes; and First Lady Lucretia Rudolph Garfield (1826-1902), wife of James Garfield. The mortality of the wives of presidents and vice presidents during Brady's career was shocking, undoubtedly at least partly attributable to death during pregnancy and childbirth and the general state of women's healthcare in the early to mid-19th century. The wives of vice presidents Richard M. Johnson, William A. Weaver, Martin Van Buren (also a president), Chester A. Arthur (also a president), and Henry Wilson died before their husbands took office. Vice President William R. King was unmarried. The purpose of this study is to assemble all the First and Second Ladies photographs taken by Brady and never collected together before.

KINESIOLOGY AND HEALTH SCIENCES

Exploring Correlates of Domestic Violence and Homelessness: A Review of the Literature

Linnette Wong

Weber State University

Domestic violence is a traumatic event, and the aftermath can be devastating. Victims of domestic violence may experience multiple issues, such as homelessness, while trying to recover from this trauma. Whether the victim is trying to escape an abusive situation, homelessness has been observed as a trend among those impacted. The purpose of this literature review was to provide an extensive summary of the impact that domestic violence had on an individual's life. This literature review analyzed the available literature using keywords to help identify important articles that were pertinent to the topic. The outcome of the literature review revealed a total of eight relevant articles relating to the keywords. The results suggested positive correlates of domestic violence and homelessness. The findings have important implications for the design of health and social programs targeting homelessness.

LANGUAGE AND LITERATURE

Humor within the Horrors of *The Two Gentlemen of Verona*

Madalynn Belliston

Southern Utah University

Readers and theorists often contemplate how William Shakespeare came to understand classical comedy as inherently humorous. More importantly, they wonder how he came to define humor itself. As a woman, I question why so much of Shakespeare's humor seems to be founded on female gender degradation. In my paper, I explore how women are depicted in Shakespeare's first comedy, *The Two Gentlemen of Verona*. I will apply principles of social feminism and humor theory to argue that the play's humor derives primarily from the social oppression and degradation of its female characters, creating a disturbing comedic paradox where Shakespeare seems to imagine that the potential horrors of maltreatment and abuse are softened and made comic through the play's ignorant, irrational characters.

LANGUAGE AND LITERATURE

Ambivalent Villains: Tracing the Binary Perception of Heroism Across Three Narratives

Brandan Ivie

Southern Utah University

Heroism cannot exist without opposing villainy; no hero can rise without the conflict caused by the villain. Traditional hero narratives are centered on struggles between good and evil; they present a clear dichotomy between hero and villain. Morally ambiguous heroes or villains are nevertheless common in literature and culture, and they challenge this binary. My paper explores three morally ambiguous villains—Satan from John Milton's *Paradise Lost*, Frankenstein's monster from Mary Shelley's *Frankenstein*, and Killmonger from the Marvel film "Black Panther" (2018)—to show how, despite embodying certain heroic impulses, each character is confined to a villain's status by plot-based and structural conventions that dictate audience perceptions.

LANGUAGE AND LITERATURE

Rhetorics of Advocacy in Disability Accommodation

Rachel Bryson and Peter Call

Utah State University

For both students and faculty in higher education, the disability accommodation process can be fraught with uncertainty. Institutional documentation processes may inadvertently create separation between students and faculty, leaving those involved unsure about how to begin conversations about accommodations and accessibility, especially when disabilities may be defined as less apparent. Our presentation will show how accommodation documents can become a starting point for collaboration and advocacy from both student and faculty perspectives. Using a disability studies methodology developed by Margaret Price, we will consider the institutional accommodation process as framed by access, activism, identification, and representation to argue that institutional accommodation and documentation processes can become sites of advocacy and self-advocacy for both faculty and students with disabilities.

PHYSICAL SCIENCES

Mercury for Dinner? Aqueous Heavy Metal Sequestration

Jacob Kjeldahl Jensen, Christopher F. Monson

Southern Utah University

Heavy metals threaten aquatic life and are a danger to human health. Multiple sites are reporting an increase in heavy metal concentration. It is possible to responsibly remove the toxic metals through a three-step process: pumping, separation, and removal/sequestration. A pumping device will provide a microfluidic separation device with a continuous solution flow. The separation device will utilize electric field-flow-fractionation to produce a concentrated metal ion solution. The metal ions will reduce onto a charged gold mesh (electroplating), which can be removed and disposed of in an environmentally responsible manner. The efficiency of the setup will be evaluated using various analytical techniques, including cyclic voltammetry and UV–visual spectroscopy.

PHYSICAL SCIENCES

A three-electrode microfluidic for the quantitation of dissolved oxygen

Cameron C. Stokes, K. Brayden Bailey, Christopher H. Abraham, Mariah Clayson, Madison J. Evans, Christopher F. Monson

Southern Utah University

The concentration of dissolved oxygen in aqueous environments is relevant in both biological and chemical processes. Variations in oxygen levels may critically change metabolic and other chemical pathways. We previously developed a microfluidic device modeled after the STOX electrode to measure dissolved oxygen. The STOX electrode is the most sensitive electrochemical device currently available for the quantitation of dissolved oxygen; however, it is fragile and expensive. Our device is constructed from PDMS and is thus more rugged and inexpensive to produce. We have further developed our device to make it simpler and require three electrodes instead of eight. We also used a 3D-printed capsule to simplify device construction and a new microfluidic oxygen exchange segment. This device will allow oxygen measurements to be made more sensitively, quickly, and cheaply than is currently possible.

PHYSICAL SCIENCES

Investigation of Manganese Nanoparticles with Various Capping Ligands and Their Effects on *Raphanus sativus*

Taytum Stratton, Christopher F. Monson, Elizabeth Pierce

Southern Utah University

Nanoparticles have recently been studied in agriculture to mitigate abiotic stress in crops because of their small size and unique characteristics. We investigated the use of manganese nanoparticles to increase stress tolerance in *Raphanus sativus*. Few studies have been conducted on the synthesis and uses of manganese nanoparticles. We were among the first to synthesize manganese nanoparticles using a microfluidic device. Manganese acetate was used as an ion source, sodium dithionite was the reducing agent, and oleic acid was the capping ligand. Fluorescence spectroscopy and scanning electron microscopy were used to confirm that the particles synthesized were in the nanoscale

size range. When foliarly applied to *R. sativus* that had been exposed to stress, the nanoparticles significantly increased both chlorophyll content and growth rate, indicating an increase in stress tolerance. In addition, several other capping ligands were used for the manganese nanoparticles. We expressed and purified a red fluorescent protein in *Escherichia coli*. This protein, along with a Texas-Red labeled BSA protein, were successfully used as capping ligands for the manganese nanoparticles. The nanoparticles capped with the proteins were foliarly applied to *R. sativus*. We investigated to see whether the protein could successfully travel through the plant cell membrane without being denatured by looking at a change in red fluorescence in the leaves of the plants. If the proteins can successfully make it into the plant cell without denaturing, it is possible that manganese nanoparticles could be used as a delivery method for proteins involved in gene editing technologies in plants, and future studies will investigate this.

PHYSICAL SCIENCES

Incorporating Authentic Research Experiences into an Undergraduate Course in Computational Chemistry

Elena N Laricheva

Utah Valley University

Computational methods have become ubiquitous in chemical and biological research—from aiding the prediction of protein structures to assisting the development of new materials and the design of new drugs. Therefore, exposing undergraduate students to such methods early in their careers is critical for ensuring they can tackle computationally intensive research tasks after they graduate. Framing the teaching of computational methods in the context of an authentic research experience increases the relevance of the techniques taught. This talk will describe incorporating authentic research experiences into an undergraduate course in computational chemistry. Initially designed to illustrate the main principles of molecular mechanics and classical molecular dynamics simulations, the course has recently been expanded to include electronic structure calculations. As a part of their research experience in the course, students have explored the effect of single-point mutations on binding between the two cell surface receptors involved in the mammalian fertilization process. In another project, they have investigated the effect of structural changes on the optoelectronic properties of graphene and hexagonal boron nitride-like systems.

PHYSICAL SCIENCES

Tunings and Temperaments: Mathematical Circles and Spirals

Jonathan Tyler and Larry Smith

Snow College

Musicians do not need to be expert mathematicians to produce beautiful music, but music is based on mathematical principles that require some choices on the part of musicians, so an understanding of the mathematical underpinnings of music theory is useful. Connections between the math of circular pitch class space and spiral pitch space and the musical concepts of tunings and temperaments are shown.

PHYSICAL SCIENCES

Character Table of Permutation Group in 4-Dimensional Space

Chin-yah Yeh

Salt Lake Community College

Permutation of points reflects the symmetry of a space. Here we shall focus on the permutation between individual points in a space and hope to shed light on the structure of spaces. 1-D spaces have even and odd symmetries. 2-D spaces have three kinds of basic symmetries. 3-D spaces have a symmetry corresponding to that of the regular and chiral octahedron, O . The group O is isomorphic to the 4-point permutation group. With interest in the properties of 4-D spaces, we shall build the character table of the 5-point permutation by starting with 4-point permutation, S_4 . The octahedral symmetry group O or the 4-point permutation group S_4 consists of 24 elements. The elements are divided into five classes, each characterized by a cycle notation. These classes are also described by Young tableaus shown in the second row. The character table contains five irreducible representations, IR_0 to IR_4 . The 5-point permutation S_5 group has the same size as the icosahedral group but is more symmetrical. We use S_4 as a scaffolding to build the S_5 group table. IR_0 corresponds to a total symmetry. IR_1 is an antisymmetry reflecting the parity of space. The next irreducible representation, IR_2 , is not extended from that of S_4 group but has a dimension 4. IR_2 is obtained from IR_0 and IR_3 . The set of characters become $\{4, 2, 0, 1,$

0} and correspond to the five classes in S_4 padded with a 1. The rest of the seven classes are (32) and (5), which have -1 as their characters. IR3 is a counterpart of IR2, with the characters of the classes, (2111), (32), and (41), negated. IR6 is easily guessed by its orthogonality to the rest of the IRs.

PHYSICAL SCIENCES

Neutron Star Kick-Off as a Consequence of Asymmetric Neutrino Diffusion

Alexander Panin

Utah Valley University

Some neutron stars move with velocities in the 500-2000 km/sec range, which is well in excess of Milky Way galactic orbital speeds (200-300 km/sec). The origin of such strong kick-off is still debated. Stars are known to have strong and often asymmetric magnetic fields. Combined with star rotation, it is unrealistic to expect spherically symmetric collapse of a star or of its core. We estimate analytically what kick-off could result from asymmetric collapse of star core and subsequent asymmetric diffusion of neutrino radiation in rapidly cooling neutron star. It turns out that high opacity of dense forming neutron matter to neutrino radiation may result in development of a “hot side” of neutron star (to which diffusion wave reaches first)—which radiates “hot” neutrinos first—versus opposite side radiating later and thus radiating colder neutrinos. Difference in momenta of radiated neutrinos of different energies can indeed accelerate neutron star to the observed high kick-off velocities.

PHYSICAL SCIENCES

Single X-Ray Photon Diffraction Experiments

Alexander M. Panin

Utah Valley University

It is very difficult to demonstrate single-photon diffraction in visible range because it requires very low intensity sources and very sensitive detectors. In contrast, in the x-ray range of the electromagnetic spectrum, these conditions are much more relaxed because of a higher probability

of spontaneous emission and much higher energy of photons. Experiments with single-photon diffraction can be relatively easily arranged with ordinary x-ray sources (like x-ray tube) and ordinary detectors (like Geiger counter, CCD array, etc). We have performed such experiments in both single-photon and multi-photon modes. Results of our experiments, as well as analytical comparison of single-photon diffraction of x-rays with diffraction in visible light, are presented in the talk.

PHYSICAL SCIENCES

Testing Quantum Mechanics on Quantum Computers

M. Thomas Hoffman, Jean-Francois Van Huele

Brigham Young University

Quantum computers have proven to be a valuable resource for complex calculations, but they also provide a new tool to probe quantum theory. One basic tenet of quantum mechanics (QM) is that the probabilities for measurement outcomes are given by the moduli squares of the quantum amplitudes. Sorkin has designed a test based on the use of multi-slit interference to investigate this fact. Sadana et al. applied the Sorkin test to a quantum computer. In this talk, I will analyze this interpretation and study the Sorkin test to see to what extent quantum computers can tell us about the fundamental laws of QM.

PHYSICAL SCIENCES

Optimizing Quantum Resources in Short-Distance Teleportation Scenarios

Aidan Gillam, Jean-Francois Van Huele

Brigham Young University

Quantum teleportation is a powerful example of current quantum technology that allows an unknown quantum state to be communicated from one location to another without physically transporting the particle to which the state is attached. I discuss ideal quantum teleportation involving the sharing of a maximally entangled pair of qubits and the sending of two bits of classical information. I show how teleportation is expressed in the language of quantum circuitry. I then discuss the

possible minimization of quantum resources in short-distance teleportation scenarios. I explain its potential application in quantum computers and quantum chips.

PHYSICAL SCIENCES

Finding the Quantum in Novel Self-Gravity Experiments

Leif Hagen, Jean-Francois Van Huele

Brigham Young University

Gravity, by far the weakest fundamental force, has proven extremely difficult to experimentally access at small scales. This has contributed to our inability to reconcile our best theories of gravity with those of quantum mechanics. Two “tabletop” experiments have recently been proposed that could measure the gravitational interaction between two simple quantum systems and confirm the need to quantize gravity. Each of these experiments uses gravity to entangle particles across a pair of interferometers. They differ in the type of interferometers used (Humpty-Dumpty vs. Mach-Zehnder). I compare these two methods and argue, alongside Hatifi and Durt, that they can be further simplified by exploiting self-gravity rather than ignoring it.

POSTER: BIOLOGICAL SCIENCES

The Predicted Structure of a Thermophilic Malate Synthase

Shaelee Nielsen, Jantzen Orton, and Bruce R. Howard

Southern Utah University

Our project aims to solve the structure of the crenarchaeal *Sulfolobus acidocaldarius* enzyme malate synthase. Other known malate synthase enzymes have been found to require a magnesium ion in the active site to carry out catalytic activities, but a study reported that *S. acidocaldarius* malate synthase does not require magnesium. This suggests a novel mechanism for this enzyme. Additionally, the mature *S. acidocaldarius* protein is approximately 100 residues larger than any other structurally characterized malate synthase. It has also been reported to form a dimer, while previously solved structures have only displayed

monomeric, trimeric, and hexameric arrangements. We plan to use X-ray crystallography to determine the structure experimentally; however, major advances in the accuracy of protein structure prediction were made recently by AlphaFold, an artificial intelligence system developed by DeepMind, that have revolutionized the field and apparently solved the protein folding problem. A similar AI system, RoseTTAFold, developed by David Baker's lab at the University of Washington, has been made publicly available. Here we report our analysis of the structure of this protein, predicted using the RoseTTAFold algorithm, and of a predicted structural model for the dimeric form of the enzyme using ClusPro. Our results provide strong support for a conserved catalytic mechanism, requiring magnesium, in common with all previously solved malate synthase isoforms. Our results also provide potential insight into evolutionary relationships with these other various isoforms.

POSTER: BIOLOGICAL SCIENCES

Single Sample Survey of Halophilic Host and Phage Pairs

Preston D. Capener, Joshua R. Mott, Matthew B. Crook, Matthew J Domek

Weber State University

Bacteria growing in the Great Salt Lake (GSL) are halophilic in nature because of the high salt concentration and are represented by a large number of diverse species. Previous studies from this laboratory have found phage that infect *Halomonas*, *Idiomarina*, *Salinovibrio*, and *Marinobacter*. The host and the phage were isolated over several years of sampling. In this study, we used three different halophilic media formulations to address the diversity in a single sample of GSL water. The water sample was isolated from Bridger Bay in the GSL. The water sample was plated on the three different media, and colonies were isolated. Isolates were selected based on colony morphology. A portion of the water sample was centrifuged at 10K×g for 10 minutes and then filtered through a 0.2-micron filter. The filtered water sample served as the phage source and was mixed with each isolate. The samples were inoculated in a 48-well plate. Growth was measured at 600 nm on a Tecan M200 multimode plate reader at 25°C for 30 hours. Lysis by phage was detected by an initial increase in absorbance followed by a rapid decrease. Control isolates showed an increase in absorbance followed by a stationary phase. Confirmation of the phage infection was

followed up by performing phage spot plates. Phage infections are noted by a zone of clearance. Host and phage identification are ongoing.

POSTER: BIOLOGICAL SCIENCES

Selective Media for the Isolation of *Paucilactobacillus wasatchensis*

Chase Wahlstrom, Matthew Domek, Michele Culumber, and Craig Oberg

Weber State University

Paucilactobacillus wasatchensis causes late gas defects in aging cheese. The ability to quickly and accurately isolate *P. wasatchensis*, especially when present at low concentrations compared with other bacteria in cheese, would benefit the dairy industry because the current protocol is time intensive and lacks sensitivity. The goal of this study was to develop a plating medium to detect *P. wasatchensis* within 72 h when as few as 10^3 CFUs per gram are present while inhibiting competing starter lactic acid bacteria (SLAB) and nonstarter lactic acid bacteria (NSLAB). Carbohydrate-restricted MRS (CR-MRS) medium with varying concentrations of vancomycin and 2-deoxyglucose, a glucose analog that inhibits glycolysis, was developed. Utilizing 5 SLAB and NSLAB strains along with the *P. wasatchensis* for each variable, CR-MRS broth containing 1% ribose, 2% Oxyrase, and either .01% 2-deoxyglucose or various vancomycin concentrations was screened. Application testing was then conducted using CR-MRS agar plates containing 1% ribose, 5 mg/mL vancomycin, and various concentrations of 2-deoxyglucose (0.01-0.1%) incubated anaerobically for 72 h. Results showed WDC04 growth was not inhibited by the experimental medium, where SLAB and other NSLAB such as *Lactocaseibacillus casei* and *Lactocaseibacillus paracasei* showed limited inhibition and *Lactococcus lactis* was inhibited due to the 2-deoxyglucose and/or the vancomycin. However, the media can be used to differentiate *L. casei* and *L. paracasei* from WDC04 because they appear as pinpoint colonies. Incorporation of 0.01% 2-deoxyglucose and 5mg/mL vancomycin into CR-MRS+1% ribose agar is a selective plating medium for *P. wasatchensis* based on its selective and differential properties. This medium could be used to determine the presence of *P. wasatchensis* in cheese when it is found in low concentrations (10^3 CFU per gram) versus the high concentration of SLAB (10^8 CFU per gram) that obscure its detection with current isolation techniques.

POSTER: BIOLOGICAL SCIENCES

Effects of the Flavonoid Epicatechin on Mitochondrial Respiration and Glucose-Regulated Glucagon Secretion in the Pancreatic Alpha Cell

Chad Mourino and Ethan Crawford

Brigham Young University

Type 2 diabetic individuals have elevated blood glucose levels. This is caused by an inability of tissues like the muscle, adipose, and liver to sense insulin and remove glucose from circulation. Interestingly, the elevated blood glucose corresponds with increased circulating insulin and glucagon levels. The elevated insulin levels are due to compensation in response to target tissue unresponsiveness. The elevated glucagon induces the liver to undergo gluconeogenesis and continuously increase circulating glucose levels. Many foods contain flavonoids, and we previously showed that the flavonoid epicatechin is sufficient to enhance beta cell glucose-stimulated insulin secretion by enhancing beta cell mitochondrial activity. Increased insulin secretion, early in type 2 diabetes, is sufficient to maintain normal blood glucose levels. Given that the mechanisms for inducing beta cell insulin secretion and blocking alpha cell glucagon secretion are very similar, we hypothesize that epicatechin may be sufficient to keep glucagon levels in check over a wider range of glucose concentrations than normally occurs with glucose alone.

POSTER: BIOLOGICAL SCIENCES

In sickness and health: Student perceptions of viruses pre- and post-pandemic

**Kayci K. Younger, Landon K. McKinnon, Jennifer L. Momsen,
Lisa B. Wiltbank**

Weber State University

In 2020, the onset of the COVID-19 pandemic began to affect the way that the general public related to viruses. Suddenly, everyday conversations used terms like antivirals, pandemic, transmission rates, and vaccines. In 2016, “before COVID-19 was on the scene,” we were interested in what the general public knew about viruses and bacteria. To get at this information, we decided to survey students from general

education biology classes about their knowledge of microbiology. These students were not biology majors. Half of the students received questions about viruses and half of the students about bacteria. We also distributed the same survey in majors and upper-level classes. By Fall 2020, the COVID-19 pandemic was a prominent topic on news media and at dinner tables. This led us to expand our study to incorporate the students' awareness of microbiology post-pandemic, with the hope that their knowledge improved. We distributed the same survey to students in the same classes that we surveyed in 2016 to see whether general knowledge about viruses had increased (n=614 students in 2016; n=379 students in 2020). In this presentation, we will present our findings of students' knowledge of viruses and bacteria pre- and post- COVID-19. Overall, in our efforts to compare 2020 to pre-COVID data, we found little evidence of differences in student knowledge or perceptions of viruses at the two timepoints. Interestingly, roughly half of the students surveyed in 2020 perceived that their knowledge of microbiology had increased from before the pandemic. We will present data summarizing our findings from a few key survey questions.

POSTER: BIOLOGICAL SCIENCES

Conserving parasites and their symbiotic microbes— keystone species in Great Basin Desert life zones

Robert L. Bossard

Bossard Consulting

Recognition of how pathosystems of parasites and their symbiotes in disease foci are keystone ecological engineers constitutes a revolution in our understanding of ecosystem function. Life zones, biomes, and specialized habitat such as caves are distinct biocenoses of plant and fungal parasites, plus animal ectoparasites, such as ticks, mites, mosquitoes, fleas, and lice, and internal parasites, such as tapeworms and nematodes, further associated with symbiotic microbiota of protists, bacteria, and the virosphere. Biomes show homeostasis, small scale but affecting the biosphere in the Gaian "Daisyworld" sense of Locklock, undergoing reoccurring, fairly predictable successions after disturbance resulting in repeated species interactions, notably including those of endemic parasites with their hosts in coevolved subgroup selection that can result counterintuitively in parasites benefitting their hosts. These indirect and third party interactions facilitate the "prudent parasite" paradox. Mistletoe parasitizing Juniper-Pinyon woodland feeds birds,

aiding seed dispersal of its hosts; woodrat (*Neotoma*) nests, shrews (*Sorex*) in wetlands, and caves shelter complements of fleas and mites in nest and fur, helminths, trypanosomes, and apicomplexa; the Alpine zone (above 3,000') harbors pikas (*Ochotona*) with mites and fleas (*Amphilius runatus*, *Ctenophyllus armatus*, *Megabothris abantis*), and invading rodent pathogens as climate warms. Processes such as predation stabilize population densities along with alternation between fragile dispersers and robust, resistant stages in a metapopulation, especially for insects with complex life cycles. Invasive flea-borne plague transforms landscapes by altering nutrient cycling and food chain length. Ecotones further connect biomes. "Fleas to Trees" hypothesizes that fleas and by implication, other parasites, regulate seed-eating deer mice (*Peromyscus*), fostering seedlings and regenerating forest after fires. In addition to the charismatic megafauna, flora, and pollinators, parasites too, and their symbiotes, are critical for conservation initiatives such as "30×30," 30% area conserved by 2030, and "Half-Earth," 50% of natural terrestrial and marine areas preserved.

POSTER: BIOLOGICAL SCIENCES

Characterization of metformin's repression of chemokine reduction in triple-negative breast cancer cells

B. Drake Alton

Weber State University

Numerous studies have demonstrated that the anti-hyperglycemia drug, metformin, exhibits both antiproliferative and antimetastatic effects on cancer cells. For patients diagnosed with triple-negative breast cancer, these in vitro effects are associated with life-prolonging outcomes in vivo. Although the antimetastatic potential of metformin is striking, the mechanism by which the drug exerts this effect is unclear. Generally, the number of tumor-associated macrophages (TAMs) found in solid tumors portends poorer prognoses. TAMs are recruited to solid tumors not only by tumor-infiltrating stromal and inflammatory cells but also by tumor cells themselves. Tumor cell production of monocyte-recruiting chemokines has been well-documented for a number of cancer types, including triple-negative breast cancers. We hypothesized that metformin exerts its antimetastatic effects, at least in part, by inhibiting tumor cell chemokine production. To test this hypothesis, two triple-negative breast cancer cell lines were treated with varying concentrations

of metformin and at varying timepoints. Metformin treatment diminished the production of several key C-C chemokines as measured via real-time PCR.

POSTER: PHYSICAL SCIENCES

Particle Detector and Einstein's Theory of Relativity

Sota Nakahama

Southern Utah University

Einstein's Theory of Special Relativity was an invaluable contribution to modern science, turning the notion of an immutable time on its head. Einstein's Theory of Special Relativity theorized that as the speed of the object that has mass increases, time dilates. The implications of special relativity have been tested repeatedly and have always shown the theory's accuracy, but more testing does not hurt. In this work, we revisit the cosmic muon experiment that originally showed the accuracy of special relativity, but at higher altitudes, in order to see a corresponding shift in the number of muons detected. These results are then compared with theory to ensure that special relativity is indeed correct. To conduct this experiment, we are going to build a particle detector by using a scintillator and photomultipliers. This device will allow us to detect muons at a given altitude. The measurement given by the device will allow us to experimentally help show the accuracy of Einstein's theory.

POSTER: PHYSICAL SCIENCES

PDMS Frit Fabrication and Applications

Kylee Stoddard, Christopher F. Monson

Southern Utah University

Frits are filters that can remove micrometer-sized particulates from solution; they are typically fabricated from glass beads. We have developed a method to make frits by mixing magnesium particles and PDMS, a silicone elastomer, followed by magnesium dissolution. Our frits exhibit surprising abilities to remove large molecules from solution, at times showing the ability to exclude medium proteins and possibly smaller molecules. They are also more heat stable than traditional dialysis membranes and so might offer significant advantages.

Additional applications of the PDMS frits are being explored, including vesicle separation and superhydrophobicity.

POSTER: PHYSICAL SCIENCES

Investigating the effect of structural changes on optoelectronic properties of benzenoids and their boron nitrogen analogs

Benjamin A. Smith, Joshua Thomson, Michelle A. Chicas Aslett, Adam Cluff, Mitchell Asper, Lance Jagerson, Elena N Laricheva
Utah Valley University

The bandgap is an intrinsic characteristic of a material that determines its electric conductivity and is linked to the optical gap energy. Depending on the magnitude of the bandgap (E_{gap}), all materials are classified as conductors ($E_{\text{gap}} < 3 \text{ eV}$) or semiconductors ($E_{\text{gap}} > 10 \text{ eV}$). Tuning the bandgap of 2D materials has long been a subject of great interest for their applications in nanophotonics and nanoelectronics. Among known 2D structures, graphene and hexagonal boron nitride (h-BN) are especially promising. However, they are also some of the most difficult materials to engineer the bandgap in. Graphene is a zero-gap electrical conductor, and h-BN functions as a wide-gap insulator. Several strategies have been employed to open the bandgap in graphene and reduce the one in h-BN, with limited success. A complete understanding of the factors affecting the electronic structure and the bandgap in materials such as graphene and h-BN is still missing. In this project, a series of benzenoids and their boron–nitrogen analogs with varying ribbon lengths (1–6 rings) and structural patterns (linear, zigzag, and helical) were investigated computationally. The structures, which serve as the prototypical building blocks of 2D materials such as graphene and h-BN, were optimized at the B3LYP level of theory with the def2-SVP and def2-TZVP basis sets. The calculated HOMO and LUMO energies were used to approximate the bandgap for each structure. Additionally, the UV/Vis spectra were computed using the time-dependent density functional theory to find the maximum of absorption (λ_{max}) that corresponds to the optical bandgap. The data analysis showed how changing structural patterns, extending ribbon length, and making atomic substitutions affects optoelectronic properties in graphene and h-BN-like systems.

POSTER: PHYSICAL SCIENCES**Preparation of novel mono-, bis- and tris-ligated PyrOx–Ir complexes****Blake Woodward, Seth Smith, Matthew B. Prater***Southern Utah University*

Ir-based complexes, particularly tris-bipyridine complexes, have been the subject of much study because of their unique photochemical properties. Such complexes have been used for photoredox chemistry, hydrogenation, and as a chemical sensor for hypochlorite ions. Coordination compounds of this nature are studied in intermediate inorganic chemistry courses; however, the ligand utilized in these experiments is often a symmetric diimine. We proposed the use of an asymmetric diimine ligand to form mono-, bis-, and tris-ligated Ir complexes. Formation of these compounds can be confirmed using analytical techniques such as UV-vis and IR spectroscopy, magnetic susceptibility, and X-ray diffraction. Currently, efforts to characterize these complexes is underway.

POSTER: PHYSICAL SCIENCES**Direct One-pot Grignard Formation and Addition to Imine Electrophiles****Austin Flynn, Matthew B. Prater***Southern Utah University*

Alkylamines represent an important class of organic molecules that include biologically active natural products and pharmaceuticals. They are found in important compounds such as morphine, dopamine, DNA, and all proteins. The formation of alkylamines is crucial for the production of better medicines. The Grignard reaction is a well-known reaction consisting of a Grignard reagent and an electrophile. We plan to use an alternative form of the Grignard reaction to form alkylamines. The proposed reaction could make it easier for chemists to produce alkylamines. In Grignard syntheses, the Grignard reagent contains an alkane with a magnesium-halide bond. The disassociation of the magnesium and halide group allows for the alkane to act as a nucleophile to attack an electrophile. It has been shown that an alkyl halide, in the presence of magnesium, will cause the Grignard reaction to occur. After

reviewing the literature, it is apparent that no reports exist of the production of amines by this method. We propose to carry out the Grignard reaction to form alkylamines without prepared Grignard reagents by using only the alkyl halide and the presence of magnesium in the solution.

POSTER: SOCIAL SCIENCES

Is Confession Good for the “Soul”?

Sarah Foote and Emily Putnam

Brigham Young University and Salt Lake Community College

This literature review investigates the role and impact of confession on psychological well-being. It investigates and differentiates between confession related to criminal behavior and non-criminal disclosures that may also be described as confessionals. This literature review also examines the role of “confessions” in religion and the potential impacts on the confessors mental and psychological well-being. We also explore a psychodynamic perspective of the role of “confession” in bringing the unconscious to consciousness. Overall, this review examines the role of confessions in psychological interventions as well as in more forensic roles.

SOCIAL SCIENCE

Belief Stories and the Social Construction of Reality using Religion as a Case Study

Matthew Smith-Lahrman

Dixie State University

A basic sociological question asks “Why do people act?” The short answer is that people act based on perceived realities. If one believes it to be real, one acts as if it is real. To answer the first question, then, we must answer another, “What do people perceive to be real?” I suggest that people’s actions are “belief stories,” presentations of what they believe to be real. Through language, especially, people let others know what they think is going on, who they think they are, and who they think others are. People act because they believe in particular realities and they let others know about those realities through their actions. In this talk, I

define and develop the idea of belief stories using empirical data gathered from 14 months of observations of religious services in Southern Utah. I first discuss the sociological theoretical tradition known as the social construction of reality, then describe the setting and methods I used to gather data, and finally present a few empirical examples of belief stories from my fieldwork. The bulk of my talk comes from the pages of a book I wrote on the subject.

SOCIAL SCIENCE

Clearance Rate Correlation to Pandemic-Era Increased Homicide Rates in American Cities

John Hill

Salt Lake Community College

During the Pandemic Era (2020-21), over a dozen American cities have seen record rates of homicide. Clearance rates for these crimes has declined, concurrently. This research analyzes correlation and antecedents for same.

SOCIAL SCIENCE

Tupac Shakur and Kendrick Lamar: A Legacy of Hip Hop Resistance

Theresa A. Martinez

University of Utah

From its very beginnings in the 1970s, rap music has reflected the profound disenfranchisement of African Americans living in the nation's neglected and abandoned inner cities. Rap was only one aspect of hip hop that emerged in the South Bronx in that time period—along with graffiti and breakdancing, among others. Rap could be playful, catchy, sexy, and humorous, but it also intoned a forceful cultural critique of on-going and horrendous disparities facing Black communities, including police violence, systemic inequity in the criminal justice system, housing discrimination, and educational disparity. This paper examines two hip hop artists—one legendary artist from the 1990s and one contemporary hip hop artist who is already making a sizable mark on the genre—as they reflect on and unpack the sociohistorical contexts of their times. The

paper unpacks the lyrics of our two hip hop artists through a theoretical lens that evokes oppositional cultures or cultures of resistance within distinct social locations or cultural formations—a nuanced response to appalling structural disparity then and now.

SOCIAL SCIENCE

Understanding Us: Undergraduate Research to Support a Community Partner Working on Homelessness

Dan Poole, Kambry Woodbury

Salt Lake Community College

Understanding Us is a non-profit organization that provides several programs focusing on individuals experiencing homelessness in Salt Lake City. Currently, Understanding Us runs a Tai Chi program at the downtown library four days a week. In 2018, a group of Salt Lake Community College students, working with Professor Poole, collected preliminary demographic survey data to help the organization better understand the population they are serving in order to best meet the needs of participants. We have updated the survey by adding new questions and rewording some of the past questions to make them more clear. In addition to the demographic survey data that was collected, we have added anecdotal examples and insight from participants in the Tai Chi program to our presentation.

SOCIAL SCIENCE

Smoke Season: Exploring the Human Geographies of Transient Wildfire Smoke along the Wasatch Front

Jeremy Bryson, Jeff Montague

Weber State University

Wildfire seasons around the American West have been intensifying as the effects of climate change are reshaping the region. Smoke seasons in Utah are also intensifying so that when places like California and Oregon experience massive wildfires, the smoke from those fires can descend on the Wasatch Front for weeks during the late summer. This transient smoke from cross-border wildfires can cause the air quality in Utah's dominant urban region to become among the worst in the world. How

are urban places along the urbanized Wasatch Front experiencing transient wildfire smoke? What efforts are state leaders making to alleviate the negative impacts of the smoke? Which residents are most impacted? What specific challenges do the smoke incursions create for the Wasatch Front's human, environmental, and economic health? How is the smoke changing the way we live in the places we live? In this paper, we use an urban political ecology approach to explore the contested human geographies of transient wildfire smoke along the urban corridor of the Wasatch Front.

SOCIAL SCIENCE

“I Was Answered That I Must Join None of Them”: Irreligion Among Former Latter-day Saints in Utah

Rick Phillips

University of North Florida

Within the United States, religious switching is common. However, when members of The Church of Jesus Christ of Latter-day Saints change their denominational status, they tend to abandon organized religion altogether. This pattern has been observed for almost 40 years. However, the number of Latter-day Saints leaving religion has accelerated in the 21st century, particularly in Utah. Using ethnographic data collected along the Wasatch Front, this paper presents a sociological framework for studying religious disaffiliation in Utah, and examines why Latter-day Saints are less likely than others to switch to a new denomination when they leave their religion. I provide cultural, demographic, and political reasons for this phenomenon.

SOCIAL SCIENCE

Geospatial Analysis of Drug-Related Crimes in Local Communities in Utah

Erin Crump, Yong Seog Kim

Utah State University

According to the 2021 World Drug Report released by the United Nations Office on Drugs and Crime, over 36 million people among 275 million people who used drugs worldwide suffered from drug use

disorders in 2020 alone. In addition, the number of people who use drugs is estimated to increase by 11% globally by 2030. Therefore, there exists a strong need to further understand drug usage and drug-related crimes to address prevention and intervention policies. In particular, the identification of geographical locations with frequent drug-related crimes is very critical for law enforcement agencies and state/federal governments to establish strategies to curb such crime activities. At the same time, it is also important for the public in general to be aware of and avoid such dangerous areas for safety reasons. To this end, we collect, analyze, and visualize crime data sets collected through incident-based reporting by local police and sheriff's offices from 2011 through 2019 to explore geospatial and temporal characteristics of drug- and alcohol-related crimes in several local communities in Utah. We find natural grouping of the geographic locations via a density-based clustering algorithm, which finds 10 clusters in addition to outliers automatically. As we expected, many cities in Utah are distinguished by various level of incidents of drug- and alcohol-related crimes over years. However, we find across all cities that both the overall crime incidents and the number of drug-related incidents increase significantly during the winter season (October through April). Most of all, we find several geospatial locations of such crimes close to public parks, residential areas, or school districts, which may inform proactive policing in these communities.